



THÈSE

Pour obtenir le grade de

DOCTEUR DE L'UNIVERSITÉ SAVOIE MONT BLANC

Spécialité : **Mathématiques Appliquées**

Arrêtée ministériel : 25 mai 2016

Présentée par

Eloi MARTINET (doctorant)

Thèse dirigée par **Dorin DUCUR** (directeur)
et codirigée par **Edouard OUDET** (co-directeur)

préparée au sein du **Laboratoire LAMA**
dans **l'École Doctorale MSTII**

Optimisation spectrale de formes sans énergie d'interface

Thèse soutenue publiquement le **13 octobre 2023**,
devant le jury composé de :

Eric Bonnetier

Institut Fourier, UGA, Président

Yannick Privat

IECL, Univ. Lorraine, Rapporteur

Zakaria Belhachmi

LMIA, Univ. Haute Alsace, Rapporteur

Ilaria Lucardesi

IECL, Univ. Lorraine, Examinatrice

Dorin Bucur

LAMA, USMB, Directeur de thèse

Edouard Oudet

LJK, UGA, Co-Directeur de thèse

"Qu'est-ce que ça peut bien vouloir dire tous ces hiéroglyphes là ?"
Obélix, Astérix et Obélix : Mission Cléopâtre.

Remerciements

Comment écrire des remerciements concis sans oublier personne ? Si je devais écrire ma gratitude à tous ceux et toutes celles qui ont contribué à me faire rendre ma thèse aujourd’hui, il me faudrait plus que ce manuscrit (même s’il n’est, j’en conviens, pas bien long). Plutôt qu’oublier trop de gens, j’ai fait le choix de recourir à l’euphémisme qui, en plus de m’économiser quelques caractères, me permet d’arborer une pudeur aussi solennelle que factice.

Je remercie tout d’abord Yannick Privat et Zakaria Belhachmi d’avoir pris le soin de relire ma thèse et pointer certaines erreurs ou imperfections. Il en reste sans doute, mais déjà moins grâce à vous ! Merci pour vos compliments qui m’ont beaucoup touché et que je ne suis pas certain de mériter.

Afin de n’oublier personne, je vais maintenant procéder par ordre plus ou moins chronologique. Je commencerai donc par remercier mon premier mentor en mathématiques, a.k.a. "Papa". Depuis ma plus tendre enfance, tu m’as éveillé aux curiosités des chiffres, aux constructions géométriques, étonnantes et esthétiques ainsi qu’aux plaisirs de la réflexion mathématique. Outre ton apport intellectuel, tu as toujours été là, tant pour accueillir mes doutes que pour me dissuader d’entrer dans l’Éducation Nationale.

D’autres mentors plus ou moins éphémères se sont succédé durant mes enseignements à l’ENSIMAG. Merci à Emmanuel et Clément de m’avoir fait découvrir que les mathématiques appliquées peuvent aussi cacher une grande beauté au-delà de leur aspect utilitaire. Merci aussi à Charles pour m’avoir conforté dans l’idée que l’optimisation de formes est - très objectivement - la meilleure discipline des mathématiques. Un immense merci à Boris, toujours prêt à discuter, toujours passionné. Tu m’as ouvert les portes de la recherche académique et j’ai pu reconnaître à travers nos discussions une conception des mathématiques qui m’était familière. Tu as été une inspiration et un soutien qui m’a permis d’être ici aujourd’hui.

Not last and definitely not least, merci à Catriona. Par ces papiers griffonnés sur des coins de tables collantes et bancales, tu as fini de sceller mon amour des maths. Merci pour ta patience, merci pour cette étincelle communicative, merci de m’avoir fait comprendre la noblesse qu’il y a à partager une passion. À défaut de devenir un grand chercheur, peut-être pourrais-je à l’avenir en mettre sur la voie.

Pour terminer la liste non-exhaustive de ceux qui ont contribué à développer mes connaissances et mon amour pour les mathématiques, je remercie mes tuteurs, Édouard et Dorin. Merci pour vos conseils très souvent fructueux lors de nos nombreuses discussions. Je rends particulièrement hommage à la patience de Dorin qui a dû m’accueillir presque quotidiennement dans son bureau en début de thèse.

Merci à tous mes amis du LAMA et de l’IMAG, pour les fous rires, les repas, les bars, les gribouillages sur tableau blanc, les pauses un peu trop longues, les sessions d’escalade (chacun se reconnaîtra dans une catégorie ou plus), et pour m’avoir fait découvrir que la recherche universitaire était un milieu d’islamo-gauchistes. Merci spécialement à toi Mickaël, pour tes conseils éclairés, pour nos discussions toujours intéressantes, et pour m’avoir appris que la recherche se faisait aussi très bien sur Messenger.

Cette thèse, comme la plupart, n’a pas été de tout repos et le moral a souvent été assez bas. Pour ces moments de doutes et l’humour parfois massacrante qui les accompagnaient, je remercie Margaux du fond du cœur. Ton soutien et ton amour quotidien ont permis d’alléger le poids de cette thèse. Accroche-toi, le post-doc arrive.

Dans le même registre, il serait impossible de ne pas remercier ma mère. À la fois maman, confidente et punching-ball, tu as toujours été là pour moi sans jamais juger, même lorsque tu ne comprenais pas grand-chose à mes soucis de jeune chercheur (c’est vrai, qu’est-ce que ça peut bien faire qu’il ne converge pas cet algo ?).

Merci à mes plus proches amis qui ont toujours été présents pour accueillir mes plaintes (il faut dire que ça fait quand même trois mois qu’il ne converge pas cet algo) : Margaux, Elisa, Riwan, Caro, Merco et tous les parisiens. Le rôle de ce manuscrit de thèse n’étant pas de me permettre d’écrire à quel point vous comptez dans ma vie, je m’en abstiens ici.

Enfin, à vous mes frères pour qui la profondeur de mon attachement ne pourrait pas même être ternie par le caractère discutable de vos engagements politiques - mais qu’ont bien pu rater vos deux fonctionnaires de parents ? J’espère que vous serez aussi fiers de moi que je suis fier de vous.

Contents

1	Introduction (version française)	1
1.1	Principaux résultats antérieurs	2
1.1.1	Optimisation pour des domaines de \mathbb{R}^n	2
1.1.2	Optimisation pour les domaines de la sphère	3
1.1.3	Comportement des valeurs propres de Neumann	3
1.1.4	L'argument de Weinberger	5
1.1.5	Etude numérique des problèmes aux valeurs propres	8
1.2	Structure de la thèse	8
1.2.1	Chapitre 2 : Une sélection d'outils pour l'optimisation numérique des valeurs propres	9
1.2.2	Chapitre 3 : Maximisation des valeurs propres de Neumann dans une classe de densités	9
1.2.3	Chapitre 4 : Inégalités optimales pour les valeurs propres de Neumann sur la sphère	11
1.2.4	Chapitre 5 : Optimisation numérique des valeurs propres de Neumann sur des domaines de la sphère	12
1	Introduction (English version)	16
1.1	Key previous results	17
1.1.1	Optimization in domains of \mathbb{R}^n	17
1.1.2	Optimization for domains on the sphere	18
1.1.3	Behavior of Neumann Eigenvalues	18
1.1.4	The Weinberger argument	20
1.1.5	Numerical Study of Eigenvalue Problems	23
1.2	Thesis structure	23
1.2.1	Chapter 2: A selection of tools for numerical eigenvalue optimization	23
1.2.2	Chapter 3: Maximization of Neumann eigenvalues in a class of densities	24
1.2.3	Chapter 4: Optimal Inequalities for Neumann Eigenvalues on the Sphere	25
1.2.4	Chapter 5: Numerical Optimization of Neumann Eigenvalues on Spherical Domains	26
2	A selection of tools for the numerical optimization of eigenvalues	30
2.1	Eigenvalues of self-adjoint operators	31
2.2	Finite elements approximation of eigenvalue problems	33
2.3	Directional shape derivative of Laplace eigenvalues	35
2.4	Shape optimization by the level set method : basic ideas	41
3	Maximization of Neumann eigenvalues in a class of densities	43
3.1	Introduction	44
3.2	A global existence result for densities	47
3.3	Study of the one dimensional case	52
3.4	Pólya conjecture and Kröger inequalities	60
3.5	Numerical approximation of optimal densities	62
4	Sharp inequalities for Neumann eigenvalues on the sphere	68
4.1	Introduction	69
4.2	Topological results	71
4.3	Proof of optimality for μ_2	75
4.4	General proof for the harmonic mean	77
4.5	Further remarks and open questions	79

5 Numerical optimization of Neumann eigenvalues of domains in the sphere	82
5.1 Introduction	83
5.2 Existence and approximation of the optimal density	83
5.3 Density method	85
5.4 Results : density method.	88
5.5 Level-set method	95
5.6 Results : level-set method.	98
5.7 Explorations on a torus	102
5.8 Discussion	103

References

I

List of figures

V

List of tables

VII

1

Introduction (version française)

Dans ce manuscrit, nous allons traiter de problèmes d'optimisation des valeurs propres du laplacien sous contrainte de volume. Dans la suite, Ω sera un ouvert borné de \mathbb{S}^n ou \mathbb{R}^n vérifiant certaines hypothèses de régularité dont on note $|\Omega|$ le volume. On dit que μ est une valeur propre du laplacien avec conditions de Neumann s'il existe une fonction $u \in \mathbf{H}^1(\Omega) \setminus \{0\}$ appelée fonction propre telle que

$$\begin{cases} -\Delta u = \mu u & \text{dans } \Omega, \\ \partial_\nu u = 0 & \text{sur } \partial\Omega \end{cases} \quad (1.1)$$

où Δ représente l'opérateur de Laplace (resp. Laplace-Beltrami) de \mathbb{R}^n (resp. \mathbb{S}^n) et $\partial_\nu u$ est la dérivée normale au bord de Ω . Prenant en compte les multiplicités, les valeurs propres d'un tel problème forment une suite vérifiant

$$0 = \mu_0(\Omega) \leq \mu_1(\Omega) \leq \dots \leq \mu_k(\Omega) \leq \dots \rightarrow \infty.$$

Un problème voisin est le problème aux valeurs propres avec conditions de Dirichlet

$$\begin{cases} -\Delta u = \lambda u & \text{dans } \Omega, \\ u = 0 & \text{sur } \partial\Omega \end{cases}$$

qui lui aussi admet un spectre de valeurs propres

$$0 < \lambda_1(\Omega) \leq \lambda_2(\Omega) \leq \dots \leq \lambda_k(\Omega) \leq \dots \rightarrow \infty.$$

On s'intéressera principalement à la maximisation des valeurs propres avec conditions de Neumann. Formellement, les problèmes considérés sont de la forme

$$\max_{|\Omega|=m} \mu_k(\Omega) \quad (1.2)$$

où $m > 0$ et $\Omega \subseteq \mathbb{R}^n$ ou $\Omega \subseteq \mathbb{S}^n$.

Les problèmes d'optimisation de formes impliquant la solution d'équations aux dérivées partielles avec conditions de Neumann apparaissent naturellement dans différents modèles mathématiques allant de la mécanique des structures à l'analyse d'image en passant par la biologie, etc. L'analyse mathématique de tels problèmes est, en général, une tâche complexe dûe à l'absence d'une énergie de bord venant contrôler les interactions entre la géométrie de la forme et la solution de l'équation aux dérivées partielles. En effet, contrairement aux conditions de Robin qui possèdent une telle énergie, son absence dans le cas de Neumann soulève de sérieuses difficultés. Dans certaines situations (par exemple les modèles de propagation de fissures ou l'étude de la fonctionnelle de Mumford-Shah), une pénalisation de la longueur du bord est naturellement présente et vient régulariser le problème, ce qui n'est pas le cas pour le problème de Neumann (1.2).

L'objectif de cette thèse est l'étude des questions théoriques liées à ces problèmes grâce au support de simulations numériques.

1.1 Principaux résultats antérieurs

1.1.1 Optimisation pour des domaines de \mathbb{R}^n

L'étude théorique des problèmes d'optimisation spectrale de formes remonte au début du XXème siècle. Le prototype d'un tel problème est l'inégalité de Faber-Krahn [53, 1925] [72, 1925], confirmant une conjecture de Lord Rayleigh stipulant que parmi les membranes d'aire donnée, celle ayant la fréquence fondamentale la plus grave est le disque :

Théorème 1.1.1 (Faber-Krahn). *Soit $\Omega \in \mathbb{R}^n$ un ouvert tel que $|\Omega| = 1$. Alors*

$$\lambda_1(\Omega) \geq \lambda_1(\mathbf{B}^{|\Omega|})$$

où $\mathbf{B}^{|\Omega|}$ est une boule de mesure $|\Omega|$.

Il faudra attendre une trentaine d'années avant d'avoir un énoncé similaire pour la première valeur propre non triviale du problème de Neumann. Dans [71, 1952], Kornhauser et Stackgold justifient par un argument de perturbation que sous réserve d'existence, μ_1 doit être optimale sur la boule. Un tel résultat fut d'abord prouvé par Szegö pour les ouverts lisses simplement connexes de \mathbb{R}^2 [98, 1954] puis en toute généralité par Weinberger [102, 1956] :

Théorème 1.1.2 (Weinberger). *Soit $\Omega \in \mathbb{R}^n$ un ouvert borné Lipschitz. Alors*

$$\mu_1(\Omega) \leq \mu_1(\mathbf{B}^{|\Omega|}).$$

Une question apparaissant naturellement ensuite est de connaître, s'il existe, un domaine maximisant des valeurs propres d'ordre plus élevé. Alors qu'en général, la question de l'existence reste ouverte, on sait désormais que le domaine maximisant la seconde valeur propre non-triviale μ_2 est l'union disjointe de deux boules de même mesure. Ce résultat a d'abord été prouvé pour des domaines lisses et simplement connexes de \mathbb{R}^2 par Girouard, Nadirashvili et Polterovich [60, 2009] puis en toute généralité par Bucur et Henrot [33, 2019] :

Théorème 1.1.3 (Bucur-Henrot). *Soit $\Omega \in \mathbb{R}^n$ un ouvert borné Lipschitz. Alors*

$$\mu_2(\Omega) \leq \mu_2(\mathbf{B}^{|\Omega|/2} \sqcup \mathbf{B}^{|\Omega|/2})$$

avec $\mathbf{B}^{|\Omega|/2} \sqcup \mathbf{B}^{|\Omega|/2}$ l'union disjointe de deux boules de mesure $|\Omega|/2$.

Pour être exact, ce théorème reste valable dans un cadre beaucoup plus large que les domaines, à savoir un cadre où il est possible de définir des valeurs propres de *densités*. Nous y reviendrons un peu plus loin.

Le problème de l'optimisation des valeurs propres du laplacien est étroitement lié à la *conjecture de Pólya*. Cette conjecture stipule que le premier terme de la formule asymptotique de Weyl [104]

$$\mu_k(\Omega) \sim 4\pi^2 \left(\frac{k}{\omega_n |\Omega|} \right)^{2/n} \quad \text{quand } k \rightarrow \infty$$

(où ω_n est le volume de la boule unité de \mathbb{R}^n) est en réalité une borne supérieure des valeurs propres de Neumann, i.e.

Conjecture 1.1.1 (Pólya). *Pour tout $k \in \mathbb{N}^*$, $\mu_k(\Omega) \leq 4\pi^2 \left(\frac{k}{\omega_n |\Omega|} \right)^{2/n}$.*

Si les précédents théorèmes nous disent que cette conjecture est vérifiée pour $k = 1$ et 2 , elle est encore complètement ouverte pour tout $n \geq 2$ et $k \geq 3$. Un résultat allant dans le sens de la conjecture a cependant été donné par Kröger [75, 1992] :

Théorème 1.1.4 (Kröger). *Pour tout $k \in \mathbb{N}^*$,*

$$\mu_k(\Omega) \leq \left(\frac{n+2}{2} \right)^{2/n} 4\pi^2 \left(\frac{k}{\omega_n |\Omega|} \right)^{2/n}.$$

Bien que ne faisant pas l'objet de cette thèse, un aspect important des problèmes d'optimisation de formes est les problèmes de *stabilité*. Pour les valeurs propres de Neumann, la stabilité consiste à se demander si la proximité de $\mu_k(\Omega)$ avec $\mu_k(\Omega^*)$, où Ω^* désigne le maximiseur de (1.2), implique la proximité en un certain sens de Ω et Ω^* . Pour μ_1 , on a en effet le résultat de stabilité suivant, dû à Brasco et Pratelli [31, 2012] :

Théorème 1.1.5 (Brasco-Pratelli).

$$\mu_1(\mathbf{B}^{|\Omega|}) - \mu_1(\Omega) \geq \mu_1(\mathbf{B}^{|\Omega|}) c_n \mathcal{A}(\Omega)^2$$

où

$$\mathcal{A}(\Omega) = \inf \left\{ \frac{|\Omega \Delta B|}{|\Omega|} : B \text{ est une boule et } |B| = |\Omega| \right\}$$

désigne l'assymétrie de Fraenkel de Ω et c_n est une constante dimensionnelle.

1.1.2 Optimisation pour les domaines de la sphère

Un autre aspect de cette thèse sera l'optimisation des valeurs propres de Neumann dans des variétés et principalement dans certains domaines de la sphère $\Omega \subseteq \mathbb{S}^n \subseteq \mathbb{R}^{n+1}$. On considère toujours le problème (1.1) où Δ désigne l'opérateur de Laplace-Beltrami de \mathbb{S}^n . Des résultats généralisant le théorème de Weinberger existent dans la littérature. Par exemple, dans l'espace hyperbolique, il a été prouvé par Ashbaugh et Benguria que le maximiseur pour μ_1 est toujours la boule (géodésique) [18, 1995]. De même, Freitas et Laugesen ont montré que le maximiseur pour μ_2 est toujours l'union disjointe de deux boules de même mesure [56, 2020]. Dans les deux cas, le résultat est vérifié en toute dimension et les preuves font encore une fois appel à de forts arguments topologiques. Cependant, de manière assez étonnante, aucun résultat complet n'avait jamais été établi pour des domaines de \mathbb{S}^n . Le premier pas dans ce sens se trouve dans le même article [18, 1995] où Ashbaugh et Benguria montrent par une méthode semblable à Weinberger le théorème suivant :

Théorème 1.1.6 (Ashbaugh-Benguria). *Notons*

$$\mathbb{S}_+^n = \{(x_1, \dots, x_{n+1}) \in \mathbb{R}^{n+1} \mid x_1^2 + \dots + x_{n+1}^2 = 1 \text{ et } x_{n+1} > 0\}$$

et considérons l'ensemble des domaines $\Omega \subseteq \mathbb{S}_+^n$. Alors

$$\mu_1(\Omega) \leq \mu_1(\mathbf{B}^{|\Omega|})$$

où $\mathbf{B}^{|\Omega|}$ est une boule géodésique de mesure $|\Omega|$.

La condition - très forte - pour Ω d'être contenu dans un hémisphère impose notamment que $|\Omega| \leq \frac{|\mathbb{S}^n|}{2}$ et on pourrait se demander si cette seule contrainte de mesure ne serait pas suffisante pour garantir le résultat. Très récemment, Langford et Laugesen [76, 2022] ont montré le résultat suivant dans \mathbb{S}^2 , étendant un précédent résultat de Bandle [21, 1972] :

Théorème 1.1.7 (Langford-Laugesen). *Soit $\Omega \subseteq \mathbb{S}^2$ un domaine simplement connexe tel que $0 < |\Omega| < 0.94|\mathbb{S}^2|$. Alors*

$$\mu_1(\Omega) \leq \mu_1(\mathbf{B}^{|\Omega|}).$$

Ils ont donc remplacé la condition de Ashbaugh et Benguria par une autre hypothèse forte sur la dimension et la topologie des domaines.

1.1.3 Comportement des valeurs propres de Neumann

Il est connu que les valeurs propres de Dirichlet jouissent de plus de stabilité que les valeurs propres de Neumann par rapport à la géométrie du domaine. Par exemple, si $\Omega_1 \subseteq \Omega_2$ alors pour tout $k \in \mathbb{N}$, $\lambda_k(\Omega_1) \geq \lambda_k(\Omega_2)$, relation qui n'est pas satisfaite pour les valeurs propres de Neumann. En particulier, considérons la suite de spirales "épaissies" à n spires

$$\Omega_n := \bigcup_{p \in \mathcal{P}_n} \mathbf{B}_{p, \frac{1}{2^n}},$$

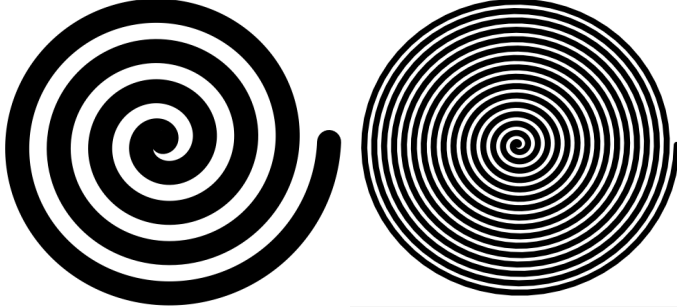


Figure 1.1: Représentation de \mathcal{S}_4 (gauche) et \mathcal{S}_{16} (droite)

où

$$\mathcal{S}_n := \{(r \cos(2\pi nr), r \sin(2\pi nr)) \in \mathbb{R}^2 \mid r \in [0, 1]\}$$

et $\mathbf{B}_{p,r}$ est la boule de centre p et de rayon r . On trouvera une représentation de \mathcal{S}_4 et \mathcal{S}_{16} Figure 1.1. On peut montrer que $\Omega_n \subseteq \mathbf{B}_{0,2}$ pour tout $n > 0$ et $\mu_k(\Omega_n) \xrightarrow{n \rightarrow \infty} 0$. Ce manque de monotonie empêche notamment l'utilisation d'un résultat général d'existence du type Buttazzo-Dal Maso [37, 1993], permettant de déduire l'existence de domaines optimaux pour des domaines inclus dans un ouvert borné fixé.

Une autre propriété importante des valeurs propres de Dirichlet est que si deux domaines Ω_1 et Ω_2 sont "proches" en un certain sens alors les valeurs propres $\lambda_k(\Omega_1)$ et $\lambda_k(\Omega_2)$ le sont aussi. Dans ce sens, on a par exemple le théorème de Šverak [107]:

Théorème 1.1.8 (Šverak). *Soit $B \subseteq \mathbb{R}^2$ un compact et $(\Omega_n)_{n \geq 0}$ une suite d'ouverts de B qui converge vers un ouvert Ω au sens de la distance de Hausdorff du complémentaire. On suppose que le nombre de composantes connexes de $B \setminus \Omega_n$ est uniformément borné. Alors pour tout $k > 0$,*

$$\lambda_k(\Omega_n) \rightarrow \lambda_k(\Omega).$$

Cette propriété échoue pour les valeurs propres de Neumann. L'exemple classique décrivant ce type de comportement est donné Figure 1.2. On peut montrer que les valeurs propres de Dirichlet d'un tel ensemble

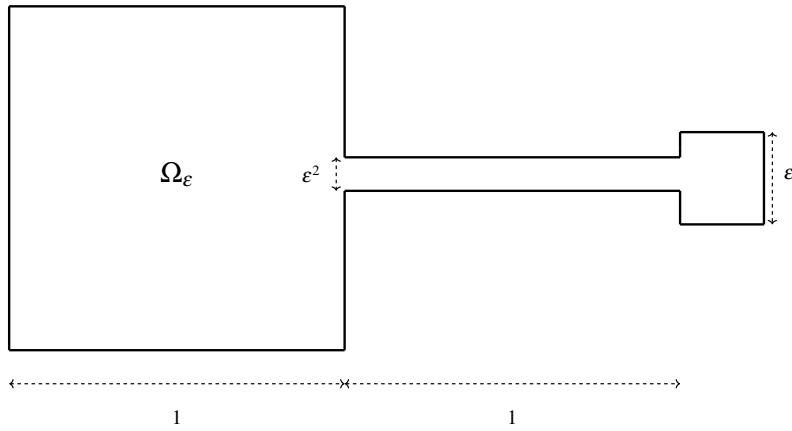


Figure 1.2: Ensemble Ω_ε consistant en l'union du carré unité et d'un carré de côté ε relié par un fin rectangle de hauteur ε^2 .

Ω_ε convergent vers celles du carré unité, alors que $\mu_1(\Omega_\varepsilon) \xrightarrow{\varepsilon \rightarrow 0} 0 \neq \mu_1((0, 1)^2)$.

Remarque 1.1.9. En réalité, les hypothèses du théorème de Šverak montrent que Ω_n converge vers Ω au sens de la γ -convergence, qui à son tour implique la convergence en norme des opérateurs résolvants et donc des valeurs propres. Dans le cas de Neumann, les hypothèses de Šverak ne permettent pas de conclure à une telle convergence des opérateurs résolvants. On peut cependant avoir un résultat de semi-continuité supérieure, voir [32, Th. 7.4.7].

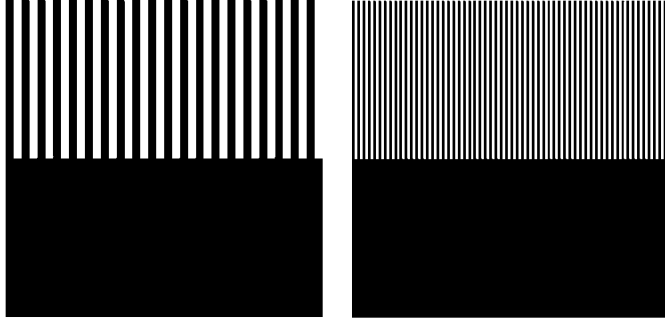


Figure 1.3: Exemple de domaine en peigne avec respectivement 20 (gauche) et 60 dents (droite).

Un autre cas particulièrement pathologique est celui du "peigne", que l'on peut trouver notamment dans [22] et illustré Figure 1.3. En effet, si on note Ω_n le peigne à n dents créé à partir du carré $D = (-1, 1)^2$ où $\omega = (-1, 1) \times (-1, 0)$ est la partie pleine et où chaque "dent" est de largeur $1/n$, on peut formellement écrire que $\mu_k(\Omega_n)$ tend vers la k -ème valeur propre du problème dégénéré

$$\inf_{S \in \mathcal{S}_{k+1}} \max_{u \in S \setminus \{0\}} \frac{\int_{\omega} |\nabla u|^2 + \frac{1}{2} \int_{D \setminus \omega} |\partial_y u|^2}{\int_{\omega} u^2 + \frac{1}{2} \int_{D \setminus \omega} u^2}$$

où \mathcal{S}_k est l'ensemble des sous espaces de dimension k de $\mathbf{H}^1(D)$. On peut observer dans ce cas que les fonctions propres sont principalement supportées sur les dents du peigne.

Malgré ces comportements, on peut tout de même obtenir la continuité des valeurs propres de Neumann pour la distance de Hausdorff en imposant des hypothèses géométriques suffisamment fortes sur les domaines. En effet, considérons le problème de type Poisson

$$\begin{cases} -\Delta u_n + u_n = f \text{ dans } \Omega_n \\ \partial_v u_n = 0 \text{ sur } \partial \Omega_n \end{cases}, \quad (1.3)$$

où $(\Omega_n)_{n \geq 0}$ est une famille d'ouvert incus dans un même compact $B \subseteq \mathbb{R}^n$ et $f \in \mathbf{L}^2(B)$. Un résultat de Chenais [42] nous permet de construire des opérateurs d'extension uniformément bornés de $\mathbf{H}^1(\Omega)$ dans $\mathbf{H}^1(B)$, résultat permettant à son tour d'avoir la propriété de continuité suivante :

Théorème 1.1.10. Soit $B \subseteq \mathbb{R}^n$ un compact et $(\Omega_n)_{n \geq 0}$ une suite d'ouvert de B qui converge vers un ouvert Ω au sens de la distance de Hausdorff. Sous l'hypothèse que les Ω_n vérifient la propriété du ε -cône uniforme (voir par exemple [67, Def. 2.4.1]), alors pour tout $k \geq 0$,

$$\mu_k(\Omega_n) \rightarrow \mu_k(\Omega).$$

Toujours pour les problèmes de type (1.3), on peut citer le résultat de Chambolle et Doveri [40]. Si $\Omega_n \rightarrow \Omega$ au sens de la distance de Hausdorff, les auteurs donnent la convergence des solutions u_n vers la solution u de (1.3) sur Ω sous contrainte de périmètre et de connexité de $\partial \Omega_n$. Dans [36], Bucur et Varchon montrent un résultat similaire sous contrainte de mesure et de borne uniforme sur les composantes connexes des $\partial \Omega_n$. Enfin, dans le Chapitre 2, nous montrons un résultat de continuité des valeurs propres de Neumann pour des déformations suffisamment lisses d'un domaine de référence. Pour plus d'informations sur ces questions, nous référons le lecteur à [64, Chap. 2].

1.1.4 L'argument de Weinberger

La preuve de Weinberger étant à l'origine d'une grande variété de résultats concernant l'optimisation des valeurs propres de Neumann, nous allons ici en donner les idées principales. Si le lecteur n'est pas tout à fait familier avec les outils utilisés ici, nous le référons au Chapitre 2.

Soit $\Omega \in \mathbb{R}^n$ un ouvert borné Lipschitz. Rappelons tout d'abord que la première valeur propre non triviale du problème de Neumann peut s'écrire sous la forme variationnelle

$$\mu_1(\Omega) = \min_{v \in \mathbf{H}^1(\Omega) \setminus \{0\}, \int_{\Omega} v = 0} \frac{\int_{\Omega} |\nabla v|^2}{\int_{\Omega} v^2} \quad (1.4)$$

grâce à la formule de Courant-Fisher. L'idée de Weinberger est d'utiliser des extensions des fonctions propres de la boule $\mathbf{B}^{|\Omega|}$ (centrée en 0) comme fonctions test dans (1.4). Le cœur de la preuve (et la principale difficulté pour son adaptation aux valeurs propres d'ordre supérieur) est de montrer que ces fonctions peuvent satisfaire la condition $\int_{\Omega} v = 0$ en translatant convenablement Ω .

Soit R le rayon de $\mathbf{B}^{|\Omega|}$. On peut montrer que les fonctions propres associées à $\mu_1(\mathbf{B}^{|\Omega|})$ sont les fonctions

$$x \mapsto \frac{g(|x|)}{|x|} x_i, \quad i \in \{1, \dots, n\}$$

où $g : (0, R) \rightarrow \mathbb{R}$ est la solution de l'équation différentielle

$$\begin{cases} g''(r) + \frac{n-1}{r} g'(r) + \left(\mu_1(\mathbf{B}^{|\Omega|}) - \frac{n-1}{r^2} \right) g(r) = 0 \\ g(0) = 0 \\ g'(R) = 0 \end{cases}. \quad (1.5)$$

Cette équation s'obtient par séparation des variables en coordonnées sphériques et la solution g est la seconde fonction de Bessel de première espèce, parfois notée J_1 . Posons maintenant

$$\tilde{g}(r) = \begin{cases} g(r) & \text{si } r \leq R \\ g(R) & \text{si } r \geq R \end{cases}$$

et pour tout $i \in \{1, \dots, n\}$,

$$G_i(x) = \frac{\tilde{g}(|x|)}{|x|} x_i.$$

Conformément à ce qui a été dit précédemment, supposons que l'on ait

$$\int_{\Omega} G_i(x) dx = 0 \quad i \in \{1, \dots, n\}. \quad (1.6)$$

Cette condition sera démontrée ci-après. Sous cette hypothèse, chaque G_i est une fonction test dans (1.4) et donc :

$$\mu_1(\Omega) \leq \frac{\int_{\Omega} \frac{\tilde{g}'(|x|)^2}{|x|^2} x_i^2 + \frac{\tilde{g}(|x|)^2}{|x|^2} \left(1 - \frac{x_i^2}{|x|^2}\right) dx}{\int_{\Omega} \frac{\tilde{g}(|x|)^2}{|x|^2} x_i^2 dx}.$$

En sommant sur i , on obtient

$$\mu_1(\Omega) \leq \frac{\int_{\Omega} \tilde{g}'(|x|)^2 + \frac{n-1}{|x|^2} \tilde{g}(|x|)^2 dx}{\int_{\Omega} \tilde{g}(|x|)^2 dx}.$$

En étudiant les variations des intégrandes au numérateur et au dénominateur, on peut voir que :

- $r \mapsto \tilde{g}^2(r)$ est croissante car $g(0) = 0$ et $g'(R)$ est le premier zéro de g' ;
- $r \mapsto \tilde{g}'(r)^2 + \frac{n-1}{r^2} \tilde{g}(r)^2$ est décroissante. En effet, la fonction est constante si $r \geq R$. Sinon,

$$\begin{aligned} \frac{d}{dr} \left(\tilde{g}'(r)^2 + \frac{n-1}{r^2} \tilde{g}(r)^2 \right) &= 2\tilde{g}'\tilde{g}'' + 2\frac{N-1}{r^3}(r\tilde{g}\tilde{g}' - \tilde{g}^2) \\ &= -2\mu_1(\mathbf{B}^{|\Omega|})gg' - \frac{n-1}{r^3}(rg' - g)^2 \\ &\leq 0 \end{aligned}$$

où on a utilisé (1.5) dans la dernière égalité.

Ainsi,

$$\int_{\Omega} \tilde{g}^2 = \int_{\Omega \cap \mathbf{B}^{|\Omega|}} \tilde{g}^2 + \int_{\Omega \setminus \mathbf{B}^{|\Omega|}} \tilde{g}^2 = \int_{\Omega \cap \mathbf{B}^{|\Omega|}} \tilde{g}^2 + \tilde{g}^2(R)|\Omega \setminus \mathbf{B}^{|\Omega|}|$$

d'une part et

$$\int_{\mathbf{B}^{|\Omega|}} \tilde{g}^2 = \int_{\Omega \cap \mathbf{B}^{|\Omega|}} \tilde{g}^2 + \int_{\mathbf{B}^{|\Omega|} \setminus \Omega} \tilde{g}^2 \leq \int_{\Omega \cap \mathbf{B}^{|\Omega|}} \tilde{g}^2 + \tilde{g}^2(R)|\mathbf{B}^{|\Omega|} \setminus \Omega|.$$

Mais puisque $|\Omega| = |\mathbf{B}^{|\Omega|}|$, on a $|\mathbf{B}^{|\Omega|} \setminus \Omega| = |\Omega \setminus \mathbf{B}^{|\Omega|}|$ et donc

$$\int_{\mathbf{B}^{|\Omega|}} \tilde{g}(|x|)^2 \leq \int_{\Omega} \tilde{g}(|x|)^2.$$

En menant les mêmes calculs au numérateur, on obtient

$$\int_{\mathbf{B}^{|\Omega|}} \tilde{g}'(|x|)^2 + \frac{n-1}{|x|^2} \tilde{g}(|x|)^2 \geq \int_{\Omega} \tilde{g}'(|x|)^2 + \frac{n-1}{|x|^2} \tilde{g}(|x|)^2$$

ce qui nous donne enfin

$$\mu_1(\Omega) \leq \mu_1(\mathbf{B}^{|\Omega|}).$$

Remarque 1.1.11. Le principe consistant à ramener toute la masse de Ω dans $\mathbf{B}^{|\Omega|}$ est parfois nommé "transplantation de masse" dans la littérature [55] [33] [56]. En effet, on voit formellement que ramener de la masse de $x \in \Omega \setminus \mathbf{B}^{|\Omega|}$ vers $x' \in \mathbf{B}^{|\Omega|} \setminus \Omega$ ne peut qu'augmenter le quotient de Rayleigh. Cette nomenclature est une analogie à la "transplantation conforme" utilisée notamment dans la preuve de Szegö, où les fonctions propres du domaine Ω sont ramenées sur le disque par le biais d'une application conforme.

Il reste maintenant à prouver la condition d'orthogonalité (1.6). Ce type de condition se retrouve aussi bien chez Weinberger, qui dans sa démonstration invoque le théorème de point fixe de Brouwer, que dans celle de Szegö qui fait appel à l'indice d'un lacet du plan complexe. Cependant, il a été remarqué dans [33] pour la preuve du Théorème 1.1.3 qu'un tel argument était insuffisant pour les valeurs propres d'ordre supérieur. En effet, le quotient de Rayleigh pour $\mu_2(\Omega)$ devient

$$\mu_2(\Omega) = \min \frac{\int_{\Omega} |\nabla v|^2}{\int_{\Omega} v^2}$$

où le minimum porte sur toutes les fonctions $v \in \mathbf{H}^1(\Omega) \setminus \{0\}$ vérifiant les conditions

$$\int_{\Omega} v = 0 \quad \text{et} \quad \int_{\Omega} vu_1 = 0,$$

u_1 étant la fonction propre associée à $\mu_1(\Omega)$. La notion plus générale utilisée par les auteurs est le *degré topologique*, qui permet dans certains cas de déterminer aisément si une équation du type $f(x) = 0$ possède une solution. Puisque celui-ci nous sera utile dans le Chapitre 3, nous rappelons ici les propriétés utiles, qui peuvent être retrouvées dans [93] :

Définition 1.1.2 (Degré d'une application C^1). Soit $\varphi : \overline{\Omega} \rightarrow \mathbb{R}^n$ une application C^1 . On suppose que 0 est une valeur régulière de φ (i.e. on a $\text{Jac}_{\varphi}(x) \neq 0$ pour tout $x \in \Omega$ tel que $\varphi(x) = 0$ où $\text{Jac}_{\varphi}(x)$ désigne le déterminant jacobien de φ) tel que $0 \notin \varphi(\partial\Omega)$. Le degré de φ est défini par

$$\deg_{\Omega} \varphi := \sum_{x \in \Omega, \varphi(x)=0} \text{signJac}_{\varphi}(x).$$

Grâce au théorème de Sard et à la densité des fonctions de classe C^1 dans l'espace fonctions continues, on peut étendre le degré en une application $\deg_{\Omega} : C^0(\overline{\Omega}, \mathbb{R}^n) \rightarrow \mathbb{Z}$. Ainsi défini, le degré d'une application continue vérifie toujours que

$$\deg_{\Omega} \varphi \neq 0 \implies \exists x \in \Omega, \varphi(x) = 0,$$

ce qui lui donne son intérêt dans les théorèmes d'existence. De plus, on a la propriété suivante, indiquant que le degré est invariant par homotopie tant qu'aucun zéro ne traverse la frontière $\partial\Omega$:

Proposition 1.1.3. Soit $h : [0, 1] \times \overline{\Omega} \rightarrow \mathbb{R}^n$ tel que pour tout $t \in [0, 1]$, $h(t, \cdot) \in C^0(\overline{\Omega}, \mathbb{R}^n)$ et $t \mapsto h(t, \cdot)$ est continue pour la topologie uniforme. Supposons de plus que pour tout $t \in [0, 1]$, $0 \notin h(t, \partial\Omega)$. Alors

$$\deg_{\Omega} h(0, \cdot) = \deg_{\Omega} h(1, \cdot).$$

Afin de terminer la preuve de Weinberger, nous allons nous servir du résultat suivant :

Proposition 1.1.4. Soit $\mathbf{B} \in \mathbb{R}^n$ une boule centrée à l'origine et $\varphi : \mathbf{B} \rightarrow \mathbb{R}^n$ une fonction telle que $\varphi(p) \cdot p \leq 0$ et $\varphi(p) \neq 0$ pour tout $p \in \partial\mathbf{B}$. Alors

$$\deg_{\mathbf{B}} \varphi = (-1)^n.$$

Démonstration. On pose $h(t, p) = (1-t)\varphi(p) - tp$ avec $t \in [0, 1]$ et $p \in \mathbf{B}$. Alors $\deg_{\mathbf{B}} h(0, .) = \deg_{\mathbf{B}} \varphi$ et $\deg_{\mathbf{B}} h(1, .) = \deg_{\mathbf{B}} (-\text{id}) = \text{signJac}_{-\text{id}}(0) = (-1)^n$.

Or, pour $p \in \partial\mathbf{B}$ et $t \in (0, 1]$,

$$(1-t)\varphi(p) \cdot p - tp \cdot p < 0$$

et $h(0, p) = \varphi(p) \neq 0$. Grâce à la proposition précédente, on a $\deg_{\mathbf{B}} \varphi = \deg_{\mathbf{B}} (-\text{id}) = (-1)^n$. \square

Nous pouvons désormais utiliser ce nouvel outil pour terminer la preuve. Soit $\mathbf{B} \supset \Omega$ une boule centrée à l'origine et

$$\begin{aligned}\varphi: \mathbf{B} &\longrightarrow \mathbb{R}^n \\ p &\longmapsto \int_{\Omega} G(x-p) dx\end{aligned}$$

où $G(x) = (G_i(x))_{1 \leq i \leq n}$. On veut trouver $p^* \in B$ tel que $\varphi(p^*) = 0$ grâce à la proposition précédente. Le problème aux valeurs propres étant invariant par translations, on pourra choisir p^* comme nouvelle origine, justifiant (1.6). Si il existe $p^* \in \partial\mathbf{B}$ tel que $\varphi(p^*) = 0$ alors c'est fini. Sinon, on remarque que

$$\begin{aligned}\varphi(p) \cdot p &= \left(\int_{\Omega} G(x-p) dx \right) \cdot p \\ &= \int_{\Omega} \underbrace{\frac{\tilde{g}(|x-p|)}{|x-p|}}_{\geq 0} \underbrace{(x-p) \cdot p}_{\leq 0} dx \leq 0.\end{aligned}$$

Ainsi, $\deg_{\mathbf{B}} \varphi = (-1)^n \neq 0$ et il existe p^* tel que $\varphi(p^*) = 0$. \square

1.1.5 Etude numérique des problèmes aux valeurs propres

Comme nous avons pu l'entrevoir, l'étude théorique des problèmes d'optimisation spectrale de formes est un problème ardu. Dans certains cas, il peut être suffisant de trouver une approximation de l'optimum; c'est pourquoi depuis une trentaine d'années, l'optimisation numérique des problèmes aux valeurs propres a reçu une attention croissante, portée par les capacités de calcul grandissantes des ordinateurs. Du côté industriel, on peut notamment penser aux problèmes d'optimisation de structures vibrantes [84] [4] [50] [83] [59], de cristaux photoniques [46] [69] [79] ou les problèmes de fluides [88], [81]. Dans cette optique, une large variété de méthodes a été utilisée, comme la variation de domaine, la méthode level set, les méthodes de type champ de phase ou encore les méthodes d'homogénéisation. Cette dernière est devenue un standard dans les problèmes d'optimisation de formes en élasticité et en conductivité [5].

Un autre intérêt de l'optimisation numérique des problèmes aux valeurs propres est son utilisation à des fins exploratoires, là où la théorie est encore lacunaire, ce qui peut permettre de déléguer à la machine une partie de l'intuition nécessaire au mathématicien. On peut citer par exemple [89] où l'auteur traite de l'optimisation des premières valeurs propres de Dirichlet dans \mathbb{R}^2 sous contrainte de volume. Ces simulations numériques ont permis de mettre en défaut la conjecture de Troesch [99] selon laquelle le domaine en forme de stade maximiserait la seconde valeur propre de Dirichlet, conjecture finalement réfutée dans [66] (notons que Troesch avait lui-même formulé cette conjecture sur la base de calculs numériques). Toujours pour les valeurs propres de Dirichlet, il est possible de mener des simulations similaires dans \mathbb{R}^3 [13] ou \mathbb{R}^4 [15], ou sous d'autres contraintes comme des contraintes de convexité [11] ou des problèmes de partition du plan [30]. On trouvera aussi des calculs pour l'optimisation de valeurs propres avec conditions de Neumann [16] [9], de Steklov [29] [12], de Robin [14] [17] ou encore de Wentzell [27]. Cette liste, loin d'être exhaustive, montre l'intérêt grandissant pour l'approche numérique des questions théoriques d'optimisation spectrale.

1.2 Structure de la thèse

Cette thèse portera donc sur l'optimisation des valeurs propres du laplacien avec conditions de Neumann. Un fort accent sera mis sur l'exploration numérique. C'est pourquoi le premier chapitre, sans

apporter de contribution originale, se veut être un rappel sur l'optimisation numérique des valeurs propres. Dans le second chapitre, intitulé *Maximisation des valeurs propres de Neumann dans une classe de densités*, on s'intéresse à l'optimisation des valeurs propres de *densités* généralisant les valeurs propres de domaines de \mathbb{R}^n . Le troisième chapitre, *Inégalités optimales pour les valeurs propres de Neumann sur la sphère* adressera la maximisation de μ_2 pour des domaines de la sphère entière, avec notamment une généralisation du théorème de Ashbaugh et Benguria. Dans le quatrième chapitre, *Optimisation numérique des valeurs propres de Neumann sur des domaines de la sphère*, on s'occupe de l'optimisation numérique des trois premières valeurs propres de Neumann sur la sphère et le tore, à la fois dans la classe des densités et des domaines. Les observations numériques issues de ces expériences permettront la formulation de plusieurs problèmes ouverts.

Nous allons ci-dessous décrire plus en détail les principaux résultats de chaque partie.

1.2.1 Chapitre 2 : Une sélection d'outils pour l'optimisation numérique des valeurs propres

Ce chapitre a pour but de rappeler les outils de base concernant l'optimisation numérique des problèmes aux valeurs propres. Dans un première partie, nous rappelons sans les démontrer quelques théorèmes classiques de la théorie spectrale pour les opérateurs elliptiques, à savoir le Théorème Spectral et le théorème de Courant-Fisher donnant la caractérisation variationnelle des valeurs propres. En second lieu, on montre comment approcher les valeurs propres d'un domaine par la méthode des éléments finis (FEM), avec une preuve élémentaire de convergence. La troisième partie fournit une courte introduction aux problèmes de différentiabilité des valeurs propres par rapport au domaine : on donnera notamment la preuve de l'expression de la dérivée directionnelle des valeurs propres de Neumann de multiplicité supérieure à 1. Enfin, une des questions centrales en optimisation de formes concerne la manière de paramétriser le domaine Ω que l'on va faire évoluer. On y rappellera le principe de la méthode level set, une méthode flexible en ce qu'elle autorise certains changements de topologie de se faire de manière totalement transparente.

1.2.2 Chapitre 3 : Maximisation des valeurs propres de Neumann dans une classe de densités

Ce chapitre est basé sur le travail publié en [35]. On y étudie la généralisation de la notion de valeurs propres de Neumann proposée initialement par Bucur et Henrot [33] : partant de la formulation variationnelle des valeurs propres

$$\mu_k(\Omega) = \min_{S \in \mathcal{S}_{k+1}} \max_{u \in S \setminus \{0\}} \frac{\int_{\Omega} |\nabla u|^2}{\int_{\Omega} u^2},$$

avec \mathcal{S}_k l'ensemble des sous espaces de dimension k dans $H^1(\Omega)$, on peut définir une notion de valeur propre généralisée pour une densité $\rho \in \mathbf{L}^1(\mathbb{R}, [0, 1])$ de la manière suivante :

$$\mu_k(\rho) := \inf_{S \in \mathcal{S}_{k+1}} \max_{u \in S \setminus \{0\}} \frac{\int_{\mathbb{R}^n} \rho |\nabla u|^2}{\int_{\mathbb{R}^n} \rho u^2}$$

où \mathcal{S}_k est cette fois l'ensemble des sous espaces de dimension k de

$$\{u \cdot 1_{\{\rho(x) > 0\}} : u \in C_c^\infty(\mathbb{R}^n)\}.$$

Si Ω est suffisamment régulier, on retrouve bien $\mu_k(\mathbf{1}_\Omega) = \mu_k(\Omega)$ pour tout $k \in \mathbb{N}$. Dans [33, 2019], cette généralisation a été motivée par le fait que l'optimisation dans la classe des densités était équivalente à l'optimisation dans la classe des domaines pour $k = 1$ et $k = 2$, c'est à dire que la densité optimale pour μ_1 (resp. μ_2) est l'indicatrice d'une boule (resp. de deux boules disjointes). Une question naturelle est de savoir si ce comportement perdure pour $k \geq 3$; en outre, il est désormais possible d'étudier la généralisation du problème original (1.2) en le substituant par

$$\max_{\int \rho = m} \mu_k(\rho) \tag{1.7}$$

ou $m > 0$. La valeur propre étant homogène (i.e. $\mu_k(t\Omega) = \frac{\mu_k(\Omega)}{t^2}$), on peut par ailleurs choisir $m = 1$. On note μ_k^* la valeur maximale de ce problème.

On donne en premier lieu un résultat d'existence dans \mathbb{R}^n :

Théorème 1.2.1. Pour tout k , le maximum de (1.7) est atteint. Plus précisément, il existe $j \in \mathbb{N}$, $j \leq k$, $\rho_1, \dots, \rho_j : \mathbb{R}^n \rightarrow [0, 1]$ et $n_1, \dots, n_j \in \mathbb{N}$ avec $n_1 + \dots + n_j = k + 1 - j$ tel que

$$\sum_{i=1}^j \int_{\mathbb{R}^n} \rho_i = 1 \quad \text{et} \quad \mu_k^* = \mu_{n_1}(\rho_1) = \dots = \mu_{n_j}(\rho_j).$$

Il faut noter que si on imposait que $\text{supp}(\rho) \subseteq U$ avec $|U| < \infty$, le résultat suivrait de manière (assez) élémentaire par la méthode directe du calcul des variations.

Dans ce nouveau cadre, le cas de la dimension 1 n'est plus évident. On montre le résultat suivant :

Théorème 1.2.2. Dans \mathbb{R} , $\forall k \in \mathbb{N}$

$$\mu_k^* = \pi^2 k^2.$$

L'égalité est atteinte lorsque ρ est la fonction caractéristique de l'union disjointe de k segments de longueur $1/k$.

Ce théorème implique que la généralisation naturelle de la conjecture de Pólya pour les densités en une dimension est vérifiée :

$$\forall k \in \mathbb{N}, \quad \mu_k(\rho) \leq \frac{\pi^2 k^2}{(\int_{\mathbb{R}} \rho)^2}.$$

On peut alors se questionner quant à la validité de la conjecture de Pólya en toute dimension pour les densités. On montre un résultat plus faible avec une constante non optimale qui généralise le Théorème 1.1.5 de Kröger :

Théorème 1.2.3. Soit $N \geq 2$, $\rho \in \mathbf{L}^1(\mathbb{R}^n, [0, 1])$, $\rho \not\equiv 0$. Alors

$$\forall k \in \mathbb{N}, \quad \mu_k(\rho) \leq \left(\frac{n+2}{2} \right)^{2/n} 4\pi^2 \left(\frac{k}{\omega_n \int_{\mathbb{R}^n} \rho} \right)^{2/n}.$$

Dans une dernière partie, on utilise la méthode des éléments finis pour calculer les valeurs propres généralisées associées aux densités afin de résoudre numériquement le Problème (1.7). Cependant, cette méthode ne permet pas directement de calculer des valeurs propres de densités qui ne soient pas associées à des problèmes elliptiques : nous allons montrer que nous pouvons asymptotiquement nous ramener à ce cas. Considérant une boîte de travail $D \subseteq \mathbb{R}^n$ (ouvert, borné) et $\rho : D \rightarrow [0, 1]$, on définit

$$\mu_k^\varepsilon(\rho) := \min_{S \in \mathcal{S}_{k+1}} \max_{u \in S \setminus \{0\}} \frac{\int_D (\rho + \varepsilon) |\nabla u|^2}{\int_D (\rho + \varepsilon^2) u^2}.$$

$\mu_k^\varepsilon(\rho)$ est alors la valeur propre associée au problème (bien posé) suivant

$$\begin{cases} -\text{div}[(\rho + \varepsilon) \nabla u] = \mu_k^\varepsilon(\rho) (\rho + \varepsilon^2) u \text{ on } D, \\ \partial_\nu u = 0 \text{ on } \partial D \end{cases} \quad (1.8)$$

et l'approximation est justifiée par

Proposition 1.2.1. Soit $0 < m < |D|$. Alors

$$\max_{\int_D \rho = m} \mu_k^\varepsilon(\rho) \xrightarrow{\varepsilon \rightarrow 0} \max_{\int_D \rho = m} \mu_k(\rho).$$

En pratique, l'optimisation repose sur une méthode de gradient. L'une des difficultés bien connue pour l'application d'une telle méthode est que la fonction $\rho \mapsto \mu_k^\varepsilon(\rho)$ n'est pas différentiable lorsque la valeur propre est multiple [50] [16]. Cependant, les maxima semblent atteints pour des valeurs propres de multiplicité plus grande que 2. Nous proposons dans ce chapitre une méthode heuristique d'optimisation de telles valeurs propres, en ajoutant la contrainte

$$\sum_{i=0}^{m_k-1} (\mu_{k+i}^\varepsilon(\rho) - \mu_k^\varepsilon(\rho))^2 = 0$$

durant l'optimisation, où m_k est la multiplicité supposée de $\mu_k^\varepsilon(\rho)$. Cette contrainte a pour but de forcer des valeurs propres proches à le rester. Une autre méthode, donnant de meilleurs résultats de stabilité pour l'optimisation des valeurs propres de densités définies sur la sphère, est présentée dans le Chapitre 5.

Les résultats pour les 8 premières valeurs propres non triviales sont donnés Figure 1.4.

On peut voir que contrairement aux deux premières valeurs propres, les densités optimales pour $k \geq 3$ ne semblent pas être la fonction caractéristique d'une forme. C'est un comportement que nous retrouverons pour certaines valeurs propres pour des densités définies sur la sphère et qui sera discutée dans le chapitre associé.

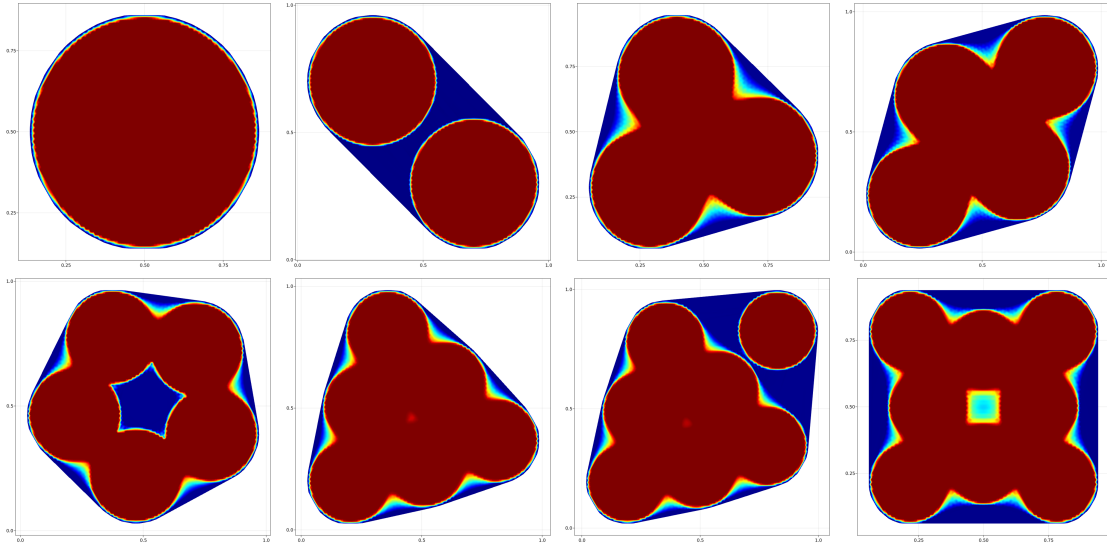


Figure 1.4: Approximation des huit premières densités optimales.

1.2.3 Chapitre 4 : Inégalités optimales pour les valeurs propres de Neumann sur la sphère

Ce chapitre est associé à l'article [34]. Alors que le problème d'optimisation des valeurs propres dans \mathbb{R}^n est essentiellement invariant par dilatation, ce n'est plus le cas pour un espace courbe. On peut donc s'attendre à des comportements différents de la part des domaines optimaux selon la valeur de la contrainte de mesure m . Dans ce chapitre, on aborde le problème d'optimisation de la seconde valeur propre non triviale de domaines de la sphère $\Omega \subseteq \mathbb{S}^n$. La contribution principale de cet article est la suivante :

Théorème 1.2.4. Soit $\Omega \subset \mathbb{S}^n$ un ouvert Lipschitz. Alors

$$\sum_{i=2}^n \frac{1}{\mu_i(\Omega)} \geq \sum_{i=2}^n \frac{1}{\mu_i(B^{|\Omega|/2} \sqcup B^{|\Omega|/2})} \left(= \frac{n-1}{\mu_1(B^{|\Omega|/2})} \right).$$

L'égalité est atteinte lorsque Ω est l'union disjointe de deux boules géodésiques de même mesure.

Ce théorème implique en particulier une borne supérieure sur la seconde valeur propre non triviale :

$$\mu_2(\Omega) \leq \mu_2(B^{\frac{|\Omega|}{2}} \sqcup B^{\frac{|\Omega|}{2}}) = \mu_1(B^{\frac{|\Omega|}{2}}).$$

La preuve est semblable au cas du plan [33], utilisant encore une fois un invariant topologique permettant de correctement construire des fonctions test orthogonales aux deux premières fonctions propres du domaine Ω . La difficulté principale pour établir le résultat provient du défaut d'unicité du "centre de masse de Weinberger" qui était un ingrédient indispensable tant dans le plan [33] que dans l'espace hyperbolique [58].

Remarquons qu'un tel résultat n'a pas encore été établi en toute généralité pour μ_1 . En effet, une première obstruction pour appliquer l'argument de transplantation de masse est de trouver une extension \mathbf{H}^1 des fonctions propres de $B^{|\Omega|}$ à la sphère \mathbb{S}^n . Une telle extension n'est pas triviale pour le cas de μ_1 , et les simulations faites au Chapitre 5 suggèrent qu'il ne s'agit pas d'une simple technicité. Cependant et de manière tout à fait surprenante, le précédent théorème permet une généralisation directe du théorème de Ashbaugh et Benguria [18], qui prend la forme suivante (on rappelle que dans le Théorème 1.1.7 de Ashbaugh et Benguria, la condition était $\Omega \subset \mathbb{S}_+^n$):

Corollaire 1.2.2. Soit $0 < m < |\mathbb{S}^n|$ et $\Omega \subset \mathbb{S}^n \setminus \mathbf{B}^m$ un ouvert Lipschitz tel que $|\Omega| = m$. Alors

$$\mu_1(\Omega) \leq \mu_1(\mathbf{B}^m).$$

Dans une dernière partie, on s'intéresse à l'optimisation dans la classe des densités, de manière similaire au cas du plan. En revenant sur le cas de μ_1 , on montre numériquement que l'indicatrice d'une boule n'est pas toujours optimale dans la classe des densités. En effet, pour $m = 6$, on exhibe une densité axisymétrique ρ^6 étant strictement meilleure que la valeur propre de la boule géodésique de même masse (voir Figure 1.5). Nous verrons dans le chapitre suivant que pour μ_1 et μ_3 , ce comportement est générique pour certaines plages de masses m .

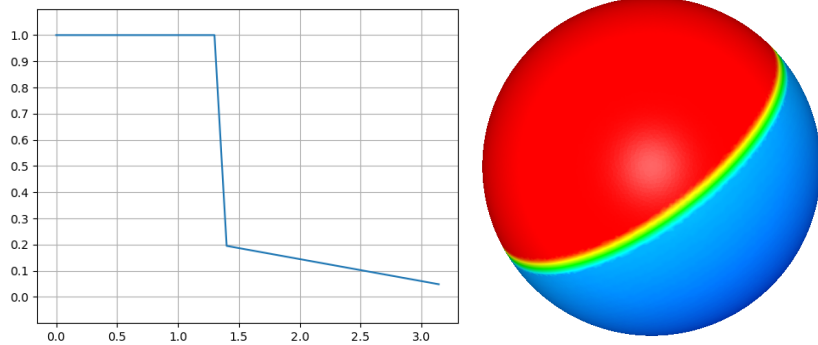


Figure 1.5: Graphe de ρ^6 comme une fonction de la latitude $\theta \in [0, \pi]$ (gauche) et sa représentation sur la sphère (droite).

1.2.4 Chapitre 5 : Optimisation numérique des valeurs propres de Neumann sur des domaines de la sphère

Ce chapitre, issu de [85], a une vocation purement expérimentale. Il a pour objectif d'explorer plus avant certaines questions soulevées par le précédent chapitre. On commence par montrer l'existence d'une densité optimale sur la sphère par la méthode directe du calcul des variations :

Théorème 1.2.5. Soit $0 \leq m \leq |\mathbb{S}^n|$. Alors le problème

$$\sup \left\{ \mu_k(\rho) \mid \rho : \mathbb{S}^n \rightarrow [0, 1], \int_{\mathbb{S}^n} \rho = m \right\}$$

possède une solution.

Remarque 1.2.6. Contrairement au cas de \mathbb{R}^n , on a ici l'existence d'une seule densité et non d'une collection de densités. En outre, une distinction fondamentale par rapport au cas de \mathbb{R}^n réside dans la dépendance de la densité/du domaine optimal par rapport à la masse totale m , l'homogénéité des valeurs propres étant perdue.

L'application de la méthode d'optimisation numérique utilisée dans le Chapitre 2, en imposant une proximité entre les valeurs propres multiples, s'est révélée infructueuse. Cette approche a conduit à la convergence vers des maxima locaux plutôt que vers un maximum global, en raison de la multiplicité des valeurs propres. Plusieurs autres méthodes ont été explorées, mais la méthode suivante s'est avérée la plus stable. L'idée sous-jacente consiste à régulariser le problème afin de le rendre différentiable. En supposant (ce qui est généralement vérifié en pratique) que $\mu_k^\varepsilon(\rho)$ reste toujours loin de $\mu_{k-1}^\varepsilon(\rho)$ pendant l'optimisation, et qu'il fait partie d'un ensemble $\mu_k^\varepsilon(\rho), \dots, \mu_{k+m_k-1}^\varepsilon(\rho)$ de valeurs propres "proches", nous avons alors naturellement :

$$\mu_k^\varepsilon(\rho) = \min \left\{ \mu_k^\varepsilon(\rho), \dots, \mu_{k+m_k-1}^\varepsilon(\rho) \right\}.$$

Pour $p > 0$ suffisamment grand, il est possible d'approcher le minimum d'un ensemble $\{x_0, \dots, x_{m_k-1}\}$ par :

$$\min \{x_0, \dots, x_{m_k-1}\} \approx \left(\sum_i x_i^{-p} \right)^{-1/p}.$$

Nous optimisons alors la fonction :

$$\rho \mapsto \left(\sum_i \mu_{k+i}^\varepsilon(\rho)^{-p} \right)^{-1/p},$$

qui est supposée être différentiable au voisinage de ρ si la multiplicité de $\mu_k(\rho)$ est effectivement m_k . En procédant à une approximation de $\mu_k(\rho)$ par une valeur propre bien définie $\mu_k^\varepsilon(\rho)$, nous optimisons ainsi les valeurs propres μ_1, μ_2 et μ_3 pour différentes valeurs de m . Quelques résultats de cette optimisation sont présentés dans la Figure 1.6.

On remarque que le cas de μ_2 est bien conforme à la théorie. Pour μ_1 , on remarque que pour m suffisamment grand, la boule n'est pas optimale. Cependant, une analyse un peu plus fine de ce cas permet de formuler la conjecture suivante :

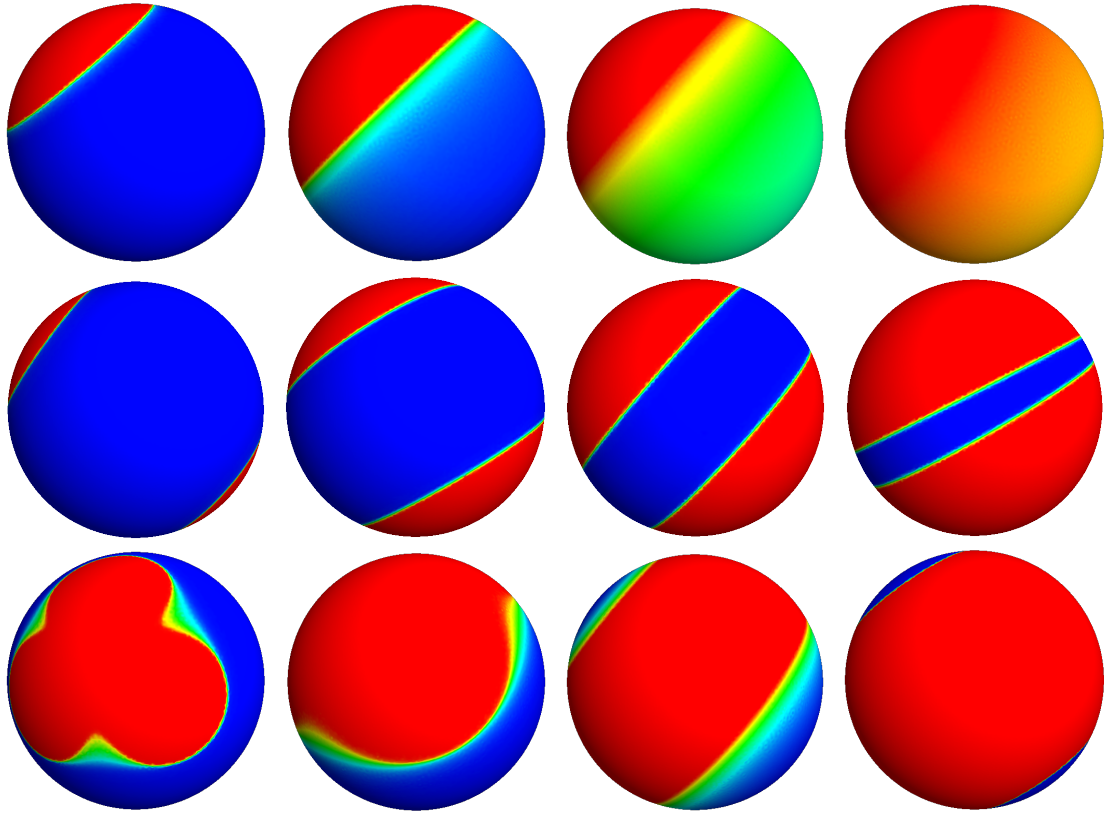


Figure 1.6: Exemples de densités optimales pour μ_1, μ_2, μ_3 (respectivement première, deuxième et troisième ligne) pour différentes valeurs de m .

Conjecture 1.2.3. Il existe $\delta > 0$ tel que pour tout $0 < m < \delta$ et tout $\rho : \mathbb{S}^n \rightarrow [0, 1]$, $\int_{\mathbb{S}^n} \rho = m$ on a

$$\mu_1(\rho) \leq \mu_1(\mathbf{B}^m).$$

Dans la deuxième partie du Chapitre 5, on considère l'optimisation de formes du problème

$$\sup \{ \mu_k(\Omega) : \Omega \subset \mathbb{S}^n, |\Omega| = m, \Omega \text{ ouvert, Lipschitz} \}.$$

L'optimisation fait appel à la méthode *level set*, qui consiste à représenter un domaine $\Omega(t)$ dépendant d'un temps fictif t par une fonction ϕ vérifiant

$$\forall x \in \mathbb{S}^n, \forall t \in [0, T], \begin{cases} \phi(t, x) < 0 & \text{if } x \in \Omega(t) \\ \phi(t, x) = 0 & \text{if } x \in \partial\Omega(t) \\ \phi(t, x) > 0 & \text{if } x \in \mathbb{S}^n \setminus \overline{\Omega(t)} \end{cases}.$$

Si $\Omega(t)$ évolue selon le flot d'un champ de vecteurs $V : \mathbb{S}^n \rightarrow T\mathbb{S}^n$ alors il est équivalent de faire évoluer ϕ selon l'équation

$$\partial_t \phi(t, x) + V(x) \cdot \nabla \phi(t, x) = 0.$$

Le choix d'un champ de vecteurs V qui fasse localement augmenter $\mu_k(\Omega(t))$ fait appel à la notion de dérivée de forme de μ_k . On peut encore une fois utiliser un algorithme de gradient pour trouver les optima des trois premières valeurs propres dont des exemples sont donnés Figure 1.7.

On remarque immédiatement que pour de grandes valeurs de m , μ_1 exhibe un comportement singulier, cherchant à remplir une calotte et à compléter le reste de la sphère par une calotte criblée de trous. On ne peut donc pas espérer montrer un résultat analogue à Langford et Laugesen [76] en l'absence de l'hypothèse de simple connexité.

Remarque 1.2.7. Pour l'optimisation de μ_1 dans la classe des densités, la boule semble bien être optimale pour toute masse $0 < m < \delta$ avec $\delta \approx 4.5$. Pour l'optimisation dans la classe des domaines, cela semble

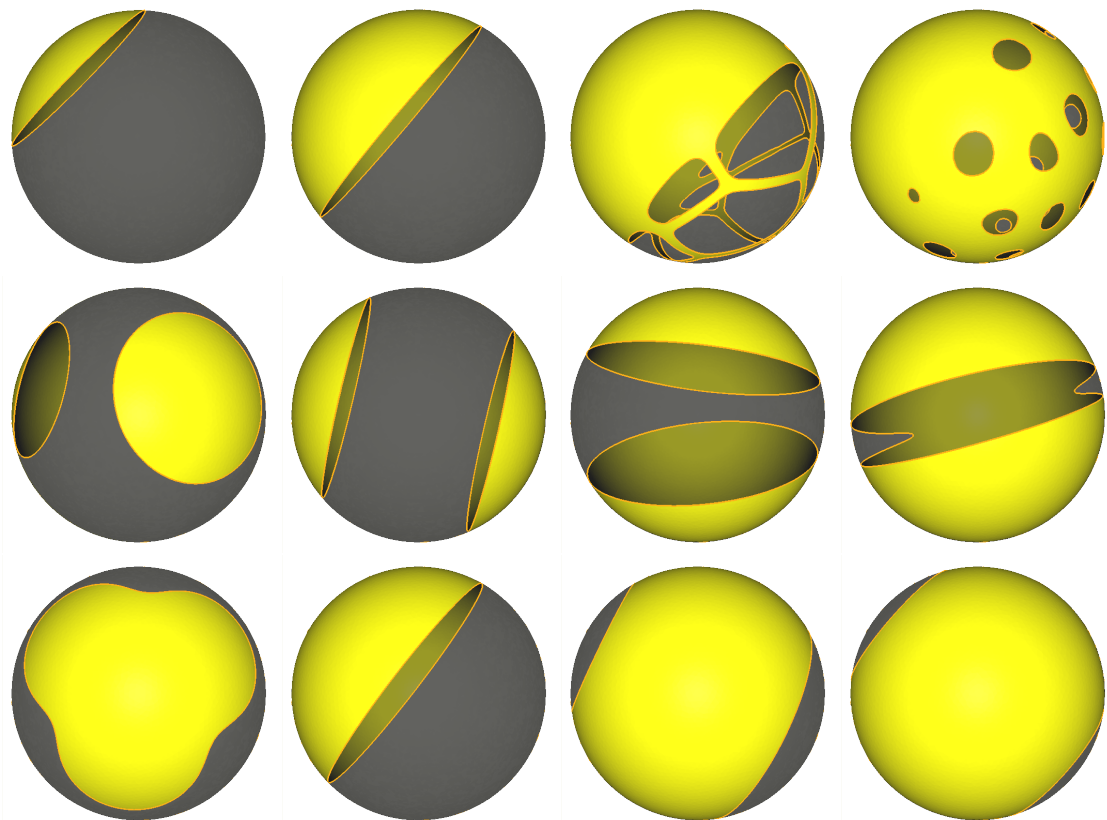


Figure 1.7: Exemples de domaines optimaux pour μ_1, μ_2, μ_3 (respectivement première, deuxième et troisième ligne) pour différentes valeurs de m .

vrai pour $0 < m < \delta' \approx 8$. Or, nous avons vu précédemment l'argument de transplantation de masse de Weinberger : il se trouve que cet argument est encore valide dans la classe des densités. Ainsi tous les résultats prouvés par un argument de ce type pour les domaines doivent être vrais pour les densités (sur ce point, voir [33]). Il ne faut donc pas espérer pouvoir prouver l'optimalité de la boule pour $\delta < m < \delta'$ par transplantation de masse, bien que cela puisse être possible pour $0 < m < \delta$.

Pour $m > \delta'$, l'optimisation en domaines semble aussi vouloir homogénéiser en créant un grand nombre de trous, ce qui pourrait laisser penser à la non-existence d'un domaine optimal.

Notons que ces arguments sont aussi valides dans le plan pour les valeurs propres où la densité optimale n'est pas un domaine; il sera donc nécessaire de développer de nouveaux outils pour traiter théoriquement tous ces cas. Une piste dans ce sens pourrait être celle de l'optimisation périodique (voir par exemple [7]).

Enfin, dans une dernière partie, on utilise les outils développés pour la sphère pour mener la même analyse sur un tore $\mathbb{T} \subseteq \mathbb{R}^3$.

1

Introduction (English version)

In this manuscript, we will address optimization problems of eigenvalues of the Laplace operator under measure constraint. Throughout, Ω will denote a bounded domain in \mathbb{S}^n or \mathbb{R}^n satisfying certain regularity assumptions, and $|\Omega|$ represents its measure. A real number μ is said to be an eigenvalue of the Laplace operator with Neumann conditions if there exists a function $u \in \mathbf{H}^1(\Omega) \setminus \{0\}$, called an eigenfunction, such that

$$\begin{cases} -\Delta u = \mu u & \text{in } \Omega, \\ \partial_\nu u = 0 & \text{on } \partial\Omega. \end{cases} \quad (1.1)$$

Here, Δ represents the Laplace (resp. Laplace-Beltrami) operator in \mathbb{R}^n (resp. \mathbb{S}^n) and $\partial_\nu u$ is the normal derivative of u on the boundary of Ω . Taking the multiplicities into account, the eigenvalues of such a problem form a sequence satisfying

$$0 = \mu_0(\Omega) \leq \mu_1(\Omega) \leq \dots \leq \mu_k(\Omega) \leq \dots \rightarrow \infty.$$

A related problem is the eigenvalue problem with Dirichlet conditions given by

$$\begin{cases} -\Delta u = \lambda u & \text{in } \Omega, \\ u = 0 & \text{on } \partial\Omega. \end{cases}$$

which also possesses a spectrum of eigenvalues

$$0 < \lambda_1(\Omega) \leq \lambda_2(\Omega) \leq \dots \leq \lambda_k(\Omega) \leq \dots \rightarrow \infty.$$

We will primarily focus on the maximization of eigenvalues with Neumann conditions. Formally, the considered problems take the form

$$\max_{|\Omega|=m} \mu_k(\Omega), \quad (1.2)$$

where $m > 0$ and $\Omega \subset \mathbb{R}^n$ or $\Omega \subset \mathbb{S}^n$.

Optimization problems involving the shape of domains and the solution of partial differential equations with Neumann conditions naturally arise in various mathematical models, including structural mechanics, image analysis, biology, and more. The mathematical analysis of such problems is generally a challenging task due to the absence of a boundary energy that controls the interactions between the domain's geometry and the solution of the partial differential equation. Unlike Robin conditions, which possess such an energy, the absence of it in the Neumann case presents serious difficulties. In certain situations (e.g., crack propagation models or the study of the Mumford-Shah functional), a penalization of the boundary length is naturally present and regularizes the problem. However, this is not the case for the Neumann problem (1.2).

The objective of this thesis is to study the theoretical aspects related to these problems, supported by numerical simulations.

1.1 Key previous results

1.1.1 Optimization in domains of \mathbb{R}^n

The theoretical study of spectral shape optimization problems dates back to the early 20th century. The prototype of such a problem is the Faber-Krahn inequality [53, 1925] [72, 1925], confirming a conjecture by Lord Rayleigh stating that among membranes of given area, the one with the smallest fundamental frequency is the disk:

Theorem 1.1.1 (Faber-Krahn). *Let $\Omega \subset \mathbb{R}^n$ be an open set with $|\Omega| = 1$. Then*

$$\lambda_1(\Omega) \geq \lambda_1(\mathbf{B}^{|\Omega|}),$$

where $\mathbf{B}^{|\Omega|}$ is a ball of measure $|\Omega|$.

It took about thirty years before a similar result was obtained for the first nontrivial Neumann eigenvalue. In [71, 1952], Kornhauser and Stackgold showed by a perturbation argument that under the assumption that an optimal set exists, μ_1 must be optimal on the ball. Such a result was first proved by Szegő for smooth simply connected open sets in \mathbb{R}^2 [98, 1954], and then in full generality by Weinberger [102, 1956]:

Theorem 1.1.2 (Weinberger). *Let $\Omega \subset \mathbb{R}^n$ be a bounded Lipschitz domain. Then*

$$\mu_1(\Omega) \leq \mu_1(\mathbf{B}^{|\Omega|}).$$

A naturally arising question is then to determine, if it exists, a domain that maximizes higher-order eigenvalues. While the question of existence remains open in general, it is now known that the domain maximizing the second non-trivial eigenvalue μ_2 is the disjoint union of two balls of equal measure. This result was first proved for smooth, simply connected domains in \mathbb{R}^2 by Girouard, Nadirashvili, and Polterovich [60, 2009], and then in full generality by Bucur and Henrot [33, 2019]:

Theorem 1.1.3 (Bucur-Henrot). *Let Ω be a bounded Lipschitz open set in \mathbb{R}^n . Then*

$$\mu_2(\Omega) \leq \mu_2(\mathbf{B}^{|\Omega|/2} \sqcup \mathbf{B}^{|\Omega|/2})$$

where $\mathbf{B}^{|\Omega|/2} \sqcup \mathbf{B}^{|\Omega|/2}$ is the disjoint union of two balls of measure $|\Omega|/2$.

To be precise, this theorem remains valid in a much broader framework than domains, namely a framework where it is possible to define eigenvalues for *densities*. We will come back to this a little later.

The problem of optimizing the eigenvalues of the Laplacian is closely related to the *Pólya Conjecture*. This conjecture states that the leading term of the Weyl's asymptotic formula [104]

$$\mu_k(\Omega) \sim 4\pi^2 \left(\frac{k}{\omega_n |\Omega|} \right)^{2/n} \quad \text{as } k \rightarrow \infty$$

(where ω_n is the volume of the unit ball in \mathbb{R}^n) is actually an upper bound for the Neumann eigenvalues, i.e.,

Conjecture 1.1.4 (Pólya). *For any $k \in \mathbb{N}^*$, $\mu_k(\Omega) \leq 4\pi^2 \left(\frac{k}{\omega_n |\Omega|} \right)^{2/n}$.*

While the previous theorems tell us that this conjecture is true for $k = 1$ and 2 , it remains completely open for all $n \geq 2$ and $k \geq 3$. However, a result supporting the conjecture has been provided by Kröger [75, 1992]:

Theorem 1.1.5 (Kröger). *For any $k \in \mathbb{N}^*$,*

$$\mu_k(\Omega) \leq \left(\frac{n+2}{2} \right)^{2/n} 4\pi^2 \left(\frac{k}{\omega_n |\Omega|} \right)^{2/n}.$$

Although not the focus of this thesis, an important aspect of shape optimization problems is the issue of *stability*. For the Neumann eigenvalues, stability refers to the question of whether the proximity of $\mu_k(\Omega)$ to $\mu_k(\Omega^*)$, where Ω^* denotes the maximizer of (1.2), implies the proximity in a certain sense of Ω and Ω^* . For μ_1 , we indeed have the following stability result, established by Brasco and Pratelli [31, 2012]:

Theorem 1.1.6 (Brasco-Pratelli).

$$\mu_1(\mathbf{B}^{|\Omega|}) - \mu_1(\Omega) \geq \mu_1(\mathbf{B}^{|\Omega|}) c_n \mathcal{A}(\Omega)^2$$

where

$$\mathcal{A}(\Omega) = \inf \left\{ \frac{|\Omega \Delta B|}{|\Omega|} : B \text{ is a ball and } |B| = |\Omega| \right\}$$

denotes the *Fraenkel asymmetry* of Ω , and c_n is a dimensional constant.

1.1.2 Optimization for domains on the sphere

Another aspect of this thesis is the optimization of Neumann eigenvalues on manifolds, particularly on certain domains in the sphere $\Omega \subset \mathbb{S}^n \subset \mathbb{R}^{n+1}$. We still consider the problem (1.1), where Δ denotes the Laplace-Beltrami operator on \mathbb{S}^n . Results generalizing the Weinberger theorem exist in the literature. For example, in hyperbolic space, Ashbaugh and Benguria proved that the maximizer for μ_1 is always the (geodesic) ball [18, 1995]. Similarly, Freitas and Laugesen showed that the maximizer for μ_2 is always the disjoint union of two balls with equal measure [56, 2020]. In both cases, the result holds in any dimension, and the proofs once again rely on strong topological arguments. However, surprisingly, no comprehensive results had been established for domains on \mathbb{S}^n . The first step in this direction is found in the same article [18, 1995] where Ashbaugh and Benguria prove, using a method similar to Weinberger's, the following theorem:

Theorem 1.1.7 (Ashbaugh-Benguria). *Let*

$$\mathbb{S}_+^n = \{(x_1, \dots, x_{n+1}) \in \mathbb{R}^{n+1} \mid x_1^2 + \dots + x_{n+1}^2 = 1 \text{ and } x_{n+1} > 0\}$$

and consider the set of domains $\Omega \subset \mathbb{S}_+^n$. Then

$$\mu_1(\Omega) \leq \mu_1(\mathbf{B}^{|\Omega|}),$$

where $\mathbf{B}^{|\Omega|}$ is a geodesic ball of measure $|\Omega|$.

The condition - which is very strong - for Ω to belong to a hemisphere implies, among other things, that $|\Omega| \leq \frac{|\mathbb{S}^n|}{2}$. One could wonder if this measure constraint alone would be sufficient to guarantee the result.

Recently, Langford and Laugesen [76, 2022] proved the following result in \mathbb{S}^2 , extending a previous result by Bandle [21, 1972]:

Theorem 1.1.8 (Langford-Laugesen). *Let $\Omega \subset \mathbb{S}^2$ be a simply connected domain such that $0 < |\Omega| < 0.94|\mathbb{S}^2|$. Then*

$$\mu_1(\Omega) \leq \mu_1(\mathbf{B}^{|\Omega|}).$$

They have thus replaced Ashbaugh and Benguria's condition with another strong assumption on the dimension and topology of the domains.

1.1.3 Behavior of Neumann Eigenvalues

It is well-known that Dirichlet eigenvalues exhibit greater stability than Neumann eigenvalues with respect to the geometry of the domain. For instance, if $\Omega_1 \subseteq \Omega_2$, then for any $k \in \mathbb{N}$, $\lambda_k(\Omega_1) \geq \lambda_k(\Omega_2)$. This relationship is not satisfied for Neumann eigenvalues. In particular, let us consider the sequence of "thickened" spirals with n turns given by

$$\Omega_n := \bigcup_{p \in \mathcal{S}_n} \mathcal{B}_{p, \frac{1}{2n}},$$

where

$$\mathcal{S}_n := \{(r \cos(2\pi nr), r \sin(2\pi nr)) \in \mathbb{R}^2 \mid r \in [0, 1]\}$$

and $\mathcal{B}_{p,r}$ denotes the ball centered at p with radius r . Figure 1.1 provides a representation of \mathcal{S}_4 and \mathcal{S}_{16} . It can be shown that $\Omega_n \subseteq \mathcal{B}_{0,2}$ for all $n > 0$, and $\mu_k(\Omega_n) \xrightarrow{n \rightarrow \infty} 0$. This lack of monotonicity notably prevents the use of a general existence result such as the Buttazzo-Dal Maso theorem [37, 1993], which deduces the existence of optimal domains for domains contained in a fixed bounded open set.

Another important property of Dirichlet eigenvalues is that if two domains Ω_1 and Ω_2 are "close" in a certain sense, then the eigenvalues $\lambda_k(\Omega_1)$ and $\lambda_k(\Omega_2)$ are also close. In this regard, we have, for example, the theorem of Šverák [107]:

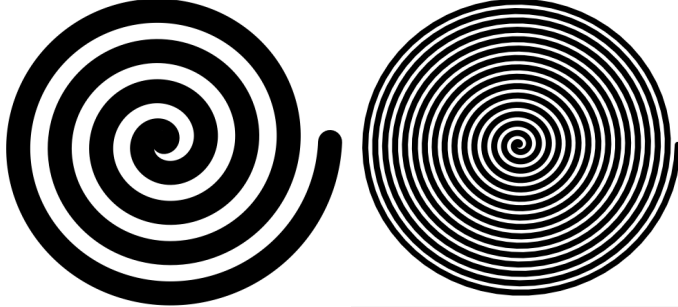


Figure 1.1: Representation of \mathcal{S}_4 (left) and \mathcal{S}_{16} (right).

Theorem 1.1.9 (Šverák). *Let $B \subseteq \mathbb{R}^2$ be a compact set and $(\Omega_n)_{n \geq 0}$ be a sequence of open sets in B that converges to an open set Ω in the sense of the Hausdorff distance of the complements. Suppose that the number of connected components of $B \setminus \Omega_n$ is uniformly bounded. Then, for all $k > 0$,*

$$\lambda_k(\Omega_n) \rightarrow \lambda_k(\Omega).$$

This property fails for Neumann eigenvalues. The classical example describing this type of behavior is depicted in Figure 1.2. It can be shown that the Dirichlet eigenvalues of such a set Ω_ε converge to those of

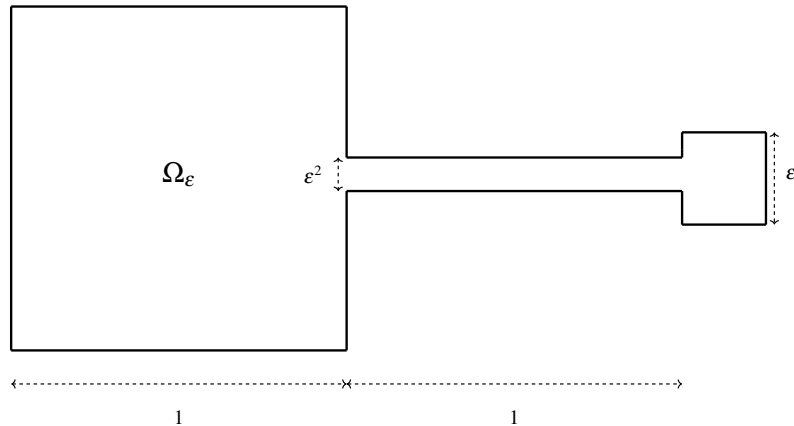


Figure 1.2: Set Ω_ε consisting in the union of the unit square and a square of size ε linked by a thin rectangle of height ε^2 .

the unit square, while $\mu_1(\Omega_\varepsilon) \xrightarrow[\varepsilon \rightarrow 0]{} 0 \neq \mu_1((0, 1)^2)$.

In fact, the assumptions of Šverák's theorem demonstrate that Ω_n converges to Ω in the sense of γ -convergence, which in turn implies the norm convergence of the resolvent operators and hence convergence of the eigenvalues. However, in the case of Neumann eigenvalues, Šverák's assumptions do not lead to such convergence of the resolvent operators. Nevertheless, a result of upper semicontinuity can be obtained, see [32, Th. 7.4.7].

Another particularly pathological case is that of the "comb" shape, which can be found, for example, in [22] and illustrated in Figure 1.3. Indeed, if we denote Ω_n as the comb with n teeth created from the square $D = (-1, 1)^2$, where $\omega = (-1, 1) \times (-1, 0)$ is the solid part and each "tooth" has a width of $1/n$, we can formally write that $\mu_k(\Omega_n)$ tends to the k -th eigenvalue of the degenerate problem

$$\inf_{S \in \mathcal{S}_{k+1}} \max_{u \in S \setminus \{0\}} \frac{\int_{\omega} |\nabla u|^2 + \frac{1}{2} \int_{D \setminus \omega} |\partial_y u|^2}{\int_{\omega} u^2 + \frac{1}{2} \int_{D \setminus \omega} u^2}$$

where \mathcal{S}_k is the set of k -dimensional subspaces of $\mathbf{H}^1(D)$. In this case, it can be observed that the eigenfunctions are mainly supported on the teeth of the comb.

Despite these behaviors, continuity of the Neumann eigenvalues with respect to the Hausdorff distance can still be obtained by imposing sufficiently strong geometric assumptions on the domains. Indeed, con-

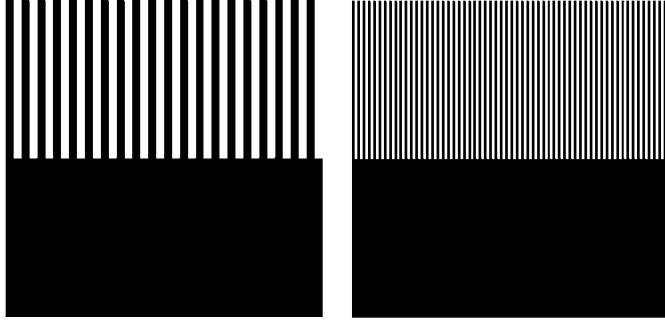


Figure 1.3: Example of a comb-shaped domain with 20 (left) and 60 teeth (right).

sider the Poisson-type problem

$$\begin{cases} -\Delta u_n + u_n = f \text{ in } \Omega_n \\ \partial_\nu u_n = 0 \text{ on } \partial\Omega_n \end{cases}, \quad (1.3)$$

where $(\Omega_n)_{n \geq 0}$ is a family of open sets contained in the same compact $B \subseteq \mathbb{R}^n$, and $f \in \mathbf{L}^2(B)$. A result by Chenais [42] allows us to construct uniformly bounded extension operators from $\mathbf{H}^1(\Omega)$ to $\mathbf{H}^1(B)$, which in turn leads to the following continuity property:

Theorem 1.1.10. *Let $B \subseteq \mathbb{R}^n$ be a compact set, and $(\Omega_n)_{n \geq 0}$ be a sequence of open sets in B converging to an open set Ω in the sense of the Hausdorff distance. Under the assumption that the Ω_n satisfy the uniform ε -cone property (see, for example, [67, Def. 2.4.1]), then for all $k \geq 0$,*

$$\mu_k(\Omega_n) \rightarrow \mu_k(\Omega).$$

Still for problems of the type (1.3), we can mention the result by Chambolle and Doveri [40]. If $\Omega_n \rightarrow \Omega$ in the sense of the Hausdorff distance, the authors establish the convergence of the solutions u_n to the solution u of (1.3) on Ω under the constraint of perimeter and connectivity of $\partial\Omega_n$. In [36], Bucur and Varchon prove a similar result under the constraint of measure and uniform bound on the connected components of $\partial\Omega_n$. Finally, in Chapter 2, we present a result on the continuity of Neumann eigenvalues for sufficiently smooth deformations of a reference domain. For more information on these issues, we refer the reader to [64, Chap. 2].

1.1.4 The Weinberger argument

The proof by Weinberger, which originated a wide range of results concerning the optimization of Neumann eigenvalues, will be presented here, outlining its main ideas. If the reader is not entirely familiar with the tools used in this proof, we refer them to Chapter 2.

Let $\Omega \subset \mathbb{R}^n$ be a bounded Lipschitz domain. First, let us recall that the first nontrivial eigenvalue of the Neumann problem can be expressed in the variational form:

$$\mu_1(\Omega) = \min_{v \in \mathbf{H}^1(\Omega) \setminus \{0\}, \int_\Omega v = 0} \frac{\int_\Omega |\nabla v|^2}{\int_\Omega v^2}, \quad (1.4)$$

thanks to the Courant-Fisher formula. Weinberger's idea is to use extensions of the eigenfunctions of the ball $\mathbf{B}^{|\Omega|}$ (centered at the origin) as test functions in (1.4). The core of the proof (and the main difficulty for its adaptation to higher-order eigenvalues) lies in showing that these functions can satisfy the condition $\int_\Omega v = 0$ by suitably translating Ω .

Let R be the radius of $\mathbf{B}^{|\Omega|}$. It can be shown that the eigenfunctions associated with $\mu_1(\mathbf{B}^{|\Omega|})$ are given by

$$x \mapsto \frac{g(|x|)}{|x|} x_i, \quad i \in \{1, \dots, n\},$$

where $g : (0, R) \rightarrow \mathbb{R}$ is the solution of the differential equation

$$\begin{cases} g''(r) + \frac{n-1}{r} g'(r) + \left(\mu_1(\mathbf{B}^{|\Omega|}) - \frac{n-1}{r^2} \right) g(r) = 0 \\ g(0) = 0 \\ g'(R) = 0 \end{cases}. \quad (1.5)$$

This equation is obtained by separating variables in spherical coordinates, and the solution g is the second-kind Bessel function, sometimes denoted as J_1 . Now, let us define

$$\tilde{g}(r) = \begin{cases} g(r) & \text{if } r \leq R \\ g(R) & \text{if } r \geq R \end{cases}$$

and for each $i \in \{1, \dots, n\}$,

$$G_i(x) = \frac{\tilde{g}(|x|)}{|x|} x_i.$$

In line with what was mentioned earlier, assume that we have

$$\int_{\Omega} G_i(x) dx = 0, \quad i \in \{1, \dots, n\}. \quad (1.6)$$

This condition will be proven below. Under this assumption, each G_i is a test function in (1.4), and thus:

$$\mu_1(\Omega) \leq \frac{\int_{\Omega} \frac{\tilde{g}'(|x|)^2}{|x|^2} x_i^2 + \frac{\tilde{g}(|x|)^2}{|x|^2} \left(1 - \frac{x_i^2}{|x|^2}\right) dx}{\int_{\Omega} \frac{\tilde{g}(|x|)^2}{|x|^2} x_i^2 dx}.$$

Summing over i , we obtain:

$$\mu_1(\Omega) \leq \frac{\int_{\Omega} \tilde{g}'(|x|)^2 + \frac{n-1}{|x|^2} \tilde{g}(|x|)^2 dx}{\int_{\Omega} \tilde{g}(|x|)^2 dx}.$$

By studying the variations of the integrands in the numerator and denominator, we can observe that:

- The function $r \mapsto \tilde{g}^2(r)$ is increasing since $g(0) = 0$ and $g'(R)$ is the first zero of g' .
- The function $r \mapsto \tilde{g}'(r)^2 + \frac{n-1}{r^2} \tilde{g}(r)^2$ is decreasing. Indeed, the function is constant if $r \geq R$. Otherwise,

$$\begin{aligned} \frac{d}{dr} \left(\tilde{g}'(r)^2 + \frac{n-1}{r^2} \tilde{g}(r)^2 \right) &= 2\tilde{g}'\tilde{g}'' + 2\frac{n-1}{r^3}(r\tilde{g}\tilde{g}' - \tilde{g}^2) \\ &= -2\mu_1(\mathbf{B}^{|\Omega|})gg' - \frac{n-1}{r^3}(rg' - g)^2 \\ &\leq 0 \end{aligned}$$

where we used (1.5) in the last equality.

Thus,

$$\int_{\Omega} \tilde{g}^2 = \int_{\Omega \cap \mathbf{B}^{|\Omega|}} \tilde{g}^2 + \int_{\Omega \setminus \mathbf{B}^{|\Omega|}} \tilde{g}^2 = \int_{\Omega \cap \mathbf{B}^{|\Omega|}} \tilde{g}^2 + \tilde{g}^2(R)|\Omega \setminus \mathbf{B}^{|\Omega|}|$$

on one hand, and

$$\int_{\mathbf{B}^{|\Omega|}} \tilde{g}^2 = \int_{\Omega \cap \mathbf{B}^{|\Omega|}} \tilde{g}^2 + \int_{\mathbf{B}^{|\Omega|} \setminus \Omega} \tilde{g}^2 \leq \int_{\Omega \cap \mathbf{B}^{|\Omega|}} \tilde{g}^2 + \tilde{g}^2(R)|\mathbf{B}^{|\Omega|} \setminus \Omega|.$$

But since $|\Omega| = |\mathbf{B}^{|\Omega|}|$, we have $|\mathbf{B}^{|\Omega|} \setminus \Omega| = |\Omega \setminus \mathbf{B}^{|\Omega|}|$, and therefore,

$$\int_{\mathbf{B}^{|\Omega|}} \tilde{g}(|x|)^2 \leq \int_{\Omega} \tilde{g}(|x|)^2.$$

By performing the same computations for the numerator, we obtain

$$\int_{\mathbf{B}^{|\Omega|}} \tilde{g}'(|x|)^2 + \frac{n-1}{|x|^2} \tilde{g}(|x|)^2 \geq \int_{\Omega} \tilde{g}'(|x|)^2 + \frac{n-1}{|x|^2} \tilde{g}(|x|)^2,$$

which finally gives us

$$\mu_1(\Omega) \leq \mu_1(\mathbf{B}^{|\Omega|}).$$

Remark 1.1.11. *The principle of transferring the entire mass of Ω to $\mathbf{B}^{|\Omega|}$ is sometimes referred to as "mass transplantation" in the literature [55] [33] [56]. Indeed, we can formally see that transferring mass from $x \in \Omega \setminus \mathbf{B}^{|\Omega|}$ to $x' \in \mathbf{B}^{|\Omega|} \setminus \Omega$ can only increase the Rayleigh quotient. This nomenclature is an analogy to "conformal transplantation" used, in particular, in Szegő's proof, where the eigenfunctions of the domain Ω are transferred to the disk through a conformal mapping.*

Now we need to prove the orthogonality condition (1.6). This type of condition is found in both Weinberger's proof, where he invokes Brouwer's fixed-point theorem, and in Szegö's proof, which uses the winding number of a curve in the complex plane. However, it was noticed in [33] for the proof of Theorem 1.1.3 that such an argument was insufficient for higher-order eigenvalues. Indeed, the Rayleigh quotient for $\mu_2(\Omega)$ becomes:

$$\mu_2(\Omega) = \min \frac{\int_{\Omega} |\nabla v|^2}{\int_{\Omega} v^2},$$

where the minimum is taken over all functions $v \in \mathcal{H}^1(\Omega) \setminus \{0\}$ satisfying the conditions:

$$\int_{\Omega} v = 0 \quad \text{and} \quad \int_{\Omega} vu_1 = 0,$$

where u_1 is the eigenfunction associated with $\mu_1(\Omega)$. The more general notion used by the authors is the *topological degree*, which in certain cases allows for easy determination of whether an equation of the form $f(x) = 0$ has a solution. Since this will be useful in Chapter 3, we recall here the relevant properties, which can be found in [93]:

Definition 1.1.12 (Degree of a C^1 mapping). *Let $\varphi : \overline{\Omega} \rightarrow \mathbb{R}^n$ be a C^1 mapping. We assume that 0 is a regular value of φ (i.e. $\text{Jac}_{\varphi}(x) \neq 0$ for all $x \in \Omega$ where $\varphi(x) = 0$ and $\text{Jac}_{\varphi}(x)$ is the Jacobian determinant of φ) such that $0 \notin \varphi(\partial\Omega)$. The degree of φ is defined by:*

$$\deg_{\Omega} \varphi := \sum_{x \in \Omega, \varphi(x)=0} \text{sign}(\text{Jac}_{\varphi}(x)).$$

Thanks to the Sard's theorem and the density of C^1 functions in the space of continuous functions, we can extend the degree to a mapping $\deg_{\Omega} : C^0(\overline{\Omega}, \mathbb{R}^n) \rightarrow \mathbb{Z}$. As defined, the degree of a continuous mapping always satisfies:

$$\deg_{\Omega} \varphi \neq 0 \implies \exists x \in \Omega, \varphi(x) = 0,$$

which makes it useful in existence theorems. Moreover, we have the following property, indicating that the degree is invariant under homotopy as long as no zero crosses the boundary $\partial\Omega$:

Proposition 1.1.13. *Let $h : [0, 1] \times \overline{\Omega} \rightarrow \mathbb{R}^n$ such that for all $t \in [0, 1]$, $h(t, \cdot) \in C^0(\overline{\Omega}, \mathbb{R}^n)$ and the mapping $t \mapsto h(t, \cdot)$ is continuous for the uniform topology. Suppose that for all $t \in [0, 1]$, $0 \notin h(t, \partial\Omega)$. Then:*

$$\deg_{\Omega} h(0, \cdot) = \deg_{\Omega} h(1, \cdot).$$

To complete Weinberger's proof, we will use the following result:

Proposition 1.1.14. *Let $\mathbf{B} \in \mathbb{R}^n$ be a ball centered at the origin, and $\varphi : \mathbf{B} \rightarrow \mathbb{R}^n$ be a function such that $\varphi(p) \cdot p \leq 0$ and $\varphi(p) \neq 0$ for all $p \in \partial\mathbf{B}$. Then:*

$$\deg_{\mathbf{B}} \varphi = (-1)^n.$$

Proof. We set $h(t, p) = (1-t)\varphi(p) - tp$ for $t \in [0, 1]$ and $p \in \mathbf{B}$. Then $\deg_{\mathbf{B}} h(0, \cdot) = \deg_{\mathbf{B}} \varphi$, and

$$\deg_{\mathbf{B}} h(1, \cdot) = \deg_{\mathbf{B}}(-\text{id}) = \text{sign}(\text{Jac}_{-\text{id}}(0)) = (-1)^n.$$

By the invariance of the degree under homotopy, we conclude that $\deg_{\mathbf{B}} \varphi = (-1)^n$. □

We can now use this new tool to complete the proof. Let $\mathbf{B} \supset \Omega$ be a ball centered at the origin, and define the function $\varphi : \mathbf{B} \rightarrow \mathbb{R}^n$ by

$$\varphi(p) = \int_{\Omega} G(x-p) dx,$$

where $G(x) = (G_i(x))_{1 \leq i \leq n}$. We want to find $p^* \in \mathbf{B}$ such that $\varphi(p^*) = 0$ using the previous proposition. Since the eigenvalue problem is translation invariant, we can choose p^* as the new origin, justifying (1.6). If there exists $p^* \in \partial\mathbf{B}$ such that $\varphi(p^*) = 0$, then we are done. Otherwise, we observe that

$$\begin{aligned} \varphi(p) \cdot p &= \left(\int_{\Omega} G(x-p) dx \right) \cdot p \\ &= \int_{\Omega} \underbrace{\frac{\tilde{g}(|x-p|)}{|x-p|}}_{\geq 0} \underbrace{(x-p) \cdot p}_{\leq 0} dx \leq 0. \end{aligned}$$

Thus, $\deg_{\mathbf{B}} \varphi = (-1)^n \neq 0$, and there exists p^* such that $\varphi(p^*) = 0$. □

1.1.5 Numerical Study of Eigenvalue Problems

As we have seen, the theoretical study of spectral shape optimization problems is a challenging task. In some cases, it may be sufficient to find an approximation of the optimum; therefore, over the past thirty years, numerical optimization of eigenvalue problems has received increasing attention, driven by the growing computational capabilities of computers. From an industrial perspective, this applies notably to optimization problems in vibrating structures [84] [4] [50] [83] [59], photonic crystals [46] [69] [79], or fluid problems [88], [81]. In this context, a wide variety of methods have been used, such as domain variation, level set methods, phase field-like methods, or homogenization methods. The latter has become a standard in shape optimization problems in elasticity and conductivity [5].

Another interest in numerical optimization of eigenvalue problems lies in its exploratory use, particularly in cases where the theory is still incomplete. This allows delegating some of the necessary intuition to the machine, which can be beneficial for mathematicians. For example, in [89], the author deals with the optimization of the first Dirichlet eigenvalues in \mathbb{R}^2 under volume constraints. These numerical simulations helped refute Troesch's conjecture [99], which postulated that a stadium-shaped domain would maximize the second Dirichlet eigenvalue. This conjecture was ultimately disproven in [66], although it is worth noting that Troesch formulated it based on numerical computations himself. For Dirichlet eigenvalues, similar simulations can be conducted in \mathbb{R}^3 [13] or \mathbb{R}^4 [15], or under other constraints such as convexity constraints [11] or planar partition problems [30]. Moreover, there are computations for optimizing eigenvalues with Neumann conditions [16] [9], Steklov conditions [29] [12], Robin conditions [14] [17], or even Wentzell conditions [27]. This list, though not exhaustive, demonstrates the growing interest in the numerical approach to theoretical questions related to spectral optimization.

1.2 Thesis structure

This thesis will focus on the optimization of eigenvalues of the Laplacian with Neumann conditions. A strong emphasis will be placed on numerical exploration. Therefore, the first chapter, although not providing original contributions, serves as a reminder of numerical optimization of eigenvalues. In the second chapter, titled *Maximization of Neumann eigenvalues in a class of densities*, we focus on the optimization of eigenvalues of "densities" that generalize eigenvalues of domains in \mathbb{R}^n . The third chapter, *Sharp inequalities for Neumann eigenvalues on the sphere*, addresses the maximization of μ_2 for domains on the entire sphere, including a generalization of the Ashbaugh-Benguria theorem. In the fourth chapter, *Numerical optimization of Neumann eigenvalues on domain on the sphere*, we deal with the numerical optimization of the first three Neumann eigenvalues on the sphere and torus, both in the class of densities and domains. The numerical observations resulting from these experiments will lead to the formulation of several open problems.

Below, we provide a more detailed description of the main results of each part.

1.2.1 Chapter 2: A selection of tools for numerical eigenvalue optimization

The purpose of this chapter is to review the basic tools related to numerical optimization of eigenvalue problems. In the first part, we recall, without proving them, some classical theorems from spectral theory for elliptic operators, namely, the Spectral Theorem and the Courant-Fisher Theorem, which provide the variational characterization of eigenvalues. Secondly, we show how to approximate the eigenvalues of a domain using the finite element method (FEM), with an elementary proof of convergence. The third part provides a brief introduction to the differentiability of eigenvalues with respect to the domain. In particular, we present the proof of the expression for the directional derivative of Neumann eigenvalues with multiplicity greater than 1. Finally, one of the central questions in shape optimization is how to parameterize the evolving domain Ω . We review the principle of the level set method, a flexible approach that allows for transparent changes in topology.

1.2.2 Chapter 3: Maximization of Neumann eigenvalues in a class of densities

This chapter is based on the work published in [35]. We study the generalization of the concept of Neumann eigenvalues initially proposed by Bucur and Henrot [33]. Starting from the variational formulation of the eigenvalues

$$\mu_k(\Omega) = \min_{S \in \mathcal{S}_{k+1}} \max_{u \in S \setminus \{0\}} \frac{\int_{\Omega} |\nabla u|^2}{\int_{\Omega} u^2},$$

where \mathcal{S}_k is the set of subspaces of dimension k in $H^1(\Omega)$, we can define a notion of generalized eigenvalue for a density $\rho \in \mathbf{L}^1(\mathbb{R}, [0, 1])$ as follows:

$$\mu_k(\rho) := \inf_{S \in \mathcal{S}_{k+1}} \max_{u \in S \setminus \{0\}} \frac{\int_{\mathbb{R}^n} \rho |\nabla u|^2}{\int_{\mathbb{R}^n} \rho u^2},$$

where \mathcal{S}_k is now the set of subspaces of dimension k of

$$\{u \cdot 1_{\{\rho(x) > 0\}} : u \in C_c^\infty(\mathbb{R}^n)\}.$$

If Ω is sufficiently regular, we recover $\mu_k(\mathbf{1}_\Omega) = \mu_k(\Omega)$ for all $k \in \mathbb{N}$. In [33, 2019], this generalization was motivated by the fact that optimization in the class of densities was equivalent to optimization in the class of domains for $k = 1$ and $k = 2$, meaning that the optimal density for μ_1 (resp. μ_2) is the indicator function of a ball (resp. two disjoint balls). A natural question is whether this behavior persists for $k \geq 3$, and now it is possible to study the generalization of the original problem (1.2) by substituting it with

$$\max_{\int \rho = m} \mu_k(\rho) \tag{1.7}$$

where $m > 0$. Since the eigenvalue is homogeneous (i.e., $\mu_k(t\Omega) = \frac{\mu_k(\Omega)}{t^2}$), we can choose $m = 1$. Let μ_k^* denote the maximum value of this problem.

First, we provide an existence result in \mathbb{R}^n :

Theorem 1.2.1. *For any k , the maximum of (1.7) is achieved. More precisely, there exist $j \in \mathbb{N}$, $j \leq k$, $\rho_1, \dots, \rho_j : \mathbb{R}^n \rightarrow [0, 1]$ and $n_1, \dots, n_j \in \mathbb{N}$ with $n_1 + \dots + n_j = k + 1 - j$ such that*

$$\sum_{i=1}^j \int_{\mathbb{R}^n} \rho_i = 1 \quad \text{and} \quad \mu_k^* = \mu_{n_1}(\rho_1) = \dots = \mu_{n_j}(\rho_j).$$

It should be noted that if we imposed $\text{supp}(\rho) \subseteq U$ with $|U| < \infty$, the result would follow in a (fairly) elementary way from the direct method of calculus of variations.

In this new framework, the case of dimension 1 is no longer evident. We prove the following result:

Theorem 1.2.2. *In \mathbb{R} , for all $k \in \mathbb{N}$,*

$$\mu_k^* = \pi^2 k^2.$$

Equality is achieved when ρ is the characteristic function of the disjoint union of k segments of length $1/k$.

This theorem implies that the natural generalization of Pólya's conjecture for densities in one dimension is satisfied:

$$\forall k \in \mathbb{N}, \quad \mu_k(\rho) \leq \frac{\pi^2 k^2}{(\int_{\mathbb{R}} \rho)^2}.$$

We can then question the validity of Pólya's conjecture for densities in any dimension. We prove a weaker result with a non-optimal constant that generalizes Kröger's Theorem 1.1.5:

Theorem 1.2.3. *Let $N \geq 2$, $\rho \in \mathbf{L}^1(\mathbb{R}^n, [0, 1])$, $\rho \not\equiv 0$. Then*

$$\forall k \in \mathbb{N}, \quad \mu_k(\rho) \leq \left(\frac{n+2}{2} \right)^{2/n} 4\pi^2 \left(\frac{k}{\omega_n \int_{\mathbb{R}^n} \rho} \right)^{2/n}.$$

In the last part, we use the finite element method to compute the generalized eigenvalues associated with densities in order to numerically solve Problem (1.7). However, this method does not directly allow us to compute eigenvalues of densities that are not associated with elliptic problems. We will show that we

can asymptotically reduce this problem to the elliptic case. Considering a *working domain* $D \subseteq \mathbb{R}^n$ (open and bounded) and $\rho : D \rightarrow [0, 1]$, we define

$$\mu_k^\varepsilon(\rho) := \min_{S \in \mathcal{S}_{k+1}} \max_{u \in S \setminus \{0\}} \frac{\int_D (\rho + \varepsilon) |\nabla u|^2}{\int_D (\rho + \varepsilon^2) u^2}.$$

Then $\mu_k^\varepsilon(\rho)$ is the eigenvalue associated with the well-posed problem

$$\begin{cases} -\operatorname{div}[(\rho + \varepsilon) \nabla u] = \mu_k^\varepsilon(\rho) (\rho + \varepsilon^2) u & \text{on } D, \\ \partial_n u = 0 & \text{on } \partial D \end{cases} \quad (1.8)$$

and the approximation is justified by

Proposition 1.2.4. *Let $0 < m < |D|$. Then*

$$\max_{\int_D \rho = m} \mu_k^\varepsilon(\rho) \xrightarrow{\varepsilon \rightarrow 0} \max_{\int_D \rho = m} \mu_k(\rho).$$

In practice, optimization is based on a gradient method. One well-known difficulty in applying such a method is that the function $\rho \mapsto \mu_k^\varepsilon(\rho)$ is not differentiable when the eigenvalue is multiple [50] [16]. However, maxima seem to be achieved for eigenvalues with multiplicity greater than 2. In this chapter, we propose a heuristic method for optimizing such eigenvalues by adding the constraint

$$\sum_{i=0}^{m_k-1} (\mu_{k+i}^\varepsilon(\rho) - \mu_k^\varepsilon(\rho))^2 = 0$$

during optimization, where m_k is the assumed multiplicity of $\mu_k^\varepsilon(\rho)$. This constraint aims to ensure that close eigenvalues remain close. Another method, which yields better stability results for optimizing eigenvalues of densities defined on the sphere, is presented in Chapter 5.

The results for the first 8 non-trivial eigenvalues are shown in Figure 1.4.

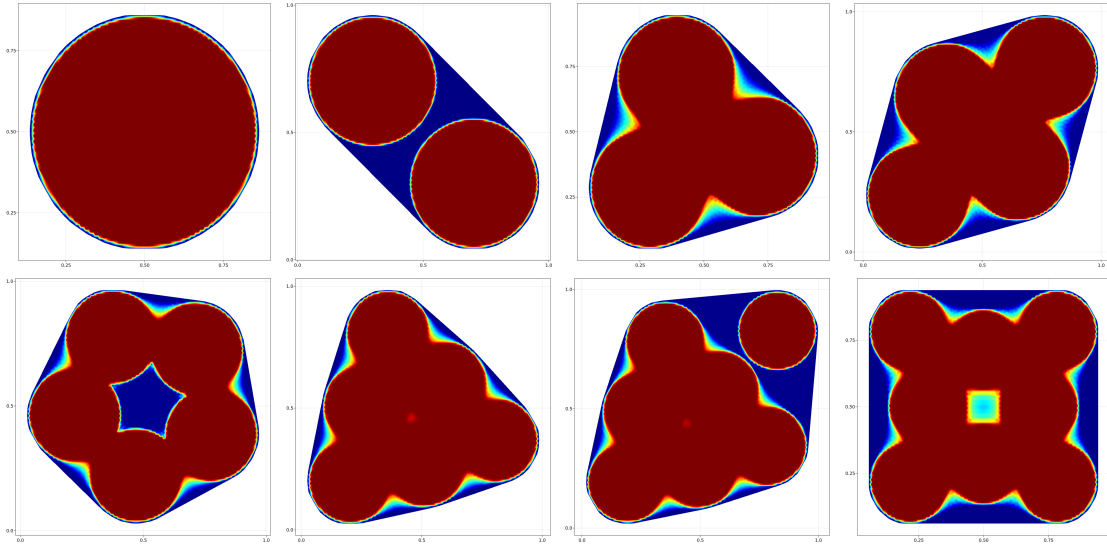


Figure 1.4: Approximation of the first eight optimal densities.

We can see that unlike the first two eigenvalues, the optimal densities for $k \geq 3$ do not appear to be the characteristic function of a shape. This behavior will be observed for certain eigenvalues of densities defined on the sphere and will be discussed in the associated chapter.

1.2.3 Chapter 4: Optimal Inequalities for Neumann Eigenvalues on the Sphere

This chapter is associated with the article [34]. While the optimization problem for eigenvalues in \mathbb{R}^n is essentially scale-invariant, this is no longer the case for curved spaces. Therefore, we can expect different behaviors of optimal domains depending on the value of the measure constraint m . In this chapter, we consider the optimization problem for the second non-trivial eigenvalue of domains on the sphere $\Omega \subset \mathbb{S}^n$. The main contribution of this article is the following result:

Theorem 1.2.5. *Let $\Omega \subset \mathbb{S}^n$ be a Lipschitz open set. Then*

$$\sum_{i=2}^n \frac{1}{\mu_i(\Omega)} \geq \sum_{i=2}^n \frac{1}{\mu_i(B^{|\Omega|/2} \sqcup B^{|\Omega|/2})} \left(= \frac{n-1}{\mu_1(B^{|\Omega|/2})} \right).$$

Equality is achieved when Ω is the disjoint union of two geodesic balls of equal measure.

This theorem implies, in particular, an upper bound on the second non-trivial eigenvalue:

$$\mu_2(\Omega) \leq \mu_2(B^{|\Omega|/2} \sqcup B^{|\Omega|/2}) = \mu_1(B^{|\Omega|/2}).$$

The proof is similar to the planar case [33], once again using a topological invariant that allows for the construction of test functions orthogonal to the first two eigenfunctions of the domain Ω . The main difficulty in establishing the result comes from the lack of uniqueness of the "center of mass of Weinberger," which was an essential ingredient in both the planar case [33] and the hyperbolic space [58].

It should be noted that such a result has not yet been established in full generality for μ_1 . One obstruction to applying the mass transplantation argument is finding an extension \mathcal{H}^1 of the eigenfunctions from $B^{|\Omega|}$ to the sphere \mathbb{S}^n . Such an extension is not trivial for the case of μ_1 , and simulations performed in Chapter 4 suggest that it is not a simple technicality. However, quite surprisingly, the previous theorem allows for a direct generalization of the theorem by Ashbaugh and Benguria [18], which takes the following form (recall that in Theorem 1.1.7 by Ashbaugh and Benguria, the condition was $\Omega \subset \mathbb{S}_+^n$):

Corollary 1.2.6. *Let $0 < m < |\mathbb{S}^n|$ and $\Omega \subset \mathbb{S}^n \setminus \mathbf{B}^m$ be a Lipschitz open set such that $|\Omega| = m$. Then*

$$\mu_1(\Omega) \leq \mu_1(\mathbf{B}^m).$$

In the final part, we consider optimization within the class of densities, similar to the planar case. Returning to the case of μ_1 , we numerically demonstrate that the indicator function of a ball is not always optimal in the class of densities. Indeed, for $m = 6$, we exhibit an axisymmetric density ρ^6 that is strictly better than the eigenvalue of the geodesic ball with the same mass (see Figure 1.5). We will see in the

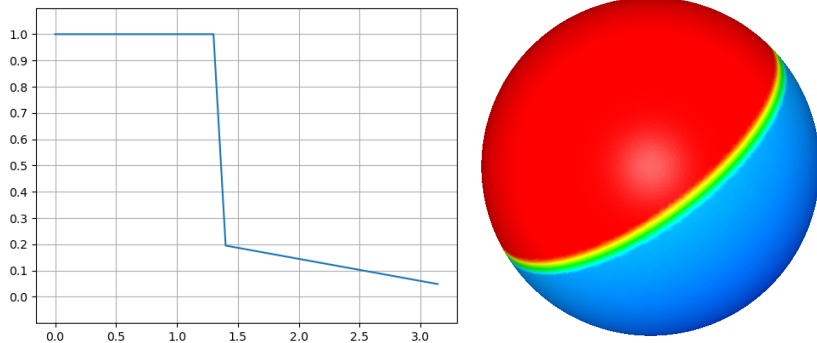


Figure 1.5: Graph of ρ^6 as a function of latitude $\theta \in [0, \pi]$ (left) and its representation on the sphere (right).

following chapter that this behavior is generic for μ_1 and μ_3 in certain ranges of masses m .

1.2.4 Chapter 5: Numerical Optimization of Neumann Eigenvalues on Spherical Domains

This chapter, derived from [85], has a purely experimental purpose. Its objective is to further explore some of the questions raised in the previous chapter. We begin by demonstrating the existence of an optimal density on the sphere using the direct method of calculus of variations:

Theorem 1.2.7. *Let $0 \leq m \leq |\mathbb{S}^n|$. Then the problem*

$$\sup \left\{ \mu_k(\rho) \mid \rho : \mathbb{S}^n \rightarrow [0, 1], \int_{\mathbb{S}^n} \rho = m \right\}$$

has a solution.

Remark 1.2.8. Unlike the case of \mathbb{R}^n , here we have the existence of a single density instead of a collection of densities. Furthermore, a fundamental distinction from the case of \mathbb{R}^n lies in the dependence of the optimal density/domain on the total mass m , leading to a loss of eigenvalue homogeneity.

Applying the numerical optimization method used in Chapter 2, which imposes proximity between multiple eigenvalues, proved to be unsuccessful. This approach led to convergence to local maxima rather than a global maximum, due to the multiplicity of eigenvalues. Several other methods were explored, but the following approach proved to be the most stable. The underlying idea is to regularize the problem to make it differentiable. Assuming (which is generally verified in practice) that $\mu_k^\varepsilon(\rho)$ remains far from $\mu_{k-1}^\varepsilon(\rho)$ during optimization and is part of a set $\mu_k^\varepsilon(\rho), \dots, \mu_{k+m_k-1}^\varepsilon(\rho)$ of "close" eigenvalues, we naturally have:

$$\mu_k^\varepsilon(\rho) = \min \left\{ \mu_k^\varepsilon(\rho), \dots, \mu_{k+m_k-1}^\varepsilon(\rho) \right\}.$$

For sufficiently large $p > 0$, it is possible to approximate the minimum of a set $\{x_0, \dots, x_{m_k-1}\}$ by:

$$\min \left\{ x_0, \dots, x_{m_k-1} \right\} \approx \left(\sum_i x_i^{-p} \right)^{-1/p}.$$

We then optimize the function:

$$\rho \mapsto \left(\sum_i \mu_{k+i}^\varepsilon(\rho)^{-p} \right)^{-1/p},$$

which is assumed to be differentiable in the vicinity of ρ if the multiplicity of $\mu_k(\rho)$ is indeed m_k . By approximating $\mu_k(\rho)$ with a well-defined eigenvalue $\mu_k^\varepsilon(\rho)$, we optimize the eigenvalues μ_1, μ_2 , and μ_3 for different values of m . Some results of this optimization are presented in Figure 1.6.

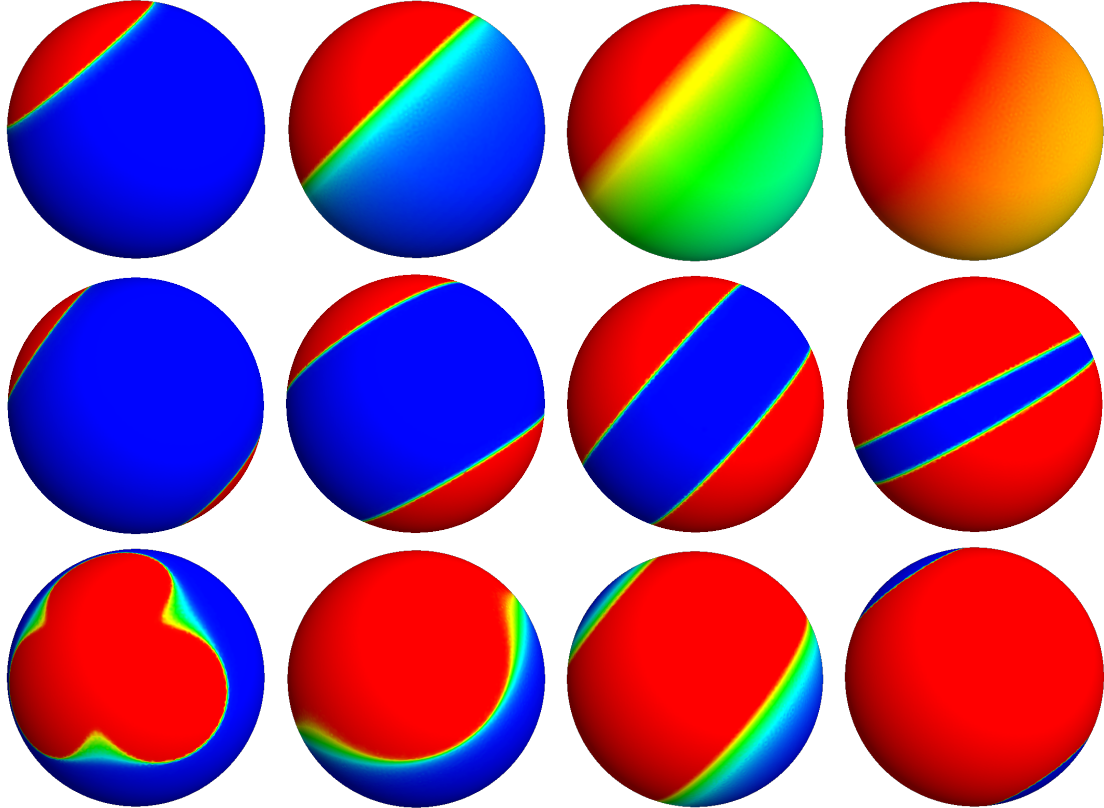


Figure 1.6: Examples of optimal densities for μ_1, μ_2, μ_3 (respectively first, second and third row) for different values of m .

We notice that the case of μ_2 is consistent with the theory. For μ_1 , we observe that for sufficiently large m , the ball is not optimal. However, a more detailed analysis of this case leads to the following conjecture:

Conjecture 1.2.9. *There exists $\delta > 0$ such that for all $0 < m < \delta$ and all $\rho : \mathbb{S}^n \rightarrow [0, 1]$ with $\int_{\mathbb{S}^n} \rho = m$, we have*

$$\mu_1(\rho) \leq \mu_1(\mathbf{B}^m).$$

In the second part of Chapter 5, we consider shape optimization of the problem

$$\sup \{ \mu_k(\Omega) : \Omega \subset \mathbb{S}^n, |\Omega| = m, \Omega \text{ open, Lipschitz} \}.$$

The optimization involves the use of the "level set" method, which consists in representing a domain $\Omega(t)$ depending on a fictitious time t by a function ϕ satisfying

$$\forall x \in \mathbb{S}^n, \forall t \in [0, T], \begin{cases} \phi(t, x) < 0 & \text{if } x \in \Omega(t) \\ \phi(t, x) = 0 & \text{if } x \in \partial\Omega(t) \\ \phi(t, x) > 0 & \text{if } x \in \mathbb{S}^n \setminus \overline{\Omega(t)} \end{cases}.$$

If $\Omega(t)$ evolves according to the flow of a vector field $V : \mathbb{S}^n \rightarrow T\mathbb{S}^n$, then it is equivalent to evolve ϕ according to the equation

$$\partial_t \phi(t, x) + V(x) \cdot \nabla \phi(t, x) = 0.$$

The choice of a vector field V that locally increases $\mu_k(\Omega(t))$ involves the concept of shape derivative of μ_k . Once again, a gradient algorithm can be used to find the optima of the first three eigenvalues, and examples are given in Figure 1.7. We immediately notice that for large values of m , μ_1 exhibits a singular behavior,

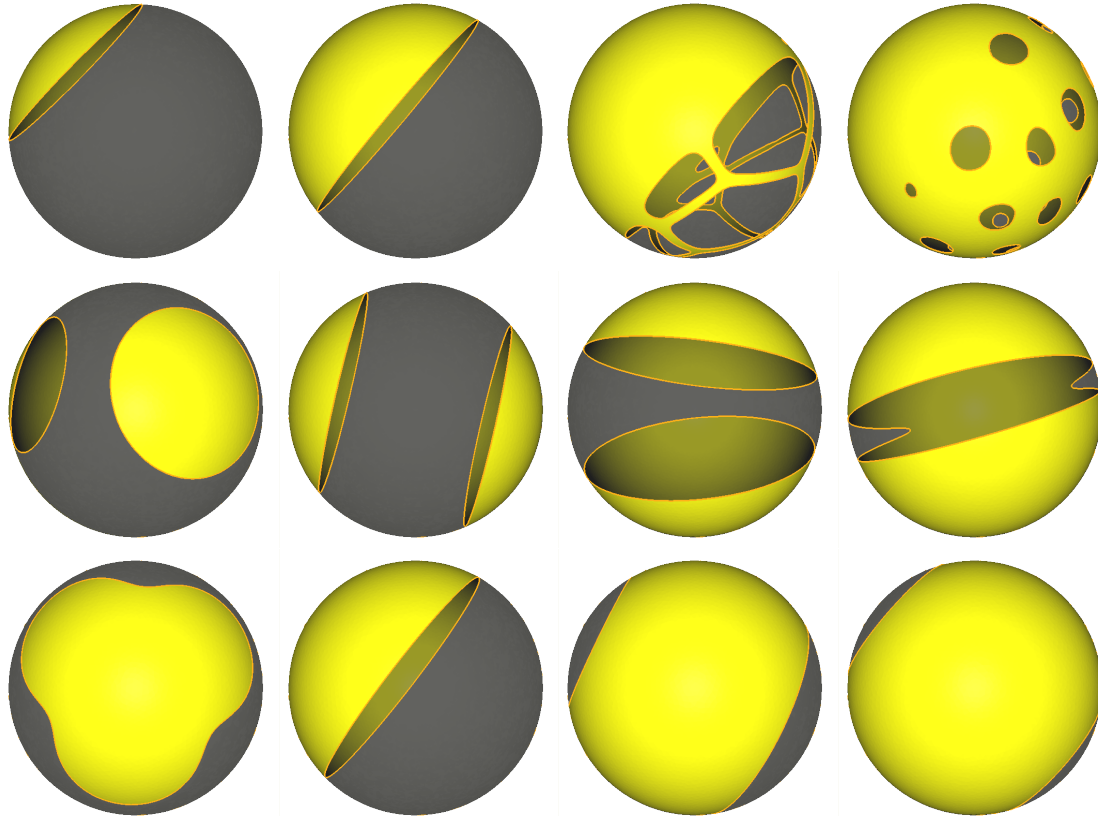


Figure 1.7: Examples of optimal domains for μ_1, μ_2, μ_3 (respectively, the first, second, and third row) for different values of m .

trying to fill a cap and complete the rest of the sphere with a cap riddled with holes. Therefore, we cannot hope to show a result similar to Langford and Laugesen [76] in the absence of the assumption of simple connectivity.

Remark 1.2.10. *For the optimization of μ_1 within the class of densities, the ball seems to be optimal for any mass $0 < m < \delta$ with $\delta \approx 4.5$. For optimization within the class of domains, this seems to hold true for*

$0 < m < \delta' \approx 8$. However, we have previously seen Weinberger's mass transplantation argument: it turns out that this argument is still valid within the class of densities. Thus, all results proven by an argument of this type for domains must also hold true for densities (on this point, see [33]). Therefore, we cannot expect to prove the optimality of the ball for $\delta < m < \delta'$ using mass transplantation, although it may be possible for $0 < m < \delta$.

For $m > \delta'$, the optimization in domains also seems to homogenize by creating a large number of holes, which could suggest the non-existence of an optimal domain.

Note that these arguments are also valid in the plane for eigenvalues where the optimal density is not a domain. Therefore, it will be necessary to develop new tools to theoretically treat all these cases. One possibility in this direction could be periodic optimization (see, for example, [7]).

Finally, in a last part, we use the tools developed for the sphere to carry out the same analysis on a torus $\mathbb{T} \subset \mathbb{R}^3$.

2

A selection of tools for the numerical optimization of eigenvalues

Contents

2.1	Eigenvalues of self-adjoint operators	31
2.2	Finite elements approximation of eigenvalue problems	33
2.3	Directional shape derivative of Laplace eigenvalues	35
2.4	Shape optimization by the level set method : basic ideas	41

In this chapter we address the main fundamental tools used for the numerical optimization of eigenvalue problems. It aims at providing the unfamiliar reader with enough knowledge to understand the subsequent chapters. First we will cover the Spectral Theorem for compact self-adjoint operators. This theorem allows to decompose the space into a sum of subspaces invariant under the action of the operator. This will lead to the study of the notion of eigenvalues of an operator and their fundamental properties. Secondly we will see how to numerically approximate the eigenvalues of a domain. Relying on the concept of shape derivatives we then explain how to optimize a functional which depends on the eigenvalues of the domain. Finally, in order to implement a numerical method allowing for topological changes during the optimization procedure, we discuss the advantages of the level set method.

2.1 Eigenvalues of self-adjoint operators

For details about this section, we refer to [2].

The problem we will consider is the following one : for an open bounded set $\Omega \subseteq \mathbb{R}^n$ or $\Omega \subseteq \mathbb{S}^n$ with Lipschitz boundary, find a non-zero $u \in \mathbf{H}^1(\Omega)$ and $\mu \in \mathbb{R}$ such that

$$\begin{cases} -\Delta u &= \mu u \text{ in } \Omega, \\ \frac{\partial u}{\partial n} &= 0 \text{ on } \partial\Omega, \end{cases} \quad (2.1)$$

This problem arises in a very natural way when considering time-dependent PDEs like the heat equation :

$$\begin{cases} \Delta \mathbf{u}(t, x) &= \partial_t \mathbf{u}(t, x) \text{ in } \mathbb{R}^+ \times \Omega, \\ \partial_n \mathbf{u}(t, x) &= 0 \text{ on } (0, T) \times \partial\Omega, \\ \mathbf{u}(0, x) &= v \text{ on } \{0\} \times \Omega \end{cases} \quad (2.2)$$

where $\mathbf{u} : \mathbb{R}^+ \times \Omega \rightarrow \mathbb{R}$ is the solution and $v \in L^2(\Omega)$ is the initial datum. This represents the time evolution of temperature inside a domain Ω which is supposed to be completely insulated from the outside. If we suppose that $\mathbf{u}(t, x) = \phi(t)u(x)$, then equation (2.2) can be reformulated as

$$\frac{\partial_t \phi}{\phi} = -\frac{\Delta u}{u}.$$

Hence this quantity must be constant with respect to t and x . By denoting this constant by μ , the problem comes to solve equation (2.1). Indeed, if we suppose that there exists couples $(\mu_k, u_k)_{k \geq 1} \in \mathbb{R} \times \mathbf{H}^1(\Omega)$ solving (2.1) such that $(u_k)_k$ is an Hilbert basis of $L^2(\Omega)$, we can write $v = \sum_k \alpha_k u_k$ and

$$\mathbf{u}(t, x) = \sum_k \alpha_k \exp(-\mu_k t) u_k(x)$$

is solution of (2.2).

Remark 2.1.1. *This point of view allows to get some physical insight concerning eigenvalues. In the case of the heat equation, the first non-zero eigenvalue can be interpreted as a characteristic time for the diffusion of the heat inside the domain Ω . Maximizing the first eigenvalue among domains of fixed volume amounts at finding the shape reaching the fastest equilibrium. When dealing with the wave equation with homogeneous Dirichlet boundary condition on a domain Ω , the eigenvalues are the square roots of the natural audible frequencies of a membrane of shape Ω .*

We will see in the sequel that there is a countably infinite family of eigenvalues

$$0 = \mu_0(\Omega) \leq \mu_1(\Omega) \leq \dots \leq \mu_k(\Omega) \leq \dots \rightarrow \infty$$

thanks to the spectral theorem for compact self-adjoint operators, which reads as follows (note that all the Hilbert spaces we considered are real):

Theorem 2.1.2 (Spectral theorem). *Let V be an infinite-dimensional Hilbert space and $A : V \rightarrow V$ a compact and self-adjoint linear operator. Then there exists a non increasing sequence of eigenvalues $(\lambda_k)_{k \geq 1}$ and an Hilbert basis of eigenvectors $(u_k)_{k \geq 1}$ such that for all $k \geq 1$*

$$Au_k = \lambda_k u_k$$

and $\lambda_k \xrightarrow{k \rightarrow \infty} 0$.

Using this theorem, we can establish the following result which is more convenient when working with partial differential equations :

Theorem 2.1.3. *Let V and H two real Hilbert spaces such that $V \subset H$ with compact embedding and suppose V is dense in H . Let $a : V \times V \rightarrow \mathbb{R}$ be a symmetric continuous bilinear form with the condition that there exists $v > 0$ such that*

$$a(v, v) \geq v \|v\|_V^2 \quad (2.3)$$

for all $v \in V$. Then there exists eigenvalues $(\mu_k)_{k \geq 1}$ and associated eigenvectors $(u_k)_{k \geq 1}$ such that for all $k \geq 1$ and $v \in V$,

$$a(u_k, v) = \mu_k \langle u_k, v \rangle_H.$$

Moreover, we have that $(u_k)_{k \geq 1}$ is an Hilbert basis of V and

$$0 \leq \mu_1 \leq \mu_2 \leq \dots \leq \mu_k \leq \dots \rightarrow \infty.$$

To relate the problem (2.1) with the previous theorem, we need to introduce the weak formulation of (2.1). First, we get rid of the constant functions which corresponds to the 0 eigenvalue that we denote by μ_0 by considering the space

$$V = \left\{ v \in \mathbf{H}^1(\Omega) \mid \int_{\Omega} v = 0 \right\}$$

which is isomorphic to $H^1(\Omega)/\mathbb{R}$. The variationnal formulation reads as follows : find $(\mu, u) \in \mathbb{R} \times V$ such that for all $v \in V$,

$$\int_{\Omega} \nabla u \cdot \nabla v = \mu \int_{\Omega} uv.$$

This formulation is obtained by multiplying (2.1) by a test function v and integrating by parts using the homogeneous Neumann boundary condition. Then we can set $H = \mathbf{L}^2(\Omega)$ and $a(u, v) = \int_{\Omega} \nabla u \cdot \nabla v$. The application a is obviously symmetric and bilinear and the continuity is given by the Cauchy-Schwarz inequality, while the coercivity constraint (2.3) is a consequence of the Poincaré-Wirtinger inequality. Finally, the Rellich's theorem ensures that $\mathbf{H}^1(\Omega)$ (and hence V) is compactly embedded in $\mathbf{L}^2(\Omega)$ (for these classical results, see [52]). Thus, thanks to Theorem 2.1.3, there exists a sequence of eigenvalues

$$0 = \mu_0(\Omega) \leq \mu_1(\Omega) \leq \mu_2(\Omega) \leq \dots \leq \mu_k(\Omega) \leq \dots \rightarrow \infty$$

(we make the dependance on the domain explicit since it will vary in further considerations).

An important result in the study of symmetric eigenvalue problems is the Courant-Fisher theorem, which gives a variationnal formulation of eigenvalues. It will be of capital importance in all the following chapters :

Theorem 2.1.4 (Courant-Fisher). *Let V , H and $a : V \times V \rightarrow \mathbb{R}$ verify the same assumptions as before. Let \mathcal{S}_k be the set of all subspaces of dimension k in V . Then we have*

$$\mu_k = \min_{S \in \mathcal{S}_k} \max_{u \in S, u \neq 0} \frac{a(u, u)}{\|u\|_H^2} = \max_{W \in \mathcal{S}_{k-1}} \min_{u \in W^\perp, u \neq 0} \frac{a(u, u)}{\|u\|_H^2} \quad (2.4)$$

Remark 2.1.5. *In the case of the Neumann eigenvalues on Ω , the first equality reads :*

$$\mu_k(\Omega) = \min_{S \in \mathcal{S}_{k+1}} \max_{u \in S, u \neq 0} \frac{\int_{\Omega} |\nabla u|^2}{\int_{\Omega} u^2},$$

where \mathcal{S}_k is the family of all subspaces of dimension k in $H^1(\Omega)$. This will be of first importance in this thesis since it is the starting point of a notion of "generalized eigenvalues".

2.2 Finite elements approximation of eigenvalue problems

In this section, we follow the lines of [91]. Another reference is [26].

In this thesis, numerical simulations has been extensively used. Such simulations has the enormous advantage to give insights when tackling a new problem. It can help to unveil patterns and properties thanks to computations inaccessible for humans. For instance, in Chapter 5, numerical computations are used to rule out some existing conjecture or establish new ones. To this extent, we will use the Finite Element Method (FEM). The idea of FEM is to approximate the natural space in which our PDE is set (in our case, the space $V = \mathbf{H}^1(\Omega)$) by some sets $V_h \subset V$ such that each V_h is of finite dimension and

$$V_h \xrightarrow[h \rightarrow 0]{} V$$

where the last "convergence" will be made rigorous in a moment. In the FEM, the space V_h is build using a triangulation \mathcal{T}_h of the set Ω (which is supposed to be polygonal) with triangles being of size of order h . Then the space V_h consists of functions build on this mesh, e.g. continuous functions which are affine on each triangle of \mathcal{T}_h (this the so-called \mathcal{P}_1 finite element method). See [2] for more informations. That being said, we have the following approximation result (see [91])

Theorem 2.2.1 (Numerical approximation of eigenvalues). *Let $V_h \subset V$ such that for all $u \in V$*

$$\lim_{h \rightarrow 0} \left(\inf_{v_h \in V_h} \|u - v_h\|_V^2 \right) = 0. \quad (2.5)$$

Let us call

$$\mu_1 \leq \mu_2 \leq \dots \rightarrow \infty$$

the eigenvalues of the problem : find $(\mu, u) \in \mathbb{R} \times V$ such that

$$a(u, v) = \mu \langle u, v \rangle_H \text{ for all } v \in V$$

and

$$\mu_1^h \leq \mu_2^h \leq \dots \leq \mu_{\dim(V_h)}^h$$

the eigenvalues of the problem : find $(\mu^h, u_h) \in \mathbb{R} \times V_h$ such that

$$a(u_h, v_h) = \mu^h \langle u_h, v_h \rangle_H \text{ for all } v_h \in V_h.$$

Then for all $k \geq 1$, $\mu_k^h \xrightarrow[h \rightarrow 0]{} \mu_k$.

Remark 2.2.2. The condition (2.5) makes the heuristic statement " $V_h \xrightarrow[h \rightarrow 0]{} V$ " rigorous. This condition is indeed fulfilled for \mathcal{P}_1 finite elements when the size of the triangles of the mesh becomes small enough.

Proof. Let $k \geq 1$ and suppose that for all h , $\dim(V_h) \geq k$. Thanks to Theorem 2.1.4, we already know that $\mu_k \leq \mu_k^h$ thus we only need the inequality

$$\mu_k^h \leq \mu_k + \underset{h \rightarrow 0}{o}(1).$$

Let us define

$$\Pi_h : V \rightarrow V_h$$

the orthogonal projection associated to the bilinear form a , i.e.

$$\forall u \in V, \forall v_h \in V_h, a(\Pi_h u - u, v_h) = 0.$$

Let us denote by u^i (resp. u_h^i) the eigenvector associated to μ_i (resp. μ_i^h) and $V^{(k)} = \text{span}(u^1, \dots, u^k)$. We claim that the space $E_k := \Pi_h V^{(k)}$ is such that $\dim(E_k) = k$. Indeed, for $u \in V$ and $v_h \in V_h$,

$$\begin{aligned} v \|\Pi_h u - u\|_V^2 &\leq a(\Pi_h u - u, \Pi_h u - u) \\ &\leq a(\Pi_h u - u, v_h - u) \quad \text{for all } v_h \in V_h \\ &\leq M \|\Pi_h u - u\|_V \inf_{v_h \in V_h} \|v_h - u\|_V \end{aligned}$$

which leads to

$$\|\Pi_h u - u\|_V \leq \frac{M}{\mathbf{v}} \inf_{v_h \in V_h} \|v_h - u\|_V \xrightarrow[h \rightarrow 0]{} 0$$

that is, for h small enough, $\|\Pi_h u - u\|_V \leq \frac{1}{2} \|u\|_V$. Hence $\Pi_h : V^{(k)} \rightarrow E_k$ is injective since

$$\|\Pi_h u\|_V \geq \|u\|_V - \|\Pi_h u - u\|_V \geq \frac{1}{2} \|u\|_V.$$

Then Π_h is bijective so $\dim(E_k) = \dim(V_k) = k$. Using the Courant-Fisher theorem,

$$\begin{aligned} \mu_k^h &= \min_{U \subset V_h, \dim U = k} \max_{v_h \in U, v_h \neq 0} \frac{a(v_h, v_h)}{\|v_h\|_H^2} \leq \max_{v_h \in E_k, v_h \neq 0} \frac{a(v_h, v_h)}{\|v_h\|_H^2} \\ &\leq \max_{v \in V^{(k)}, \|v\|_H = 1} \frac{a(\Pi_h v, \Pi_h v)}{\|\Pi_h v\|_H^2} \\ &\leq \max_{v \in V^{(k)}, \|v\|_H = 1} \frac{a(v, v)}{\|\Pi_h v\|_H^2} \quad \text{since } a(\Pi_h v, \Pi_h v) \leq a(v, v) \\ &\leq \mu_k \max_{v \in V^{(k)}, \|v\|_H = 1} \frac{1}{\|\Pi_h v\|_H^2} \quad \text{thanks to Courant-Fisher again} \\ &\leq \left(\min_{v \in V^{(k)}, \|v\|_H = 1} \|\Pi_h v\|_H^2 \right)^{-1} \mu_k. \end{aligned}$$

Now we only have to prove that the factor $\left(\min_{v \in V^{(k)}, \|v\|_H = 1} \|\Pi_h v\|_H^2 \right)^{-1}$ is $1 + o_{h \rightarrow 0}(1)$. For $\|v\|_H = 1$,

$$\|\Pi_h v\|_H^2 \geq (\|v\|_H - \|v - \Pi_h v\|_H)^2 \geq 1 - 2\|v - \Pi_h v\|_H$$

which implies that

$$\min_{v \in V^{(k)}, \|v\|_H = 1} \|\Pi_h v\|_H^2 \geq 1 - 2 \max_{v \in V^{(k)}, \|v\|_H = 1} \|v - \Pi_h v\|_H.$$

For $0 \leq x \leq 1/2$, $\frac{1}{1-x} \leq 1 + 2x$ so assuming $\max_{v \in V^{(k)}, \|v\|_H = 1} \|v - \Pi_h v\|_H \xrightarrow[h \rightarrow 0]{} 0$ then for h small enough we would have

$$\left(\min_{v \in V^{(k)}, \|v\|_H = 1} \|\Pi_h v\|_H^2 \right)^{-1} \leq 1 + 4 \max_{v \in V^{(k)}, \|v\|_H = 1} \|v - \Pi_h v\|_H.$$

This is indeed the case : for $i \in \{0, \dots, k-1\}$, the eigenvector u_i verifies

$$\|\Pi_h u_i - u_i\|_H \leq \frac{M}{\mathbf{v}} \min_{v \in V_h} \|v_h - u_i\|_H^2 \rightarrow 0.$$

Let $v \in V^{(k)}$ such that $\|v\|_H = 1$. There exists a_1, \dots, a_k such that $v = \sum a_i u_i$ and $|a_i| \leq 1$ for all i . This implies

$$\|v - \Pi_h v\|_H \leq \sum |a_i| \|u_i - \Pi_h u_i\|_H \xrightarrow[h \rightarrow 0]{} 0$$

and we can pass to the sup at the left. Finally, for h small enough, we get :

$$\mu_k \leq \mu_k^h \leq \left(1 + 4 \max_{v \in V^{(k)}, \|v\|_H = 1} \|v - \Pi_h v\|_H \right) \mu_k \xrightarrow[h \rightarrow 0]{} \mu_k.$$

□

Remark 2.2.3. Notice that we only proved the convergence of the eigenvalues without any guarantee on the speed of convergence with respect to the mesh size h . Moreover, we can also prove some notion of convergence of the eigenfunctions (see [26] for more informations).

It is possible to show that for \mathcal{P}_1 finite elements defined on a sequence of regular meshes \mathcal{T}_h , then the condition (2.5) holds. It is based on the construction of the *interpolation operator* $r_h : V \rightarrow V_h$ which associates to each continuous function the \mathcal{P}_1 function which has the same value at the vertices of \mathcal{T}_h . A proof can be found in [2, Prop 6.3.16].

2.3 Directional shape derivative of Laplace eigenvalues

We will now consider the problem of optimizing an eigenvalue with respect to the domain. Namely, for $k \geq 0$ and $m \in \mathbb{R}^+$ we will consider the problem

$$\sup \{\mu_k(\Omega) : \Omega \subset \mathbb{R}^n, \Omega \text{ bounded, open and Lipschitz}, |\Omega| = m\}. \quad (2.6)$$

Notice that in general, we don't know if the sup is attained by a certain set Ω . The strategy will be to define some kind of "gradient" of the function $\Omega \mapsto \mu_k(\Omega)$, which will allow to derive some gradient-based optimization method. The idea, which goes back to Hadamard [62], is to use a vector field to move the domain then compute the variation of the cost function with respect to an infinitesimal variation of the shape with respect to the vector field. Explicitly, let $V \in \mathbf{W}^{1,\infty}(\mathbb{R}^n, \mathbb{R}^n)$ be a Lipschitz vector field and $\psi_t = \text{id} + tV$ where $t \in \mathbb{R}$. Let us define $\Omega_t = \psi_t(\Omega)$. Then the (directional) shape derivative of μ_k at Ω in the direction V is defined by

$$\mu'_k(\Omega)(V) = \lim_{t \rightarrow 0^+} \frac{\mu_k(\Omega_t) - \mu_k(\Omega)}{t}. \quad (2.7)$$

Remark 2.3.1. Usually, the definition of shape derivative is expressed as the Frechet derivative of the functional and the standard method to prove its differentiability makes use of the implicit function theorem. One important hurdle in spectral shape optimization is the fact that eigenvalues are not differentiable if not of multiplicity one preventing such proof to work in our case. However, there always exists directional derivatives as defined above as we will show hereafter.

Remark 2.3.2. Numerically, the directional derivative is used to approximate the set that maximizes the k^{th} eigenvalue as follows : start from an arbitrary domain Ω^0 . For this Ω^0 , suppose that we can find a vector field V_0 such that $\mu'_k(\Omega^0)(V_0) > 0$. This means that for a $\delta t > 0$ small enough,

$$\mu_k(\Omega_{\delta t}^0) \approx \mu_k(\Omega^0) + \delta t \mu'_k(\Omega^0)(V_0) > \mu_k(\Omega^0).$$

We can then take $\Omega^1 := \Omega_{\delta t}^0$; for this new domain, we search for V_1 as before such that $\Omega^2 := \Omega_{\delta t}^1$ verifies $\mu_k(\Omega^2) > \mu_k(\Omega^1)$. Iteratively, we construct a sequence of domains Ω^m with the expectation that

$$\mu_k(\Omega^m) \xrightarrow[m \rightarrow \infty]{} \max_{\Omega} \mu_k(\Omega).$$

The method to prove and compute the derivative is taken from [39] where the authors use a result by Delfour and Zolésio [51, Chapter 10, Theorem 2.1]. We reproduce it here with similar notations and arguments.

Theorem 2.3.3. Let X be an arbitrary set and $\tau > 0$ and $G : [0, \tau] \times X \rightarrow \mathbb{R}$. We define :

$$g(t) = \inf_{u \in X} G(t, u)$$

$$X(t) = \{u \in X : G(t, u) = g(t)\}$$

$$g'(0^+) = \lim_{t \rightarrow 0^+} \frac{g(t) - g(0)}{t}.$$

Assume that the following conditions are satisfied :

- (**H1**): $\forall t \in [0, \tau], X(t) \neq \emptyset$
- (**H2**): $\forall u \in \bigcup_{t \in [0, \tau]} X(t), \partial_t G(t, u)$ exists on $[0, \tau]$
- (**H3**): There exists a topology \mathcal{T} on X s.t. for any sequence $(t_n)_n \in]0, \tau]$ converging to 0, there exists $u_\infty \in X(0)$ and a subsequence $(t_{n_k})_k$ of $(t_n)_n$ such that there exists $u_{n_k} \in X(t_{n_k})$ verifying
 - (**H3i**): $u_{n_k} \xrightarrow{\mathcal{T}} u_\infty$
 - (**H3ii**): $\liminf_{k \rightarrow \infty} \partial_t G(t_{n_k}, u_{n_k}) \geq \partial_t G(0, u_\infty)$
- (**H4**): $\forall u \in X(0), t \mapsto \partial_t G(t, u)$ is upper semi-continuous at $t = 0$.

Then

$$g'(0^+) = \min_{u \in X(0)} \partial_t G(0, u).$$

Proof. See Theorem 2.1, Chapter 10 of [51] □

The hypothesis of this theorem are quite heavy, but are also quite easy to verify if one follows the proof step by step. For the moment, let us focus on the first non-trivial eigenvalue. The case of μ_k being handled by similar arguments, working with μ_1 saves us from carrying unnecessarily heavy notations.

Theorem 2.3.4. *Let Ω be a Lipschitz domain and $V \in \mathbf{W}^{1,\infty}(\mathbb{R}^n, \mathbb{R}^n)$. Then $\mu'_1(\Omega)(V)$ exists. Moreover, if Ω is of class C^2 and $V \in C^2(\mathbb{R}^n, \mathbb{R}^n)$ then*

$$\mu'_1(\Omega)(V) = \inf_{u \in E_1(\Omega)} \frac{\int_{\partial\Omega} (|\nabla u|^2 - \mu_1(\Omega)u^2) (V \cdot \mathbf{n})}{\int_{\Omega} u^2} \quad (2.8)$$

where $E_1(\Omega)$ is the eigenspace associated to $\mu_1(\Omega)$.

The proof is rather long and will take advantage of some technical, yet classical lemmas. The first step is to match the notations with Theorem 2.3.3. First, for t small enough, let

$$g(t) := \mu_1(\Omega_t) = \min_{u \in \mathbf{H}^1(\Omega_t), \int_{\Omega_t} u=0} \frac{\int_{\Omega_t} |\nabla u|^2}{\int_{\Omega_t} u^2} = \min_{u \in \mathbf{H}^1(\Omega), \int_{\Omega_t} u \circ \psi_t^{-1}=0} \frac{\int_{\Omega_t} |\nabla(u \circ \psi_t^{-1})|^2}{\int_{\Omega_t} (u \circ \psi_t^{-1})^2}$$

The last identity is justified by the following lemmas :

Lemma 2.3.5. *Let $\phi \in \mathbf{W}^{1,\infty}(\mathbb{R}^n, \mathbb{R}^n)$ a bi-Lipschitz map. Then*

$$\begin{aligned} \mathbf{H}^1(\Omega_t) &\longrightarrow \mathbf{H}^1(\Omega) \\ u &\longmapsto u \circ \psi_t^{-1} \end{aligned}$$

is an isomorphism.

Proof. This is a consequence of the formula of change of variables and density for \mathcal{C}^∞ functions in $\mathbf{H}^1(\Omega)$. □

Lemma 2.3.6. *The application*

$$\begin{aligned} \mathbf{W}^{1,\infty}(\mathbb{R}^n, \mathbb{R}^n) &\longrightarrow \mathbf{L}^\infty(\mathbb{R}^n, \mathbb{R}^n) \\ \theta &\longmapsto (\text{id} + \theta)^{-1} \end{aligned}$$

is well defined and differentiable for $\|\theta\|_{1,\infty} < 1$.

This allows to define the function

$$\begin{aligned} G: [0, \delta) \times \mathbf{H}^1(\Omega) &\longrightarrow \mathbb{R} \\ (t, u) &\longmapsto \frac{\int_{\Omega_t} |\nabla(u \circ \psi_t^{-1})|^2}{\int_{\Omega_t} (u \circ \psi_t^{-1})^2} \end{aligned}$$

where δ will be chosen during the course of the proof. Also let

$$\begin{aligned} X(t) &:= \left\{ u \in \mathbf{H}^1(\Omega) : g(t) = G(t, u) \text{ and } \int_{\Omega} u^2 = 1 \right\} \\ &= \left\{ u \in \mathbf{H}^1(\Omega) : u \circ \psi_t^{-1} \in E_1(\Omega_t) \text{ and } \int_{\Omega} u^2 = 1 \right\}. \end{aligned}$$

We know have to verify that all the hypotheses of Theorem 2.3.3 are fulfilled. The hypothesis (H1) is ensured thanks to the Spectral Theorem 2.1.2. Let us verify that (H2) holds : for $t > 0$ small enough and $u \in \mathbf{H}^1(\Omega)$ such that $\int_{\Omega} u^2 = 1$, by a change of variable, we have that

$$\int_{\Omega_t} (u \circ \psi_t^{-1})^2 = \int_{\Omega} u^2 |\det(D\psi_t)| = \int_{\Omega} u^2 |\det(I + t\nabla V)|$$

where $\nabla V \in \mathbf{L}^\infty(\mathbb{R}^n, \mathbb{R}^{n \times n})$ is the Jacobian matrix of V . Now remark that $t \mapsto \det(I + t\nabla V)$ is continuous at 0 so for $t > 0$ small enough, $|\det(I + t\nabla V)| = \det(I + t\nabla V)$. Moreover, this map is differentiable and its differential is bounded; by the Dominated Convergence Theorem the map

$$t \mapsto \int_{\Omega_t} (u \circ \psi_t^{-1})^2 = \int_{\Omega} u^2 \det(I + t\nabla V)$$

is differentiable for $t > 0$ small enough. In the same way, the function

$$\begin{aligned} t \mapsto \int_{\Omega_t} |\nabla(u \circ \psi_t^{-1})|^2 &= \int_{\Omega_t} |((D\psi)^{-1}\nabla u) \circ \psi_t^{-1}|^2 \\ &= \int_{\Omega} \det(I + t\nabla V)(I + t\nabla V)^{-1}(I + t\nabla V)^{-T} |\nabla u|^2. \end{aligned}$$

is differentiable. Finally,

$$\lim_{t \rightarrow 0^+} \int_{\Omega_t} (u \circ \psi_t^{-1})^2 = \int_{\Omega} u^2 = 1$$

so for t near 0, $\int_{\Omega_t} (u \circ \psi_t^{-1})^2 > 0$. This implies that for all $u \in \mathbf{H}^1(\Omega)$ such that $\int_{\Omega} u^2 = 1$,

$$t \mapsto \partial_t G(t, u)$$

is differentiable hence **(H2)** holds. In fact, the previous arguments also show that this application is continuous hence **(H4)** holds. We will now prove **(H3)**. The main issue is to find the convenient topology. We will show that the hypothesis holds for the strong \mathbf{H}^1 topology, but first we provide an intermediate lemma which the reader may find interesting on its own :

Lemma 2.3.7. *Under the previous assumptions,*

$$\mu_1(\Omega_t) \xrightarrow[t \rightarrow 0^+]{} \mu_1(\Omega).$$

Proof. We will proceed by showing the \limsup - \liminf inequalities. First let us show that

$$\limsup_{t \rightarrow 0^+} \mu_1(\Omega_t) \leq \mu_1(\Omega)$$

by building good test functions for $\mu_1(\Omega_t)$ from eigenfunctions of $\mu_1(\Omega)$. Indeed, consider $u \in E_1(\Omega)$ and

$$u_t := u - \frac{1}{\Omega_t} \int_{\Omega_t} u \det(I + t\nabla V) \implies \int_{\Omega_t} u_t \circ \psi_t^{-1} = 0. \quad (2.9)$$

which implies that

$$\mu_1(\Omega_t) \leq \frac{\int_{\Omega_t} |\nabla(u_t \circ \psi_t^{-1})|^2}{\int_{\Omega_t} (u_t \circ \psi_t^{-1})^2}.$$

Then we can show the limits $\int_{\Omega_t} (u_t \circ \psi_t^{-1})^2 \xrightarrow[t \rightarrow 0^+]{\longrightarrow} \int_{\Omega} u^2$ and $\int_{\Omega_t} \nabla(u_t \circ \psi_t^{-1})^2 \xrightarrow[t \rightarrow 0^+]{\longrightarrow} \int_{\Omega} \nabla u^2$ so passing to the \limsup in (2.9), we get

$$\begin{aligned} \limsup \mu_1(\Omega_t) &\leq \lim_{t \rightarrow 0^+} \frac{\int_{\Omega_t} |\nabla(u_t \circ \psi_t^{-1})|^2}{\int_{\Omega_t} (u_t \circ \psi_t^{-1})^2} \\ &\leq \frac{\int_{\Omega} |\nabla u|^2}{\int_{\Omega} u^2} \\ &\leq \mu_1(\Omega). \end{aligned}$$

For the reverse inequality we need this time to build test function for $\mu_1(\Omega)$ from eigenfunctions of $\mu_1(\Omega_t)$. Let $u_t \in \mathbf{H}^1(\Omega)$ such that $u_t \circ \psi_t^{-1} \in E_1(\Omega_t)$ and $\int_{\Omega_t} (u \circ \psi_t^{-1})^2 = 1$ so $\mu_1(\Omega_t) = \int_{\Omega_t} |\nabla(u \circ \psi_t^{-1})|^2$. We can extract a subsequence $(u_{t_n})_{n \in \mathbb{N}}$, such that

$$\lim_{n \rightarrow +\infty} \int_{\Omega_{t_n}} |\nabla(u_{t_n} \circ \psi_{t_n}^{-1})|^2 = \liminf_{t \rightarrow 0^+} \mu_1(\Omega_t)$$

Since $\liminf_{t \rightarrow 0^+} \mu_1(\Omega_t) < +\infty$, the sequence (u_{t_n}) is bounded in $\mathbf{H}^1(\Omega)$. Using the Banach-Alaoglu and the Rellich theorem, there exists $u_\infty \in \mathbf{H}^1(\Omega)$ such that up to a subsequence,

$$u_{t_n} \xrightarrow{\mathbf{H}^1(\Omega)} u \text{ and } u_{t_n} \xrightarrow{\mathbf{L}^2(\Omega)} u.$$

This implies that $\int_{\Omega} u_\infty^2 = 1$. Moreover, the function

$$\begin{aligned} \mathbf{H}^1(\Omega) &\longrightarrow \mathbb{R} \\ v &\longmapsto \int_{\Omega} |\nabla v|^2 \end{aligned}$$

is convex, strongly continuous hence weakly semicontinuous in $\mathbf{H}^1(\Omega)$. This allows us to write

$$\begin{aligned} \int_{\Omega} |\nabla u_\infty|^2 &\leq \liminf \int_{\Omega} |\nabla u_{t_n}|^2 \\ &\leq \liminf \int_{\Omega_{t_n}} |\nabla(u_{t_n} \circ \psi_{t_n}^{-1})|^2. \end{aligned}$$

where the last inequality comes from

$$\left| \int_{\Omega_{t_n}} |\nabla(u_{t_n} \circ \psi_{t_n}^{-1})|^2 - \int_{\Omega} |\nabla u_{t_n}|^2 \right| \leq \int_{\Omega} |(A(t) - \mathbf{I}) \nabla u_{t_n} \cdot \nabla u_{t_n}| \xrightarrow[n \rightarrow +\infty]{} 0$$

since $A(t) := \det(\mathbf{I} + t_n V)(\mathbf{I} + t_n \nabla V)^{-1}(\mathbf{I} + t_n \nabla V)^{-T} \xrightarrow[n \rightarrow +\infty]{\mathbf{L}^\infty(\mathbb{R}^n, \mathbb{R}^{n \times n})} \mathbf{I}$. This leads to

$$\mu_1(\Omega) \leq \frac{\int_{\Omega} |\nabla u_\infty|^2}{\int_{\Omega} u_\infty^2} \leq \liminf \mu_1(\Omega_t)$$

hence the property. \square

The proof of the previous Lemma will help us prove (H3). Indeed, consider the previous subsequence (t_n) and take $u_n := \frac{u_{t_n}}{\|u_{t_n}\|_{\mathbf{L}^2}}$. Then $u_n \in X(t_n)$ and for $t > 0$ small enough, there exists $C > 0$ (which depends on the lowest eigenvalue of $A(t)$ which goes to 1 when t goes to 0) such that

$$\begin{aligned} C \int_{\Omega} |\nabla(u_n - u_\infty)|^2 &\leq \int_{\Omega} |A(t) \nabla(u_n - u_\infty) \cdot (\nabla u_n - \nabla u_\infty)| \\ &\leq \underbrace{\int_{\Omega} A(t) \nabla u_n \cdot \nabla u_n}_{\substack{n \sim \mu_1(\Omega_{t_n}) \\ \xrightarrow{n \rightarrow \infty} \mu_1(\Omega)}} + \underbrace{\int_{\Omega} A(t) \nabla u_\infty \cdot \nabla u_\infty}_{\substack{n \rightarrow \infty \\ \xrightarrow{n \rightarrow \infty} \int_{\Omega} |\nabla u_\infty|^2 = \mu_1(\Omega)}} - 2 \underbrace{\int_{\Omega} A(t) \nabla u_n \cdot \nabla u_\infty}_{\substack{n \rightarrow \infty \\ \xrightarrow{n \rightarrow \infty} \int_{\Omega} |\nabla u_\infty|^2 = \mu_1(\Omega)}} \end{aligned}$$

which shows that u_n converges strongly to u_∞ in \mathbf{H}^1 . By continuity of $\partial_t G$ and this new convergence, we have

$$\lim \partial_t G(t_n, u_n) = \partial_t G(0, u_\infty).$$

All the hypothesis of the theorem are verified so

$$\mu'_1(\Omega)(V) = g'(0^+) = \inf_{u \in X(0)} \partial_t G(0, u).$$

The last step is to compute $\partial_t G(0, u)$. To this purpose, we will need more regularity on the eigenfunctions $u \in E_1(\Omega)$ in order to compute second-order derivatives. By standard elliptic regularity results (see [52]), if Ω is of class \mathcal{C}^2 then the eigenfunctions associated to $\mu_1(\Omega)$ are in $\mathbf{H}^2(\Omega)$. The following lemma gives the main technical results to finish the computation of $\mu'_1(\Omega)(V)$:

Lemma 2.3.8. *Let Ω and V be as before and let $u \in \mathbf{H}^1(\Omega)$. Then :*

$$\partial_t \left(\int_{\Omega_t} (u \circ \psi_t^{-1})^2 \right)_{t=0} = \int_{\partial\Omega} u^2 (V \cdot n) - 2 \int_{\Omega} u (V \cdot \nabla u). \quad (2.10)$$

Moreover, suppose Ω is of class \mathcal{C}^2 and let $u \in \mathbf{H}^2(\Omega)$

$$\partial_t \left(\int_{\Omega_t} |\nabla(u \circ \psi_t^{-1})|^2 \right)_{t=0} = \int_{\partial\Omega} |\nabla u|^2 (V \cdot n) - 2 \int_{\Omega} \nabla u \cdot \nabla(V \cdot \nabla u) \quad (2.11)$$

Proof. First let prove (2.10) :

$$\begin{aligned}\partial_t \left(\int_{\Omega_t} (u \circ \psi_t^{-1})^2 \right)_{t=0} &= \partial_t \left(\int_{\Omega} \det(I + tV) u^2 \right)_{t=0} \\ &= \int_{\Omega} \operatorname{div}(V) u^2.\end{aligned}$$

Integrating and using Stokes formula on

$$\operatorname{div}(Vu^2) = \operatorname{div}(V)u^2 + 2u(V \cdot \nabla u)$$

we get

$$\int_{\Omega} \operatorname{div}(V)u^2 = \int_{\partial\Omega} u^2(V \cdot n) - 2 \int_{\Omega} u(V \cdot \nabla u).$$

Now let prove (2.11) :

$$\partial_t \left(\int_{\Omega_t} |\nabla(u \circ \psi_t^{-1})|^2 \right)_{t=0} = \int_{\Omega} A'(0) \nabla u \cdot \nabla u.$$

Using the two identities

$$\operatorname{div}(V|\nabla u|^2) = (\operatorname{div}V)|\nabla u|^2 + 2(\operatorname{Hess}u)\nabla u \cdot V$$

$$\nabla(V \cdot \nabla u) = (\operatorname{Hess}u)V + (\nabla V)\nabla u$$

the latter of which implies

$$2\nabla(V \cdot \nabla u) \cdot \nabla u = 2(\operatorname{Hess}u)\nabla u \cdot V + (\nabla V + (\nabla V)^T)\nabla u \cdot \nabla u$$

we get

$$A'(0)\nabla u \cdot \nabla u = \operatorname{div}(V|\nabla u|^2) - 2\nabla(V \cdot \nabla u) \cdot \nabla u$$

which after integration and Stokes formula leads to

$$\int_{\Omega} A'(0) \nabla u \cdot \nabla u = \int_{\partial\Omega} |\nabla u|^2(V \cdot n) - 2 \int_{\Omega} \nabla u \cdot \nabla(V \cdot \nabla u).$$

□

We can now finish the proof. Using

$$\mu'_1(\Omega)(V) = g(0^+) = \min_{u \in E_1(\Omega)} \partial_t G(0, u)$$

we can compute for $u \in E_1(\Omega)$

$$\begin{aligned}\partial_t G(0, u) &= \frac{\partial_t \left(\int_{\Omega_t} |\nabla(u \circ \psi_t^{-1})|^2 \right)_{t=0} \left(\int_{\Omega} u^2 \right) - \left(\int_{\Omega} |\nabla u|^2 \right) \partial_t \left(\int_{\Omega_t} (u \circ \psi_t^{-1})^2 \right)_{t=0}}{\left(\int_{\Omega} u^2 \right)^2} \\ &= \frac{\partial_t \left(\int_{\Omega_t} |\nabla(u \circ \psi_t^{-1})|^2 \right)_{t=0} - \mu_1(\Omega) \partial_t \left(\int_{\Omega_t} (u \circ \psi_t^{-1})^2 \right)_{t=0}}{\int_{\Omega} u^2} \\ &= \frac{\int_{\partial\Omega} (|\nabla u|^2 - \mu_1(\Omega)u^2)(V \cdot n)}{\int_{\Omega} u^2} - 2 \underbrace{\frac{1}{\int_{\Omega} u^2} \int_{\Omega} \nabla u \cdot \nabla(V \cdot \nabla u) - \mu_1(\Omega)u(V \cdot \nabla u)}_{=0}\end{aligned}$$

hence the result. □

Remark 2.3.9. To conclude, this method adapts well to the directional derivative of multiple eigenvalues, when Frechet differentiability fails. Moreover, it uses classical tools of calculus of variations (weak compactness, convexity...) and does not need to differentiate either the eigenvalue equation (2.1) nor the eigenvector associated to $\mu_1(\Omega_t)$ as it would be the case with the usual method based on the implicit function theorem (see for instance [67]).

Theorem 2.3.10. Let k and m be such that $\mu_{k-1}(\Omega) < \mu_k(\Omega) = \dots = \mu_{k+m-1}(\Omega) < \mu_{k+m}(\Omega)$ and Ω, V be as before. Then

$$\mu'_k(\Omega)(V) = \inf_{u \in E_k(\Omega)} \frac{\int_{\partial\Omega} (|\nabla u|^2 - \mu_1(\Omega)u^2) (V \cdot \mathbf{n})}{\int_{\Omega} u^2}.$$

Proof. The proof is similar to what have been done for μ_1 , except that we need to work on the space $\text{span}(\mathbf{1}, u_1, \dots, u_{k-1})^\perp$ instead of $\mathbf{1}^\perp$ where u_1, \dots, u_{k-1} are the eigenfunctions associated to $\mu_1(\Omega), \dots, \mu_{k-1}(\Omega)$. \square

Remark 2.3.11. In the previous theorem, we make the assumption that the eigenvalue we want to optimize is distinct from the lower one, which may not always be the case. In practice, we can see that when trying to maximize μ_k , the multiplicity comes always "from above", i.e. we are always within the assumptions of the previous theorem. This, however, is still an open problem [65].

Numerical considerations

When implementing a gradient-based optimization algorithm, this multiplicity will have to be taken into account. The simplest approach consists in ignoring completely the multiplicity by considering that $\mu_k(\Omega)$ is simple. Then the derivative is

$$\mu'_k(\Omega)(V) = \frac{\int_{\partial\Omega} (|\nabla u_k|^2 - \mu_1(\Omega)u_k^2) (V \cdot \mathbf{n})}{\int_{\Omega} u_k^2}$$

where u_k is an eigenfunction associated to $\mu_k(\Omega)$. We can then construct a vector field V which verifies

$$V|_{\partial\Omega} = (|\nabla u_k|^2 - \mu_1(\Omega)u_k^2) \mathbf{n}.$$

Under the assumption that $\mu_k(\Omega)$ is simple, for $t > 0$ small enough, we would have

$$\mu_k(\Omega_t) \approx \mu_k(\Omega) + t \underbrace{\mu'_k(\Omega)(V)}_{>0} > \mu_k(\Omega)$$

hence V is a good gradient direction. In practice, we observe that the eigenvalue is never simple near the optimum. It leads to instabilities that may prevent such gradient-based method from converging.

Another approach, developped in [50], really take advantage of the boundary expression (2.8) by searching at each step the "best" vector field V in the sense that it is chosen as the solution to the problem

$$\max_{\|V\|_{L^2(\partial\Omega)} \leq 1} \mu'_k(\Omega)(V)$$

which can be efficiently solved by Semi-Definite Programming procedures. We refer to the original paper for more informations.

In this thesis, we will see two other heuristic methods based on the regularization of the eigenvalue functionnal.

Shape derivative on the sphere

In the Chapter 5, we will actually make use of the concept of shape derivative for domains on the sphere. Since we will be moving on a curved surface we will need to change a bit our point of view on the variation of domains (based on perturbation of the identity) and adopt the so-called *velocity method* (see [51, Chap. 3], from which we borrow the notations). Indeed, let $V : \mathbb{S}^n \rightarrow T\mathbb{S}^n$ be a smooth enough vector field on the sphere. For all $x \in \mathbb{S}^n$, the flow of this vector field is defined as

$$\begin{cases} \chi'(x, t) = V(\chi(x, t)) \text{ for } (t, x_0) \in \mathbb{R}^+ \times \mathbb{R}^n \\ \chi(x, 0) = x \in \mathbb{S}^n \end{cases}$$

Let $\Omega \subseteq \mathbb{S}^n$ be a open Lipschitz domain. By putting $\psi_t = \chi(., t)$ for $t > 0$, we now define the domains $\Omega_t := \psi_t(\Omega)$ as the advection of the domain Ω by the flow of V , and the directional shape derivative of $\mu_k(\Omega)$ in the direction of V is defined as

$$\mu'(\Omega)(V) := \lim_{t \rightarrow 0^+} \frac{\mu_k(\Omega_t) - \mu_k(\Omega)}{t}.$$

Remark 2.3.12. In \mathbb{R}^n we can show that both approaches lead to the same first-order shape derivatives, as discussed in [51, Chap. 3].

The Theorem 2.3.10 may be reformulated as follows in the context of the sphere :

Theorem 2.3.13. Let $\Omega \subseteq \mathbb{S}^n$ a C^2 open set and $V : \mathbb{S}^n \rightarrow T\mathbb{S}^n$ a C^2 vector field. Let k and m be such that $\mu_{k-1}(\Omega) < \mu_k(\Omega) = \dots = \mu_{k+m-1}(\Omega) < \mu_{k+m}(\Omega)$. Then

$$\mu'_k(\Omega)(V) = \inf_{u \in E_k(\Omega)} \frac{\int_{\partial\Omega} (|\nabla u|^2 - \mu_1(\Omega)u^2) (V \cdot \mathbf{n})}{\int_{\Omega} u^2}.$$

where \mathbf{n} is the conormal to $\partial\Omega$ in \mathbb{S}^n .

2.4 Shape optimization by the level set method : basic ideas

All the previous section was based on the assumption that the topology of the original domain is preserved by the transformation ψ_t . In practice, one rarely knows the topology of the optimal domain (if it exists). From this point of view, it would be interesting to allow at least *some* change of topology during the optimization process. For this, a good representation of the shape is necessary. However, a given parametrization may be particularly inconvenient in representing complex topologies. For instance, one could represent a shape $\Omega \subseteq \mathbb{R}^2$ by a polar parametrization of its boundary $\rho : (0, 2\pi) \rightarrow \mathbb{R}^+$ by, for instance, a truncated Fourier series [28], but this would only allows for the representation of star-shaped domains. Another method consists in representing Ω by a mesh [90]; however the topology would stay the same during all the optimization. From this point of view, the possibility of topological changes is one of the main advantages of the so-called *level set method*. An introduction to the level set method applied to shape optimization is given in [6]. In this section, we recall the basic principles.

Suppose that we aim at optimizing the eigenvalue μ_k for domains on the sphere. As we have seen before, we would like to construct iteratively a sequence of domains $(\Omega_m)_{m \in \mathbb{N}}$ of \mathbb{S}^n such that for all m , $\Omega_{m+1} = \psi_{\delta t}^m(\Omega_m)$ where ψ_t^m is the flow of a well-chosen vector field $V_m : \mathbb{S}^n \rightarrow T\mathbb{S}^n$. At each step, V_m is found using the shape derivative of $\mu_k(\Omega_m)$ and δt is chosen in such a way that $\mu_k(\Omega_{m+1}) > \mu_k(\Omega_m)$. In the limit where $\delta t \rightarrow 0$, we formally get back a continuous family of domains Ω_t and of velocity fields $\mathcal{V}(t, x)$ advecting the domains

$$\begin{cases} \partial_t X(x, t) = \mathcal{V}(t, X(x, t)) \text{ for } (t, x) \in \mathbb{R}^+ \times \mathbb{S}^n \\ X(x, 0) = x \in \mathbb{S}^n \end{cases}$$

in such a way that $\Omega_t = X(\Omega_0, t)$. The main idea of the level set method is to represent this moving domain Ω_t as the zero sublevel set of a function ϕ :

$$\forall x \in \mathbb{S}^n, \forall t \in [0, T], \begin{cases} \phi(t, x) < 0 & \text{if } x \in \Omega_t \\ \phi(t, x) = 0 & \text{if } x \in \partial\Omega_t \\ \phi(t, x) > 0 & \text{if } x \in \mathbb{S}^n \setminus \Omega_t \end{cases}.$$

The advantage of this representation is that the motion of Ω_t is equivalent to the advection of ϕ by the equation

$$\partial_t \phi(t, x) + V(t, x) \cdot \nabla \phi(t, x) = 0.$$

During a single time step $[t_m, t_{m+1}]$, we can consider $V(t, x) \approx V_m(x)$ and solve

$$\partial_t \phi(t, x) + V_m(x) \cdot \nabla \phi(t, x) = 0$$

instead. At each time step, this equation can be solved using, for instance, the method of characteristics [52].

In practice, the level set method allows to evolve a function ϕ defined on a fix mesh of \mathbb{S}^n , saving the important computational cost of remeshing. This, however, is at the price of less precise computation since the boundary of the domain $\partial\Omega_t$ does not lie on the mesh. On the other hand, it is possible to remesh the interface $\partial\Omega_t$ at each step, gaining precision but losing performance; more on this in Chapter 5.

3

Maximization of Neumann eigenvalues in a class of densities

This chapter essentially comes from the paper [35].

Contents

3.1	Introduction	44
3.2	A global existence result for densities	47
3.3	Study of the one dimensional case	52
3.4	Pólya conjecture and Kröger inequalities	60
3.5	Numerical approximation of optimal densities	62

3.1 Introduction

We focus in this chapter on a class of problems which involve the spectrum of the Laplace operator with Neumann boundary conditions. Let $N \geq 1$ and $\Omega \subset \mathbb{R}^N$ be an open, bounded, Lipschitz set. As it has been seen in Chapter 2, the Laplace operator with Neumann boundary conditions has a spectrum consisting on eigenvalues, denoted (counting their multiplicities)

$$0 = \mu_0(\Omega) \leq \mu_1(\Omega) \leq \mu_2(\Omega) \leq \dots \rightarrow +\infty.$$

and by the Courant-Fisher formula, every $k \geq 1$, we have

$$\mu_k(\Omega) = \min_{S \in \mathcal{S}_{k+1}} \max_{u \in S \setminus \{0\}} \frac{\int_{\Omega} |\nabla u|^2 dx}{\int_{\Omega} u^2 dx},$$

where \mathcal{S}_k is the family of all subspaces of dimension k in $H^1(\Omega)$. Then, for some $u \in H^1(\Omega) \setminus \{0\}$

$$\begin{cases} -\Delta u = \mu_k(\Omega)u \text{ in } \Omega, \\ \frac{\partial u}{\partial n} = 0 \text{ on } \partial\Omega, \end{cases}$$

in a weak sense (which is also strong as soon as Ω is of class C^2).

We are concerned with the following shape optimization problem: given $m > 0$, solve

$$\max \{\mu_k(\Omega) : \Omega \subset \mathbb{R}^N, \Omega \text{ bounded, open and Lipschitz, } |\Omega| = m\}. \quad (3.1)$$

This question is, in general, open. For the Laplace operator with Dirichlet boundary conditions, the similar (minimizing) question has been intensively investigated in last 30 years. Since the seminal existence result by Buttazzo and Dal Maso [38], a series of results, both of analytical and numerical type, have been obtained (see the recent survey [68]). In the Dirichlet case, the description of relaxed problems is known. This is due to full understanding of the Gamma convergence limits for the energy functionals (and hence of the spectrum), while local analysis by free boundary techniques leads to qualitative information on the optimal shapes. If Dirichlet boundary conditions are replaced by Neumann conditions, as in problem (3.1), several deep, new difficulties appear, changing completely the nature of the problem.

First, on nonsmooth domains the resolvent of the Neumann Laplacian is not necessarily compact, so that the spectrum may not consist on eigenvalues. Keeping track of the Lipschitz character of a maximizing sequence is an impassable challenge. Second, there is no Gamma convergence description of limits of the energy functionals, and even if such a result was available, it would not be enough for the control of the spectrum, because of the absence of collective compactness of Sobolev spaces $H^1(\Omega)$ in $L^2(\mathbb{R}^N)$. Third, local analysis to search some regularity of the free boundary seems out of reach, since problem (3.1) is of max-min-max type; consequently, one can not test maximality by local perturbations of the eigenfunctions. Fourth, the absence of any interface energy makes the final answer different from the case of Dirichlet (or Robin) boundary conditions, being unclear: for some values of k optimal shapes do exist, while for others, this may not be the case.

Another point of interest in problem (3.1) is related to the long standing Pólya conjecture, which states that

$$\forall k \in \mathbb{N}, \quad \mu_k(\Omega) \leq \frac{4\pi^2 k^2}{(\Omega_N |\Omega|)^{\frac{2}{N}}}.$$

This inequality is known to hold only for some particular domains in \mathbb{R}^N , like those tiling the space [78] or with a particular geometric structure [57]. In general, for arbitrary domains, it has only been proved for $k = 1, 2$. Any qualitative information on the solution to problem (3.1) may provide useful information on the Pólya conjecture.

Coming back to Problem (3.1), let us briefly recall the known results. For $k = 1$ the solution of problem (3.1) corresponds to a ball of volume m . This was proved by Szegő [98] (for smooth simply connected domains in \mathbb{R}^2) and by Weinberger [103] (for Lipschitz domains in \mathbb{R}^N). For $k = 2$ the solution is the union of two disjoint equal balls. This result was proved in \mathbb{R}^2 for smooth simply connected sets by Girouard, Nadirashvili and Polterovich in [60] and for general domains in \mathbb{R}^N by Bucur and Henrot in [33]. As a consequence, the Pólya conjecture holds for $k = 1, 2$. In this direction, for $k \geq 3$ Kröger found in [73] a series of bounds larger than the conjectured ones, however, respecting the growth of the Weyl law.

Although it puzzled the spectral geometry community in the last years, problem (3.1) remains largely open for $k \geq 3$ (and $N \geq 2$). We can only refer to several numerical approximations of suspected geometries

which maximize μ_k , see for instance [8, 9, 25], but the optimal geometries are not even proved to exist! The case $N = 1$ is trivial and the answer is the union of k segments of length $\frac{m}{k}$ (possibly joining at their extremities).

The main observation motivating this chapter comes from [33]. Precisely, there it is proved for $k = 1, 2$ that the optimal geometries (a ball, two equal balls, respectively) are in fact optimal in the larger class of (possibly degenerate) densities satisfying a mass constraint. In this class, a Lipschitz set is identified with the density equal to its characteristic function. Out of this observation, a natural question emerges: is this phenomenon true for every k ? A positive answer would open the way to the proof of existence of optimal sets in (3.1) for every k , while a negative answer would even raise more questions.

Let $\rho : \mathbb{R}^N \rightarrow [0, 1]$ be a measurable function such that $0 < \int_{\mathbb{R}^N} \rho dx < +\infty$. We consider the *possibly degenerate* eigenvalue problem defined via the relaxation of the Rayleigh quotient: for every integer $k \geq 0$, we set

$$\mu_k(\rho) := \inf_{S \in \mathcal{S}_{k+1}} \max_{u \in S} \frac{\int_{\mathbb{R}^N} \rho |\nabla u|^2 dx}{\int_{\mathbb{R}^N} \rho u^2 dx}, \quad (3.2)$$

where \mathcal{S}_{k+1} is the family of all subspaces of dimension $k+1$ in

$$\{u \cdot 1_{\{\rho(x) > 0\}} : u \in C_c^\infty(\mathbb{R}^N)\}. \quad (3.3)$$

Clearly, if ρ satisfies some suitable assumptions (for instance if it equals the characteristic function of a bounded, open, Lipschitz set or if it is a Gaussian measure in \mathbb{R}^N , etc.), the Rayleigh quotient above leads to a classical spectrum associated to a positive, self-adjoint, compact operator. If ρ is just arbitrary, the definition (3.2) itself is correct in the sense that the numbers $\mu_k(\rho)$ are well defined, but there is no an interpretation in terms of the spectrum of a well defined operator. By abuse of language, we still call them *eigenvalues of the density ρ* .

It is natural to consider the (relaxed) problem

$$\sup \left\{ \mu_k(\rho) : \rho : \mathbb{R}^N \rightarrow [0, 1], \int_{\mathbb{R}^N} \rho dx = m \right\}, \quad (3.4)$$

or its scale invariant version

$$\mu_k^* := \sup \left\{ \left(\int_{\mathbb{R}^N} \rho dx \right)^{\frac{2}{N}} \mu_k(\rho) : \rho : \mathbb{R}^N \rightarrow [0, 1] \right\}, \quad (3.5)$$

and to observe that, in general, this value is not smaller than the one given by problem (3.1), from the simple fact that the class of Lipschitz sets is implicitly contained in the class of densities. In [33] it was proved that for $k = 1, 2$ problems (3.1) and (3.4) are indeed equivalent, the maximizers being the same, corresponding to one and two equal balls, respectively.

This observation raises several questions.

Does problem (3.5) have a solution? Our first result is that problem (3.5) has a solution in \mathbb{R}^N possibly consisting in a *collection* of at most k densities.

Theorem 3.1.1. *The maximal value μ_k^* in (3.5) is attained. Precisely, there exist $j \in \mathbb{N}$, $j \leq k$, $\rho_1, \dots, \rho_j : \mathbb{R}^N \rightarrow [0, 1]$ and $n_1, \dots, n_j \in \mathbb{N}$ with $n_1 + \dots + n_j = k+1-j$ such that*

$$\sum_{i=1}^j \int_{\mathbb{R}^N} \rho_i dx = 1 \quad \text{and} \quad \mu_k^* = \mu_{n_1}(\rho_1) = \dots = \mu_{n_j}(\rho_j).$$

Note that each ρ_i is optimal for the maximization of μ_{n_i} under its own mass constraint. This property is straightforward; we refer to the paper by Wolf and Keller [105] to describe the phenomenon.

Related to the distribution of eigenvalues, the notion of collection of densities in Theorem 3.1.1 plays a similar role as the connected components of an open set. We also point out that the existence result above extends to general functionals of eigenvalues

$$\rho \rightarrow F(\mu_1(\rho), \dots, \mu_k(\rho)),$$

where F is nondecreasing in each variable and upper semicontinuous. The key technical point in the proof of Theorem 3.1.1 is to get some control of the concentration of mass for a maximizing sequence of densities;

this is a difficult task because of the absence of any interface energy. In general, we are not able to prove or disprove the nondegeneracy of optimal densities.

Following [33], for $k = 1, 2$ problems (3.1) and (3.4) are equivalent. For $k \geq 3$, not only this is a highly challenging question which requires regularity analysis of optimal densities, but the answer might be negative, as our numerical results suggest. To this question, we give a complete answer in dimension one of the space, i.e. for $N = 1$, where we prove that an optimal density corresponds to a union of equal segments of lengths $\frac{m}{k}$, possibly touching at their extremities.

Theorem 3.1.2 (One dimension of the space). *In \mathbb{R} , $\forall k \in \mathbb{N}$*

$$\mu_k^* = \pi^2 k^2.$$

Equality is attained for ρ being the characteristic function associated to the union of at most k open, pairwise disjoint segments of total length equal to $m := \int_{\mathbb{R}} \rho dx$, each one with length an entire multiple of $\frac{m}{k}$.

The argument requires fine arguments from topological degree theory and, in fact, leads to a slightly stronger inequality (see Lemma 3.3.4). In particular, Theorem 3.1.2 provides sharp upper bounds for Sturm-Liouville eigenvalues (see [74] for a related problem involving concave density functions).

Does the Pólya conjecture hold for densities? A second consequence of Theorem 3.1.2 is the validity of the Pólya conjecture for densities. Precisely, for every $\rho \in \mathbf{L}^1(\mathbb{R}, [0, 1])$ we have

$$\forall k \in \mathbb{N}, \mu_k(\rho) \leq \frac{\pi^2 k^2}{\left(\int_{\mathbb{R}} \rho dx \right)^2}.$$

A natural question is whether for every $N \geq 2$ the Pólya conjecture holds for densities in \mathbb{R}^N

$$\forall k \in \mathbb{N}, \mu_k(\rho) \leq \frac{4\pi^2 k^{\frac{2}{N}}}{(\Omega_N \int_{\mathbb{R}^N} \rho dx)^{\frac{2}{N}}}?$$

While for $k = 1, 2$ the inequality is true, we prove that the estimates obtained by Kröger [73] in the classical setting, continue to hold for densities. This result brings support to the thesis that the Pólya conjecture might hold for densities. With respect to the classical setting, the main improvement is that an optimal density does exist for each k !

Theorem 3.1.3 (Kröger estimates for densities). *Let $N \geq 2$, $\rho \in \mathbf{L}^1(\mathbb{R}^N) \cap \mathbf{L}^\infty(\mathbb{R}^N, \mathbb{R}^+)$, $\rho \not\equiv 0$. Then*

$$\forall k \in \mathbb{N}, \mu_k(\rho) \leq 4\pi^2 \left(\frac{(N+2)k}{2\Omega_N} \frac{\|\rho\|_\infty}{\|\rho\|_1} \right)^{2/N},$$

where Ω_N is the volume of the unit ball of \mathbb{R}^N .

What is the geometry of the optimal densities? We build up a numerical approach and give approximations of optimal densities in \mathbb{R}^2 , for $k = 1, \dots, 8$. Contrary to the shape optimization problem (3.1), our numerical procedure is justified and, formally, leads to an approximation of the solution. A natural question is to compare our optimal densities with the previous results for optimal shapes from [8, 9, 25]. For $k = 1, 2$ we recover the theoretical results proved in [33], while for $k = 3, \dots, 8$ the numerical values for the optimal densities are quite close to the optimal values for domains from [8, 9, 25], being, as expected, larger. Moreover, the densities are close to be characteristic functions. However, some surprising non simply connected geometries of their level sets are observed for $k = 5$ and $k = 8$, suggesting that the numerical optimal shapes previously known could be improved. Although we can not rigorously justify that the optimal densities do not correspond to domains for $k = 3, \dots, 8$, the numerical computations seem to suggest this fact.

The chapter is organized as follows. In Section 3.2 we prove Theorem 3.1.1, Section 3.3 contains the analysis of the one dimensional case with the proof of Theorem 3.1.2, Section 3.4 contains the discussion about the Pólya conjecture and the proof of Theorem 3.1.3 while Section 5 is dedicated to the numerical computations.

3.2 A global existence result for densities

For every $m > 0$ and open set $D \subset \mathbb{R}^N$, let us denote

$$\begin{aligned}\mathbf{L}^1(D, [0, 1]) &:= \{\rho : D \rightarrow [0, 1] : \rho \in \mathbf{L}^1(D)\} \\ \mathbf{L}_m^1(D, [0, 1]) &:= \left\{ \rho \in \mathbf{L}^1(D, [0, 1]) : \int_D \rho dx = m \right\}.\end{aligned}$$

In order to analyse existence of a solution to Problem (3.5) in $\mathbf{L}^1(\mathbb{R}^N, [0, 1])$ the main technical difficulty is related to handling the behavior of densities with unbounded support. For instance, if $(\rho_n)_n$ is a maximizing sequence such that, after possible translations, there exists a ball which contains all supports of ρ_n , then the existence of an optimal density would follow immediately as a consequence of an upper semicontinuity result for \mathbf{L}^∞ weak-* convergence of densities (Lemma 3.3.3 below) and the preservation of the constraint at the limit. Nevertheless, a maximizing sequence could, a priori, have densities with very large, or unbounded support. In this case, the upper semicontinuity result still works, but it is not enough to prove existence. In fact, there is no guarantee that a limit density does satisfy the constraint since the constant function 1 does not belong to $\mathbf{L}^1(\mathbb{R}^N)$. In other words, to prove that the constraint is satisfied by a limit density one should gather qualitative information on the maximizing sequence itself. Our idea is to prove that a maximizing sequence enjoys some mass concentration properties around at most k spots. Contrary to the case of Dirichlet boundary conditions we can not perform a surgery of the domains in order to remove possibly insignificant parts of a density (for instance long and thin tails of their support). This is a consequence of the max-min-max structure of Problem (3.5).

There is a second issue related to the behavior of the spectrum for disconnected sets. The maximizer of μ_2 is known to be the union of two equal balls. The spectrum of the union of balls is the union of spectra of each ball, multiplicity being counted. In case of densities, we have to mimic this behaviour in terms of a collection of densities, since the notion of connectedness is somehow unclear.

We begin with technical upper semicontinuity result. Below, by convention, if $\rho = 0$ then $\forall k \geq 0, \mu_k(\rho) = +\infty$.

Lemma 3.2.1. *Assume $\rho, \rho_n \in \mathbf{L}^1(\mathbb{R}^N, [0, 1])$ satisfy $\rho_n \rightharpoonup \rho$ weak-* in $\mathbf{L}^\infty(\mathbb{R}^N)$. Then*

$$\forall k \geq 1, \mu_k(\rho) \geq \limsup_{n \rightarrow +\infty} \mu_k(\rho_n).$$

Proof. The proof of the result is standard. Assume $\rho \neq 0$, otherwise the inequality is trivially true. Let $\varepsilon > 0$ be fixed and let $S = \text{span}\{u_0 1_{\{\rho > 0\}}, \dots, u_k 1_{\{\rho > 0\}}\}$ with $u_0, \dots, u_k \in C_c^\infty(\mathbb{R}^N)$ be an admissible subspace for the computation of $\mu_k(\rho)$ such that

$$\mu_k(\rho) \geq \max_{u \in S \setminus \{0\}} \frac{\int_{\mathbb{R}^N} |\nabla u|^2 \rho dx}{\int_{\mathbb{R}^N} u^2 \rho dx} - \varepsilon.$$

For each index n , assume that

$$u_n := \sum_{i=0}^k \alpha_i^n u_i$$

attains the maximum of

$$\max_{u \in S^n \setminus \{0\}} \frac{\int_{\mathbb{R}^N} |\nabla u|^2 \rho_n dx}{\int_{\mathbb{R}^N} u^2 \rho_n dx},$$

where $S^n = \text{span}\{u_0 1_{\rho_n > 0}, \dots, u_k 1_{\rho_n > 0}\}$. Note that for n large, this space is of dimension $k+1$ so that $\mu_k(\rho_n) \leq \max_{u \in S^n \setminus \{0\}} \frac{\int_{\mathbb{R}^N} |\nabla u|^2 \rho_n dx}{\int_{\mathbb{R}^N} u^2 \rho_n dx}$. Without restricting the generality, we may assume that

$$\sum_{i=0}^k (\alpha_i^n)^2 = 1, \quad \alpha_i^n \rightarrow \alpha_i.$$

Denoting $\tilde{u} := \sum_{i=0}^k \alpha_i u_i$, we have

$$\lim_{n \rightarrow +\infty} \int_{\mathbb{R}^N} |\nabla u_n|^2 \rho_n dx = \int_{\mathbb{R}^N} |\nabla \tilde{u}|^2 \rho dx \quad \text{and} \quad \lim_{n \rightarrow +\infty} \int_{\mathbb{R}^N} u_n^2 \rho_n dx = \int_{\mathbb{R}^N} \tilde{u}^2 \rho dx, \quad (3.6)$$

so that

$$\mu_k(\rho) + \varepsilon \geq \limsup_{n \rightarrow +\infty} \mu_k(\rho_n).$$

Taking $\varepsilon \rightarrow 0$, we conclude the proof. \square

Collection of densities.

Given the non-zero densities $\rho_1, \rho_2, \dots, \rho_j$, we formally denote their collection as

$$\bar{\rho} = \rho_1 \sqcup \rho_2 \sqcup \cdots \sqcup \rho_j$$

and define the eigenvalues of the collection, as follows. We consider the family of eigenvalues of each density, take their union

$$\bigcup_{i=1}^j \{\mu_k(\rho_i) : k \geq 0\},$$

keep track of multiplicity and relabel them $\mu_k(\bar{\rho})$ in increasing order. It can be easily noticed that $\mu_0(\bar{\rho}) = \mu_1(\bar{\rho}) = \cdots = \mu_{j-1}(\bar{\rho}) = 0$.

Of course, if the supports of ρ_i are all bounded, then we can build a density ρ in \mathbb{R}^N such that $\mu_k(\rho) = \mu_k(\bar{\rho})$ by just translating the supports of each density, to place them pairwise at strictly positive distance. If at least one support is unbounded, we are not, in general, able to build such a density.

Let $\bar{\rho} = \rho_1 \sqcup \rho_2 \sqcup \cdots \sqcup \rho_j$ and let $\bar{\rho}' = \rho_1 \sqcup \rho_2 \sqcup \cdots \sqcup \rho_{j-1}$. Then, from the definition,

$$\forall k \geq 1, \mu_k(\bar{\rho}) \leq \mu_k(\bar{\rho}').$$

In other words, if we drop a component of $\bar{\rho}$, the eigenvalues can not decrease. We have the following.

Lemma 3.2.2. Assume $\rho_n \in \mathbf{L}^1(\mathbb{R}^N, [0, 1])$ is such that $\rho_n = \rho_n^0 + \rho_n^1 + \cdots + \rho_n^j$, $\int_{\mathbb{R}^N} \rho_n^0 dx \rightarrow 0$, and for every $l = 1, \dots, j$, for some sequences $(y_n^l)_n$ we have $\rho_n^l(y_n^l + \cdot) \rightharpoonup \rho^l$ weak-* in $\mathbf{L}^\infty(\mathbb{R}^N)$. Assume that for all $1 \leq l \neq h \leq j$, $\text{dist}(\{\rho_n^l > 0\}, \{\rho_n^h > 0\}) \rightarrow +\infty$. Then, denoting $\bar{\rho} = \rho_1 \sqcup \rho_2 \sqcup \cdots \sqcup \rho_j$, we have

$$\forall k \geq 1, \mu_k(\bar{\rho}) \geq \limsup_{n \rightarrow +\infty} \mu_k(\rho_n).$$

Proof. By definition, there exists k_1, \dots, k_j such that $k_1 + \cdots + k_j + (j - 1) = k$ and

$$\mu_k(\bar{\rho}) = \mu_{k_1}(\rho_1),$$

$$\forall l = 1, \dots, j, \mu_{k_l+1}(\rho_l) \geq \mu_k(\bar{\rho}) \geq \mu_{k_l}(\rho_l).$$

We follow the same arguments as in Lemma 3.2.1. For some $\varepsilon > 0$, we choose $\forall l = 1, \dots, j$, $u_0^l, \dots, u_{k_l}^l$, such that $S_{k_l+1}^l = \text{span}\{u_0^l 1_{\rho_l > 0}, \dots, u_{k_l}^l 1_{\rho_l > 0}\}$ is of dimension $k_l + 1$ and satisfies

$$\mu_{k_l}(\rho_l) \geq \max_{u \in S_{k_l+1}^l \setminus \{0\}} \frac{\int_{\mathbb{R}^N} |\nabla u|^2 \rho_l dx}{\int_{\mathbb{R}^N} u^2 \rho_l dx} - \varepsilon.$$

For each $l = 1, \dots, j$, for each index n , we consider the set of test functions $\{u_i^l(\cdot - y_n^l) : l = 1, \dots, j, i = 0, \dots, k_l\}$. For n large enough, the dimensions of $S_{k_l+1}^{n,l} = \text{span}\{u_0^l(\cdot - y_n^l) 1_{\rho_n > 0}, \dots, u_{k_l}^l(\cdot - y_n^l) 1_{\rho_n > 0}\}$ equal $k_l + 1$. Since the supports of u_i^l are bounded and $\text{dist}(\{\rho_n^l > 0\}, \{\rho_n^h > 0\}) \rightarrow +\infty$, the space

$$S^n = \text{span}\{u_i^l(\cdot - y_n^l) 1_{\rho_n > 0} : l = 1, \dots, j, i = 0, \dots, k_l\}$$

is of dimension $k + 1$ and for every $l \neq s$ the supports of $u_i^l(\cdot - y_n^l)$ and $u_r^s(\cdot - y_n^s)$ are disjoint so that

$$\mu_k(\rho_n) \leq \max_{u \in S^n \setminus \{0\}} \frac{\int_{\mathbb{R}^N} |\nabla u|^2 \rho_n dx}{\int_{\mathbb{R}^N} u^2 \rho_n dx}.$$

Following the same arguments as in Lemma 3.2.1 applied for every $l = 1, \dots, j$, we conclude the proof. \square

In order to prove Theorem 3.1.1, we formulate the following problem

$$\max \left\{ \mu_k(\bar{\rho}) : \bar{\rho} = \rho_1 \sqcup \rho_2 \sqcup \cdots \sqcup \rho_k, \rho_j : \mathbb{R}^N \rightarrow [0, 1], \sum_{j=1}^k \int_{\mathbb{R}^N} \rho_j dx = m \right\}. \quad (3.7)$$

Of course, a solution may have $k - 1$ vanishing densities, in which case their eigenvalues equal $+\infty$ and they do not contribute to the computation of $\mu_k(\bar{\rho})$. Roughly speaking, the number of nonzero densities in the maximization of μ_k can not exceed k , otherwise μ_k equals to 0. The number of nonvanishing densities mimics the number of the connected components of an optimal set.

Proof of Theorem 3.1.1. The case $k = 1, 2$ is known from [33]. Let fix $k \geq 3$ and note that if we consider two different values of m , the solutions will be the same, up to some rescaling. In order to prove Theorem 3.1.1, we start with several technical results. We recall the following result from [61, Corollary 3.12].

Lemma 3.2.3 (Grigor'yan-Netrusov-Yau). *Let $\rho \in \mathbf{L}_m^1(\mathbb{R}^N, [0, 1])$. There exists a dimensional constant c_N and k annuli $(A_{x_i, r_i, R_i})_{i=1, k}$ such that*

$$\forall i = 1, \dots, k, \int_{A_{x_i, r_i, R_i}} \rho dx \geq \frac{c_N m}{k},$$

$(A_{x_i, \frac{r_i}{2}, 2R_i})_{i=1, k}$ are pairwise disjoint.

Below, we give a first result relating the value of the k -th eigenvalue of ρ to its concentration of mass.

Lemma 3.2.4 (Geometric control of the spectrum). *Let $\rho \in \mathbf{L}_m^1(\mathbb{R}^N, [0, 1])$ such that $\mu_k(\rho) > 0$. There exists a ball \mathbf{B}_{x, R^*} with*

$$R^* = \sqrt{\frac{4(k+1)}{c_N \mu_k(\rho)}}$$

such that

$$\int_{\mathbf{B}_{x, R^*}} \rho dx \geq \frac{c_N m}{k+1}.$$

The meaning of this result is the following: if $\mu_k(\rho)$ is large (as we expect it as a maximizer), then an important fraction of the mass of ρ concentrates on a ball of small, controlled radius R^* .

Proof. We start by applying Lemma 3.2.3 for $k+1$ and get the annuli $(A_{x_i, r_i, R_i})_{i=1, k+1}$ such that $(A_{x_i, \frac{r_i}{2}, 2R_i})_{i=1, k+1}$ are pairwise disjoint and

$$\forall i = 1, \dots, k+1, \int_{A_{x_i, r_i, R_i}} \rho dx \geq \frac{c_N m}{k+1}.$$

We perform the following transformation of the annuli: if A_{x_i, r_i, R_i} does not contain another annulus inside (i.e. inside the ball \mathbf{B}_{x_i, r_i}) we fill it and replace it with the ball \mathbf{B}_{x_i, R_i} (roughly speaking corresponding to $r_i = 0$). The statement of Lemma 3.2.3 continues to be valid. From now on, we work with this new family of annuli.

We claim that for every $r_i > 0$ there exists some R_j such that

$$R_j < r_i. \quad (3.8)$$

Indeed, since $r_i > 0$, in view of our transformation above, inside the ball \mathbf{B}_{x_i, r_i} there should be another annulus A_{x_j, r_j, R_j} , so that $R_j < r_i$.

Let us denote

$$R^* = \min\{r_i, r_i > 0\} \cup \{R_j : j = 1, \dots, k+1\}.$$

In view of the previous observation, R^* equals some R_j . We build the following test functions.

- On an annulus $A_{x_i, \frac{r_i}{2}, 2R_i}$

$$\varphi_i(x) = \begin{cases} 1 & \text{if } x \in A_{x_i, r_i, R_i} \\ \frac{d(x, \mathbf{B}_{x_i, \frac{r_i}{2}})}{\frac{r_i}{2}} & \text{if } x \in A_{x_i, \frac{r_i}{2}, R_i} \\ \frac{d(x, \mathbf{B}_{x_i, 2R_i}^c)}{R_i} & \text{if } x \in A_{x_i, R_i, 2R_i} \\ 0 & \text{elsewhere.} \end{cases} \quad (3.9)$$

- On a ball \mathbf{B}_{x_i, R_i}

$$\varphi_i(x) = \begin{cases} 1 & \text{if } x \in \mathbf{B}_{x_i, R_i} \\ \frac{d(x, \mathbf{B}_{x_i, 2R_i}^c)}{R_i} & \text{if } x \in A_{x_i, R_i, 2R_i} \\ 0 & \text{elsewhere.} \end{cases} \quad (3.10)$$

Then for every φ defined above we have

$$\forall x \in \mathbb{R}^N, |\nabla \varphi(x)| \leq \frac{2}{R^*},$$

$$\int |\nabla \varphi|^2 \rho dx \leq \frac{4m}{(R^*)^2},$$

$$\int \varphi^2 \rho dx \geq \frac{c_N m}{k+1}.$$

Since all functions φ_i have pairwise disjoint support, we can use them as test for μ_k and get

$$\mu_k(\rho) \leq \frac{\frac{4m}{(R^*)^2}}{\frac{c_N m}{k+1}}.$$

This implies

$$R^* \leq \sqrt{\frac{4(k+1)}{c_N \mu_k(\rho)}}.$$

In view of (3.8), R^* is attained by some R_j , so that the ball \mathbf{B}_{x_j, R_j} satisfies the conclusion of the lemma. \square

Lemma 3.2.5 (Enhanced geometric control of the spectrum). *Let $\rho \in \mathbf{L}_m^1(\mathbb{R}^N, [0, 1])$ such that $\rho = \rho_0 + \rho_1 + \dots + \rho_j$ and let $R > 0$. Assume that*

$$\forall 1 \leq l \neq i \leq j, \text{ dist}(\{\rho_l > 0\}, \{\rho_i > 0\}) \geq 3R.$$

Moreover, assume $\forall 1 \leq l \leq j, m_l = \int \rho_l dx > 0$ and denote $m_0 = \int \rho_0 dx$.

Then, for every $l \in 1, \dots, j$, there exists $R_l^* > 0$ and $x_l \in \mathbb{R}^N$ satisfying

$$\frac{1}{R_l^*} \geq \left[\frac{1}{2} \left(\frac{\mu_k(\rho) c_N m_l}{(k+1)(m_l + m_0)} \right)^{\frac{1}{2}} - \frac{1}{2R} \right]^+ \quad (3.11)$$

and

$$\int_{\mathbf{B}_{x_l, R_l^*}} \rho_l \geq \frac{c_N m_l}{k+1}.$$

This lemma gives a control on the concentration of masses in a dichotomy situation. If $\mu_k(\rho)$ is not small, then on every large region where there is some positive mass of ρ , there should also be some concentration of this mass on a ball with controlled radius, the control being in terms of $\mu_k(\rho)$.

Proof. We rely again on Lemma 3.2.3 which is applied separately for each ρ_l , $1 \leq l \leq j$ and for $k+1$. As previously, we fill the annuli if they do not contain any other and define R_l^* in a similar way. The test functions φ are build as in (3.9)-(3.10) with the following new constraint: for ρ_l we take the minimum between each φ_i and $1 - \frac{d(x, \{\rho_l > 0\}) \wedge R}{R}$,

In this way, the supports of the test functions for $l \neq i$ do not intersect and their gradient is still controlled by $\frac{2}{R_l^*} + \frac{1}{R}$. Then

$$\mu_k(\rho) \leq \frac{\left(\frac{2}{R_l^*} + \frac{1}{R} \right)^2 (m_l + m_0)}{\frac{c_N m_l}{k+1}},$$

which leads to inequality (3.11). \square

Proof. (of Theorem 3.1.1, continuation) Consider $(\bar{\rho}_n)_n$, a maximising sequence for problem (3.7),

$$\bar{\rho}_n = \rho_1 \sqcup \rho_2 \sqcup \dots \sqcup \rho_k.$$

In view of the definition of the eigenvalue of $\bar{\rho}_n$, we can identify the densities ρ_n^j such that $\int \rho_n^j dx \rightarrow 0$. If this is the case, we just drop them out without decreasing the k -th eigenvalue. The new sequence is also maximizing (possibly after rescalings in order to satisfy the mass constraint) but with less components. For this new maximizing sequence, up to extracting a subsequence and reliable the densities composing $\bar{\rho}_n$, we get that for $1, \dots, j$, with $j \leq k$, that

$$\int \rho_n^j dx \rightarrow m_j > 0$$

and $(\rho_n^j)_n$ is maximizing sequence for problem (3.7), associated to some eigenvalue index k_j and mass m_j .

Relabeling again the indices, it is enough to consider only the case in which a sequence of densities $(\rho_n)_n$ complemented by 0, i.e. $\bar{\rho}_n = \rho_n \sqcup 0 \sqcup \dots \sqcup 0$ is maximizing for problem (3.7) (possibly with a different k and m), hence

$$\mu_k(\rho_n) \rightarrow \sup \{ \mu_k(\rho) : \rho \in \mathbf{L}_m^1(\mathbb{R}^N, [0, 1]) \} > 0.$$

Then $\int_{\mathbb{R}^N} \rho_n dx = m$. We shall use the concentration compactness principle of P.-L. Lions [82] to describe the behaviour of the sequence $(\rho_n)_n$. There are three possibilities.

1. *Compactness.* There exists a subsequence $(\rho_{n_j})_j$ and a sequence of vectors $y_{n_j} \in \mathbb{R}^N$ such that

$$\rho_{n_j} \rightharpoonup \rho, \text{ weakly-* in } L^\infty(\mathbb{R}^N)$$

and $\int_{\mathbb{R}^N} \rho dx = m$. Since

$$\mu_k(\rho) \geq \limsup_{j \rightarrow +\infty} \mu_k(\rho_{n_j}),$$

we conclude with the optimality of ρ from Lemma 3.2.1, since ρ satisfies the mass constraint.

- 2 *Vanishing.* For every $R > 0$, we have that

$$\sup_{y \in \mathbb{R}^N} \int_{B(y, R)} \rho_n dx \rightarrow 0, \text{ when } n \rightarrow +\infty.$$

This situation can not occur for a maximizing sequence, as a consequence of the geometric control of the spectrum, Lemma 3.2.4. Indeed, we know that there exists R^* such that

$$\int_{B_{y_n, R^*}} \rho_n \geq \frac{c_N m}{k+1}$$

uniform in n , as soon as $\mu_k(\rho_n) \geq M > 0$, which is expected from a maximizing sequence.

3. *Dichotomy.* As vanishing does not occur, we know that there exists a concentration of mass somewhere. Assume that for some subsequence and some translations if necessary we have some concentration of mass

$$m > m_1 = \lim_{R \rightarrow +\infty} \lim_{n \rightarrow +\infty} \sup_y \int_{B_{y, R}} \rho_n dx > 0.$$

Then for a subsequence, still denoted with the same index, we find a density ρ_1 such that

$$\rho_n \rightharpoonup \rho_1, \text{ weakly-* in } L^\infty(\mathbb{R}^N), \int_{\mathbb{R}^N} \rho_1 dx = m_1.$$

We define R_n such that $\int_{B_{R_n}} \rho_n dx \geq m_1 - \frac{1}{n}$ and define

$$\rho_n^2 = \rho_n|_{B_{3R_n}} \text{ and } \rho_n^0 = \rho_n - \rho_n^1 - \rho_n^2.$$

Then, $R_n \rightarrow +\infty$,

$$\int_{\mathbb{R}^N} \rho_n^2 dx \rightarrow m - m_1 > 0 \text{ and } \int_{\mathbb{R}^N} \rho_n^0 dx \rightarrow 0.$$

In view of the enhanced geometric control of the spectrum, Lemma 3.2.5, the sequence of densities $(\rho_n^2)_n$ has also a concentration of mass on balls of uniform radius. Let us denote the maximal mass concentration $m_2 > 0$.

If $m_2 = m - m_1$, this means that the sequence $(\rho_n^2)_n$ satisfies the compactness assumption, so we get a limit ρ^2 . Then $\bar{\rho} = \rho_1 \cup \rho_2$ is optimal using the upper semicontinuity result from Lemma 3.2.2 since it satisfies the mass constraint.

If $m_2 < m - m_1$, we continue the process and find another concentration of mass, and so on. This procedure stops after at most k steps, since a density with $k+1$ disjoint concentrations of mass has the k -th eigenvalue equal to 0, so it is not maximizing.

□

Remark 3.2.6. Let $F : \mathbb{R}_+^k \rightarrow \mathbb{R}$ be upper semicontinuous and non decreasing in each variable. Then the following problem

$$\max\{F(\mu_1(\bar{\rho}), \dots, \mu_k(\bar{\rho})) : \bar{\rho} = \rho_1 \sqcup \rho_2 \sqcup \dots \sqcup \rho_k, \rho_j : \mathbb{R}^N \rightarrow [0, 1], \sum_{j=1}^k \int_{\mathbb{R}^N} \rho_j dx = m\}$$

has a solution. A typical example is

$$F(\mu_1(\bar{\rho}), \dots, \mu_k(\bar{\rho})) = \sum_{i=1}^k \mu_i(\bar{\rho}).$$

The proof does not require any further argument with respect to Theorem 3.1.1.

3.3 Study of the one dimensional case

This section is devoted to the proof of Theorem 3.1.2. The most of results of this section are one dimensional. However, some technical points hold true in any dimension of the space. If this is the case, we shall state the results in the most general framework.

The proof of Theorem 3.1.2 has two distinctive parts. In the first part, we shall prove the inequality

$$\forall k \in \mathbb{N}, \mu_k(\rho) \leq \frac{\pi^2 k^2}{\left(\int_{\mathbb{R}} \rho dx \right)^2}$$

for non degenerate densities: $\rho : [0, a] \rightarrow [\delta, 1]$ with $\delta > 0$. In the second part, we shall consider general densities and we shall use an approximation argument. The approximation argument is itself quite technical and requires to regularize the density in different manners on the numerator and denominator. This is to avoid the presence of spurious modes in the approximation procedure.

In order to compare eigenvalues of a density with the eigenvalues of union of segments, we shall use the technique of mass transplantation, implicitly introduced by Weinberger in [103]. The prototype situation is the following: let $\rho_1, \rho_2 \in L^1(\mathbb{R}, [0, 1])$ such that $\int_{\mathbb{R}} \rho_1(x) dx = \int_{\mathbb{R}} \rho_2(x) dx$. Let also $f : \mathbb{R} \rightarrow \mathbb{R}$ belong to $L^1(\mathbb{R})$. We seek the following inequality

$$\int_{\mathbb{R}} \rho_1(x) f(x) dx \leq \int_{\mathbb{R}} \rho_2(x) f(x) dx.$$

The interpretation of this inequality as "mass transplantation" comes from the fact that, formally speaking, we transport the mass of the measure of density ρ_1 onto the measure of density ρ_2 , in such a way that the values of f are controlled along the transportation process. For instance, in our future applications, we consider a density ρ and a measurable set A such that $\int_{\mathbb{R}} \rho dx = |A|$. If $\text{esssup}_{\mathbb{R} \setminus A} f \leq \text{essinf}_A f$ the inequality is true. Indeed, this is equivalent to

$$\int_{\mathbb{R} \setminus A} \rho(x) f(x) dx \leq \int_A (1 - \rho(x)) f(x) dx,$$

which is a consequence of

$$\begin{aligned} \int_{\mathbb{R} \setminus A} \rho(x) f(x) dx &\leq \text{esssup}_{\mathbb{R} \setminus A} f \int_{\mathbb{R} \setminus A} \rho(x) dx = \text{esssup}_{\mathbb{R} \setminus A} f \int_A (1 - \rho(x)) dx \\ &\leq \text{essinf}_A f \int_A (1 - \rho(x)) dx \leq \int_A (1 - \rho(x)) f(x) dx. \end{aligned}$$

This inequality can be interpreted as a consequence of the mass transportation of the density $\rho \cdot 1_{\mathbb{R} \setminus A}$ towards $(1 - \rho) \cdot 1_A$.

We shall use the following classical result on the nodal points of a linear combination of eigenfunctions of a well posed Sturm-Liouville problem, for which we refer to the original paper of Sturm [97] and to [24, Theorem 1.4 and Theorem 3.2].

Lemma 3.3.1. (*Extended Courant nodal domain property*) Assume $\rho : [0, a] \rightarrow [\delta, 1]$. If u_k is a nonzero eigenfunction associated to $\mu_k(\rho)$, then u_k has precisely k zeros. Moreover, any linear combination

$$\sum_{i=0}^k a_i u_i$$

of the eigenfunctions u_0, \dots, u_k has at most k zeros, multiplicities being counted.

Proof. (of Theorem 3.1.2) In a first step, we assume $\rho : [0, a] \rightarrow [\delta, 1]$ so that the problem is elliptic and the eigenvalue problem is well posed on the interval $(0, a)$. In a second step we shall use a double approximation procedure to deal with degenerate densities, and reduce the argument to the elliptic case.

Step 1. Assume $\rho : [0, a] \rightarrow [\delta, 1]$ and $\int \rho dx = 1$. This assumption will not reduce generality. In fact, a is intended to be large, asymptotically infinite, and δ to be small, asymptotically vanishing. Once Theorem 3.1.2 is proved for such densities (depending on a and δ), the general case follows by approximation.

The proof of Theorem 3.1.2 in this particular situation is based on the construction of a test function g which is ρ -orthogonal to the eigenfunctions $1, u_1, \dots, u_{k-1}$ and satisfies

$$\frac{\int_0^a \rho(g')^2 dx}{\int_0^a \rho g^2 dx} \leq \frac{\pi^2 k^2}{\left(\int_0^a \rho dx\right)^2}. \quad (3.12)$$

This will readily give the conclusion. The difficulty to build g is that u_1, \dots, u_{k-1} are not known (the constant function 1 is identified with u_0). This technical point popped up in [33], in the case $k=2$ (with only one unknown function) and was dealt with a topological degree argument (see as well [56]). Here, we have $k-1$ unknown functions but we have the advantage of the dimension being equal to 1. We shall also use a topological degree argument, in the spirit of [33], however more sophisticated here, since orthogonality is searched on k functions simultaneously.

Let $P = (b_1, \dots, b_k) \in \mathbb{R}^k$ and assume that

$$b_1 \leq b_2 \leq \dots \leq b_k.$$

We associate to P the function g_P , built as follows. Let first introduce the function (see Figure 3.1)

$$h(x) = -1_{(-\infty, -\frac{1}{2k})}(x) + \sin(k\pi x)1_{[-\frac{1}{2k}, \frac{1}{2k}]}(x) + 1_{(\frac{1}{2k}, +\infty)}(x),$$

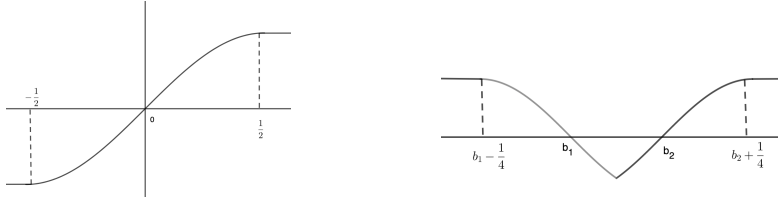


Figure 3.1: The function h for $k=1$ and a function g_P for $k=2$.

and for every $j = 1, \dots, k$ define

$$g_j(x) = h(x - b_j).$$

On any interval (b_j, b_{j+1}) we define

$$g_P = (-1)^j \min\{|g_i|, |g_{i+1}|\},$$

while on $(-\infty, b_1)$ $g_P = -g_1$ and on $(b_k, +\infty)$ $g_P = (-1)^k g_k$.

Validity of the functions g_P . Assume we find some point P such that

$$\forall 0 \leq i \leq k-1, \int_0^a g_P u_i \rho dx = 0. \quad (3.13)$$

Then,

$$\mu_k(\rho) \leq \frac{\int_0^a \rho(g'_P)^2 dx}{\int_0^a \rho g_P^2 dx}.$$

The structure of the function g_P is a union of segments where g_P equals 1 or -1 and of k intervals $J_i = [b_i - b'_i, b_i + b''_i]$ with $0 \leq b'_i, b''_i \leq \frac{1}{2k}$ where g_P is the sinus branch $(-1)^i \sin(\pi k(x - b_i))$. In order to use the mass transplantation technique, we can formally split the set $[0, a] \setminus \cup_{i=1}^k J_i$ in a union of disjoint sets A_1, \dots, A_k such that

$$\forall i = 1, \dots, k, \int_{A_i \cup J_i} \rho(x) dx = \frac{1}{k}.$$

Then, we transplant the mass of $\rho \cdot 1_{A_i}$ onto $1_{[b_i - \frac{1}{2k}, b_i + \frac{1}{2k}]} - \rho \cdot 1_{J_i}$ to get

$$\int_{A_i \cup J_i} \rho g_P^2 dx \geq \int_{[b_i - \frac{1}{2k}, b_i + \frac{1}{2k}]} \sin^2(\pi k(x - b_i)) dx,$$

and

$$\int_{A_i \cup J_i} \rho(g'_P)^2 dx \leq \pi^2 k^2 \int_{[b_i - \frac{1}{2k}, b_i + \frac{1}{2k}]} \cos^2(\pi k(x - b_i)) dx.$$

Note that both inequalities above are true since g_P^2 equals 1 and g'_P equals 0 on A_i .

Summing those inequalities we get

$$\frac{\int_0^a \rho(g'_P)^2 dx}{\int_0^a \rho g_P^2 dx} \leq \pi^2 k^2.$$

Existence of an admissible function g_P . This is the most technical part. In fact we shall prove a more precise statement in order to be able to use a topological degree argument. Let us denote

$$U_{ad} = \{(a_1, \dots, a_k) \in \mathbb{R}^k : a_1 < a_2 < \dots < a_k\}.$$

We notice that U_{ad} is open and if a point $(a_1, \dots, a_k) \in \mathbb{R}^k$ belongs to its boundary ∂U_{ad} , then there exists at least one j such that $a_j = a_{j+1}$.

Lemma 3.3.2. *There exists a unique point $P = (a_1, \dots, a_k) \in U_{ad}$ satisfying (3.13). Moreover $-\frac{1}{2k} < a_1, a_k < a + \frac{1}{2k}$.*

Proof. We will use a cyclic induction argument on k ,

$$\dots \text{existence for } k \implies \text{uniqueness for } k \implies \text{existence for } k+1 \dots$$

Start ($k=1$). In this case, both existence and uniqueness are trivial. The existence follows as a consequence of the intermediate value property for a continuous function, while uniqueness is a consequence of the connectedness of the support of ρ . Indeed, it is enough to assume that for two different points $-\frac{1}{2k} < b < b' < a + \frac{1}{2k}$ one has $\int_0^a \rho g_b dx = \int_0^a \rho g_{b'} dx = 0$. The strict lower and upper bounds $-\frac{1}{2k}, a + \frac{1}{2k}$ occur, otherwise $\int_0^a \rho g dx = \pm 1 \neq 0$. But $g_{b'} \geq g_b$ on \mathbb{R} , this inequality being strict between $b - \frac{1}{2k}$ and $b' + \frac{1}{2k}$. Since $\rho \geq \delta > 0$ on $[0, a]$ and $(b - \frac{1}{2k}, b' + \frac{1}{2k}) \cap (0, a) \neq \emptyset$ we get $\int_0^a \rho(g_{b'} - g_b) dx > 0$, in contradiction with our assumptions.

Existence for k . Assume the assertion is true up to $k-1$. We shall prove the assertion for k , starting with the existence part. We know that there exists

$$Q = (b_1, \dots, b_{k-1}) \text{ such that } \forall i = 0, \dots, k-2, \int_{\mathbb{R}} g_Q u_i \rho dx = 0.$$

We fix $M > 0$ large enough, say $M \geq a + 2k + 2$, and define

$$F : [-M, M]^k \cap U_{ad} \rightarrow \mathbb{R}^k,$$

$$F(a_1, \dots, a_k) = \left(\int_0^a \rho g_P dx, \int_0^a u_1 \rho g_P dx, \dots, \int_0^a u_{k-1} \rho g_P dx \right).$$

Above $P = (a_1, \dots, a_k)$. Our purpose is to prove that there exists $P \in [-M, M]^k \cap U_{ad}$ such that $F(P) = 0$.

We introduce the segments $S_i = (a + 2i, a + 2i + \frac{1}{k})$ and the deformation of F^t of F , by $\forall t \in [0, 1]$, $\forall 0 \leq i \leq k-2$, $F_i = F_i^t$ and

$$F_{k-1}^t(P) = t \int \rho u_{k-1} g_P dx + \alpha(1-t) \int_{S_k} g_P dx,$$

where $\alpha \in \{-1, 1\}$ will be chosen later.

Clearly, this deformation is continuous. Let us prove that no zero crosses $\partial([-M, M]^k \cap U_{ad})$. Assume for some t that $F^t(a_1, \dots, a_k) = 0$ and that $a_1 = -M$ or $a_k = M$. Let us chose one of them: assume first that $a_k = M$. Then, in the definition of g_P the point a_k has no influence on the support of ρ . In this way, denoting $P' = (a_1, \dots, a_{k-1})$ we get

$$\forall 0 \leq i \leq k-2, \int \rho u_i g_P dx = 0.$$

Using the induction hypothesis, the point $P' = (b_1, \dots, b_{k-1})$ is necessarily the unique point given by the induction hypothesis for $k-1$. Now, we look to the sign of $\int \rho u_{k-1} g_P$ (assuming this quantity is not equal to zero, in which case the existence problem is solved). If nonnegative we chose $\alpha = -1$, if nonpositive, we chose $\alpha = 1$ (and denote it α_k from now on), so that for every $t \in [0, 1]$.

$$t \int \rho u_{k-1} g_P dx + \alpha_k(1-t) \int_{S_k} g_P dx \neq 0.$$

Assume now that $a_1 = -M$. The choice for the sign α is the same as in the previous case, since if $a_1 = -M$ then necessarily $(a_2, \dots, a_k) = (b_1, \dots, b_{k-1})$. This means that the new function g_P has opposite sign with respect to the previous one on both $[0, a]$ and S_k . This choice of α_k implies that F^t can not vanish on $[0, 1]$ on a point on $(\partial[-M, M]^k)$

Let us now prove that (a_1, \dots, a_k) can not cross ∂U_{ad} . Assume for contradiction that for some $(a_1, \dots, a_k) \in \partial U_{ad}$ we have $F^t(a_1, \dots, a_k) = 0$. Then for some index j we have $a_j = a_{j+1}$. The function g_P has at most $k-2$ sign changing.

Assume they are y_1, \dots, y_j , with $j \leq k-2$. We find β_0, \dots, β_j , not all of them vanishing, such that

$$U = \sum_{i=0}^j \beta_i u_i$$

satisfies $U(y_i) = 0, \forall i = 1, \dots, j$. This is a consequence of the fact that a linear system with j equations, $j+1$ unknowns and 0 right hand side, has a space of solutions of co-dimension at least equal to 1.

Using the extended Courant property, the number of zeros of U is at most j , in our case being exactly equal to j . Hence U has to change sign between two zeros, otherwise we would get more than j zeros, including multiplicity. Finally, this implies that $g_P U$ has constant sign. This is a contradiction with the orthogonality property

$$\int \rho g_P U dx = 0.$$

Once arrived at $t = 1$, we relabel $F^1 = F$ and continue with a second deformation, keeping constant the last component $\alpha_k \int_{S_k} g_P dx$, keeping unchanged the first $k-2$ components and deforming for $t \in [0, 1]$

$$F_{k-2}^t(P) = t \int \rho u_{k-2} g_P dx + \alpha_{k-1}(1-t) \int_{S_{k-1}} g_P dx.$$

This is again continuous and can not have a zero crossing $\partial([-M, M]^k \cap U_{ad})$. The argument is exactly the same. The only new observation comes from the fact that as $\int_{S_k} g_P dx = 0$, necessarily one point, say a_k has to be the middle of the segment S_k . More than one point can not come in touch with S_k , otherwise strictly less than $k-2$ points would be sufficient to cancel the first $k-2$ components, which is not possible by the induction property.

We continue this procedure and arrive to the final function

$$F_{fin}(P) = \left(\alpha_1 \int_{S_1} g_P dx, \dots, \alpha_k \int_{S_k} g_P dx \right).$$

This function has as (only) zero the centers of the segments S_i and the Jacobian equals $(-2)^{\lfloor \frac{k}{2} \rfloor} \prod_{i=1}^k \alpha_i$, hence it is not vanishing. Indeed, the Jacobian matrix is diagonal, and for each diagonal element one has to perform a derivative at 0 of a function equal to, up to a positive or negative sign depending on j and α_j ,

$$a \rightarrow \int_{-\frac{1}{2k}}^{\frac{1}{2k}} \sin(\pi k(x-a)) dx.$$

Finally, as the Jacobian does not vanishes at the unique zero, we conclude with the existence part of the proof.

Uniqueness for k . Assume $P_1 \neq P_2$ and

$$\forall j = 1, 2, \forall 0 \leq i \leq k-1, \int \rho g_{P_j} u_i dx = 0.$$

We get that $\forall 0 \leq i \leq k-1, \int \rho (g_{P_1} - g_{P_2}) u_i dx = 0$. In view of the structures of g_{P_1} and g_{P_2} , the function $g_{P_1} - g_{P_2}$ has at most $k-1$ zeroes where there is sign changing. To be more precise, we notice that the set of zeros of $g_{P_1} - g_{P_2}$ consists on a union of isolated points and of closed intervals (the two extremal ones being unbounded). Let $\{g_{P_1} - g_{P_2} \neq 0\} = I_1 \cup I_2 \cup \dots \cup I_m$ be the decomposition of the open set $\{g_{P_1} - g_{P_2} \neq 0\}$ as the union of ordered open, disjoint, intervals. The sign of $g_{P_1} - g_{P_2}$ may be the same on two consecutive intervals I_j, I_{j+1} . We say that we have a sign change when the sign of $g_{P_1} - g_{P_2}$ changes between I_j and I_{j+1} . There are at most $k-1$ sign changing and we can choose for each sign changing corresponding to I_j and I_{j+1} a zero of $g_{P_1} - g_{P_2}$ which lies between the intervals. In order to justify that the number of sing changing is at most $k-1$, we can formally extend each function g_P on each bounded interval $[x, y]$ where it

equals 1 by $(\min\{|t-x|, |t-y|\} + 1)$ and where it equals -1 by $(-\min\{|t-x|, |t-y|\} - 1)$. Denoting the extended functions \tilde{g}_P , we notice that each the sign changing of $g_{P_1} - g_{P_2}$ corresponds to a sign changing of $\tilde{g}_{P_1} - \tilde{g}_{P_2}$. However, for the last function, a sing changing can occur only if a strictly increasing branch of one of the functions crosses a strictly decreasing branch of the other, so at most $k-1$ times.

We use a similar argument as in the existence part. Assume they are y_1, \dots, y_j , with $j \leq k-1$. We find β_0, \dots, β_j , not all of them vanishing, such that $U = \sum_{i=0}^j \beta_i u_i$ satisfies $U(y_i) = 0, \forall i = 1, \dots, j$. From the extended Courant property, the number of zeros of U is at most j , in our case being exactly equal to j . Hence U has to change sign between two zeros, otherwise we would get more than j zeros, including multiplicity. Finally, this implies that $(g_{P_1} - g_{P_2})U$ has constant sign, against the orthogonality property

$$\int \rho(g_{P_1} - g_{P_2})U dx = 0.$$

The inequality $-\frac{1}{2k} < a_1 \leq \dots \leq a_k < a + \frac{1}{2k}$. In fact, this inequality implies that all k -points are necessarily involved in the construction of the function g . Assume this inequality is not true. Then any point out of the interval $(-\frac{1}{2k}, a + \frac{1}{2k})$ does not play any role in the geometry of the function g_P on $[0, a]$. Assume that for some $j < k$, $Q = (a_1, \dots, a_j)$ are the only points in this interval. Then

$$\int g_Q \rho u_i dx = 0, i = 0, \dots, k-1.$$

The function g_Q changes sign at most $j+1$ times and has no more than j zeros where it changes sign. There exists a linear combination of u_0, \dots, u_j with the same zeros, so that a similar argument as the previous one leads to a contradiction.

Step 2. General densities. In order to handle the approximation procedure for general densities, we need to regularize differently the numerator and the denominator. Let $\rho_1, \rho_2 : \mathbb{R}^N \rightarrow [0, +\infty)$, $\rho_1, \rho_2 \in L^1(\mathbb{R}^N) \cap L^\infty(\mathbb{R}^N)$, $\rho_2 \not\equiv 0$. For every integer $k \geq 0$, the number

$$\mu_k(\rho_1, \rho_2) := \inf_{S \in \mathcal{S}_{k+1}} \max_{u \in S \setminus \{0\}} \frac{\int_{\mathbb{R}^N} \rho_1 |\nabla u|^2 dx}{\int_{\mathbb{R}^N} \rho_2 u^2 dx}, \quad (3.14)$$

is called the k -th eigenvalue of the problem

$$-\operatorname{div}(\rho_1 \nabla u) = \mu_k(\rho_1, \rho_2) \rho_2 u$$

with Neumann boundary conditions. Above, \mathcal{S}_{k+1} is the family of all subspaces of dimension $k+1$ in

$$\{u \cdot 1_{\{\rho_2(x) > 0\}} : u \in C_c^\infty(\mathbb{R}^N)\}. \quad (3.15)$$

If $\rho_1 = \rho_2 := \rho$, we have $\mu_k(\rho_1, \rho_2) = \mu_k(\rho)$. By convention, if $\rho_2 = 0$, we set $\mu_k(\rho_1, \rho_2) = +\infty$.

The following upper semicontinuity result holds.

Lemma 3.3.3. Assume $\rho_1, \rho_2, \rho_1^n \rho_2^n \in L^1(\mathbb{R}^N, [0, 1])$ satisfy $\rho_i^n \rightharpoonup \rho_i$ weak-* in $L^\infty(\mathbb{R}^N)$, for $i = 1, 2$. Then

$$\forall k \geq 1, \mu_k(\rho_1, \rho_2) \geq \limsup_{n \rightarrow +\infty} \mu_k(\rho_1^n, \rho_2^n).$$

Proof. The proof of the result is absolutely similar to Lemma 3.2.1. □

Lemma 3.3.4. Let $\delta > 0$. Assume $\rho_1, \rho_2 : (0, a) \rightarrow [\delta, 1]$ and denote $m = \min\{\int_0^a \rho_1 dx, \int_0^a \rho_2 dx\}$. Then,

$$\mu_k(\rho_1, \rho_2) \leq \frac{\pi^2 k^2}{m^2}.$$

Proof. Assume first that $\int_0^a \rho_2 dx \leq \int_0^a \rho_1 dx$. The proof of Step 1 is valid with $m = \int_0^a \rho_2 dx$. The key point is that the inequality given by mass transplantation still occurs, since on the regions where g'_P vanishes, the value of ρ_1 is not important, while on the regions where g'_P does not vanish we replace anyway ρ_1 by 1.

In particular, this implies that

$$\left(\int_0^a \rho_2 dx \right)^2 \mu_k(1, \rho_2) \leq \pi^2 k^2. \quad (3.16)$$

If $\int \rho_2 dx \geq \int \rho_1 dx$, for some $0 < \alpha < 1$ we write $\int \alpha \rho_2 dx = \int \rho_1 dx$ and use monotonicity of the Rayleigh quotient together with the previous argument to get

$$\mu_k(\rho_1, \rho_2) \leq \mu_k(\rho_1, \alpha \rho_2) \leq \mu_k(1, \alpha \rho_2) \leq \frac{\pi^2 k^2}{\left(\int_0^a \alpha \rho_2 dx \right)^2} = \frac{\pi^2 k^2}{\left(\int_0^a \rho_1 dx \right)^2}.$$

□

Approximation of density eigenvalues by regular problems.

The following approximation results is inspired from numerical analysis, technically developed in order to avoid spurious eigenvalues in the numerical approximation (see for instance Allaire and Jouve [4] and Section 3.5). Let us denote the Gaussian measure

$$\gamma_N(A) = \frac{1}{(2\pi)^{\frac{N}{2}}} \int_A e^{-\frac{|x|^2}{2}} dx.$$

Let $\rho_1, \rho_2 \in \mathbf{L}^1(\mathbb{R}^N) \cap \mathbf{L}^\infty(\mathbb{R}^N, \mathbb{R}^+)$, $\rho_2 \not\equiv 0$. We denote

$$\rho_1^\varepsilon = \rho_1 + \varepsilon e^{-\frac{|x|^2}{2}}, \quad \rho_2^\varepsilon = \rho_2 1_{\mathbf{B}_{\frac{1}{\varepsilon}}} + \varepsilon^2 e^{-\frac{|x|^2}{2}}$$

where \mathbf{B}_r stands for the ball of radius r centered at the origin.

The problem associated to $(\rho_1^\varepsilon, \rho_2^\varepsilon)$ is regular. This is a consequence of the compact embedding $H^1(\mathbb{R}^N, \gamma_N) \subset \mathbf{L}^2(\mathbb{R}^N, \gamma_N)$ and of the ellipticity of the differential operator $u \rightarrow -\operatorname{div}(\rho_1^\varepsilon \nabla u)$ in the associated spaces.

Lemma 3.3.5. *With the previous notations, we have*

$$\forall k \in \mathbb{N}, \mu_k(\rho_1^\varepsilon, \rho_2^\varepsilon) \rightarrow \mu_k(\rho_1, \rho_2).$$

Proof. The proof is done in two steps: upper and lower semicontinuity. For the upper semicontinuity, it is enough to observe that $\rho_i^\varepsilon \rightharpoonup \rho_i$, weakly-* in $\mathbf{L}^\infty(\mathbb{R}^N)$ hence one can relay Lemma 3.3.3 to get upper semicontinuity. Let us prove

$$\mu_k(\rho_1, \rho_2) \leq \liminf_{\varepsilon \rightarrow 0} \mu_k(\rho_1^\varepsilon, \rho_2^\varepsilon). \quad (3.17)$$

To avoid heavy notations, we shall denote $\mu_k^\varepsilon := \mu_k(\rho_1^\varepsilon, \rho_2^\varepsilon)$. The ε -problem is well posed, so that we can consider eigenfunctions $u_0^\varepsilon, \dots, u_k^\varepsilon \in H^1(\mathbb{R}^N, \gamma_N)$ associated to $\mu_0^\varepsilon, \dots, \mu_k^\varepsilon$ respectively, such that

$$\int_{\mathbb{R}^N} \rho_2^\varepsilon (u_i^\varepsilon)^2 = 1 \quad (3.18)$$

$$\int_{\mathbb{R}^N} \rho_1^\varepsilon |\nabla u_i^\varepsilon|^2 = \mu_i^\varepsilon \leq M \quad (3.19)$$

$$\forall i \neq j, \int \rho_2^\varepsilon u_i^\varepsilon u_j^\varepsilon = 0 \quad (3.20)$$

where M is a common bound for all ε and all $i \in \{0, \dots, k\}$ (such a bound exists, otherwise the *liminf* in (3.17) equals $+\infty$ and so there is nothing to prove). From the first equality we have that $\varepsilon u_i^\varepsilon$ is bounded in $\mathbf{L}^2(\mathbb{R}^N, \gamma_N)$. Then up to a subsequence, there exist a $U_i \in \mathbf{L}^2(\mathbb{R}^N, \gamma_N)$ such that

$$\varepsilon u_i^\varepsilon \xrightarrow{\mathbf{L}^2(\mathbb{R}^N, \gamma_N)} U_i, \text{ weakly.}$$

In particular, if we denote by $\bar{v} := \int v d\gamma_N$, the weighted mean of v , we have that

$$\varepsilon \bar{u}_i^\varepsilon \rightarrow \bar{U}_i.$$

This is a consequence of the fact that $1 \in \mathbf{L}^1(\mathbb{R}^N, \gamma_N)$. From (3.19) we get that $(\sqrt{\varepsilon} |\nabla u_i^\varepsilon|)$ is bounded in $\mathbf{L}^2(\mathbb{R}^N, \gamma_N)$. This implies that $\varepsilon |\nabla u_i^\varepsilon| \xrightarrow{\mathbf{L}^2(\mathbb{R}^N, \gamma_N)} 0$. Thanks to the compactness of $H^1(\mathbb{R}^N, \gamma_N)$ in $\mathbf{L}^2(\mathbb{R}^N, \gamma_N)$, we have that

$$\|\varepsilon u_i^\varepsilon - \varepsilon \bar{u}_i^\varepsilon\|_{\mathbf{L}^2(\mathbb{R}^N, \gamma_N)} \rightarrow 0$$

which implies that

$$\varepsilon u_i^\varepsilon \xrightarrow{\mathbf{L}^2(\mathbb{R}^N, \gamma_N)} \bar{U}_i.$$

In the same time, u_i^ε is bounded in $\mathbf{L}^2(\mathbb{R}^N, \rho_1 1_{\mathbf{B}_n})$, for some $n \in \mathbb{N}$ such that $|\mathbf{B}_n \cap \{\rho > 0\}| > 0$ so

$$\varepsilon u_i^\varepsilon \xrightarrow{\mathbf{L}^2(\mathbb{R}^N, \rho_1 1_{\mathbf{B}_n})} 0$$

then $\bar{U}_i = 0$ from the a.e. point wise convergence. In other terms,

$$\varepsilon^2 \int_{\mathbb{R}^N} (u_i^\varepsilon)^2 e^{-\frac{|x|^2}{2}} dx \rightarrow 0$$

then by Cauchy-Schwarz

$$\varepsilon^2 \int_{\mathbb{R}^N} u_i^\varepsilon u_j^\varepsilon e^{-\frac{|x|^2}{2}} dx \rightarrow 0$$

so that

$$\int_{\mathbb{R}^N} \rho_2 1_{B_{\frac{1}{\varepsilon}}} (u_i^\varepsilon)^2 dx \rightarrow 1$$

and

$$\int_{\mathbb{R}^N} \rho_2 1_{B_{\frac{1}{\varepsilon}}} u_i^\varepsilon u_j^\varepsilon dx \rightarrow 0$$

Finally,

$$\begin{aligned} \mu_k^\varepsilon &= \frac{\int_{\mathbb{R}^N} \rho_1 |\nabla u_k^\varepsilon|^2 + \varepsilon e^{-\frac{|x|^2}{2}} |\nabla u_k^\varepsilon|^2}{\int_{\mathbb{R}^N} \rho_2 1_{B_{\frac{1}{\varepsilon}}} (u_k^\varepsilon)^2 + \varepsilon^2 e^{-\frac{|x|^2}{2}} (u_k^\varepsilon)^2} \\ &= \max_{v^\varepsilon \in \text{Span}(u_0^\varepsilon, \dots, u_k^\varepsilon)} \frac{\int_{\mathbb{R}^N} \rho_1 |\nabla v^\varepsilon|^2 + \varepsilon e^{-\frac{|x|^2}{2}} |\nabla v^\varepsilon|^2}{\int_{\mathbb{R}^N} \rho_2 1_{B_{\frac{1}{\varepsilon}}} (v^\varepsilon)^2 + \varepsilon^2 e^{-\frac{|x|^2}{2}} (v^\varepsilon)^2} \geq \max_{v^\varepsilon \in \text{Span}(u_0^\varepsilon, \dots, u_k^\varepsilon)} \frac{\int_{\mathbb{R}^N} \rho_1 |\nabla v^\varepsilon|^2}{\int_{\mathbb{R}^N} \rho_2 (v^\varepsilon)^2 + \varepsilon^2 e^{-\frac{|x|^2}{2}} (v^\varepsilon)^2}. \end{aligned}$$

Passing to the liminf and recalling that

$$\int_{\mathbb{R}^N} \varepsilon^2 e^{-\frac{|x|^2}{2}} (v^\varepsilon)^2 dx \rightarrow 0$$

for every $v^\varepsilon = \sum_{j=0}^k a_j^\varepsilon u_j^\varepsilon$ with $\sum_{j=0}^k (a_j^\varepsilon)^2 = 1$, we get

$$\liminf \mu_k^\varepsilon \geq \liminf \max_{v^\varepsilon \in \text{Span}(u_0^\varepsilon, \dots, u_k^\varepsilon)} \frac{\int_{\mathbb{R}^N} \rho_1 |\nabla v^\varepsilon|^2}{\int_{\mathbb{R}^N} \rho_2 (v^\varepsilon)^2}$$

We conclude by remarking that $\text{Span}(u_0^\varepsilon, \dots, u_k^\varepsilon) 1_{\{\rho_2 > 0\}}$ is of dimension $k+1$ for ε small enough, hence

$$\max_{v^\varepsilon \in \text{Span}(u_0^\varepsilon, \dots, u_k^\varepsilon)} \frac{\int_{\mathbb{R}^N} \rho_1 |\nabla v^\varepsilon|^2}{\int_{\mathbb{R}^N} \rho_2 (v^\varepsilon)^2} \geq \mu_k(\rho_1, \rho_2).$$

□

Proof of Theorem 3.1.2, continuation. Let now $\rho \in \mathbf{L}^1(\mathbb{R}, [0, 1])$. For every $\varepsilon > 0$, we define

$$\mu_k^\varepsilon(\rho) = \inf_{U \in S_{k+1}} \max_{u \in U} \frac{\int_{\mathbb{R}} (\rho + \varepsilon e^{-\frac{|x|^2}{2}})(u')^2 dx}{\int_{\mathbb{R}} (\rho 1_{[-\frac{1}{\varepsilon}, \frac{1}{\varepsilon}]} + \varepsilon^2 e^{-\frac{|x|^2}{2}}) u^2 dx}.$$

This problem is well posed in view of the compact embedding of the Sobolev space associated to the Gaussian measure in \mathbf{L}^2 . Moreover $\mu_k^\varepsilon(\rho) \rightarrow \mu_k(\rho)$ when $\varepsilon \rightarrow 0$.

Let us introduce the second approximation. For every $n \in \mathbb{N}$,

$$\mu_k^{\varepsilon,n}(\rho) = \inf_{U \in S_{k+1}} \max_{u \in U} \frac{\int_{-n}^n (\rho + \varepsilon e^{-\frac{|x|^2}{2}})(u')^2 dx}{\int_{-n}^n (\rho 1_{[-\frac{1}{\varepsilon}, \frac{1}{\varepsilon}]} + \varepsilon^2 e^{-\frac{|x|^2}{2}}) u^2 dx}.$$

Then, for every fixed $\varepsilon > 0$, we have

$$\forall k \geq 1, \mu_k^{\varepsilon,n}(\rho) \rightarrow \mu_k^\varepsilon(\rho), \text{ when } n \rightarrow +\infty.$$

Indeed, the upper semicontinuity is done as before. The lower semicontinuity is a consequence of the "collective compactness" property: if $\varphi_n \in H^1(-n, n)$ is such that $\int_{-n}^n (\varphi'_n)^2 e^{-x^2} dx \leq M$ and $\int_{-n}^n \varphi_n^2 e^{-x^2} dx = 1$, then there exists $\varphi \in H^1(\mathbb{R}, \gamma_1)$ such that $\varphi_n \rightharpoonup \varphi$ in $H_{loc}^1(\mathbb{R})$ and

$$\varphi_n 1_{(-n, n)} \rightarrow \varphi, \text{ strong in } \mathbf{L}^2(\mathbb{R}, \gamma_1).$$

This comes from the compact embedding $H^1(\mathbb{R}, \gamma_1) \subset L^2(\mathbb{R}, \gamma_1)$ and the uniform extension operator

$$H^1((-n, n), \gamma_1) \ni \varphi \rightarrow \tilde{\varphi} \in H^1(\mathbb{R}, \gamma_1),$$

given by the reflection against the points $n + 2n\mathbb{Z}$.

Denoting

$$m_{\varepsilon, n} := \min \left\{ \frac{\int_{-n}^n \rho + \varepsilon e^{-\frac{|x|^2}{2}} dx}{1 + \varepsilon}, \frac{\int_{-n}^n \rho 1_{[-\frac{1}{\varepsilon}, \frac{1}{\varepsilon}]} + \varepsilon^2 e^{-\frac{|x|^2}{2}} dx}{1 + \varepsilon^2} \right\},$$

we get, from Lemma 3.3.4

$$\mu_k^{\varepsilon, n}(\rho) \leq \frac{1 + \varepsilon}{1 + \varepsilon^2} \cdot \frac{\pi^2 k^2}{m_{\varepsilon, n}^2}.$$

Passing to the limit $n \rightarrow +\infty$ and then $\varepsilon \rightarrow 0$, we conclude the proof. □

□

□

Remark 3.3.6 (The equality case). *Clearly, if $\rho : [0, a] \rightarrow [\delta, 1]$ satisfies*

$$\mu_k(\rho) = \frac{\pi^2 k^2}{\left(\int_0^a \rho dx \right)^2},$$

this means that the function g_P has to be an eigenfunction and all the mass of ρ is distributed on the k segments of length $\frac{1}{k} \int_0^a \rho dx$, which have to be disjoint. This is a consequence of the mass transplantation procedure. However, the hypothesis $\rho \geq \delta 1_{[0, a]}$ prevents this situation. On the other hand, if ρ equals the characteristic function of k such segments, then equality occurs.

More interesting is the analysis of the equality case in Lemma 3.3.4. Assume now ρ equals the characteristic function of k disjoint segments of equal length. Then

$$\frac{\pi^2 k^2}{\left(\int_0^a \rho dx \right)^2} = \mu_k(\rho) \leq \mu_k(1, \rho) \leq \frac{\pi^2 k^2}{\left(\int_0^a \rho dx \right)^2}.$$

In fact, in general, the eigenvalues $\mu_j(1, \rho)$ depend on the pairwise distance between the segments and

$$\mu_j(\rho) \leq \mu_j(1, \rho).$$

The inequality is, in general, strict, except for the k -th eigenvalue, when the values are necessarily equal.

We end this section with the following sharp inequality involving the Sturm-Liouville eigenvalues.

Corollary 3.3.7 (Sharp inequalities for Sturm-Liouville eigenvalues). *Let $(\alpha, \beta) \subset \mathbb{R}$ be an interval and $\rho_1, \rho_2 : [\alpha, \beta] \rightarrow \mathbb{R}$ be positive C^1 functions. We consider the eigenvalue problem*

$$\begin{cases} -(\rho_1 u')' = \mu_k \rho_2 u & \text{on } (\alpha, \beta) \\ u'(\alpha) = u'(\beta) = 0 \end{cases}$$

Then

$$\forall k \geq 0, \quad \mu_k \leq \frac{\|\rho_2\|_\infty}{\|\rho_1\|_\infty} \frac{\pi^2 k^2}{\min\left(\frac{\int_\alpha^\beta \rho_1}{\|\rho_1\|_\infty}, \frac{\int_\alpha^\beta \rho_2}{\|\rho_2\|_\infty}\right)^2}$$

Proof. This is a consequence of Theorem 3.1.2 applied to $\frac{\int_\alpha^\beta \rho_1}{\|\rho_1\|_\infty}, \frac{\int_\alpha^\beta \rho_2}{\|\rho_2\|_\infty}$ and relies on the argument of Lemma 3.3.4. □

3.4 Pólya conjecture and Kröger inequalities

A direct consequence of Theorem 3.1.2 is the following.

Corollary 3.4.1. *The Pólya conjecture holds in one dimension of the space. Let $\rho \in \mathbf{L}^1(\mathbb{R}, [0, 1])$, $\rho \not\equiv 0$. Then*

$$\forall k \in \mathbb{N}, \mu_k(\rho) \leq \frac{\pi^2 k^2}{\left(\int_{\mathbb{R}} \rho dx \right)^2}. \quad (3.21)$$

Although the conjecture is not proved in general in any dimension of the space, a natural question is whether the validity of the conjecture could cover the density eigenvalues. This is the case for $k = 1, 2$. To bring support in this direction, our purpose is to prove that estimates obtained by Kröger for smooth sets (see [73]) are still valid in our context of (degenerate) densities. As we shall see below, the estimates hold true and naturally involve the \mathbf{L}^∞ and \mathbf{L}^1 norms of the densities. The proof is, in its main lines, the same, except the need of approximation of degenerate densities by regular problems.

Proof of Theorem 3.1.3. Let $\rho \in \mathbf{L}^1(\mathbb{R}^N) \cap \mathbf{L}^\infty(\mathbb{R}^N, \mathbb{R}^+)$, $\rho \not\equiv 0$. We want to prove that

$$\forall k \in \mathbb{N}, \mu_k(\rho) \leq 4\pi^2 \left(\frac{(N+2)k}{2\Omega_N} \frac{\|\rho\|_\infty}{\|\rho\|_1} \right)^{2/N}.$$

From Lemma 3.3.5 we know that

$$\mu_k(\rho + \varepsilon e^{-|\cdot|^2}, \rho \mathbf{1}_{B_{1/\varepsilon}} + \varepsilon^2 e^{-|\cdot|^2}) \rightarrow \mu_k(\rho) \text{ for } \varepsilon \rightarrow 0.$$

Consequently, it is enough to prove inequality (3.22) below, for the couple of densities $(\rho + \varepsilon e^{-|\cdot|^2}, \rho \mathbf{1}_{B_{1/\varepsilon}} + \varepsilon^2 e^{-|\cdot|^2})$ and then to pass to the limit

$$\mu_k(\rho_1, \rho_2) \leq 4\pi^2 \frac{\|\rho_1\|_1}{\|\rho_2\|_1} \left(\frac{(N+2)k}{2\Omega_N} \frac{\|\rho_2\|_\infty}{\|\rho_2\|_1} \right)^{2/N}. \quad (3.22)$$

So, without restricting the generality, we can assume that $\rho_1, \rho_2 \in \mathbf{L}^1(\mathbb{R}^N) \cap \mathbf{L}^\infty(\mathbb{R}^N)$ are such that there exists $\alpha, \beta > 0$ verifying

$$\alpha e^{-\frac{|x|^2}{2}} \leq \rho_1, \rho_2 \text{ and } \rho_2 \leq \beta e^{-\frac{|x|^2}{2}}.$$

In our case, $\alpha = \varepsilon^2$ and $\beta = (1 + \varepsilon^2)e^{\frac{1}{2\varepsilon^2}}$. Then the eigenvalue problem

$$\begin{cases} -\operatorname{div}[\rho_1 \nabla u] = \mu_k(\rho_1, \rho_2) \rho_2 u \text{ on } \mathbb{R}^N \\ u \in H^1(\mathbb{R}^N, \gamma_N) \end{cases}$$

is well posed.

We detail the proof of inequality (3.22) in order to show how to handle the presence of densities, but refer to the paper of Kröger [73] for the original proof (see also [43, 45]).

Let u_0, \dots, u_{k-1} be eigenfunctions associated to μ_0, \dots, μ_{k-1} which satisfy $\int_{\mathbb{R}^n} \rho_2 u_i u_j = \delta_{ij}$. Let

$$\Phi(x, y) = \sum_{j=0}^{k-1} \rho_2(x) u_j(x) u_j(y) \text{ and } h_z(y) = e^{iz \cdot y}.$$

If

$$\hat{\Phi}(z, y) = \frac{1}{(2\pi)^{\frac{N}{2}}} \int_{\mathbb{R}^N} e^{iz \cdot x} \Phi(x, y) dx$$

denotes the Fourier transform of $\Phi(., y)$ then for every $z \in \mathbb{R}^N$ the function $(2\pi)^{\frac{N}{2}} \hat{\Phi}(z, .)$ is the orthogonal projection of h_z on $\operatorname{Span}(u_0, \dots, u_{k-1})$ for the scalar product $(u, v) \rightarrow \int_{\mathbb{R}^n} \rho_2 u v$. Hence

$$\mu_k(\rho_1, \rho_2) \leq \frac{\int_{\mathbb{R}^N} \rho_1 |\nabla(h_z(y) - (2\pi)^{\frac{N}{2}} \hat{\Phi}(z, y))|^2 dy}{\int_{\mathbb{R}^N} \rho_2 |(h_z(y) - (2\pi)^{\frac{N}{2}} \hat{\Phi}(z, y))|^2 dy},$$

then by summing with respect to z over B_r for some $r > 0$, we get

$$\mu_k(\rho_1, \rho_2) \leq \frac{\int_{B_r} \int_{\mathbb{R}^N} \rho_1 |\nabla(h_z(y) - (2\pi)^{\frac{2}{N}} \hat{\Phi}(z, y))|^2 dy dz}{\int_{B_r} \int_{\mathbb{R}^N} \rho_2 |(h_z(y) - (2\pi)^{\frac{2}{N}} \hat{\Phi}(z, y))|^2 dy dz}.$$

Let's compute first the numerator:

$$\begin{aligned} \int_{B_r} \int_{\mathbb{R}^N} \rho_1 |\nabla(h_z(y) - (2\pi)^{\frac{2}{N}} \hat{\Phi}(z, y))|^2 dy dz &= \int_{B_r} \int_{\mathbb{R}^N} \rho_1 |\nabla h_z(y)|^2 dy dz \\ &\quad - 2Re \int_{B_r} \int_{\mathbb{R}^N} \rho_1 \nabla(h_z(y) - (2\pi)^{\frac{2}{N}} \hat{\Phi}(z, y)) \cdot \nabla((2\pi)^{\frac{2}{N}} \hat{\Phi}(z, y)) dy dz \\ &\quad - (2\pi)^n \int_{B_r} \int_{\mathbb{R}^N} \rho_1 |\nabla \hat{\Phi}(z, y)|^2 dy dz. \end{aligned}$$

Since $|\nabla h_z(y)| = |z|$, we get

$$\int_{B_r} \int_{\mathbb{R}^N} \rho_1 |z|^2 dy dz = \|\rho_1\|_1 \frac{r^{N+2}}{N+2} N \Omega_N$$

We have

$$\begin{aligned} Re \sum_{j=0}^k \int_{B_r} \int_{\mathbb{R}^N} \rho_1 \nabla(h_z(y) - (2\pi)^{\frac{2}{N}} \hat{\Phi}(z, y)) \cdot \nabla(\widehat{\rho_2 u_j}(z) u_j(y)) dy dz \\ = Re \sum_{j=0}^k \int_{B_r} \widehat{\rho_2 u_j}(z) \int_{\mathbb{R}^N} \rho_1 \nabla(h_z(y) - (2\pi)^{\frac{2}{N}} \hat{\Phi}(z, y)) \cdot \nabla u_j(y) dy dz = 0. \end{aligned}$$

This is a consequence of the orthogonality hypothesis together with the fact that u_j is an eigenfunction. Indeed,

$$\int_{\mathbb{R}^N} \rho_1 \nabla(h_z(y) - (2\pi)^{\frac{2}{N}} \hat{\Phi}(z, y)) \cdot \nabla u_j(y) dy = \mu_j \int_{\mathbb{R}^N} \rho_2(h_z(y) - (2\pi)^{\frac{2}{N}} \hat{\Phi}(z, y)) u_j(y) dy = 0.$$

We conclude that an upper bound of the numerator is $\|\rho_1\|_1 \frac{r^{N+2}}{N+2} N \Omega_N$.

Concerning the denominator, we similarly have

$$\begin{aligned} \int_{B_r} \int_{\mathbb{R}^N} \rho_2 |(h_z(y) - (2\pi)^{\frac{2}{N}} \hat{\Phi}(z, y))|^2 dy dz &= \int_{B_r} \int_{\mathbb{R}^N} \rho_2 |h_z(y)|^2 dy dz \\ &\quad - 2Re \int_{B_r} \int_{\mathbb{R}^N} \rho_2(h_z(y) - (2\pi)^{\frac{2}{N}} \hat{\Phi}(z, y)) ((2\pi)^{\frac{2}{N}} \hat{\Phi}(z, y)) dy dz \\ &\quad - (2\pi)^N \int_{B_r} \int_{\mathbb{R}^N} \rho_2 |\hat{\Phi}(z, y)|^2 dy dz \end{aligned}$$

We get

$$\begin{aligned} \int_{B_r} \int_{\mathbb{R}^N} \rho_2 |h_z(y)|^2 dy dz &= \|\rho_2\|_1 r^N \Omega_N, \\ Re \int_{B_r} \int_{\mathbb{R}^N} \rho_2(h_z(y) - (2\pi)^{\frac{2}{N}} \hat{\Phi}(z, y)) ((2\pi)^{\frac{2}{N}} \hat{\Phi}(z, y)) dy dz &= 0, \\ (2\pi)^N \int_{B_r} \int_{\mathbb{R}^N} \rho_2 |\hat{\Phi}(z, y)|^2 dy dz &= (2\pi)^N \sum_{j=0}^k \int_{B_r} |\widehat{\rho_2 u_j}|^2 dz \end{aligned}$$

Now $\int_{B_r} |\widehat{\rho_2 u_j}|^2 dz \leq \int_{\mathbb{R}^N} |\widehat{\rho_2 u_j}|^2 dz$. This last term is finite since $\rho_2 u_j^2 \in \mathbf{L}^1(\mathbb{R}^N)$ and ρ_2 is bounded, so that $\rho_2 u_j \in \mathbf{L}^2(\mathbb{R}^N)$. Using Plancherel's theorem

$$\begin{aligned} \int_{\mathbb{R}^N} |\widehat{\rho_2 u_j}|^2 dz &= \int_{\mathbb{R}^N} |\rho_2 u_j|^2 dz \\ &\leq \|\rho_2\|_\infty \int_{\mathbb{R}^N} \rho_2 |u_j|^2 dz \\ &= \|\rho_2\|_\infty \end{aligned}$$

Now if $\frac{r^N}{N} \|\rho_2\|_1 N \Omega_N - (2\pi)^N k \|\rho_2\|_\infty > 0$, we have :

$$\mu_k \leq \frac{\frac{r^{N+2}}{N+2} \|\rho_1\|_1 N \Omega_N}{\frac{r^N}{N} \|\rho_2\|_1 N \Omega_N - (2\pi)^N k \|\rho_2\|_\infty}$$

which leads to the desired result when

$$r = 2\pi \left(\frac{(N+2)k \|\rho_2\|_\infty}{2\Omega_N \|\rho_2\|_1} \right)^{1/N}.$$

□

3.5 Numerical approximation of optimal densities

In this section we describe a numerical approximation process of optimal densities in \mathbb{R}^2 for $k = 1, \dots, 8$. For $k = 1, 2$ we recover the theoretical results proved in [33], namely the ball and the union of two equal balls respectively. It is a challenge to prove or disprove, for $k \geq 3$, that the optimal densities correspond to a characteristic function. The numerical simulations suggest, to some extent, that the optimal densities are not characteristic functions. We compare the optimal densities with previous computations of optimal shapes and we obtain reliable better values. However, the excess of the optimal eigenvalues in the class of densities over the optimal eigenvalue in the class of domains is relatively low.

Spurious modes

Let $D = (-1, 1)^N \subset \mathbb{R}^N$. For $\varepsilon > 0$ we denote by $\mu_k^\varepsilon(\rho)$ the k -th eigenvalue of the well posed elliptic problem

$$\begin{cases} -\operatorname{div}[(\rho + \varepsilon) \nabla u] = \mu_k^\varepsilon(\rho)(\rho + \varepsilon^2)u \text{ on } D, \\ \partial_n u = 0 \text{ on } \partial D. \end{cases} \quad (3.23)$$

The following occurs.

Lemma 3.5.1. *Let D be a bounded, open Lipschitz set and $\rho \in \mathbf{L}^\infty(D, \mathbb{R}^+)$, $\rho \not\equiv 0$. With the notations above, for $\varepsilon \rightarrow 0$ we have*

$$\forall k \in \mathbb{N}, \mu_k^\varepsilon(\rho) \rightarrow \mu_k(\rho).$$

Proof. The proof is similar to Lemma 3.3.5, so we do not reproduce it here. □

We rely on this approximation result in order to numerically estimate $\mu_k(\rho)$. Notice the difference of homogeneity of the terms depending on ε and ε^2 . This kind of formulation has been introduced by Allaire and Jouve in [4] in the context of the numerical optimization of mechanical structures and is a crucial point to avoid spurious modes.

Indeed, assume $\Omega \subset D$ is a smooth domain and consider the well posed elliptic problem

$$\begin{cases} -\operatorname{div}[(\mathbf{1}_\Omega + \varepsilon) \nabla u] = \mu(\mathbf{1}_\Omega + \varepsilon)u \text{ on } D, \\ \partial_n u = 0 \text{ on } \partial D \end{cases} \quad (3.24)$$

expecting that the spectrum of this problem would converge to Neumann spectrum on Ω . In this natural, but naive, relaxation procedure, extra spurious eigenvalues are actually expected. These eigenmodes are solutions of the limit eigenvalue problem:

$$\begin{cases} -\Delta u = \mu u \text{ on } D \setminus \Omega, \\ u = 0 \text{ on } \Omega, \\ \partial_n u = 0 \text{ on } \partial D. \end{cases}$$

We observe numerically that the associated extra eigenfunctions have a Dirichlet energy concentrated in the complement of the domain Ω ! As an example, we plot the graph of the first spurious eigenfunction for

ε	$\varepsilon - \varepsilon$							$\varepsilon - \varepsilon^2$		
	μ_1	μ_2	μ_3	μ_4	μ_5	μ_6	μ_7	μ_1	μ_2	μ_3
0.1	18.50	18.50	37.36	46.16	49.84	49.84	54.46	23.24	23.24	64.29
0.05	19.64	19.64	40.91	47.10	49.28	49.28	56.08	22.34	22.34	61.80
0.01	20.81	20.81	46.07	48.06	48.63	48.63	57.64	21.41	21.41	58.92
0.005	20.98	20.98	47.14	48.20	48.53	48.53	57.86	21.28	21.28	58.51
0.001	21.11	21.11	48.20	48.32	48.45	48.45	58.04	21.18	21.18	58.17
0.0005	21.13	21.13	48.33	48.36	48.44	48.44	58.06	21.16	21.16	58.12
0.0001	21.15	21.15	48.35	48.43	48.43	48.48	58.08	21.15	21.15	58.09
5e-05	21.15	21.15	48.35	48.43	48.43	48.50	58.08	21.15	21.15	58.09
1e-05	21.15	21.15	48.35	48.43	48.43	48.51	58.08	21.15	21.15	58.08

Table 3.1: Spurious modes persistence. Eigenvalues computed with the approximation (3.24) containing spurious modes (left) and with the approximation (3.23) (right)

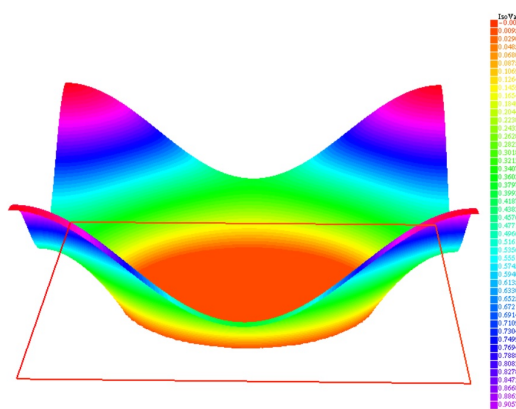


Figure 3.2: One spurious mode

$D = (-1, 1)^2$ and Ω the centered ball of radius $r = 0.4$ in Figure 3.2. Values in Table 3.1 illustrate the persistence of spurious modes even for small values of ε .

Coming back to problem (3.4), our numerical approximation is fully justified by the avoidance of spurious modes from Lemma 3.5.1 and by the following proposition.

Proposition 3.5.2. *Under the notations of (3.23), we have*

$$\max_{\rho \in \mathbf{L}_m^1(D, [0, 1])} \mu_k^\varepsilon(\rho) \xrightarrow{\varepsilon \rightarrow 0} \max_{\rho \in \mathbf{L}_m^1(D, [0, 1])} \mu_k(\rho).$$

Proof. Let $\rho^* \in \mathbf{L}_m^1(D, [0, 1])$ be a maximizer of μ_k and $\rho_\varepsilon \in \mathbf{L}_m^\infty(D, [0, 1])$ be a maximizer of μ_k^ε (their existence are immediate in view of Lemma 3.3.3). Without restricting generality, we can assume that

$$\rho_\varepsilon \xrightarrow{\mathbf{L}^\infty \rightarrow *} \tilde{\rho}$$

and $\tilde{\rho} \in \mathbf{L}_m^1(D, [0, 1])$.

Then, on the one hand

$$\limsup_{\varepsilon \rightarrow 0} \mu_k^\varepsilon(\rho_\varepsilon) \leq \mu_k(\tilde{\rho}) \leq \mu_k(\rho^*).$$

On the other hand,

$$\mu_k^\varepsilon(\rho^*) \leq \mu_k^\varepsilon(\rho_\varepsilon)$$

so that passing to the limit we get

$$\mu_k(\rho^*) \leq \liminf_{\varepsilon \rightarrow 0} \mu_k^\varepsilon(\rho_\varepsilon),$$

which implies that $\tilde{\rho}$ is also maximizer for μ_k and concludes the proof. \square

Numerical strategy

We fix $\varepsilon, m > 0$ and look for a numerical solution of

$$\max \{ \mu_k^\varepsilon(\rho) : \rho \in \mathbf{L}_m^1(D, [0, 1]) \}.$$

We implemented a finite element method for the computation of eigenvalues. Assume D is meshed by a union of triangles $(T_p)_p$. Densities from the space $\mathbf{L}_m^1(D, [0, 1])$ are approximated by standard \mathcal{P}_1 elements consisting of continuous piecewise linear functions on the given mesh (cf Chapter 2). We denote this space by V_h . Functions of $H^1(D)$ are approximated by the space U_h of standard P2 elements consisting of continuous piecewise quadratic polynomials. The canonical basis of V_h (resp. U_h) is denoted by $(\phi_i)_i$ (resp. $(\psi_i)_i$). For a given $\rho \in V_h$ we denote by ρ_i its i -th coordinate in the canonical basis of V_h . The discretized version of our eigenvalue problem is then:

$$\vec{M}^\varepsilon(\rho) \vec{u}_k^\varepsilon(\rho) = \mu_k^\varepsilon(\rho) \vec{K}^\varepsilon(\rho) \vec{u}_k^\varepsilon(\rho)$$

where

$$\begin{aligned} \vec{M}^\varepsilon(\rho)_{i,j} &= \int_D (\rho + \varepsilon) \nabla \psi_i \nabla \psi_j, \\ \vec{K}^\varepsilon(\rho)_{i,j} &= \int_D (\rho + \varepsilon^2) \psi_i \psi_j \end{aligned}$$

and $\vec{u}_k^\varepsilon(\rho)$ are the coordinates of $u_k^\varepsilon(\rho)$ in $(\psi_i)_i$.

In order to implement a gradient descent algorithm, we compute the discrete derivative of our functional

$$\begin{aligned} \mu_k^\varepsilon &: V_h \rightarrow \mathbb{R} \\ \rho &\mapsto \mu_k^\varepsilon(\rho). \end{aligned}$$

For a fixed $\varepsilon > 0$ we are interested in solving the following maximization problem:

$$\begin{aligned} \max_{\rho \in V_h} \quad & \mu_k^\varepsilon(\rho). \\ \text{s.t.} \quad & 0 \leq \rho \leq 1, \\ & \int_D \rho = m. \end{aligned}$$

Using homogeneity arguments, we can get rid of the equality constraint by considering the unconstrained problem

$$\begin{aligned} \max_{\rho \in V_h} \quad & \|\rho\|_1 \mu_k^\varepsilon(\rho) - \alpha(\|\rho\|_1 - m)^2 \\ \text{s.t.} \quad & 0 \leq \rho \leq 1 \end{aligned} \tag{3.25}$$

where $\alpha > 0$ is a parameter related to the mass constraint. When the eigenvalue is simple, a straightforward direct computation of the ρ_l -th partial derivative of μ_k^ε gives

$$\partial_{\rho_l} \mu_k^\varepsilon = \frac{(\vec{u}_k^\varepsilon)^\top \partial_{\rho_l} \vec{M}^\varepsilon \vec{u}_k^\varepsilon - \mu_k^\varepsilon (\vec{u}_k^\varepsilon)^\top \partial_{\rho_l} \vec{K}^\varepsilon \vec{u}_k^\varepsilon}{(\vec{u}_k^\varepsilon)^\top \vec{K}^\varepsilon \vec{u}_k^\varepsilon}$$

where

$$\partial_{\rho_l} \vec{M}^\varepsilon(\rho)_{i,j} = \int_D \phi_l \nabla \psi_i \nabla \psi_j$$

and

$$\partial_{\rho_l} \vec{K}^\varepsilon(\rho)_{i,j} = \int_D \phi_l \psi_i \psi_j.$$

It is standard in eigenvalue optimization to expect a multiplicity higher than one for optimal parameters. This phenomenon is known to produce numerical difficulties in the approximation procedure related to the non differentiability of the functional [94] [80]. A multiplicity higher than one causes the gradient direction to greatly change from one iteration to the next one close to the optimum causing instabilities preventing the algorithm to converge. On the other hand, symmetric combination of multiple eigenvalues are known to preserve smoothness [70].

Having this observation in mind, we introduce a straightforward (but efficient enough in our context) two phases process: When the optimization of problem (3.25) encounters a multiplicity higher than one preventing the gradient based approach to converge we switch to the equivalent smoother problem defined by

$$\begin{aligned} \max_{\rho \in V_h} \quad & \|\rho\|_1 \sum_{i=0}^{l-1} \mu_{k+i}^\varepsilon(\rho) - \alpha(\|\rho\|_1 - m)^2 \\ \text{s.t.} \quad & 0 \leq \rho \leq 1, \\ & \sum_{0 \leq i < j \leq l-1} (\mu_{k+i}^\varepsilon(\rho) - \mu_{k+j}^\varepsilon(\rho))^2 = 0 \end{aligned}$$

where $l = \max\{l \geq 0 : \mu_{k+l}^\varepsilon(\rho) - \mu_k^\varepsilon(\rho) < \sigma\}$ for some small parameter $\sigma > 0$. Notice that in this new, trivially equivalent, formulation, cost and constraint functions are both smooth in the neighborhood of the optimal density.

Technical details

The optimization process has been carried out by IPOPT, an interior point optimization method [100]. Each side of the domain $D = [0, 1]^2$ is discretized into 100 segments then triangulated leading to a total of 11658 degrees of freedom for the function space V_h . The finite elements computations have been carried out through GetFEM [92]. We used the values $\varepsilon = 0.001$, $m = 0.4$ and $\sigma = 0.1$.

After the optimization procedure, we perform a final estimation of the eigenvalue in a post-processing phase. This post-processing consists in getting rid of the areas where the density is almost zero and recomputing the eigenvalue on the remaining density on the smaller domain without using the relaxation. To this purpose, we used MMG [47] to mesh the domain $\{\rho > 0.01\}$ where the value 0.01 is arbitrarily chosen larger than $\varepsilon = 0.001$ to avoid spurious modes but sufficiently small to be close to the actual eigenvalues. However this choice is not very sensitive for the visualization of the geometry of the best density in Figure 3.3, as soon as it is small enough. Then, we interpolate ρ on a $P3$ finite element space on this new mesh and compute the now well-defined eigenvalue problem

$$\begin{cases} -\operatorname{div}(\rho \nabla u) = \mu_k(\rho) \rho u \text{ in } \{\rho > 0.01\}, \\ \frac{\partial u}{\partial n} = 0 \text{ on } \partial\{\rho > 0.01\} \end{cases} \tag{3.26}$$

to obtain precise reliable values of the eigenmodes.

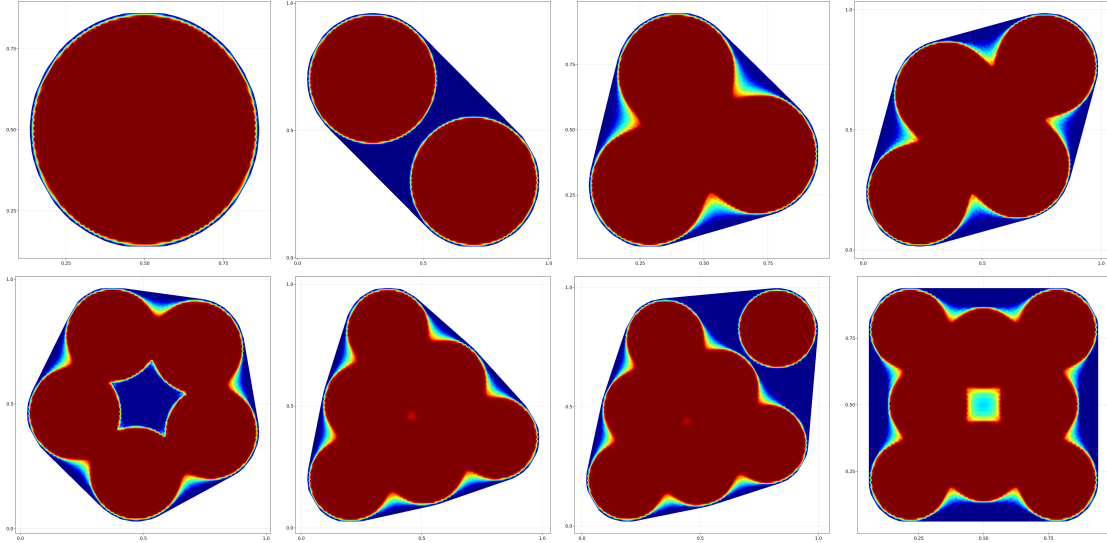


Figure 3.3: Approximation of the first eight optimal densities

Numerical Results

Figure 3.3 displays the numerical results¹ for $k = 1, \dots, 8$ plotted on the convex hull of $\{\rho > 0.01\}$. For $k = 1$ and $k = 2$, we obtained respectively one and two disks, which meets the theory. For $k \geq 3$, optimal densities looks like homogenized union of disks.

In Table 3.2 we display the numerical values obtained by our approach (for densities) compared both to the optimal values of [8] and to the ones of disjoint union of discs. We can observe that $k = 4, k = 5$ and $k = 8$ are fairly different from the result in [8]. Moreover, for $k = 5$ and $k = 8$, the "optimal" shape that one may somehow extract from an optimal density seems not to be a union of *simply connected* domains going beyond the framework in which the computation of [8] have been carried out.

	μ_1	μ_2	μ_3	μ_4	μ_5	μ_6	μ_7	μ_8
Multiplicity	2	2	3	3	3	4	4	4
Optimal densities	10.65	21.28	32.92	43.90	54.47	67.25	77.96	89.47
Optimal shapes, Antunes-Freitas [8]			32.79	43.43	54.08	67.04	77.68	89.22
Union of discs	10.65	21.30	31.95	42.60	53.25	63.90	74.55	88.85

Table 3.2: Values comparison

¹The data of the meshes and solutions is available at https://github.com/EloiMartinet/Maximization_Of_Neumann_Eigenvalues

4

Sharp inequalities for Neumann eigenvalues on the sphere

This chapter is based on the reference [34].

Contents

4.1	Introduction	69
4.2	Topological results	71
4.3	Proof of optimality for μ_2	75
4.4	General proof for the harmonic mean	77
4.5	Further remarks and open questions	79

4.1 Introduction

In this chapter, we study problems similar to Chapter 3 on \mathbb{S}^n . While it may seem that the main tools developped in \mathbb{R}^n can be readily transposed for \mathbb{S}^n , difficulties arises due to the geometrical nature of the sphere. Let $n \geq 2$ and denote by \mathbb{S}^n the unit sphere of dimension n in \mathbb{R}^{n+1} . Let $\Omega \subseteq \mathbb{S}^n$ be an open, Lipschitz set of measure $m \in (0, |\mathbb{S}^n|)$. The eigenvalues of the Laplace-Beltrami operator with Neumann boundary conditions on Ω are

$$0 = \mu_0(\Omega) \leq \mu_1(\Omega) \leq \dots \leq \mu_k(\Omega) \rightarrow +\infty,$$

multiplicity being counted. If Ω is connected then $\mu_1(\Omega) > 0$.

For each $k \in \mathbb{N}$ we have

$$\mu_k(\Omega) = \min_{S \in \mathcal{S}_{k+1}} \max_{u \in S \setminus \{0\}} \frac{\int_{\Omega} |\nabla u|^2}{\int_{\Omega} u^2},$$

where \mathcal{S}_k is the family of all subspaces of dimension k in $H^1(\Omega)$, and the integral is defined with the canonical measure on \mathbb{S}^n . Then, there exists $u \in H^1(\Omega)$, $u \neq 0$ such that

$$\begin{cases} -\Delta_{\mathbb{S}^n} u = \mu_k(\Omega) u \text{ in } \Omega, \\ \frac{\partial u}{\partial \nu} = 0 \text{ on } \partial\Omega. \end{cases}$$

The aim of this chapter is to find sharp upper bounds for the second non-trivial eigenvalue provided that the volume of the set Ω is prescribed. Shortly, we prove that

$$\mu_2(\Omega) \leq \mu_1(\mathbf{B}^{m/2}), \quad (4.1)$$

where $m = |\Omega|$ and \mathbf{B}^a denotes a geodesic ball of volume a in \mathbb{S}^n . This means that the set of volume m with maximal second non trivial Neumann eigenvalue is the union of two disjoint geodesic balls of volume $\frac{m}{2}$.

Although this is our main motivation, the result we obtain is more general, in two directions. First, we shall prove the stronger inequality for the harmonic mean of the eigenvalues of order 2 to n

$$\sum_{k=2}^n \frac{1}{\mu_k(\Omega)} \geq \frac{n-1}{\mu_1(\mathbf{B}^{m/2})}. \quad (4.2)$$

Second, the inequality (4.2) naturally extends to densities with prescribed mass. This is detailed in the last section, but we also refer to [33] for an introduction to such problems.

A (somehow surprising) consequence of inequality (4.1) is an extension of the result of Ashbaugh-Benguria stating that if Ω is contained in a hemisphere of \mathbb{S}^n (and so has volume m not larger than $\frac{|\mathbb{S}^n|}{2}$), the sharp inequality occurs

$$\mu_1(\Omega) \leq \mu_1(\mathbf{B}^m). \quad (4.3)$$

Indeed, inequality (4.1) can be applied as follows: if Ω_1, Ω_2 are two disjoint, smooth open subsets of \mathbb{S}^n , then

$$\mu_2(\Omega_1 \cup \Omega_2) \leq \mu_1\left(\mathbf{B}^{\frac{1}{2}(|\Omega_1|+|\Omega_2|)}\right).$$

This means that

$$\min\{\mu_1(\Omega_1), \mu_1(\Omega_2)\} \leq \mu_1\left(\mathbf{B}^{\frac{1}{2}(|\Omega_1|+|\Omega_2|)}\right).$$

In particular, this implies that the Ashbaugh-Benguria inequality (4.3) holds when Ω lies in the complement of a geodesic ball of volume m . The main explanation of the "ease" with which we obtain this result relies on the richness of the class of new test functions we build for testing the second eigenvalue. It is a challenge to understand whether or not this last inclusion condition can be completely dropped; we comment this issue in Section 4.5.

In the previous chapter we saw that the study of the maximization of Neumann eigenvalues in \mathbb{R}^n already draw the attention of mathematicians since the second part of the XXth century. While there have been some study on the same problem on the other manifolds of constant curvature, our knowledge of the subject is way more limited. It is already known that the main results known on the plane are valid on the hyperbolic space. In [18], Ashbaugh and Benguria show the optimality of the geodesic ball for μ_1 using Weinberger-type arguments. In [56], Laugesen and Freitas prove that the disjoint union of two geodesic balls of same measure maximizes μ_2 using topological arguments similar to [33]. On spheres, the first results are due to Chavel [41] and to Ashbaugh and Benguria [18]. Refining the Weinberger argument,

Ashbaugh and Benguria prove that given $0 < m < \frac{|\mathbb{S}^n|}{2}$ among all subsets of a hemisphere of volume m , the geodesic ball is the unique maximizer. A similar assertion for domains allowed to go beyond the hemisphere is generally an open question (even if their volumes are not larger than $\frac{|\mathbb{S}^n|}{2}$). We refer to [18, Remark (2) after Theorem 5.1] and [20, Remark (2), p. 1085] for some ideas to extend the inequality to domains on the whole sphere. However, those results are typically working only for subclasses of domains which have, in some sense, their mass balanced on sections of the sphere centered at the "center of mass" point. We comment in Section 4.5 the question of completely removing any inclusion constraint.

If $\frac{|\mathbb{S}^n|}{2} \leq m < |\mathbb{S}^n|$ the inequality for μ_1 is not well understood and it is likely to fail, at least for some values of m . The behaviour of the first Neumann eigenvalue on geodesic balls of radius larger than $\frac{\pi}{2}$ studied in [18] support this idea. For instance, the first Neumann eigenvalue of the hemisphere and of the full sphere coincide, so that the monotonicity of the first eigenvalue on geodesic balls with respect to the measure fails to be true, for values of m above the half of the sphere. This is a strong indicator that the inequality may not be true provided the volume is larger than $\frac{|\mathbb{S}^n|}{2}$. We comment this issue in Section 4.5 and refer to [85] for some numerical computation in support to this assertion.

We point out the paper [54], where Fall and Weth analyze critical sets for μ_1 on the sphere. As well, recently, in [23] the authors prove on spheres an extension of the result of Wang and Xia [101] for harmonic means, still under the constraint on Ω to be included in a hemisphere.

Here is the main result.

Theorem 4.1.1. *Let $\Omega \subset \mathbb{S}^n$ be an open, Lipschitz set. Then*

$$\sum_{i=2}^n \frac{1}{\mu_i(\Omega)} \geq \sum_{i=2}^n \frac{1}{\mu_i(\mathbf{B}^{|\Omega|/2} \sqcup \mathbf{B}^{|\Omega|/2})} \left(= \frac{n-1}{\mu_1(\mathbf{B}^{|\Omega|/2})} \right).$$

Equality is attained when Ω is the union of two equal, disjoint geodesic balls.

Note that the hemisphere inclusion hypothesis is not imposed in this result. We work with domains on the full sphere and with arbitrary measure. If Ω has three or more connected components, then $\mu_2(\Omega)$ equals to 0 and the inequality is trivially true. The relevant cases are when Ω is either connected or has two connected components.

As a consequence, μ_2 is maximal on two disjoint geodesic balls of half measure. Indeed, we get the following.

Theorem 4.1.2. *Let $\Omega \subset \mathbb{S}^n$ be an open Lipschitz set, then*

$$\mu_2(\Omega) \leq \mu_1(\mathbf{B}^{|\Omega|/2}).$$

The proof of Theorems 4.1.1 and 4.1.2 is going in the same direction as [33]. We build a pack of n test functions which are orthogonal to both constants and on the first (unknown) eigenfunction of a set Ω . While the idea of the construction is similar to the one of [33] being based on folding (Weinberger based) Ashbaugh-Benguria test functions across a hyperplane containing the center of the sphere, the main difficulty is related to the validity of the topological argument. Roughly speaking, the key difficulty comes from the non uniqueness of the "center of mass" point of an arbitrary domain on a sphere; a domain may have multiple (even infinite) family of such centers for packages of suitable test functions. The uniqueness of such a point was a crucial ingredient in both topological arguments in [33] and [56].

A consequence of this last result is an extension of the result of Ashbaugh-Benguria on the first eigenvalue.

Corollary 4.1.3. *Let $m \in (0, |\mathbb{S}^n|/2)$ and let \mathbf{B}^m be a geodesic ball of measure m in \mathbb{S}^n . Let $\Omega \subset \mathbb{S}^n \setminus \mathbf{B}^m$ be an open Lipschitz set such that $|\Omega| = m$. Then*

$$\mu_1(\Omega) \leq \mu_1(\mathbf{B}^m).$$

In the result above, the hemisphere inclusion condition of Ashbaugh-Benguria is replaced by a weaker one, namely inclusion in the complement of a geodesic ball of measure m . In several other situations the inequality above continues to be true, as, for instance, for every domain which is disjoint with one of its isometric images. Let us also mention the recent paper [77] where the authors use conformal methods to obtain $\mu_1(\Omega) \leq \mu_1(\mathbf{B}^m)$ for any simply connected set $\Omega \subset \mathbb{S}^2$ under the condition $|\Omega| = m \leq 0.94 |\mathbb{S}^2|$.

The issue of dropping completely the inclusion constraint in Corollary 4.1.3 has not a clear answer and will be discussed in the last section. In fact, we numerically identify a density, with support on the full sphere \mathbb{S}^2 and mass less than 2π which has higher first eigenvalue than the corresponding geodesic ball. The main consequence of this observation is that no mass transplantation argument such as ours can work on the full sphere.

The chapter is organized as follows. In the next section we recall some topological tools and prove the main technical result on which is based the construction of the test functions. The key argument relies on the control, along a continuous deformation, of the number of zeroes of a vector field build upon the test functions. Section 4.3 is devoted to the proof of Theorem 4.1.2 and its corollaries, while Section 4.4 is devoted to the proof of Theorem 4.1.1. We choose to switch what should be the natural order of the proofs, since the proof of Theorem 4.1.2 is a direct consequence of the topological arguments, while the proof of Theorem 4.1.1 requires some extra analysis which may hide the core ideas. Finally, in the last section we comment about possible extensions of those results and bring some numerical support for our assertions.

4.2 Topological results

Notations

We write \mathbb{S}^n the unit sphere of dimension n in \mathbb{R}^{n+1} and set $z \mapsto z_1, \dots, z_{n+1}$ its coordinate functions. For any $a \in \mathbb{S}^n$, we let

$$a^- = \{z \in \mathbb{S}^n : z \cdot a < 0\}, \quad a^\perp = \{z \in \mathbb{S}^n : z \cdot a = 0\}, \quad a^+ = \{z \in \mathbb{S}^n : z \cdot a > 0\}$$

and denote

$$R_a(z) = z - 2(z \cdot a)a,$$

$$F_a(z) = \begin{cases} R_a(z) & \text{when } z \in a^+, \\ z & \text{when } z \in a^- \sqcup a^\perp. \end{cases}$$

Above $x \cdot y$ denotes the scalar product of \mathbb{R}^{n+1} between the vectors x and y and $\text{span}(x, y)$ denotes the space spanned by x, y .

For any $w, z \in \mathbb{S}^n$, we denote $\pi_z(w) = w - (w \cdot z)z$ the projection of w on $T_z \mathbb{S}^n = z^\perp$, the tangent hyperplane at the sphere in point z .

Let $|\cdot|$ denote the n -dimensional Hausdorff measure on \mathbb{S}^n . For any $m \in (0, |\mathbb{S}^n|)$, $r \in (0, \pi)$, and $p \in \mathbb{S}^n$, we let $B_{p,r}$ be the geodesic ball in \mathbb{S}^n of center p and radius r , B_p^m the ball of center p and measure m . When p is not mentioned we may implicitly assume that $p = e_{n+1}$ (as it will not matter).

Let $g \in \mathcal{C}^0([-1, 1], \mathbb{R}_+)$ be a continuous even function such that $g > 0$ on $(-1, 1)$. We denote $G(t) = \int_0^t g(s)ds$ the primitive of g which vanishes at $t = 0$.

For any $\rho \in L^1(\mathbb{S}^n, \mathbb{R})$, and $(a, z) \in \mathbb{S}^n \times \mathbb{S}^n$ we denote

$$E_\rho(z) := \int_{\mathbb{S}^n} \rho(v) G(z \cdot v) dv$$

and

$$\mathcal{E}_\rho(a, z) := \int_{\mathbb{S}^n} \rho(v) G(z \cdot F_a v) dv.$$

Notice in particular that $\nabla E_\rho(z) = \nabla_z \mathcal{E}_\rho(-z, z)$, where “ ∇_z ” is the partial gradient in its second variable.

Counting zeroes modulo 4

Let M be a compact manifold with boundary ∂M . Suppose that we have some smooth involution without fixed point $S : M \rightarrow M$, and a $(1,1)$ tensor Q acting as a invertible linear transformation on each tangent space, meaning that for every $x \in M$ we have $Q(x) \in GL(T_x M)$.

We denote by $\mathcal{X}(M)$ be the set of continuous (tangent) vector fields V on M (with the natural \mathcal{C}^0 topology) such that

$$S_* V = QV,$$

meaning that for every $x \in M$, we have $dS(S^{-1}(x))V(S^{-1}(x)) = Q(x)V(x)$. We also let

$$\mathcal{X}^*(M) = \{V \in \mathcal{X}(M) : V|_{\partial M} \text{ does not vanish}\}.$$

When $V \in \mathcal{X}^*(M)$ is smooth (\mathcal{C}^∞), we say it is nondegenerate if for every $x \in M$ such that $V(x) = 0$, and any local chart $\varphi : \mathcal{B} \rightarrow M$ (where \mathcal{B} is a ball in Euclidian space) with $\varphi(0) = x$, then $D(\varphi^* V)(0)$ is invertible (where $\varphi^* V = (\varphi^{-1})_* V$).

Lemma 4.2.1. *There is a unique continuous function $I : \mathcal{X}^*(M) \rightarrow \mathbb{Z}/4\mathbb{Z}$ such that for every smooth nondegenerate vector field $V \in \mathcal{X}^*(M)$,*

$$I(V) = \text{Card}(\{x \in M : V(x) = 0\}) \bmod (4).$$

In particular I is invariant by homotopy in $\mathcal{X}^*(M)$. This result is similar to [87, §4], [95, Ch. 7.4].

Proof. This is a consequence of the two following facts: first, by smoothing and a classical application of Sard's theorem we have the \mathcal{C}^0 -density of vectors $V \in \mathcal{X}^*(M)$ with \mathcal{C}^∞ regularity and nondegenerate zeros. Second for any two sufficiently close, smooth and nondegenerate vector fields V, W , we have

$$\text{Card}(V^{-1}(0))(V) = \text{Card}(W^{-1}(0)) \bmod (4).$$

Indeed, letting $V_t = (1-t)V + tW$ we have an homotopy between V and W that never vanish on ∂M when $\|V - W\|_{\mathcal{C}^0(M)} < \inf_{\partial M} |V|$. Then by a perturbation argument and parametric transversality theorem (see for instance [95, Th. 7.1.1]) there is an homotopy $(H_t)_{0 \leq t \leq 1}$ in $\mathcal{X}^*(M)$ such that H_0 (respectively H_1) is an arbitrarily small perturbation of V (respectively W) and so

$$\text{Card}(V^{-1}(0)) = \text{Card}(H_0^{-1}(0)), \quad \text{Card}(W^{-1}(0)) = \text{Card}(H_1^{-1}(0)),$$

and such that $H : [0, 1] \times M \rightarrow TM$ is transversal to the null vector field. As a consequence $Z := \{(t, x) \in [0, 1] \times M : H_t(x) = 0\}$ is a compact 1-dimensional manifold that meets $\partial[0, 1] \times M$ transversally but that does not meet $[0, 1] \times \partial M$ (because the homotopy is in $\mathcal{X}^*(M)$). For every connected component c of Z there are four possibilities (due to the classification of 1-dimensional manifold, see for instance [95, Th 5.4.1]):

- c is a circle ; in this case it has no influence on counting of zeroes of H_0, H_1 .
- c is a curve (we write it $c(\tau)_{\tau \in [0, 1]}$) such that $c(0)$ and $c(1)$ are both in $\{0\} \times M$. Consider then $\tilde{c}(\tau) := (\text{Id}_{[0, 1]}, \mathcal{S}) \circ c(\tau)$; by the symmetry property of V we know it is also a connected component of Z with both ends in $\{0\} \times M$.

We claim that it is disjoint from c ; indeed for every $\tau \in [0, 1]$, $c(\tau) \neq \tilde{c}(\tau)$, however if c and \tilde{c} span the same curve then $\tilde{c} = c \circ \varphi$ for some continuous map $\varphi : [0, 1] \rightarrow [0, 1]$ with no fixed point, which is a contradiction. As a consequence $c(0), c(1), \tilde{c}(0), \tilde{c}(1)$ are all distincts, so the number of such zeroes is a multiple of 4.

- c is a curve with both ends in $\{1\} \times M$; this is the same as above.
- c is a curve with $c(0) \in \{0\} \times M, c(1) \in \{1\} \times M$; this counts the same number of zeroes on both sides.

Thus the difference of the number of zeroes of H_0 and H_1 is a multiple of 4, which ends the proof. \square

The main technical result on which is based the construction of test functions is the following.

Theorem 4.2.2. *Let $\rho, \sigma \in L^1(\mathbb{S}^n, \mathbb{R})$ with $\rho \geq 0$. Then there exists $(a, z) \in \mathbb{S}^n \times \mathbb{S}^n$ such that z is a critical point of both $\mathcal{E}_\rho(a, \cdot)$ and $\mathcal{E}_\sigma(a, \cdot)$.*

Criticality above reads

$$\int_{\mathbb{S}^n} \rho(v) g(z \cdot F_a(v)) \pi_z F_a(v) dv = \int_{\mathbb{S}^n} \sigma(v) g(z \cdot F_a(v)) \pi_z F_a(v) dv = 0.$$

The remaining part of the section is devoted to the proof of this theorem.

Proof. This is direct for any a when $\rho = 0$, so we suppose without loss of generality that $\int_{\mathbb{S}^n} \rho > 0$. We begin with a computation which will be useful in several steps of the proof.

Lemma 4.2.3. *Let $p \in \mathbb{S}^n$. For any $r \in (0, \pi/2)$, let us denote $G_r : [-1, 1] \rightarrow \mathbb{R}$ given by*

$$G_r(p \cdot z) = E_{1_{B_{p,r}}}(z).$$

Then, $G_r \in \mathcal{C}^0([-1, 1], \mathbb{R}) \cap \mathcal{C}^1((-1, 1), \mathbb{R})$ and satisfies $G'_r > 0$ in $(-1, 1)$. Moreover,

$$G'_r(p \cdot z) \pi_z(p) = \nabla E_{1_{B_{p,r}}}(z).$$

Proof. By explicit computation,

$$E_{1_{B_{p,r}}}(z) = \int_{B_{p,r}} G(z \cdot v) dv.$$

Since G is \mathcal{C}^1 , we obtain directly that $E_{1_{B_{p,r}}}$ is \mathcal{C}^1 and only depends on the scalar product $z \cdot p$. Consequently, it may be written as a function $G_r(p \cdot z)$ with $G_r \in \mathcal{C}^1((-1, 1), \mathbb{R})$.

Let us now check that $G'_r > 0$ on $(-1, 1)$. For any $z \neq \pm p$,

$$G'_r(z \cdot p) \pi_z(p) = \nabla E_{1_{B_{p,r}}}(z) = \int_{B_{p,r}} g(z \cdot v) \pi_z(v) dv.$$

We let $u = -\frac{\pi_z(p)}{|\pi_z(p)|}$ be the unique unit vector in $T_z \mathbb{S}^n \cap \text{span}(p, z)$ such that $u \cdot p < 0$. Then

$$\begin{aligned} G'_r(z \cdot p) u \cdot p &= \int_{B_{p,r}} g(z \cdot v) (u \cdot v) dv \\ &= \int_{B_{p,r} \setminus R_u(B_{p,r})} g(z \cdot v) (u \cdot v) dv < 0. \end{aligned}$$

The last inequality holds because $w \in B_{p,r} \setminus R_u(B_{p,r})$ implies $u \cdot w < 0$. □

Homotopy and zeroes of the gradient fields

Let $r \in (0, \pi/4)$ (its precise value is not important), and some $p, q \in \mathbb{S}^n$ that will be fixed later. Consider the following homotopy for $t \in [0, 1]$:

$$H_t(a, z) := \left((1-t)\mathcal{E}_\rho(a, z) + t\mathcal{E}_{1_{B_{p,r}}}(a, z), (1-t)\mathcal{E}_\sigma(a, z) + t\mathcal{E}_{1_{B_{q,r}}}(a, z) \right).$$

We claim that $\nabla_z H_t(a, z)$ has no zeroes when $a \cdot z = 0$. Indeed looking at the first component we always have

$$\begin{aligned} a \cdot \nabla_z \mathcal{E}_\rho(a, z) &= \int_{\mathbb{S}^n} \rho(v) g(z \cdot F_a v) (a \cdot \pi_z F_a v) dv = \int_{\mathbb{S}^n} \rho(v) g(z \cdot v) (a \cdot F_a v) dv < 0. \\ a \cdot \nabla_z \mathcal{E}_{1_{B_{p,r}}}(a, z) &= \int_{B_{p,r}} g(z \cdot F_a v) (a \cdot \pi_z F_a v) dv = \int_{B_{p,r}} g(z \cdot v) (a \cdot F_a v) dv < 0. \end{aligned}$$

so, by uniform continuity, the first component of $\nabla_z H_t(a, z)$ doesn't vanish for any $t \in [0, 1]$ and $(a, z) \in \mathbb{S}^n \times \mathbb{S}^n$ for which $|a \cdot z|$ is small enough.

We claim that for well-chosen points p, q ,

$$z \in a^-, \nabla_z H_1(a, z) = 0 \text{ implies } \{z, R_a(z)\} = \{p, q\}.$$

The points p, q we will be chosen to be antipodal, but it may be checked that any p, q such that $B_{p,r} \cap B_{q,r} = \emptyset$ would work as well.

Indeed,

- If $\nabla_z \mathcal{E}_{1_{B_{p,r}}}(a, z) = 0$, then $p \in \text{span}(a, z)$. This is because for any $b \in \text{span}(z, a)^\perp$, we have

$$b \cdot \nabla_z \mathcal{E}_{1_{B_{p,r}}}(a, z) = \int_{B_{p,r}} g(z \cdot F_a(v))(b \cdot v) dv = \int_{B_{p,r} \setminus B_{R_{b,p},r}} g(z \cdot F_a(v))(b \cdot v) dv,$$

which is positive (resp. negative) as soon as $b \cdot p > 0$ (resp. $b \cdot p < 0$).

- If $R_a(z) = -z$ or $B_{p,r} \subset a^- \sqcup a^+$, then $p \in \{z, R_a(z)\}$. Indeed in the first case it means $a = -z$, so z can be identified with the critical points of $E_{1_{B_{p,r}}}$, which are $\{\pm z\}$. In the second case, if $\overline{B_{p,r}}$ is fully in a^- (resp a^+), then z (resp $R_a z$) is also a critical point of $E_{B_{p,r}}$, meaning

$$p = \begin{cases} z & \text{if } p \in a^-, \\ R_a(z) & \text{if } p \in a^+ \end{cases}.$$

- If $\nabla_z \mathcal{E}_{1_{B_{p,r}}}(a, z) = 0$ and $p \notin \{z, R_a(z)\}$, then

$$c := \frac{z + R_a(z)}{|z + R_a(z)|} \in \overline{B_{p,r}}. \quad (4.4)$$

Indeed, according to the previous point $R_a(z) \neq -z$ (meaning c is well-defined) and $B_{p,r}$ meets a^\perp . Since $\overline{B(p, r)}$ and a^\perp intersect, $r < \frac{\pi}{4}$ and $p \in \text{span}(a, z)$, then necessarily $\overline{B_{p,r}}$ contains (exactly) one of $\{-c, c\}$. However, if it meets $-c$ then since $r < \frac{\pi}{4}$, $B_{p,r} \subset c^- \subset \{v : a \cdot \pi_z F_a(v) < 0\}$ so

$$a \cdot \nabla_z \mathcal{E}_{1_{B_{p,r}}}(a, z) = \int_{B_{p,r}} g(z \cdot F_a(v))(a \cdot \pi_z F_a(v)) dv < 0$$

so necessarily $c \in \overline{B_{p,r}}$.

Since we are free to choose p and q , we may take $p = e_{n+1}$, $q = -e_{n+1}$. Assume $\nabla_z H_1(a, z) = 0$ and suppose that $\{p, q\} \neq \{z, R_a z\}$. Then using the second point, necessarily $z \neq R_a z$ and either $B_{p,r}$ or $B_{q,r}$ meets c (which is as defined in equation (4.4)); without loss of generality assume $c \in \overline{B_{p,r}}$, then since $r < \frac{\pi}{4}$ we have $B_{q,r} \subset c^- \cap (a^+ \sqcup a^-)$, which is in contradiction with the fact that $q \in \{z, R_a z\}$. This prove the claim.

Counting zeroes modulo 4

Let us now make a change of parametrization; for any $(z, w) \in \mathbb{S}^n \times \mathbb{S}^n$ that are not identical, we define

$$a = a(z, w) := \frac{w - z}{|w - z|},$$

such that $z \in a^-$, $w = R_a z$, R_a acting as an isometry between $T_z \mathbb{S}^n$ and $T_w \mathbb{S}^n$. We let D be a (small) tubular neighbourhood of $\{(z, w) \in (\mathbb{S}^n)^2 : z = w\}$, $M = (\mathbb{S}^n)^2 \setminus D$, and we define, for any densities (ρ, σ) , the vector field

$$\mathcal{V}_{\rho, \sigma}(z, w) = (\nabla_z \mathcal{E}_\rho(a(z, w), z), R_a \nabla_z \mathcal{E}_\sigma(a(z, w), z)).$$

$\mathcal{V}_{\rho, \sigma}$ and $\mathcal{V}_{1_{B_{p,r}}, 1_{B_{q,r}}}$ are two tangent vector fields of M that are homotopic with no zeroes crossing ∂M when D is chosen small enough.

Define $S : (z, w) \in M \mapsto (w, z) \in M$; it is a smooth involution with no fixed point. For any $(z, w) \in M$, let $Q(z, w)$ be the linear endomorphism of $T_{z,w} M = T_z \mathbb{S}^n \times T_w \mathbb{S}^n$ defined by

$$Q(z, w). (h, k) = (R_a k, R_a h).$$

We claim that for any $(z, w) \in M$:

$$dS(w, z)\mathcal{V}_{\rho, \sigma}(w, z) = Q(z, w)\mathcal{V}_{\rho, \sigma}(z, w), \quad (4.5)$$

or in a more synthetic way that $S_*\mathcal{V}_{\rho, \sigma} = Q\mathcal{V}_{\rho, \sigma}$ as in the hypothesis of Lemma 4.2.1. Indeed, write $a := a(z, w)$, notice that $a(w, z) = -a$, that $\pi_z R_a = R_a \pi_w$ and $F_{-a} = R_a F_a$. Then

$$\begin{aligned} \mathcal{V}_{\rho, \sigma}(w, z) &= \left(\int_{\mathbb{S}^n} \rho(v) g(w \cdot F_{-a} v) \pi_w F_{-a} v dv, R_a \int_{\mathbb{S}^n} \sigma(v) g(w \cdot F_{-a} v) \pi_w F_{-a} v dv \right) \\ &= \left(R_a \int_{\mathbb{S}^n} \rho(v) g(z \cdot F_a v) \pi_z F_a v dv, \int_{\mathbb{S}^n} \sigma(v) g(z \cdot F_a v) \pi_z F_a v dv \right), \end{aligned}$$

and $dS(w, z).(h, k) = (k, h)$, so

$$\begin{aligned} dS(w, z).\mathcal{V}_{\rho, \sigma}(w, z) &= \left(\int_{\mathbb{S}^n} \sigma(v) g(z \cdot F_a v) \pi_z F_a v dv, R_a \int_{\mathbb{S}^n} \rho(v) g(z \cdot F_a v) \pi_z F_a v dv \right) \\ &= Q(z, w).\mathcal{V}_{\rho, \sigma}(z, w). \end{aligned}$$

We thus define the zero counting modulo 4 in M as in Lemma 4.2.1 and we claim that

$$I(\mathcal{V}_{1_{B_p, r}, 1_{B_q, r}}) = 2 \text{ mod } (4).$$

According to the previous discussion, the zeroes of $\mathcal{V}_{1_{B_p, r}, 1_{B_q, r}}$ are exactly $\{(p, q), (q, p)\}$. Let (z, w) be sufficiently close to (p, q) such that $\overline{B_{p,r}} \subset a(z, w)^-, \overline{B_{q,r}} \subset a(z, w)^+$. Notice that in this case

$$\begin{aligned} \nabla_z \mathcal{E}_{1_{B_p, r}}(a, z) &= \int_{B_{p,r}} g(z \cdot v) \pi_z v dv = G'_r(z \cdot p) \pi_z(p) \\ \nabla_z \mathcal{E}_{1_{B_q, r}}(a, z) &= \int_{B_{q,r}} g(z \cdot R_a(v)) \pi_z(R_a(v)) dv \\ &= R_a \left(\int_{B_{q,r}} g(w \cdot v) \pi_w(v) dv \right) \\ &= G'_r(w \cdot q) R_a(\pi_w(q)) \end{aligned}$$

because $\pi_z R_a = R_a \pi_w$. Thus $\mathcal{V}_{1_{B_p, r}, 1_{B_q, r}}(z, w)$ admits the simpler expression (when (z, w) is in a neighbourhood of (p, q))

$$\mathcal{V}_{1_{B_p, r}, 1_{B_q, r}}(z, w) = (G'_r(z \cdot p) \pi_z(p), G'_r(w \cdot q) \pi_w(q)). \quad (4.6)$$

Up to a choice of orientable chart, this is locally homotopic to $-\text{Id}|_{\mathcal{B}}$ (where \mathcal{B} is the unit Euclidian ball of \mathbb{R}^{2n}) which has a unique nondegenerate zero. When (z, w) is near (q, p) the study is the same by the symmetry property (4.5), so (q, p) counts as one nondegenerate zero. We thus get that $I(\mathcal{V}_{1_{B_p, r}, 1_{B_q, r}}) = 2 \text{ mod } (4)$ as claimed. Since $\mathcal{V}_{\rho, \sigma}$ and $\mathcal{V}_{1_{B_p, r}, 1_{B_q, r}}$ are homotopic in $\mathcal{X}^*(M)$, by invariance of I through homotopy:

$$I(\mathcal{V}_{\rho, \sigma}) = I(\mathcal{V}_{1_{B_p, r}, 1_{B_q, r}}) = 2 \text{ mod } (4).$$

Conclusion

Since $I(\mathcal{V}_{\rho, \sigma}) \neq 0 \text{ mod } (4)$ we conclude that $\mathcal{V}_{\rho, \sigma}$ has a zero (z, w) somewhere in M . Since $z \neq w$, then $(a, z) := \left(\frac{w-z}{|w-z|}, z \right)$ satisfies the conclusion of Theorem 4.2.2. \square

4.3 Proof of optimality for μ_2

Although Theorem 4.1.2 is *de facto* a consequence of Theorem 4.1.1, for expository reasons, we start with a short, independent proof of Theorem 4.1.2. The reason is that Theorem 4.1.1 requires some extra arguments related to the presence of higher order eigenvalues and so it can hide the core ideas of the proof.

Proof. (of Theorem 4.1.2) Let r be the radius of $\mathbf{B}^{|\Omega|/2}$. The first non-trivial eigenvalue of B_r (supposed to be centered in e_{n+1}) has multiplicity n and its eigenfunctions are of the form

$$v \mapsto J(\theta) \frac{v_i}{\sin(\theta)}, \quad i = 1, \dots, n$$

where $\theta = \arccos(v_{n+1})$ is the angle between v and e_{n+1} . The function $J : [0, r] \rightarrow \mathbb{R}_+$ is a non-trivial solution of the differential equation

$$\frac{1}{\sin(\theta)^{n-1}} \frac{d}{d\theta} \left[\sin(\theta)^{n-1} \frac{d}{d\theta} J(\theta) \right] + \left(\mu_1(B_r) - \frac{n-1}{\sin(\theta)^2} \right) J(\theta) = 0.$$

In [18] (see also [23]), the authors study this function and prove that $J(0) = 0$, $J'(r) = 0$, $J' > 0$ on $(0, r)$, meaning J is positive and increasing on $(0, r]$. Following [18], we extend J on $[0, \pi]$: we let it be constant (equal to $J(r)$ by continuity) on $[r, \pi/2]$, and symmetric along the reflexion $\theta \mapsto \pi - \theta$. Moreover, from [18] (see also [23]), the functions

$$\theta \in \left(0, \frac{\pi}{2}\right) \mapsto J(\theta)^2, \quad \theta \in \left(0, \frac{\pi}{2}\right) \mapsto J'(\theta)^2 + \frac{n-1}{\sin(\theta)^2} J(\theta)^2$$

are respectively nondecreasing and decreasing.

We then define for all t in $(-1, 1)$

$$g(t) := \frac{J(\arccos(t))}{\sqrt{1-t^2}}$$

and extend it by continuity in 1 and -1 with value 0. We set $G(t) = \int_0^t g$ as previously.

Consider $\rho = 1_\Omega$, $\sigma = u_1 1_\Omega$ where u_1 is a non-constant eigenfunction associated to $\mu_1(\Omega)$. When Ω is disconnected, such a function is a constant different from 0 on some of the connected components and equals to 0 elsewhere.

In order to prove the inequality $\mu_2(\Omega) \leq \mu_2(\mathbf{B}^{m/2} \sqcup \mathbf{B}^{m/2})$ the mass transplantation method used in [33] works, in relation with the properties of J recalled above. Indeed, following Theorem 4.2.2 there exists $(a, z) \in \mathbb{S}^n \times \mathbb{S}^n$ such that

$$\int_\Omega g(z \cdot F_a(v)) \pi_z F_a(v) dv = \int_\Omega u_1(v) g(z \cdot F_a(v)) \pi_z F_a(v) dv = 0.$$

Up to a rotation we may assume $z = e_{n+1}$ with $a \in e_{n+1}^-$. This means that for any $i = 1, \dots, n$, the function

$$v \mapsto g(z \cdot F_a v)(F_a v)_i$$

is orthogonal to 1 and u_1 in $L^2(\Omega)$. In particular, for each $i = 1, \dots, n$ we have

$$\mu_1(\Omega) \int_\Omega |g(z \cdot F_a v)(F_a v)_i|^2 dv \leq \int_\Omega |\nabla(g(z \cdot F_a v)(F_a v)_i)|^2 dv \quad (4.7)$$

We now define $H_{a^-} = (B(e_{n+1}, r) \cup B(-e_{n+1}, r)) \cap a^-$, and we define the first angular coordinate $\theta^- : v \mapsto \arccos(v_{n+1})$. Similary, we let $H_{a^+} = R_a(H_{a^-}) (\subset a^+)$ and $\theta^+(v) = \theta^-(R_a v)$. Then summing the previous inequality in i we get

$$\begin{aligned} \mu_2(\Omega) &\left[\int_{H_{a^-} \cap \Omega} J(\theta^-)^2 dv + \int_{H_{a^+} \cap \Omega} J(\theta^+)^2 dv + |\Omega \setminus (H_{a^-} \cup H_{a^+})| J(r)^2 \right] \\ &\leq \left[\int_{H_{a^-} \cap \Omega} b(\theta^-) dv + \int_{H_{a^+} \cap \Omega} b(\theta^+) dv + \int_{\Omega \setminus (H_{a^-} \cup H_{a^+})} b(\theta^-(R_a v)) dv \right] \end{aligned}$$

Above, we have denoted $b(\theta) := J'(\theta)^2 + \frac{n-1}{\sin(\theta)^2} J(\theta)^2$.

Using the properties of $J(\theta)$, $b(\theta)$ and the fact that $|\Omega \setminus (H_{a^-} \cup H_{a^+})| = |H_{a^-} \setminus \Omega| + |H_{a^+} \setminus \Omega|$ this reduces to

$$\begin{aligned} \mu_2(\Omega) &\leq \frac{\int_{H_{a^-} \cap \Omega} b(\theta^-) dv + \int_{H_{a^+} \cap \Omega} b(\theta^+) dv + |\Omega \setminus (H_{a^-} \cup H_{a^+})| b(r)}{\int_{H_{a^-} \cap \Omega} J(\theta^-)^2 dv + \int_{H_{a^+} \cap \Omega} J(\theta^+)^2 dv + |\Omega \setminus (H_{a^-} \cup H_{a^+})| J(r)^2} \\ &\leq \frac{\int_{H_{a^-}} b(\theta^-) dv + \int_{H_{a^+}} b(\theta^+) dv}{\int_{H_{a^-}} J(\theta^-)^2 dv + \int_{H_{a^+}} J(\theta^+)^2 dv} \\ &= \mu_1(B_r), \end{aligned}$$

which is the result. \square

Corollary 4.3.1. *Let $\Omega \subset \mathbb{S}^n$ be a Lipschitz domain and $i(\Omega) \subseteq \mathbb{S}^n$ an isometric image of Ω . Assume that $\Omega \cap i(\Omega) = \emptyset$. Then*

$$\mu_1(\Omega) \leq \mu_1(\mathbf{B}^{|\Omega|}).$$

The proof is an immediate consequence of Theorem 4.1.2 applied to $\Omega \sqcup i(\Omega)$. This result was previously known only for $i(\Omega) = -\Omega$.

Corollary 4.3.2. *Let $\Omega \subset \mathbb{S}^n$ such that $|\Omega| \leq \frac{|\mathbb{S}^n|}{2}$ and $\Omega \cap \mathbf{B}^{|\Omega|} = \emptyset$. Then*

$$\mu_1(\Omega) \leq \mu_1(\mathbf{B}^{|\Omega|}).$$

This result extends the hemisphere inclusion condition of Ashbaugh and Benguria expressed, with our notation, as $\Omega \cap \mathbf{B}^{|\mathbb{S}^n|/2} = \emptyset$.

Proof. We remind that the function

$$m \in (0, |\mathbb{S}^n|) \mapsto \mu_1(\mathbf{B}^m)$$

is continuous and decreasing on $(0, |\mathbb{S}^n|/2)$ (and actually on a slightly larger interval), as was proved in [18].

Let $\Omega \subseteq \mathbb{S}^n$ satisfying the hypotheses of Corollary 4.3.2. Consider $\varepsilon \in (0, |\Omega|)$, then $\Omega \cap \mathbf{B}^{|\Omega|-\varepsilon} = \emptyset$ and, according to Theorem 4.1.2,

$$\min \left\{ \mu_1(\Omega), \mu_1(\mathbf{B}^{|\Omega|-\varepsilon}) \right\} = \mu_2(\Omega \sqcup \mathbf{B}^{|\Omega|-\varepsilon}) \leq \mu_1(\mathbf{B}^{|\Omega|-\frac{1}{2}\varepsilon})$$

Since $\mu_1(\mathbf{B}^{|\Omega|-\varepsilon}) > \mu_1(\mathbf{B}^{|\Omega|-\frac{1}{2}\varepsilon})$, we get $\mu_1(\Omega) \leq \mu_1(\mathbf{B}^{|\Omega|-\frac{1}{2}\varepsilon})$, which implies the result as $\varepsilon \rightarrow 0$. \square

4.4 General proof for the harmonic mean

Proof of Theorem 4.1.1. In [23], it has been proved that

$$\sum_{i=1}^{n-1} \frac{1}{\mu_i(\Omega)} \geq \sum_{i=1}^{n-1} \frac{1}{\mu_i(\mathbf{B}^{|\Omega|})} \left(= \frac{n-1}{\mu_1(\mathbf{B}^{|\Omega|})} \right).$$

We mostly rely on those computations, to which we refer the reader. With the notations of the proof of Theorem 4.1.2, the main idea is to choose a suitable basis for e_{n+1}^\perp so that extra orthogonality conditions on the eigenfunctions occur. This is also the idea behind [101] and [23], however, some extra care is needed because of the structure of the test functions found in Section 4.2.

We fix again $\rho = 1_\Omega$, $\sigma = u_1 1_\Omega$ and suppose, up to a rotation, that $a \in e_{n+1}^-$ is such that e_{n+1} is a critical point of both $\mathcal{E}_\rho(a, \cdot)$ and $\mathcal{E}_\sigma(a, \cdot)$. This means that for any $\xi \in \mathbb{R}^n (\hookrightarrow \mathbb{R}^n \times \{0\} = e_{n+1}^\perp)$, the function

$$\varphi_\xi(w) := g((F_a w)_{n+1})(\xi \cdot F_a w)$$

is orthogonal to $1, u_1$ in $L^2(\Omega)$.

Lemma 4.4.1. *There is a choice of an orthonormal basis ξ_1, \dots, ξ_n of \mathbb{R}^n such that for any $i = 1, \dots, n$,*

$$\varphi_{\xi_i} \in \text{span}(1, u_1, \dots, u_i)^\perp$$

Proof. We start by choosing ξ_n . Consider the function

$$f : \xi \in \mathbb{S}^{n-1} \mapsto \left(\int_\Omega u_2 \varphi_\xi, \dots, \int_\Omega u_n \varphi_\xi \right) \in \mathbb{R}^{n-1}.$$

Then f verifies $f(-\xi) = -f(\xi)$, so by Borsuk-Ulam theorem [86] we get that f must vanish at some ξ_n . We then continue with the restriction

$$\xi \in \mathbb{S}^{n-1} \cap \xi_n^\perp \mapsto \left(\int_\Omega u_2 \varphi_\xi, \dots, \int_\Omega u_{n-1} \varphi_\xi \right) \in \mathbb{R}^{n-2}.$$

to choose ξ_{n-1} , and so on until ξ_2 such that φ_{ξ_2} is orthogonal to $1, u_1$ and u_2 . Finally, ξ_1 is then chosen in $\mathbb{S}^n \cap \text{span}(\xi_n, \dots, \xi_2)^\perp$ (there are two possibilities and we may choose the one that makes an oriented basis, although this is not important for the rest of the proof). \square

From the orthogonality properties proved above, for any $i = 1, \dots, n$ we get

$$\int_{\Omega} |\varphi_{\xi_i}|^2 \leq \frac{1}{\mu_{i+1}(\Omega)} \int_{\Omega} |\nabla \varphi_{\xi_i}|^2.$$

Assuming that $\xi_i = e_i$,

$$\begin{aligned} & \int_{a^-} (1_{\Omega} + 1_{R_a(a^+ \cap \Omega)}) J^2(\arccos(v_{n+1})) \frac{v_i^2}{1 - v_{n+1}^2} dv \leq \\ & \frac{1}{\mu_{i+1}(\Omega)} \int_{a^-} (1_{\Omega} + 1_{R_a(a^+ \cap \Omega)}) \left(\frac{J^2(\arccos(v_{n+1})) (1 - v_i^2 - v_{n+1}^2)}{(1 - v_{n+1}^2)^2} + \frac{(J'(\arccos(v_{n+1})) v_i)^2}{1 - v_{n+1}^2} \right) dv. \end{aligned}$$

Since $\theta^- = \arccos(v_{n+1})$ we simplify

$$\begin{aligned} & \int_{a^-} (1_{\Omega} + 1_{R_a(a^+ \cap \Omega)}) J^2(\theta^-) \frac{v_i^2}{\sin(\theta^-)^2} dv \leq \\ & \frac{1}{\mu_{i+1}(\Omega)} \left(\int_{a^-} (1_{\Omega} + 1_{R_a(a^+ \cap \Omega)}) \frac{J^2(\theta^-)}{\sin(\theta^-)^2} \frac{1 - v_i^2}{\sin(\theta^-)^2} dv + \int_{a^-} (1_{\Omega} + 1_{R_a(a^+ \cap \Omega)}) \frac{(J'(\theta^-) v_i)^2}{\sin(\theta^-)^2} dv \right). \end{aligned}$$

Summing for $i = 1, \dots, n$, the left hand side becomes $\int_{a^-} (1_{\Omega} + 1_{R_a(a^+ \cap \Omega)}) J(\theta^-)^2 dv$ and the monotonicity property of J leads to

$$2 \int_{H^-} J(\theta^-)^2 dv \leq \int_{a^-} (1_{\Omega} + 1_{R_a(a^+ \cap \Omega)}) J(\theta^-)^2 dv.$$

Inside the first term of the right hand side, we use the inequality

$$\sum_{i=1}^n \frac{1}{\mu_{i+1}(\Omega)} \left(1 - \frac{v_i^2}{\sin(\theta^-)^2} \right) \leq \sum_{i=2}^n \frac{1}{\mu_i(\Omega)},$$

so that

$$\begin{aligned} & \sum_{i=1}^n \frac{1}{\mu_{i+1}(\Omega)} \int_{a^-} (1_{\Omega} + 1_{R_a(a^+ \cap \Omega)}) \frac{J^2(\theta^-)}{\sin(\theta^-)^2} \frac{1 - v_i^2}{\sin(\theta^-)^2} dv \leq \\ & \sum_{i=2}^n \frac{1}{\mu_i(\Omega)} \int_{a^-} (1_{\Omega} + 1_{R_a(a^+ \cap \Omega)}) \frac{J^2(\theta^-)}{\sin(\theta^-)^2} dv. \end{aligned}$$

The second term in the right hand side vanishes outside $(\Omega \cap H^-) \cup R_a(H^+ \cap \Omega)$, hence

$$\begin{aligned} & \sum_{i=1}^n \frac{1}{\mu_{i+1}(\Omega)} \int_{a^-} (1_{\Omega} + 1_{R_a(a^+ \cap \Omega)}) \frac{(J'(\theta^-) v_i)^2}{\sin(\theta^-)^2} dv \leq \\ & \sum_{i=1}^n \frac{1}{\mu_{i+1}(\Omega)} \int_{H^-} (1_{\Omega} + 1_{R_a(a^+ \cap \Omega)}) \frac{(J'(\theta^-) v_i)^2}{\sin(\theta^-)^2} dv. \end{aligned}$$

Relying on the monotonicity property of b , we implement now the mass transplantation as follows: if a point belongs to $\Omega \cap H^-$ or $R_a(a^+ \cap \Omega) \cap H^-$ we keep the integrands unchanged. If a point belongs to $(\Omega \cap a^-) \setminus H^-$ or to $R_a(a^+ \cap \Omega) \setminus H^-$, we virtually transport it in any free point of H^- or $R_a H^-$, the overall mass being preserved.

We get

$$2 \int_{H^-} J(\theta^-)^2 dv \leq 2 \left(\sum_{i=2}^n \frac{1}{\mu_i(\Omega)} \right) \int_{H^-} \frac{J(\theta^-)^2}{\sin(\theta^-)^2} dv + 2 \sum_{i=1}^n \frac{1}{\mu_{i+1}(\Omega)} \int_{H^-} \frac{(J'(\theta^-) v_i)^2}{\sin(\theta^-)^2} dv.$$

Taking into account the symmetry of H^- and of J , we get

$$\int_{H^-} \frac{(J'(\theta^-) v_i)^2}{\sin(\theta^-)^2} dv = \frac{1}{n} \int_{H^-} (J'(\theta^-))^2 dv = \frac{1}{n} \int_{B^{|\Omega|/2}} (J'(\theta))^2 dv.$$

Since

$$\sum_{i=1}^n \frac{1}{\mu_i(\Omega)} \leq \frac{n}{n-1} \sum_{i=2}^n \frac{1}{\mu_i(\Omega)}$$

and

$$\mu_1(\mathbf{B}^{|\Omega|/2}) = \frac{\int_{H^-} \left(J'(\theta^-)^2 + \frac{J(\theta^-)^2}{\sin(\theta^-)^2} \right) dv}{\int_{H^-} J(\theta^-)^2 dv},$$

we conclude the proof. \square

4.5 Further remarks and open questions

Extension to densities

The proofs of Theorems 4.1.1 and 4.1.2 and of their corollaries are exclusively based on mass transplantation. Once the topological result of Section 4.2 can be applied to identify the suitable family of test functions, the geometry of Ω is not anymore relevant. In the spirit of [33] and the previous chapter, all results established here extend naturally to densities by defining

$$\mu_k(\rho) = \inf_{S \in \mathcal{S}_{k+1}} \sup_{u \in S \setminus \{0\}} \frac{\int_{\Omega} \rho |\nabla u|^2}{\int_{\Omega} \rho u^2}.$$

Then, Theorem 4.1.2 reads

$$\mu_2(\rho) \leq \mu_1 \left(\mathbf{B}^{\frac{1}{2} \int_{\mathbb{S}^n} \rho} \right).$$

All the other estimates for $\mu_1(\rho)$ follow from this inequality. In particular, if $m < \frac{|\mathbb{S}^2|}{2}$, $\int_{\mathbb{S}^n} \rho = m$ and $\rho = 0$ on \mathbf{B}^m , then

$$\mu_1(\rho) \leq \mu_1(\mathbf{B}^m).$$

Going beyond \mathbf{B}^m for μ_1

Two questions are in order.

[Q1.] For $m < \frac{|\mathbb{S}^2|}{2}$, can one remove the constraint $\Omega \subseteq \mathbb{S}^n \setminus \mathbf{B}^m$? The answer is not clear. One may think that it is only a technical difficulty in the construction of the test functions in order to remove the inclusion condition $\Omega \subseteq \mathbb{S}^n \setminus \mathbf{B}^m$, but the answer is more involved. In the next chapter, using the density framework, we will give some numerical examples where the optimality of the ball seems to fail if one performs the optimization in the whole sphere, without inclusion constraint. While it does not prove that the result must be false in the class of domains, it shows that it likely to be false for densities. As a consequence, even if true for every $\Omega \subseteq \mathbb{S}^n$, $|\Omega| < \frac{|\mathbb{S}^n|}{2}$, we do not expect the inequality $\mu_1(\Omega) \leq \mu_1(\mathbf{B}^m)$ could be proved by means of mass transplantations, like ours. Otherwise, this would necessarily generalize to $\mu_1(\rho)$, which is being strongly contradicted by the numerical examples given in the next chapter.

[Q2.] What happens if $m \geq \frac{|\mathbb{S}^2|}{2}$? Is there any chance that the spherical cap of prescribed volume continues to be maximal? The analysis performed in [18] leads to the suggestion that this should not be the case. A strong argument is that the first Neumann eigenvalues on the hemisphere of \mathbb{S}^2 and the full sphere do coincide. Thus, the eigenvalue is not anymore decreasing when the measure of the geodesic ball increases, at least in a neighborhood of 4π . Numerical computations performed in the next chapter suggest the existence of sets having higher first eigenvalue than the spherical cap of the same measure.

Remark 4.5.1. (Euclidean version of Theorem 4.1.1). The inequality proved in Theorem 4.1.1 comes as a consequence of the construction of the test functions and relies on the arguments of [101] and [23]. Clearly,

based on the result of [33] on the maximality of μ_2 in the Euclidean space, the following inequality can be proved, in the lines of Theorem 4.1.1: let $\Omega \subseteq \mathbb{R}^n$ be bounded, open and smooth, then

$$\sum_{i=2}^n \frac{1}{\mu_i(\Omega)} \geq \frac{n-1}{\mu_1(B_{Euc}^{|\Omega|/2})}.$$

This improves the result of [33].

5

Numerical optimization of Neumann eigenvalues of domains in the sphere

This chapter is essentially taken from [85].

Contents

5.1	Introduction	83
5.2	Existence and approximation of the optimal density	83
5.3	Density method	85
5.4	Results : density method.	88
5.5	Level-set method	95
5.6	Results : level-set method.	98
5.7	Explorations on a torus	102
5.8	Discussion	103

5.1 Introduction

In the line of the previous chapter we consider the optimization problem

$$\sup \{ \mu_k(\Omega) : \Omega \subset \mathbb{S}^n, |\Omega| = m, \Omega \text{ bounded, open and Lipschitz} \} \quad (5.1)$$

where

$$\mu_k(\Omega) = \min_{V \in \mathcal{S}_{k+1}} \max_{u \in V \setminus \{0\}} \frac{\int_{\Omega} |\nabla u|^2}{\int_{\Omega} u^2}, \quad (5.2)$$

with $k \geq 0$ and \mathcal{S}_k the family of subspaces of dimension k in $H^1(\Omega)$.

As we have seen, there is still a lot of gaps in our general knowledge concerning those problems, especially for the case of μ_1 . The purpose of this chapter is to address those problems from a numerical point of view in order to identify potential properties of the optimal domains. While the numerical shape optimization of Neumann eigenvalues of domains in the Euclidian space have drawn a lot of attention in the past years (see for instance [16] [15] [10] and Chapter 3), the litterature concerning the optimization of those eigenvalues for domains in curved spaces is sparse. The present work will address this problem by considering the optimization of several Neumann eigenvalues of domains in the sphere \mathbb{S}^n as well as on a torus.

In this chapter we implement two shape optimization methods allowing us to approximate 5.1. As mentionned in the introduction, it is well known that shape optimization problems face the difficulty of topological changes during the optimization process. That being said, we will show how to take advantage of a two-step level set method (one with *ersatz material*, another with remeshing) to infer properties on the optima while allowing complex changes in topology. This will be one of the two method.

Taking advantage of what have been done in Chapter 3, the other numerical method will rely on the following generalization of the original problem (5.2) to the class of densities $\rho \in \mathbf{L}^\infty(\mathbb{S}^n, [0, 1])$

$$\mu_k(\rho) := \inf_{V \in \mathcal{S}_{k+1}} \max_{u \in V \setminus \{0\}} \frac{\int_{\mathbb{S}^n} \rho |\nabla u|^2}{\int_{\mathbb{S}^n} \rho u^2}, \quad (5.3)$$

where \mathcal{S}_{k+1} is the family of subspaces of dimension $k+1$ in

$$\{u \cdot 1_{\{\rho(x) > 0\}} : u \in C_c^\infty(\mathbb{S}^n)\}. \quad (5.4)$$

Note that this relaxation can also be found in greater generality in the case of Riemannian manifolds in [44].

The original problem will then be replaced by

$$\sup \left\{ \mu_k(\rho) : \rho : \mathbb{S}^n \rightarrow [0, 1], \int_{\mathbb{S}^n} \rho = m \right\}. \quad (5.5)$$

which well-posedness is established below.

This formulation allows to perform some classical optimization methods such as gradient descent over the variable ρ instead of considering shape optimization problem involving potentially complex changes of topology. However, the density method is strictly more general than the problem (5.1) in the sense that optimal density may not correspond to characteristic functions of domains. This problem is not completely decorellated from the original one 5.1. Indeed, the only known method to prove the optimality of a domain in all dimension is the mass transplantation argument introduced by Weinberger [102]. As it has been noted in the previous chapter, such mass transplantation argument should hold for densities if it does for domains. This is why it is interesting to consider both optimization approaches. Following numerical experiments will show that in the case of μ_1 , the optimal density is not always the characteristic function of a domain; however, the level set method will provide some precious additional information.

In the next sections, we first see the theoretical aspects brought by the relaxation (5.3). Then we discuss the practical implementation of the two methods cited above and provide numerical results related to the first three eigenvalues for domains and densities in the sphere and the torus.

5.2 Existence and approximation of the optimal density

We start by setting a theoretical framework which makes problem (5.5) well-posed. The results follows using the same ideas as in Chapter 3. For this reason, we shall not enter too much in the details.

A natural question that directly arises is the one of the existence of an optimal density. In the Euclidian case \mathbb{R}^n , we had to rely on some concentration-compactness result to obtain the existence of some *collection* of densities. Here, the fact that the sphere has finite measure allows us to give a complete existence result easily :

Theorem 5.2.1 (Existence of an optimal density). *Let $0 \leq m \leq |\mathbb{S}^n|$. Then problem (5.5) has a solution.*

Proof. We actually prove the upper-semicontinuity of the eigenvalues with respect to the weak-* convergence. Let $k \in \mathbb{N}$ and $\rho, (\rho_n)_{n \in \mathbb{N}} \in \mathbf{L}^1(\mathbb{S}^n, [0, 1])$ be functions such that $\rho_n \rightharpoonup \rho$. Let $\varepsilon > 0$ and $V = \text{span}\{v_0 \mathbf{1}_{\{\rho > 0\}}, \dots, v_k \mathbf{1}_{\{\rho > 0\}}\}$ be such that

$$\mu_k(\rho) \geq \max_{u \in V \setminus \{0\}} \frac{\int_{\mathbb{S}^n} \rho |\nabla u|^2}{\int_{\mathbb{S}^n} \rho u^2} - \varepsilon.$$

Let us consider $V_n = \langle v_0 \mathbf{1}_{\{\rho_n > 0\}}, \dots, v_k \mathbf{1}_{\{\rho_n > 0\}} \rangle$ and $u_n = \sum_{i=0}^k \alpha_i^n v_i$ a maximizing sequence in

$$\max_{u \in V_n \setminus \{0\}} \frac{\int_{\mathbb{S}^n} \rho_n |\nabla u|^2}{\int_{\mathbb{S}^n} \rho_n u^2}.$$

For n large enough, V_n is of dimension $k+1$ hence

$$\mu_k(\rho_n) \leq \frac{\int_{\mathbb{S}^n} \rho_n |\nabla u_n|^2}{\int_{\mathbb{S}^n} \rho_n u_n^2}.$$

Note that we can suppose by homogeneity that $\sum_{i=0}^k (\alpha_i^n)^2 = 1$ for all n . Up to a subsequence, we get that $\alpha_i^n \rightarrow \alpha_i \in \mathbb{R}$ for all i . By putting $\tilde{v} = \sum_{i=0}^k \alpha_i v_i$ we get that

$$\int_{\mathbb{S}^n} \rho_n |\nabla u_n|^2 \rightarrow \int_{\mathbb{S}^n} \rho |\nabla \tilde{v}|^2$$

and

$$\int_{\mathbb{S}^n} \rho_n u_n^2 \rightarrow \int_{\mathbb{S}^n} \rho \tilde{v}^2.$$

Thus

$$\mu_k(\rho) \geq \limsup_{n \rightarrow +\infty} \mu_k(\rho_n) - \varepsilon.$$

This relation being valid for all ε , we get

$$\mu_k(\rho) \geq \limsup_{n \rightarrow +\infty} \mu_k(\rho_n).$$

Now let $(\rho_n)_{n \in \mathbb{N}}$ be some maximizing sequence of the problem (5.5). There exists a $\rho \in \mathbf{L}^1(\mathbb{S}^n, [0, 1])$ such that up to a subsequence, $\rho_n \rightharpoonup \rho$ weakly. By upper-semicontinuity, we get that $\mu_k(\rho) \geq \limsup_{n \rightarrow +\infty} \mu_k(\rho_n)$ and the fact that $1 \in \mathbf{L}^1(\mathbb{S}^n, \mathbb{R})$ ensure that the condition $\int_{\mathbb{S}^n} \rho_n = m$ is satisfied at the limit. \square

From a numerical point of view, computing the generalized eigenvalue *via* finite element method is not possible in general due to the potential vanishing of ρ on some non-negligible parts of \mathbb{S}^n . It is possible to approximate our generalized eigenvalues by well-defined ones of non-zero densities :

Theorem 5.2.2 (Approximation). *Let $\rho \in \mathbf{L}^1(\mathbb{S}^n, [0, 1])$, $\int_{\mathbb{S}^n} \rho = m > 0$. We introduce the following quantity :*

$$\mu_k^\varepsilon(\rho) := \min_{V \in \mathcal{S}_{k+1}} \max_{u \in V \setminus \{0\}} \frac{\int_{\mathbb{S}^n} (\rho + \varepsilon) |\nabla u|^2}{\int_{\mathbb{S}^n} (\rho + \varepsilon^2) u^2}$$

where \mathcal{S}_{k+1} is the family of subspace of dimension $k+1$ in $\mathbf{H}^1(\mathbb{S}^n)$.

Then :

$$\mu_k^\varepsilon(\rho) \xrightarrow[\varepsilon \rightarrow 0]{} \mu_k(\rho).$$

For the proof in the Euclidian case, we refer to [35, Lemma 14].

Remark 5.2.3. $\mu_k^\varepsilon(\rho)$ is the k -th non-trivial eigenvalue of the well posed elliptic problem

$$-\operatorname{div}[(\rho + \varepsilon) \nabla u] = \mu_k^\varepsilon(\rho)(\rho + \varepsilon^2)u$$

on \mathbb{S}^n .

Proof. The proof decomposes into proving both the limsup and the liminf. The limsup is proven in the same way as in previous theorem; let us focus on the liminf.

Let $u_0^\varepsilon, \dots, u_k^\varepsilon \in \mathbf{H}^1(\mathbb{S}^n)$ be the eigenfunctions associated to the eigenvalues $\mu_0^\varepsilon, \dots, \mu_k^\varepsilon$, orthogonal and normalized in the sense that

$$\int_{\mathbb{S}^n} (\rho + \varepsilon^2) u_i^\varepsilon u_j^\varepsilon = \delta_{i,j}. \quad (5.6)$$

This implies that

$$\int_{\mathbb{S}^n} (\rho + \varepsilon) |\nabla u_i^\varepsilon|^2 = \mu_i^\varepsilon(\rho) \quad (5.7)$$

and this quantity can be considered bounded independently of i and ε by some bound M . If not, the limsup would be infinite and the previous case would allow us to conclude. From equation 5.6 we deduce that $(\varepsilon u_i^\varepsilon)_\varepsilon$ is bounded in $\mathbf{L}^2(\mathbb{S}^n)$ for all i . Hence we can find a subsequence such that for all $0 \leq i \leq k$, the sequence $(\varepsilon u_i^\varepsilon)$ converges weakly in $\mathbf{L}^2(\mathbb{S}^n)$ to some function g_i . Denoting $\bar{v} = \frac{1}{|\mathbb{S}^n|} \int_{\mathbb{S}^n} v$, we get $\varepsilon u_i^\varepsilon \rightharpoonup \bar{g}_i$ for all i , the constant function 1 being in \mathbf{L}^2 . Moreover, the sequence $(\sqrt{\varepsilon} \nabla u_i^\varepsilon)_\varepsilon$ is bounded in $\mathbf{L}^2(\mathbb{S}^n)$ hence by we get by the Poincaré-Wirtinger inequality :

$$\|\varepsilon u_i^\varepsilon - \varepsilon \bar{g}_i\|_{\mathbf{L}^2} \leq C \|\varepsilon \nabla u_i^\varepsilon\|_{\mathbf{L}^2} \Rightarrow 0.$$

We deduce that $\varepsilon u_i^\varepsilon \rightharpoonup \bar{g}_i$ strongly in \mathbf{L}^2 . We can then conclude that $\bar{g}_i = 0$ by noticing that

$$0 = \lim_{\varepsilon \rightarrow 0} \varepsilon^2 \int_{\mathbb{S}^n} \rho (u_i^\varepsilon)^2 = \int_{\mathbb{S}^n} \rho \bar{g}_i^2 = \bar{g}_i^2 m.$$

By Cauchy-Schwarz inequality, this implies that $\int_{\mathbb{S}^n} u_i^\varepsilon u_j^\varepsilon \Rightarrow 0$ which in turn results in $\int_{\mathbb{S}^n} \varepsilon^2 (v^\varepsilon)^2 dx \Rightarrow 0$ for all $v^\varepsilon \in \text{span}\{u_0^\varepsilon, \dots, u_k^\varepsilon\}$. Using this last limit and the fact that $\text{span}\{u_0^\varepsilon 1_{\{\rho > 0\}}, \dots, u_k^\varepsilon 1_{\{\rho > 0\}}\}$ is of dimension $k+1$ for ε small enough we finally get

$$\mu_k(\rho) = \inf_{V \in \mathcal{S}_{k+1}^{\rho}} \max_{u \in V \setminus \{0\}} \frac{\int_{\mathbb{S}^n} \rho |\nabla u|^2}{\int_{\mathbb{S}^n} \rho u^2} \leq \liminf_{\varepsilon \rightarrow 0} \max_{v \in \text{span}\{u_0^\varepsilon, \dots, u_k^\varepsilon\}} \frac{\int_{\mathbb{S}^n} (\rho + \varepsilon) |\nabla u|^2}{\int_{\mathbb{S}^n} (\rho + \varepsilon^2) u^2} = \liminf_{\varepsilon \rightarrow 0} \mu_k^\varepsilon(\rho)$$

which concludes the proof. \square

Theorem 5.2.4 (Approximation of maxima). *Let $0 < m \leq |\mathbb{S}^n|$. Then*

$$\max_{\|\rho\|_{\mathbf{L}^1} = m} \mu_k^\varepsilon(\rho) = \max_{\|\rho\|_{\mathbf{L}^1} = m} \mu_k(\rho). \quad (5.8)$$

Proof. Let $(\rho^\varepsilon)_\varepsilon$ be such that $\mu_k^\varepsilon(\rho^\varepsilon) = \max_{\|\rho\|_{\mathbf{L}^1} = m} \mu_k^\varepsilon(\rho)$ and ρ^* be such that $\mu_k(\rho^*) = \max_{\|\rho\|_{\mathbf{L}^1} = m} \mu_k(\rho)$. In the same way than the upper semicontinuity in theorem 5.2.1, we have that

$$\limsup_{\varepsilon \rightarrow 0} \mu_k^\varepsilon(\rho^\varepsilon) \leq \mu_k(\tilde{\rho}) < \max_{\|\rho\|_{\mathbf{L}^1} = m} \mu_k(\rho) < +\infty$$

whenever $\rho^\varepsilon \rightharpoonup \tilde{\rho}$ weakly in \mathbf{L}^∞ . Hence the sequence $(\mu_k^\varepsilon(\rho^\varepsilon))_\varepsilon$ is bounded. Then the previous lower-semicontinuity result implies that

$$\max_{\|\rho\|_{\mathbf{L}^1} = m} \mu_k(\rho) = \mu_k(\rho^*) \leq \liminf_{\varepsilon \rightarrow 0} \mu_k^\varepsilon(\rho^\varepsilon) = \liminf_{\varepsilon \rightarrow 0} \max_{\|\rho\|_{\mathbf{L}^1} = m} \mu_k^\varepsilon(\rho^\varepsilon)$$

which concludes the proof. \square

5.3 Density method

In this section we discuss the numerical implementation of the density method, which follows the same lines as Chapter 3 with some new technical difficulties working on the sphere. The sphere is assumed to be discretized by a mesh that remains the same during the optimization process. Let $V_h = \text{span}(\phi_1, \dots, \phi_n) \subset \mathbf{H}^1(\mathbb{S}^n)$ be a finite element space. If $v = \sum_i v_i \phi_i$ we denote by $\bar{v} = (v_1, \dots, v_n)^T$ its coordinates on the basis

$(\phi_i)_i$. Even if we made the choice here to discretize both the density and the eigenfunctions on the same FE space V_h , we could have considered different ones as we did in the Euclidean case. Let $\rho \in V_h$ be a density (i.e. $\rho : \mathbb{S}^n \rightarrow [0, 1]$). We denote by $\bar{\mu}_k^\varepsilon(\rho)$ the eigenvalue of the finite-dimensional eigenvalue problem :

$$\mathbf{M}^\varepsilon(\rho)\bar{u}_k^\varepsilon(\rho) = \bar{\mu}_k^\varepsilon(\rho)\mathbf{K}^\varepsilon(\rho)\bar{u}_k^\varepsilon(\rho) \quad (5.9)$$

where

$$\mathbf{M}^\varepsilon(\rho) = \left(\int_{\mathbb{S}^n} (\rho + \varepsilon) \nabla \phi_i \nabla \phi_j \right)_{i,j}$$

and

$$\mathbf{K}^\varepsilon(\rho) = \left(\int_{\mathbb{S}^n} (\rho + \varepsilon^2) \phi_i \phi_j \right)_{i,j}.$$

Since we use a gradient-based optimization method, we need to differentiate $\bar{\mu}_k^\varepsilon(\rho)$ with respect to its coordinates (ρ_1, \dots, ρ_n) in the basis $(\phi_i)_i$. Assuming that $\bar{\mu}_k^\varepsilon(\rho)$ is simple, we can differentiate the equation (5.9) and multiply on the left by $(\bar{u}_k^\varepsilon(\rho))^T$ to get

$$\partial_l \bar{\mu}_k^\varepsilon = \frac{(\bar{u}_k^\varepsilon)^T (\partial_l \mathbf{M}^\varepsilon - \bar{\mu}_k^\varepsilon \partial_l \mathbf{K}^\varepsilon) \bar{u}_k^\varepsilon}{(\bar{u}_k^\varepsilon)^T \mathbf{K}^\varepsilon(\rho) \bar{u}_k^\varepsilon} \quad (5.10)$$

where the derivatives of the matrices are respectively

$$\partial_l \mathbf{M}^\varepsilon(\rho) = \left(\int_{\mathbb{S}^n} \phi_l \nabla \phi_i \nabla \phi_j \right)_{i,j}$$

and

$$\partial_l \mathbf{K}^\varepsilon(\rho) = \left(\int_{\mathbb{S}^n} \phi_l \phi_i \phi_j \right)_{i,j}.$$

One may remember that since we are on the sphere, we don't have scale-homogeneity of the eigenvalue as it is the case in \mathbb{R}^n . Hence we have to enforce the condition $\int_{\mathbb{S}^n} \rho = m$, which in the discrete case becomes $\bar{\rho} \cdot \mathbf{g} = m$ where

$$\mathbf{g} = \left(\int_{\mathbb{S}^n} \phi_l \right)_l.$$

Multiple eigenvalues.

One of the main hurdles in spectral shape optimization is to handle the multiplicity of the eigenvalues. Indeed, in practice, the optimal density is expected to have high multiplicity. The method presented in Chapter 3 consisted in adding a constraint forcing the eigenvalues that were close (depending on a certain threshold σ) to get even closer. While it yielded good results in the planar case, it suffered one peculiar issue here, especially in the case of μ_1 . Indeed, even if the optimal density seems to be of multiplicity 2, the third eigenvalue is observed to be close to μ_2 leading the previous method either to fall into a local maximum of multiplicity 3 if σ was too high, or to be too unstable to converge if σ was too small. One way to overcome this issue is to compute a better direction than the one given by the gradient of μ_k . Several numerical methods have been investigated in this direction, such as finding the direction h as a solution to the problem

$$\max_{h \in V_h, \|h\|=1} \min \{ d\mu_k^\varepsilon(\rho).h, \dots, d\mu_{k+m-1}^\varepsilon(\rho).h \}$$

where m is the "guessed" multiplicity, chosen such that $\mu_{k+m-1}^\varepsilon(\rho) - \mu_k^\varepsilon(\rho) \leq \sigma$ and $\mu_{k+m}^\varepsilon(\rho) - \mu_k^\varepsilon(\rho) > \sigma$. Such method has been used for instance in [15]. Heuristically, it produces a direction that increases all the selected eigenvalues by a maximal amount. Another, more rigorous method would be to consider the true directional derivative of our multiple eigenvalue in the direction h (which always exists, see Chapter 2), namely

$$(\mu_k^\varepsilon)'(\rho)(h) := \lim_{t \rightarrow 0^+} \frac{\mu_k^\varepsilon(\rho + th) - \mu_k^\varepsilon(\rho)}{t}$$

and in the same way as before, to search the direction that maximizes this variation :

$$\max_{h \in V_h, \|h\|=1} (\mu_k^\varepsilon)'(\rho)(h).$$

This has been brilliantly studied in [50]. Using the *Hilbertian extension-regularization method*, the author shows that the search of the optimal direction can be efficiently solved by a semi-definite programming method.

However, in our case, these methods did not seem to perform better than the one of Chapter 3. It turned out that a simple modification of our problem leads to a very good convergence. Instead of searching for a direction based on directional derivatives, we regularize our problem to make it differentiable. It can then be handled better from the interior point optimizer. The idea is the following : suppose that $\mu_k^\varepsilon(\rho)$ stays away from $\mu_{k-1}^\varepsilon(\rho)$ during the whole optimization process (which is always the case in practice) and is part of a cluster $\mu_k^\varepsilon(\rho), \dots, \mu_{k+m-1}^\varepsilon(\rho)$ of eigenvalues closer than σ . Then obviously

$$\mu_k^\varepsilon(\rho) = \min \{ \mu_k^\varepsilon(\rho), \dots, \mu_{k+m-1}^\varepsilon(\rho) \}. \quad (5.11)$$

But for $x_0, \dots, x_{m-1} > 0$, we have that

$$\min \{x_0, \dots, x_{m-1}\} = \lim_{p \rightarrow +\infty} \left(\sum_i x_i^{-p} \right)^{-1/p}. \quad (5.12)$$

Thus, by taking p large, we can approximately write

$$\min \{x_0, \dots, x_{m-1}\} \approx \left(\sum_i x_i^{-p} \right)^{-1/p}. \quad (5.13)$$

In this spirit, we instead optimize the functional

$$\rho \mapsto \left(\sum_i \mu_{k+i}^\varepsilon(\rho)^{-p} \right)^{-1/p}. \quad (5.14)$$

This function being a symmetric function of the eigenvalues, it is expected to be smooth near ρ if m is the actual multiplicity of $\mu_k^\varepsilon(\rho)$ [70]. If it is not, the largest eigenvalues of the cluster are mostly ignored.

Dimension 1

After running a series of simulations on the sphere, it appeared that the optimal density seems to be axially symmetric in the case of μ_1 . In order to get even more insight on the density problem, we subsequently ran simulations only in 1D, considering the density ρ as a real function of the latitude $\theta \in [0, \pi]$, i.e. the angle from one pole to a point on the sphere. By separation of variables, if $\rho : \mathbb{S}^2 \rightarrow [0, 1]$ is axially symmetric and not degenerated, then $\mu_1(\rho)$ is the least non-zero eigenvalue of the following two eigenvalue problems

$$\begin{cases} -\frac{1}{\sin(\theta)} \frac{d}{d\theta} \left(\rho(\theta) \sin(\theta) \frac{dy}{d\theta} \right) + \frac{\rho(\theta)}{\sin^2(\theta)} y = \rho(\theta) \bar{\mu} y \text{ on } (0, \pi) \\ y(0) \text{ and } y(\pi) \text{ are finite} \end{cases}$$

$$\begin{cases} -\frac{1}{\sin(\theta)} \frac{d}{d\theta} \left(\rho(\theta) \sin(\theta) \frac{dy}{d\theta} \right) = \rho(\theta) \bar{\mu} y \text{ on } (0, \pi) \\ y(0) \text{ and } y(\pi) \text{ are finite} \end{cases}.$$

See [19] for more details. Formally, by developing the derivative in the first differential equation, we can see that the condition $y(0) = y(\pi) = 0$ is forced by the term in $\frac{1}{\sin(\theta)}$, which penalizes large values of y in 0 and π . In the same way, we can see that in the second differential equation, the boundary conditions needs to be $y'(0) = y'(\pi) = 0$.

As before, since we allow ρ to vanish, we need to regularize the problem to make it elliptic. The problems that are actually solved are

$$\begin{cases} -\frac{d}{d\theta} \left((\rho(\theta) \sin(\theta) + \varepsilon) \frac{dy}{d\theta} \right) + \frac{\rho(\theta) + \varepsilon}{\sin(\theta)} y = (\rho(\theta) \sin(\theta) + \varepsilon^2) \bar{\mu} y \text{ on } (0, \pi) \\ y(0) = y(\pi) = 0 \end{cases}$$

$$\begin{cases} -\frac{d}{d\theta} \left((\rho(\theta) \sin(\theta) + \varepsilon) \frac{dy}{d\theta} \right) = (\rho(\theta) \sin(\theta) + \varepsilon^2) \bar{\mu} y \text{ on } (0, \pi) \\ y'(0) = y'(\pi) = 0 \end{cases}$$

where ε is supposed to be small.

Numerical considerations.

Our optimization procedure is carried out by IPOPT [100] while the finite element computations is perfomed in GetFEM [92]. A first optimization is carried on a coarse mesh of 2246 vertices with \mathcal{P}_1 finite elements. A second optimization is then performed with the result of the previous one as initilization on a mesh consisting in 35401 elements (the meshes that are used can be vizualized Figure 5.1). For each m , the optimization is performed multiple times with different initialization and the density giving the best value is finally kept.

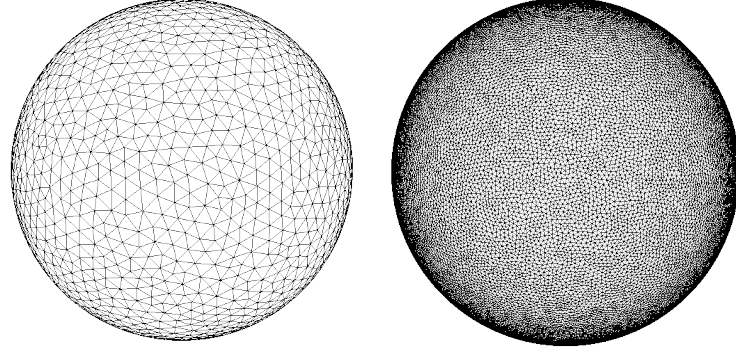


Figure 5.1: The meshes used for the density method.

For both optimizations we take $p = 20$ and $\varepsilon = 10^{-4}$.

5.4 Results : density method.

In this section we discuss the results obtained by the density method described above. We focus only on the first three eigenvalues, since they already shows a rich behaviour. In each graph, the value of the optimized eigenvalue is plotted in green as a function of the total mass m and the corresponding density is denoted by ρ^m . In order to give a comparison, for each μ_k we plot in red the corresponding eigenvalue for a union of k disjoint geodesic balls of surface area m/k (denoted UB_k^m). These values have been approximated by a finite element (FE) decomposition of the following 1D eigenvalue problem :

$$\begin{cases} -\frac{1}{\sin(\theta)} \frac{d}{d\theta} \left(\sin(\theta) \frac{dy}{d\theta} \right) + \frac{1}{\sin^2(\theta)} y = \mu y & \text{on } (0, \theta_m) \\ \frac{dy}{d\theta}(\theta_m) = 0 \\ y(0) \text{ is finite} \end{cases} \quad (5.15)$$

where $\theta_m = \arccos(1 - \frac{m}{2\pi})$ is the geodesic radius of the ball of surface area m on \mathbb{S}^2 . In practice, the solution is approximated using \mathcal{P}_1 FE with 10000 degrees of freedom.

Validation : μ_1 with constraint.

In order to validate our optimization process, we rely on Corollary 4.1.3, which states that if we run the optimization outside of a ball of the right area then the optimum is a ball. This theorem, proved by some mass transplantation technique, is hence also valid for densities and could be reformulated as follows :

Theorem 5.4.1. *Let $m \in (0, |\mathbb{S}^n|/2)$ and let \mathbf{B}^m be a geodesic ball of measure m in \mathbb{S}^n . Let $\rho : \mathbb{S}^n \rightarrow [0, 1]$ such that $\rho = 0$ on \mathbf{B}^m and $\int_{\mathbb{S}^n} \rho = m$. Then $\mu_1(\rho) \leq \mu_1(\mathbf{B}^m)$.*

In practice, we run the optimization process in the whole sphere but add the constraint that all degrees of freedom of ρ that lies inside a certain ball \mathbf{B}^m stay equal to 0. This constraint is easily handled by IPOPT. In Figure 5.2 we show on two examples that the optimal densities are indeed the characteristic functions of balls of given measure. The red color correspond to a density $\rho = 1$ while the blue color corresponds

to $\rho = 0$. In Figure 5.3 we plot the value of the approximated optima (green crosses) against the value for geodesic balls (red curve). It is clear that the eigenvalues of the approximations meet the ones of actual balls.

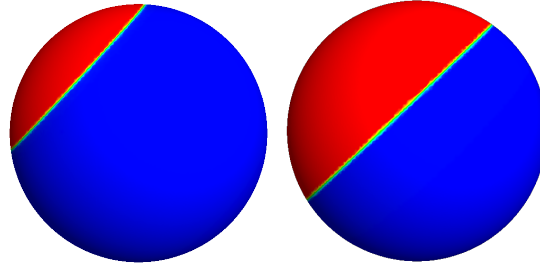


Figure 5.2: Example of optimal densities for μ_1 for $m \in \{2.17, 5.0\}$ when ρ is supported outside of a ball.

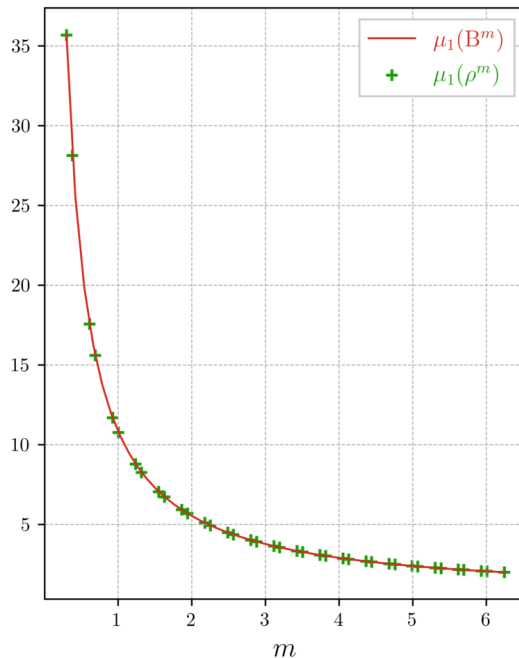


Figure 5.3: Optimal value of μ_1 obtained by the density method, with the constraint that the support of ρ is located outside of a ball.

The case of μ_1 in the whole sphere.

We now consider the case where ρ is allowed to fill the whole sphere. One first observation is that the optimal eigenvalue is expected to be never less than n . Indeed, this eigenvalue is associated to constant densities hence we can chose the density $\rho = \frac{m}{|\mathbb{S}^n|}$ which leads to $\mu_1(\rho) = \mu_1(\mathbb{S}^n) = n$. The simulations actually suggest that this value is only attained near $m = |\mathbb{S}^n|$ as shown in Figure 5.4.

Since the eigenvalue goes to infinity as m goes to 0, the graph is displayed on two different scales for a better readability. The reader should pay a particular attention to the range of the different axes. Something interesting happens : the spherical cap seems not to be optimal for values of m greater than $m \approx 4.5$. This is allowed by the fact that ρ can fill the whole sphere, which wasn't allowed with the previous ball constraint. A zoom on the range $m \in [3.5, 6.5]$ is displayed Figure 5.5.

We illustrate the behaviour of the optimal ρ in Figure 5.6 for different values of m . Deep blue color corresponds to $\rho = 0$ while red color corresponds to $\rho = 1$.

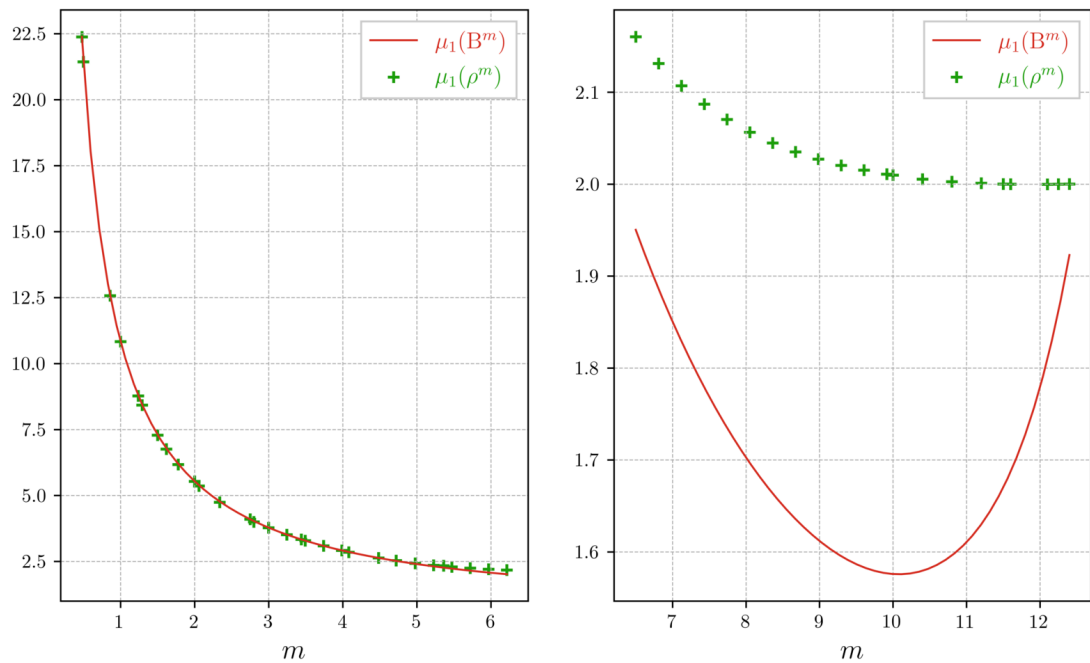


Figure 5.4: Optimal value of μ_1 obtained by the density method.

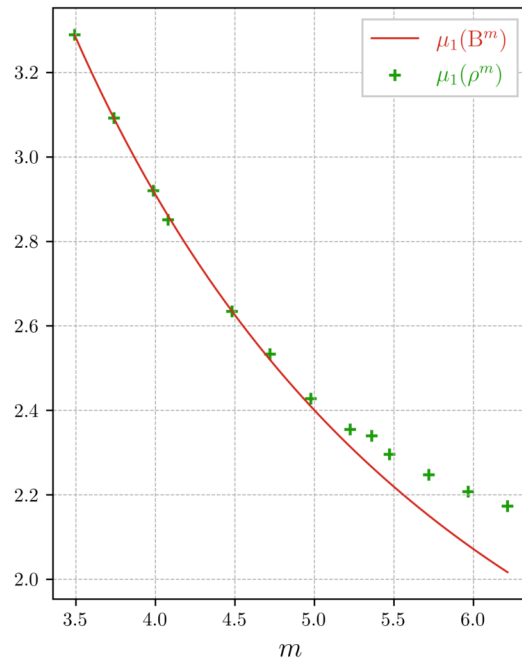


Figure 5.5: Optimal value of μ_1 near $m \approx 5.0$.

Remark 5.4.2. Apart from $m = 2.0$ which seems to be the characteristic function of a geodesic ball, the optimal density seems to be some "homogenized" spherical cap. As mentioned in the introduction, this surprising result has an important theoretical implication : even if the ball B^m were optimal for μ_1 among shapes Ω such that $|\Omega| = m \leq |\mathbb{S}^n|/2$, it would be impossible to prove it using the standard mass transplantation technique of Weinberger [102]. Indeed, the proof would also hold for densities, but the numerical results strongly indicates that it is false for $m > 4.5$. To go further, it would be interesting to investigate if this kind of "homogenization" of the sphere could be attained by some sequence of actual domains. This could for instance suggest the non-existence of optimal domains for a large enough m .

The inspection of these results leads to the following conjecture :

Conjecture 5.4.3. Let $m \in (0, |\mathbb{S}^n|)$. Then the optimal density ρ^m of the problem

$$\max \left\{ \mu_1(\rho) : \rho : \mathbb{S}^n \rightarrow [0, 1], \int_{\mathbb{S}^n} \rho = m \right\}.$$

is axially symmetric.

In the light of this conjecture, we illustrate on the same Figure 5.6 the density ρ as the result of the 1D optimization procedure.

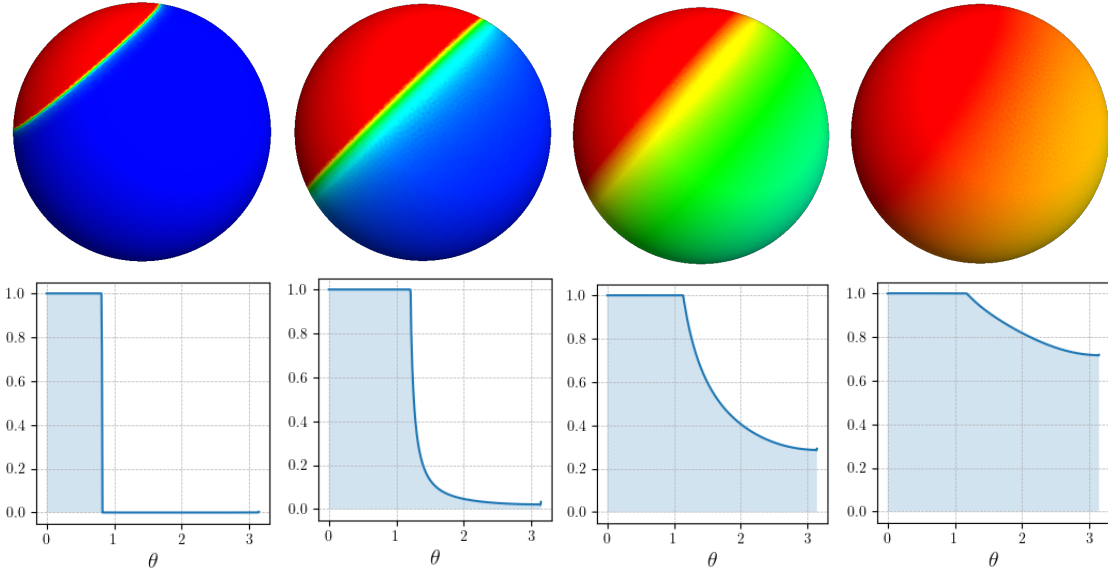


Figure 5.6: Example of optimal densities for μ_1 for $m \in \{2.0, 4.98, 8.05, 11.2\}$ (top) along with their latitudinal profile (bottom).

Note that it would be interesting to get more information on the behaviour of the density near $m = 4.5$ where it seems to start to homogenize. A good indication that the optimal density is an actual domain would be for the size of the set $\rho^m \notin \{0, 1\}$ to be always proportionnal to the size of an element under mesh refinement. On the contrary, if ρ^m is a density, then the size of this set should be independant of the size of one element. Let N be the number of elements of the segment $[0, \pi]$. For $N \in \{100, 200, 400, 800\}$, we compute the quantity

$$h_m(N) = \frac{N}{\pi} \int_0^\pi \rho^m(1 - \rho^m).$$

Since π/N is the size of one element, this quantity should be constant in N if ρ^m is a domain for the reasons stated previously. If ρ^m is not a domain, then we would expect $h_m(N)$ to double when doubling the number of points in the mesh. To compare this quantity for different N we normalize this quantity at $N = 100$ and define

$$\text{Dispersion}_m(N) = \frac{h_m(N)}{h_m(100)}$$

We plot the graph of Dispersion_m for different values of m in Figure 5.7

A few things can be deduced from this graph. For m large enough (approximately $m > 4.6$), the behaviour is the one we would observe for a density which is not a domain, as the dispersion grows with the

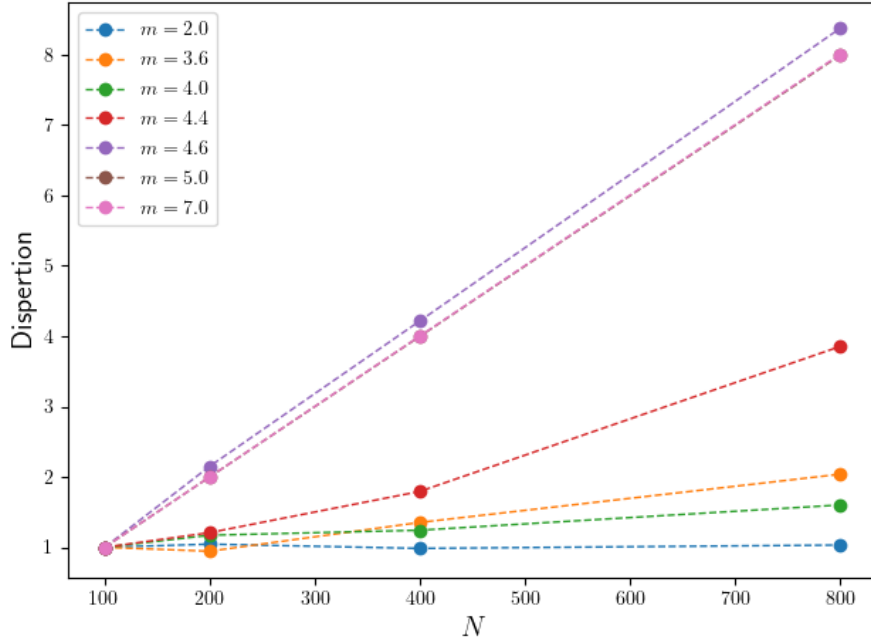


Figure 5.7: Mesh-refinement procedure une 1D for different values of m .

number of points. On the other hand, it appears that for m small enough ρ^m seems to be a domain since its dispersion is constant. It is the subject of the following conjecture.

Conjecture 5.4.4. *There exists $\delta > 0$ such that for all $m \in (0, \delta)$, $\rho^m = \mathbf{1}_{\mathbf{B}^m}$ i.e. the optimal density is the one of a geodesic ball.*

Following the numerical observations above, the value of δ would lie between 3.5 and 4.6.

Results for μ_2

Chronologically, these simulations came before Theorem 4.1.1 was established. In contrast to μ_1 , the optimization turned out to be extremely stable and gave us good confidence about the validity of Theorem 4.1.1. Indeed, no matter the value of m , the corresponding optimal density is always attained by the characteristic function of the union of two balls of the same measure as can be seen in Figure 5.8. Figure 5.9 shows the optimal densities that are obtained for some values of m .

Results for μ_3

As for the case of μ_1 , the optimization procedure for μ_3 exhibits various different behaviours depending on the value of m . Note that the union of three balls of the same surface area seems to never be optimal, as shown in Figure 5.10.

In Figure 5.11 are displayed the different types of densities that can be obtained with the density method. As it could be expected, for small m we get the same type of result than in the plane (see Chapter 3). Only the last, for large m , seems to be an actual characteristic function of some "napkin ring"-shaped domain. For $m \approx 8.0$, we get some homogenized geodesic annulus. For large m , μ_3 is expected to 2 since $\mu_1(\mathbb{S}^2)$ is of multiplicity 3 and $\mu_1(\mathbb{S}^2) = 2$, which is coherent with the results shown Figure 5.10.

Data.

All the final solutions are available in MEDIT format at https://github.com/EloiMartinet/Neumann_Sphere/. A FreeFem++ [63] script allowing to read the solutions and compute the eigenvalues is also provided for replicability purposes. See the README file for more information.

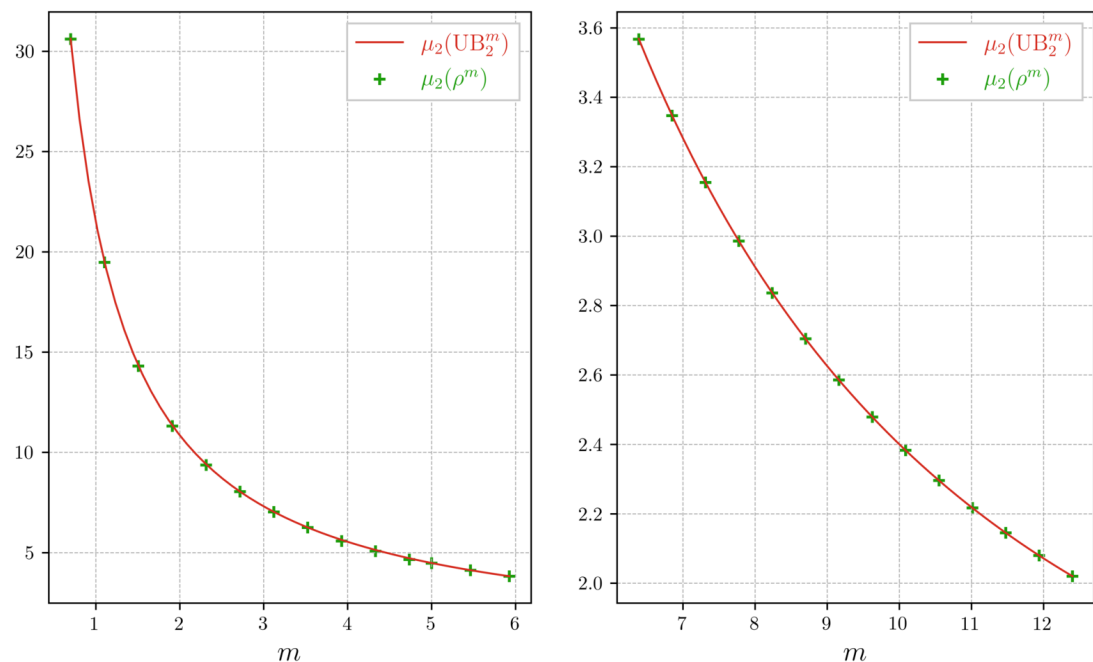


Figure 5.8: Optimal value of μ_2 obtained by the density method.

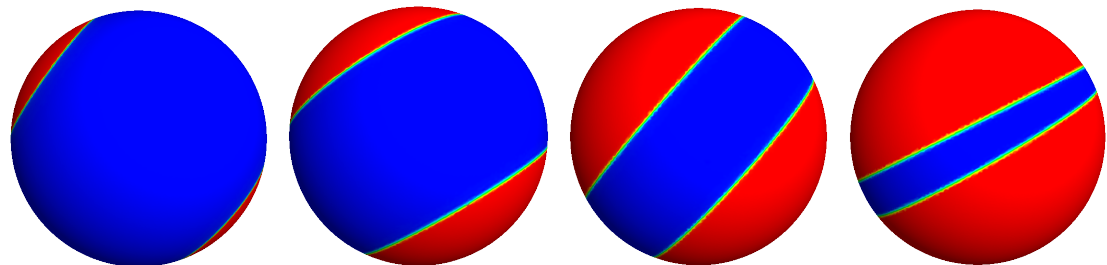


Figure 5.9: Example of optimal densities for μ_2 for $m \in \{2.31, 5.46, 8.23, 11.01\}$.

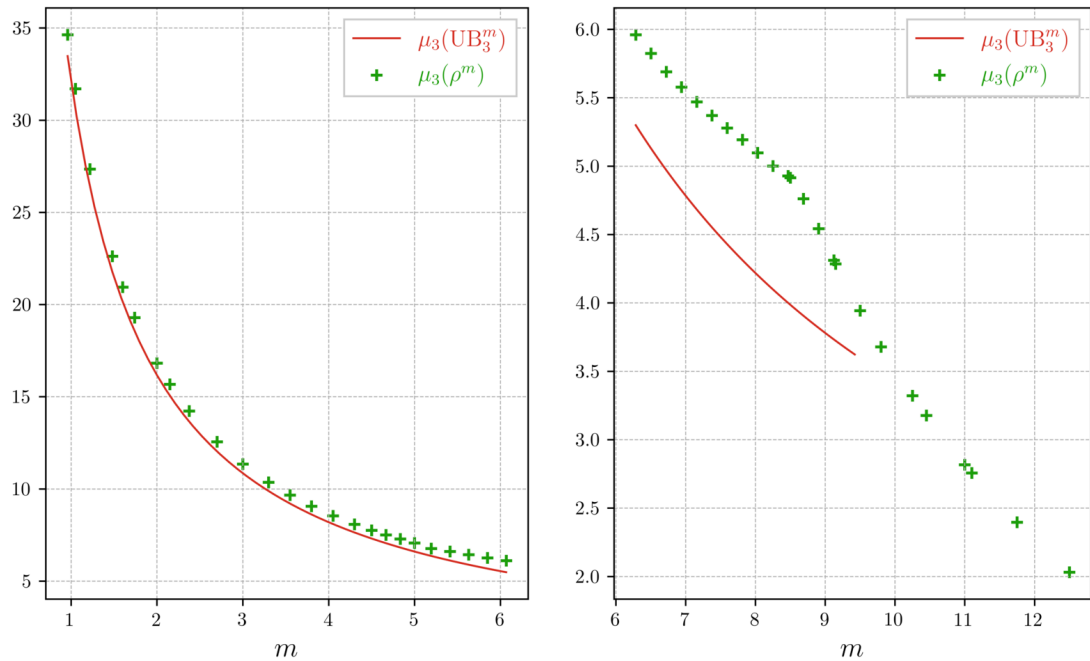


Figure 5.10: Optimal value of μ_3 obtained by the density method.

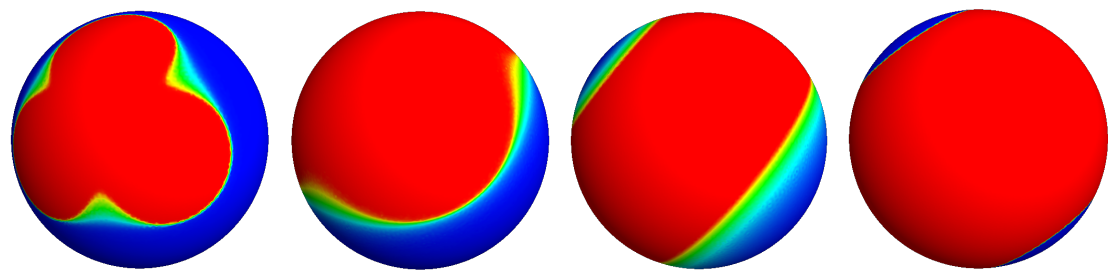


Figure 5.11: Example of optimal densities for μ_3 for $m \in \{2.0, 5.0, 8.03, 11.0\}$.

5.5 Level-set method

In this section we focus on the optimization of the original problem (5.1) through the level-set method. This allows to give more informations for the original shape optimization problem, when optima lead by the previous density method didn't match the characteristic function of an actual shape. As explained briefly in Chapter 2, the level-set method consists in representing the domain Ω as the level-set of a function. It has been extensively used for shape optimization, either for compliance or eigenvalue optimization (see for example [50], [4], [1] among others). We recall that if $(\Omega_t)_{t \in [0, T]} \subset \mathbb{S}^n$ is a domain evolving in time according to a velocity field $V : [0, T] \times \mathbb{S}^n \rightarrow \mathbb{T}\mathbb{S}^n$ then we represent our domain by a function $\phi : [0, T] \times \mathbb{S}^n \rightarrow \mathbb{R}$ such that

$$\forall x \in \mathbb{S}^n, \forall t \in [0, T], \begin{cases} \phi(t, x) < 0 & \text{if } x \in \Omega(t) \\ \phi(t, x) = 0 & \text{if } x \in \partial\Omega(t) \\ \phi(t, x) > 0 & \text{if } x \in \mathbb{S}^n \setminus \Omega(t) \end{cases}. \quad (5.16)$$

The motion of Ω_t is equivalent to the advection of ϕ by the equation

$$\partial_t \phi(t, x) + V(t, x) \cdot \nabla \phi(t, x) = 0 \text{ on } (0, T) \times \mathbb{S}^n. \quad (5.17)$$

which can be approximated during a single timestep $[t_m, t_{m+1}]$ by

$$\partial_t \phi(t, x) + V(t_m, x) \cdot \nabla \phi(t, x) = 0 \text{ on } (0, T) \times \mathbb{S}^n. \quad (5.18)$$

Numerically, this equation is solved by the method of characteristics, thanks to the "advect" toolbox that can be found at <https://github.com/ISCDtoolbox/Advection/>. This script supports \mathcal{P}_1 functions defined on surface meshes. Many thanks to the authors for their precious work.

Shape derivative

At each time step, the purpose is to find some vector field v such that advecting ϕ by (5.18) on this small time step increase the considered eigenvalue. In order to address this issue we need to compute the shape derivative of an eigenvalue of a domain of \mathbb{S}^n . This shape derivative is given by the following result (see for instance [106]):

Theorem 5.5.1 (Shape derivative). *We assume that Ω is C^1 with non-empty boundary. Let $k \in \mathbb{N}$ and $V : \mathbb{S}^n \rightarrow \mathbb{T}\mathbb{S}^n$ be a smooth vector field with compact support in the neighborhood of Ω_0 . We denote*

$$\mu'_k(\Omega_0, V) := \lim_{t \rightarrow 0^+} \frac{\mu_k(\Omega(t)) - \mu_k(\Omega_0)}{t}.$$

Moreover we assume that $\mu_k(\Omega_0)$ is simple. Then this limit exists and

$$\mu'_k(\Omega_0, V) = \int_{\partial\Omega_0} (|\nabla u|^2 - \mu_k(\Omega_0)u^2) (V \cdot n) d\sigma \quad (5.19)$$

with u an eigenfunction associated to $\mu_k(\Omega_0)$ with unitary \mathbf{L}^2 norm and n the outward normal.

The previous theorem allows us to only consider normal variations of the boundary and from this consideration $\mu'_k(\Omega_0, V) = \mu'_k(\Omega_0, v)$ where $v = V \cdot n$. Moreover, it shows that we can choose $v = |\nabla u|^2 - \mu_k(\Omega_0)u^2$ as a gradient direction. This, however, may not be the best choice as we see hereafter.

Handling area constraint

Despite being able to compute a gradient direction (5.19), we also have to fullfill the constraint $|\Omega| = m$ in the original problem (5.1). We could choose to add a penalization term and maximize the function

$$\Omega \mapsto \mu_k(\Omega) - b(|\Omega| - m')^2$$

instead, with $b > 0$ and m' a parameter allowing to control for the total mass m . However, if we consider the sequence of geodesic balls \mathbf{B}^w of mass $w > 0$ then we can fin that

$$\mu_k(\mathbf{B}^w) - b(|\mathbf{B}^w| - m')^2 \xrightarrow[w \rightarrow 0]{} +\infty$$

which establishes that the optimum is never attained for a positive area. However, a result by Strichartz allows to replace the unbounded quantity $\mu_k(\Omega)$ by the quantity $|\Omega|^{\frac{2}{n}}\mu_k(\Omega)$ even if we do not have invariance by dilation as in the Euclidian case. Indeed, using formulas (3.15) and (3.16) of [96] in the special case $n = 2$, we get the following property :

Proposition 5.5.2. *Let $\Omega \subset \mathbb{S}^2$. Then*

$$|\Omega|\mu_k(\Omega) \leq 2\pi k^2. \quad (5.20)$$

This generic bound allows to maximize the function

$$J(\Omega) := |\Omega|\mu_k(\Omega) - b(|\Omega| - m')^2 \quad (5.21)$$

which prevents the function to blow-up. Then if Ω^* maximizes (5.21), it is solution of (5.1) with $m = |\Omega^*|$.

There are two ways to implement the level set method. The so-called ersatz material approach involves a fixed mesh where the "void" part is filled with some material with good properties. The other one involves to remesh the domain at each step according to the level-set function. While the second one is more accurate, it suffers two main drawbacks, the most obvious one being its computational cost. The second one is related to the connectivity of Ω_t : suppose that we want to optimize μ_k , starting from a topologically complex domain. The level-set method allowing topological changes, it is very likely that at one point t , Ω_t splits into $k+1$ connected components. Then $\mu_0(\Omega_t) = \dots = \mu_k(\Omega_t) = 0$ and the associated eigenfunctions are constant on each connected component. This leads the shape derivative to be equal to

$$\mu'_k(\Omega, v) = -\mu_k(\Omega) \int_{\partial\Omega} v d\sigma.$$

The reader may recognise that this is proportional to the shape derivative of the function $\Omega \rightarrow |\Omega|$. This implies that the optimization process will only optimize on the volume. On the other hand, the "ersatz material" approach allows transparent topological changes and is faster than the second one since it doesn't require remeshing at each iteration. This is why we perform a first optimization using the ersatz material method and then use a remeshing approach for a final optimization of higher accuracy.

Level-set with ersatz material

In this section we assume the eigenvalues to be simple. According to the approximation theorem 5.2.2, we fix a small $\varepsilon > 0$ and solve the problem

$$-\operatorname{div}[(\mathbf{1}_\Omega + \varepsilon)\nabla u] = \mu_k^\varepsilon(\mathbf{1}_\Omega)(\mathbf{1}_\Omega + \varepsilon^2)u$$

at each step. Thanks to the above-mentioned theorem, this eigenvalue is expected to be close to the actual one for small ε . However, the function $\mathbf{1}_\Omega = 1_{\{\phi < 0\}}$, as defined on the mesh, may be highly irregular. This is why we approximate it in the following way

$$\mathbf{1}_\Omega \approx \frac{1}{2} \left(1 - \frac{\phi}{\sqrt{\phi^2 + \sigma^2}} \right)$$

with $\sigma > 0$ small. This avoids degeneracy in the denominator. Similar regularizations have been used in this framework, see for instance [3]. For the same reasons, the extended normal field is approximated by

$$\mathbf{n}_\Omega \approx \frac{\nabla\phi}{\sqrt{|\nabla\phi|^2 + \sigma^2}}$$

Initialization

It is well-known that the levelset method is prone to fall into local optima because of its sensitivity to initialization. To tackle this problem, the levelset function is initialized with a randomized trigonometric sum of the type

$$\phi(\theta, \psi) = \operatorname{Re} \left\{ \sum_{j=0}^p \sum_{k=0}^q c_{j,k} \exp(i(j\theta + k\psi)) \right\}$$

where the $c_{i,j}$ are chosen at random and $\theta, \psi \in [0, \pi] \times [0, 2\pi]$ are respectively the latitude and longitude on \mathbb{S}^2 . It is expected that the larger q and p , the more complex ϕ is and, by extension, Ω .

Multiple eigenvalues

The case of multiple eigenvalues, which always occurs in practice, is handled in the same way as in the density case.

Numerical considerations

In our simulations, we took $\varepsilon = 10^{-4}$ and $\sigma = 10^{-5}$. Moreover, to capture the variations of $\Omega(t)$ with good accuracy and because the level-set function tends to steepen near $\partial\Omega(t)$ over the iterations, we remesh the domain thanks to the MMG library [48] and recompute the signed distance function every 20 iterations thanks to the mshdist tool [49]. The maximal size of an element is $h_{max} = 10^{-1}$ and the minimal size is $h_{min} = 10^{-3}$. Just as previously, we use \mathcal{P}_1 finite elements and the FE computations are performed in GetFEM. The optimization algorithm is a simple gradient algorithm with a fixed number of $N = 600$ steps. The step size δt is chosen such that, if v is the gradient direction at a given moment then $\delta t = \frac{\gamma}{\|v\|_\infty}$ with $\gamma = 3 \cdot 10^{-2}$. The penalty term b is chosen to be equal to 5 and m' takes multiple values between 0.5 and 4π . The algorithm is presented in algorithm 1 for clarity purposes. Note that this algorithm is the one performed for a fixed m' . Finally, as in the density case, the optimization is performed multiple times with different initial level set functions and the best one is kept.

Algorithm 1 ersatz material levelset algorithm.

```

Require:  $k > 0$  ▷ The eigenvalue we optimize
Require: A mesh in MEDIT format
    Initialize the levelset  $\phi$ 
    for  $i$  from 0 to  $N$  do
        if  $N = 0 \bmod 20$  then
            Remesh using MMG.
            Reinitialize the levelset function  $\phi$ .
        end if
        Compute  $\mu_k^\varepsilon(\Omega)$  and the associated eigenfunctions using FE.
        Compute  $v$  the maximizing direction.
        Advect  $\phi$  during a time  $\delta t$ .
    end for

```

Level-set with remeshing

The following method is triggered once the previous one has converged, hence we don't expect major changes in topology which could be problematic as discussed before. In this procedure, we remesh the sphere such that $\partial\Omega = \{\phi = 0\}$ is a polygonal line of the mesh at each timestep. This then allows us to extract the mesh describing Ω and solve the original eigenvalue problem on it, without having to compute the approximation μ_k^ε . But then the optimization direction $v = |\nabla u|^2 - \mu_k(\Omega)u^2$ (with u an eigenfunction of $\mu_k(\Omega)$) is only defined on Ω while we need it to be defined in the whole sphere \mathbb{S}^n in order to advect the level-set function. In this purpose we use the well-known "extension-regularization" method which allows - as its name suggests - to extend the velocity field on all \mathbb{S}^n and regularize it at the same time [50]. Still assuming that the eigenvalue is simple, we see that $v \mapsto \mu'_k(\Omega_0, v)$ is a continuous linear form in v . Hence, we can find w the unique solution to the variational problem

$$\forall v \in \mathbf{H}^1(\mathbb{S}^n), \int_{\mathbb{S}^n} \alpha \nabla v \nabla w + vw = d\mu_k(\Omega_0, v) \quad (5.22)$$

where $\alpha > 0$. Then w is indeed an extension of $|\nabla u|^2 - \mu_k u^2$ on $\mathbf{H}^1(\mathbb{S}^n)$ with regularity depending on α . Moreover, w is a valid gradient direction since

$$d\mu_k(\Omega_0, w) = \int_{\mathbb{S}^n} \alpha |\nabla w|^2 + w^2 \geq 0.$$

Numerical considerations

The numerical values chosen for this second optimization are mostly the same as the previous procedure. One add the regularization parameter $\alpha = 0.1$ and that h_{max} is now equal to 5.10^{-2} . The step size δt_i is now adaptative : if at a given iteration i we have that $\mu_k(\Omega_i) > \mu_k(\Omega_{i+1})$ then $\delta t_{i+1} = \delta t_i/2$. Otherwise $\delta t_{i+1} = 1.1\delta t_i$. The optimization stops when $\delta t_i < 10^{-7}$ and the mesh with the best cost is kept. The pseudocode of the algorithm for a fixed m' is provided in algorithm 2.

Algorithm 2 ersatz material levelset algorithm.

```

Require:  $k > 0$  ▷ The eigenvalue we optimize
Require: The mesh and optimal domain  $\Omega$  obtained by the previous procedure.
Initialize the levelset  $\phi$  as the one of  $\Omega$ .
while  $\delta t > 10^{-7}$  do
    Remesh using MMG.
    Reinitialize the levelset function  $\phi$ .
    Extract the submesh  $\Omega$ 
    Compute  $\mu_k(\Omega)$  and the associated eigenfunctions using FE.
    Compute  $v$  the maximizing direction on  $\partial\Omega$ 
    Extend  $v$  to the whole mesh of  $\mathbb{S}^2$  by extension-regularization
    Advect  $\phi$  during a time  $\delta t$ 
    if The cost function increased then
         $\delta t \leftarrow 1.1\delta t$ 
    else
         $\delta t \leftarrow \delta t/2$ 
    end if
end while
```

5.6 Results : level-set method.

We report here the optimization results for $k \in \{1, 2, 3\}$. We denote by Ω^m the optimal domain computed with the levelset procedure verifying $|\Omega^m| = m$. The optimal eigenvalues $\mu_k(|\Omega^m|)$ are plotted in green, against the corresponding surface area m . As for the density method, we also plot in red the eigenvalue $\mu_k(UB(|\Omega^m|, k))$ of an union of k disjoints balls of total area m . Since the eigenvalue goes to ∞ as $|\Omega^m|$ goes to 0, we divide the plot on two parts $0 < |\Omega^m| \leq 2\pi$ and $2\pi < |\Omega^m| \leq 4\pi$ for better readability.

Optimization of μ_1

In Figure 5.12 are displayed the results for the optimization of μ_1 . The spherical cap seems to be the optimal shape up to $m \approx 8.0$, after which it clearly ceases to be the optimal shape. From that point up to $m = 4\pi$, complex shapes arises, consisting in a plain hemisphere and a lot of holes in the opposite one. Different views of one of those shapes can be seen in Figure 5.13, where $m \approx 11.13$ and $\mu_1(\Omega^m) \approx 1.77$ (for instance, a spherical cap of this surface area would give $\mu_1(\mathbf{B}^m) = 1.62$). This strange behaviour, combined with the density approach above, may suggest that the actual optimal may be attained by some kind of homogenization procedure. Some simple, non conclusive numerical test have been performed in this direction but this problem surely needs further investigation and may lead to interesting numerical and theoretical developements.

More optimal shapes are displayed in Figure 5.14. Looking at Ω^m for $m = 8.0$ (the third one from the left), one can imagine that it would be possible for the geodesic cap to cease to be optimal for m way lower than 8.0 but the numerical procedure wouldn't be able to "see" it because it would be necessary to create details thinner than the size of an element of the mesh. However, it seems unlikely that the spherical cap ceases to be optimal for the same mass m as the density method:

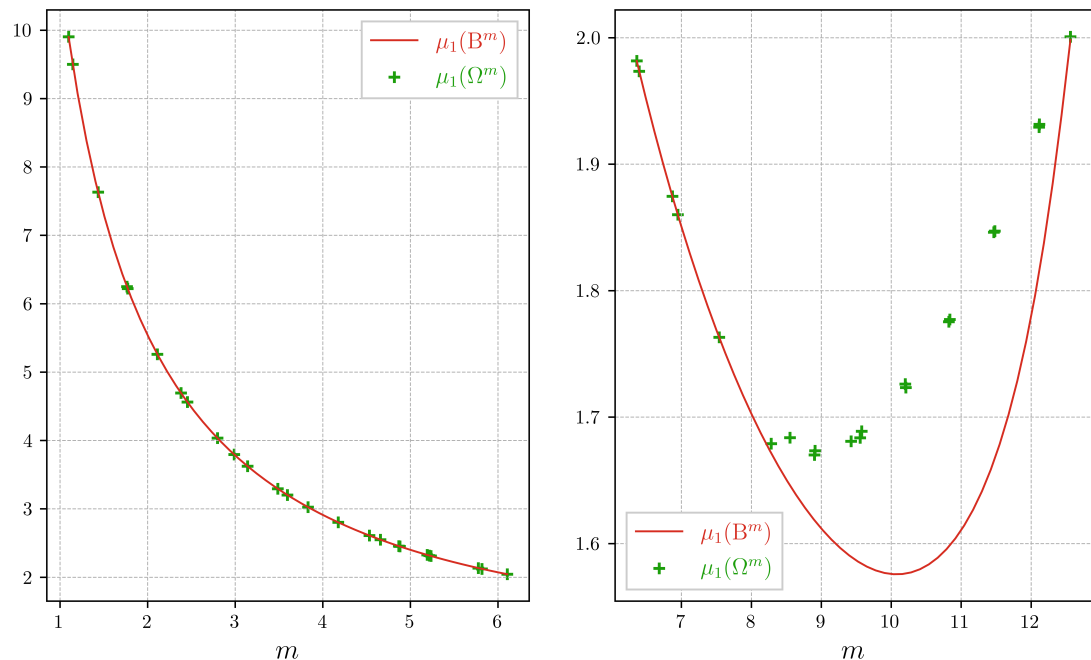


Figure 5.12: Optimal value of μ_1 obtained by the level-set method.

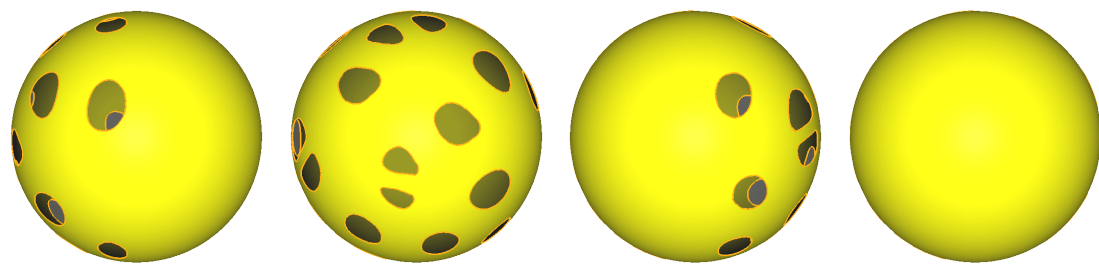


Figure 5.13: Rotational view of the optimal shape obtained by the level-set method for large m .

Conjecture 5.6.1. Let δ be the same as in Conjecture 5.4.4. Then there exists $\delta' > \delta$ such that for all $0 < m < \delta'$, $\Omega^m = B^m$.

Remark 5.6.2. The fact that $\delta' \geq \delta$ is obvious; the interesting part would be to show that the inequality is strict.

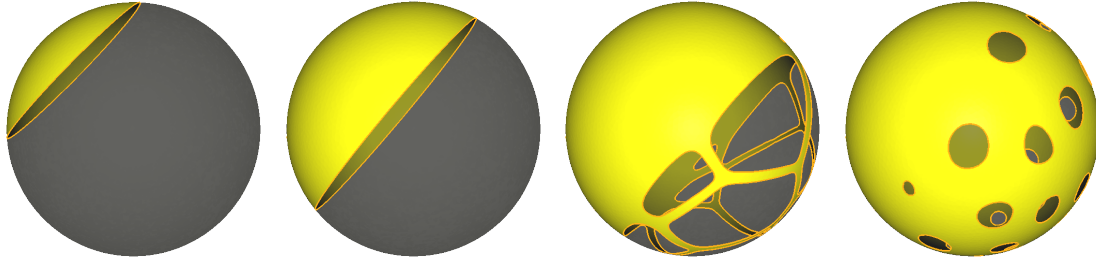


Figure 5.14: Example of optimal domains for μ_1 for $m \in \{2.03, 5.1, 8.0, 10.85\}$.

Optimization of μ_2

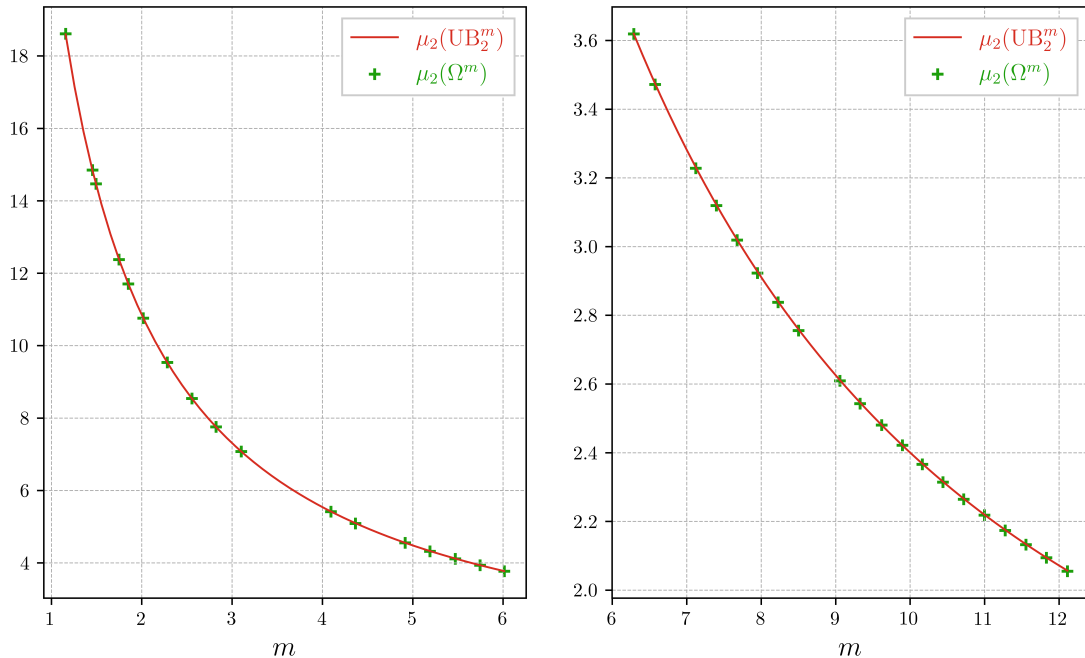


Figure 5.15: Optimal value of μ_2 obtained by the level-set method.

The optimal results for μ_2 are displayed Figure 5.15. We can see that the optimal shape is always the union of two spherical caps, as it has been proven in 4. Hence this case can be considered as a test case to support the validity of the method. In Figure 5.16 are shown the optimal shapes. For $m = 11.17$, we give an example of a shape which is not the union of two disjoint disks. Indeed, for large m , the first levelset procedure struggled to disconnect one domain into two disks due to numerical instabilities. The eigenvalue is however really close to the one of two disks.

Optimization of μ_3

In Figure 5.17 is displayed the results for the optimization of μ_3 . As for the density case, this eigenvalue shows a rich variety of behaviours depending on the value of m (see Figure 5.18).

The results seems to be in accordance with the ones given by the density method.

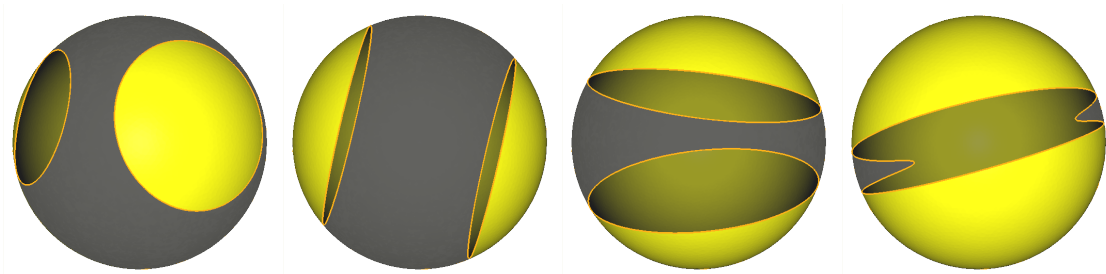


Figure 5.16: Example of optimal domains for μ_2 for $m \in \{2.12, 5.1, 8.13, 11.17\}$.

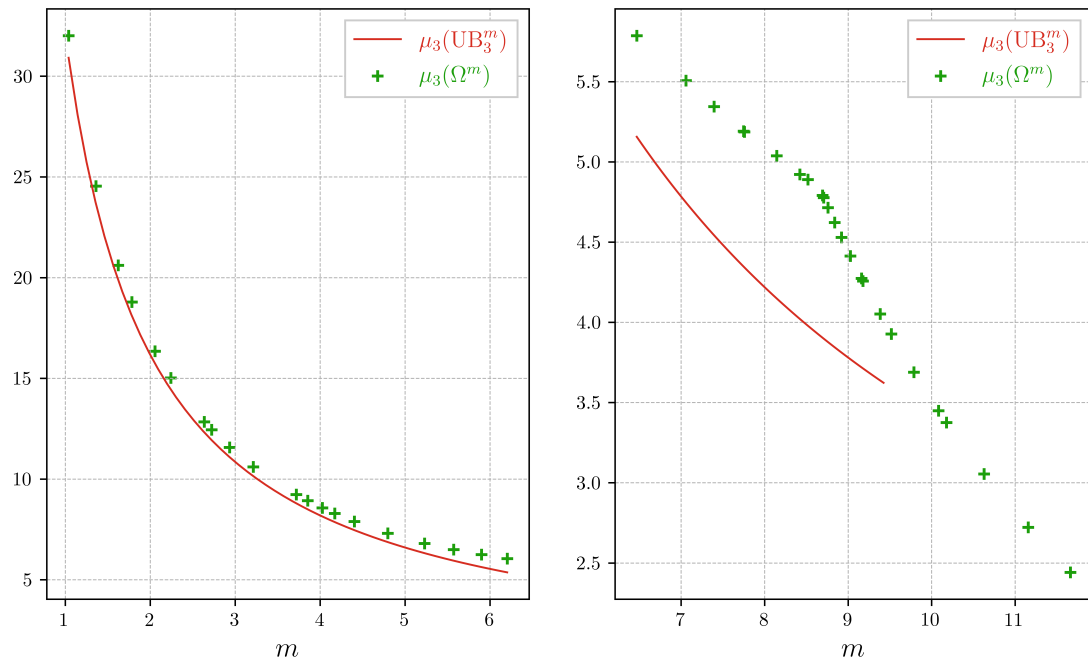


Figure 5.17: Optimal value of μ_3 obtained by the level-set method.

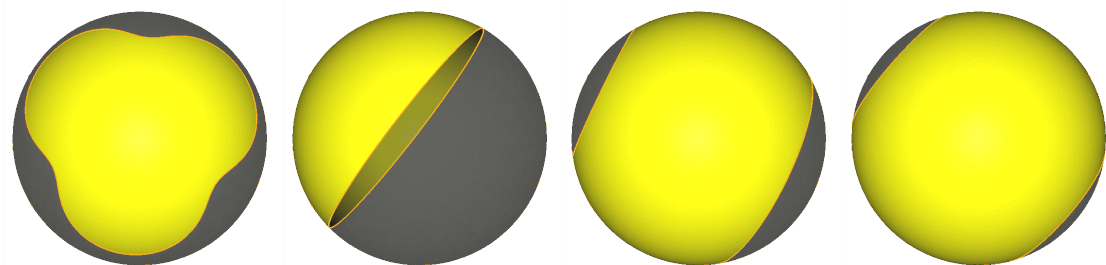


Figure 5.18: Example of optimal domains for μ_3 for $m \in \{2.0, 5.22, 8.0, 11.04\}$.

Data.

As for the results of the density method, all the final solutions are available in MEDIT format at https://github.com/EloiMartinet/Neumann_Sphere/, with a FreeFem++ script allowing to compute the eigenvalue and surface area of each solution.

5.7 Explorations on a torus

This last part is devoted to the optimization of eigenvalues on a torus. Specifically, we consider the torus \mathbb{T} in \mathbb{R}^3 parametrized by

$$(u, v) \mapsto ((R + r \cos v) \cos u, r \sin v, (R + r \cos v) \sin u),$$

that is, the torus with major radius R and minor radius r . In the sequel, we will choose $R = 2$ and $r = 1$. Knowing that the surface area of \mathbb{T} is given by

$$|\mathbb{T}| = 4\pi^2 Rr$$

we have in our case $|\mathbb{T}| \approx 78.96$.

The problem we consider now is analogous to the one on the sphere. With $\Omega \subset \mathbb{T}$ being a Lipschitz open domain, the eigenvalue problem is

$$\begin{cases} -\Delta u = \mu_k(\Omega)u \text{ in } \Omega, \\ \frac{\partial u}{\partial n} = 0 \text{ on } \partial\Omega, \end{cases}.$$

We also use the same notion of generalized eigenvalues of a density $\rho : \mathbb{T} \rightarrow [0, 1]$, we define

$$\mu_k(\rho) := \inf_{V \in \mathcal{S}_{k+1}} \max_{u \in V \setminus \{0\}} \frac{\int_{\mathbb{T}} \rho |\nabla u|^2}{\int_{\mathbb{T}} \rho u^2},$$

where \mathcal{S}_{k+1} is the family of subspaces of dimension $k+1$ in

$$\{u \cdot 1_{\{\rho(x) > 0\}} : u \in C_c^\infty(\mathbb{T})\}.$$

We then consider the two optimization problems

$$\sup \{\mu_k(\Omega) \text{ s.t. } \Omega \subset \mathbb{T}, |\Omega| = m, \Omega \text{ bounded, open and Lipschitz}\}$$

and

$$\sup \left\{ \mu_k(\rho) \text{ s.t. } \rho : \mathbb{T} \rightarrow [0, 1], \int_{\mathbb{T}} \rho = m \right\}.$$

with $0 < m < |\mathbb{T}|$ and $k > 0$.

This last formulation allows to perform the same density method performed on the sphere. These are the results presented hereafter, followed by the results obtained by the level set method.

Density optimization

We precise that the optimization parameters that have been used are the same than the ones used for the sphere. We begin to depict some of the optimal densities in Figure 5.19. For a better visualization, we recall that all the meshes and densities are available at https://github.com/EloiMartinet/Neumann_Sphere/.

We can notice that for small enough masses, the optimal densities seems to be the characteristic function of geodesic balls for $k \in \{1, 2, 3\}$. However, by comparison with the case of the plane and the sphere, the case of μ_3 must be taken with caution. A striking fact is that contrary to the case of the sphere, the optimal density for μ_1 seems to stay a charateristic function whereas we cans witness some homogenization for μ_2 . The optimal eigenvalues plotted as functions of m are shown in Figure 5.20.

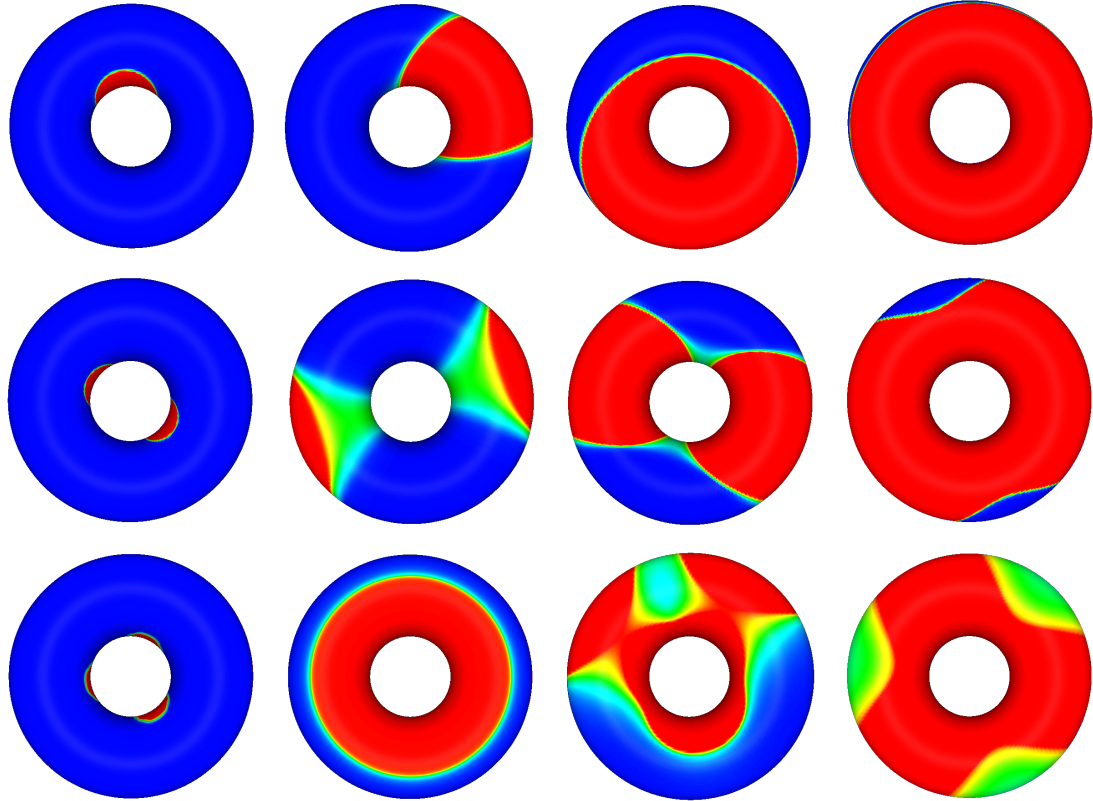


Figure 5.19: Example of optimal densities for μ_1, μ_2 and μ_3 (resp. first, second and third row) for $m \in \{3, 22, 43, 68\}$ approximately.

Level set optimization

In Figure 5.21 are the optimal domains obtained by the level set method for μ_1, μ_2, μ_3 and various masses.

The optimal eigenvalues plotted as functions of m are shown in Figure 5.22.

5.8 Discussion

We have presented two ways to explore numerically the optimization of eigenvalues of the Laplace-Beltrami operator with Neumann boundary conditions for domains in the sphere and the torus. The first one generalizes the notion of eigenvalues of domains and thus is independant of topological consideration. On the other hand, the second method relies on the level set representation of the domain, which allows topological changes.

In the case of the optimization on the sphere, this flexibility turned out to be an important feature, regarding the topological complexity of certain optimal domains for μ_1 on the sphere. Indeed, while the density optimization leads to optima that does not corresponds to domains, the level set procedure tries to create areas with a lot of holes, which might indicate non-existence of optimal domains for large enough surface area. Oppositely, it seems clear that for small enough surface area, the optimal density (and thus, optimal domain) for μ_1 on the sphere is the one of a geodesic ball. It has then been witnessed that the behaviour of μ_2 on the sphere was completely understood. For μ_3 , it might be difficult to decribe theoretically the way optima behave depending on the total surface area. Nevertheless, it would be interesting to prove some necessary conditions such domains have to meet, such as symmetry.

In the case of the optimization on the torus, we noticed that homogenization happened this time for μ_2 and not for μ_1 . Further investigations may be needed to better understand how this phenomenon is linked

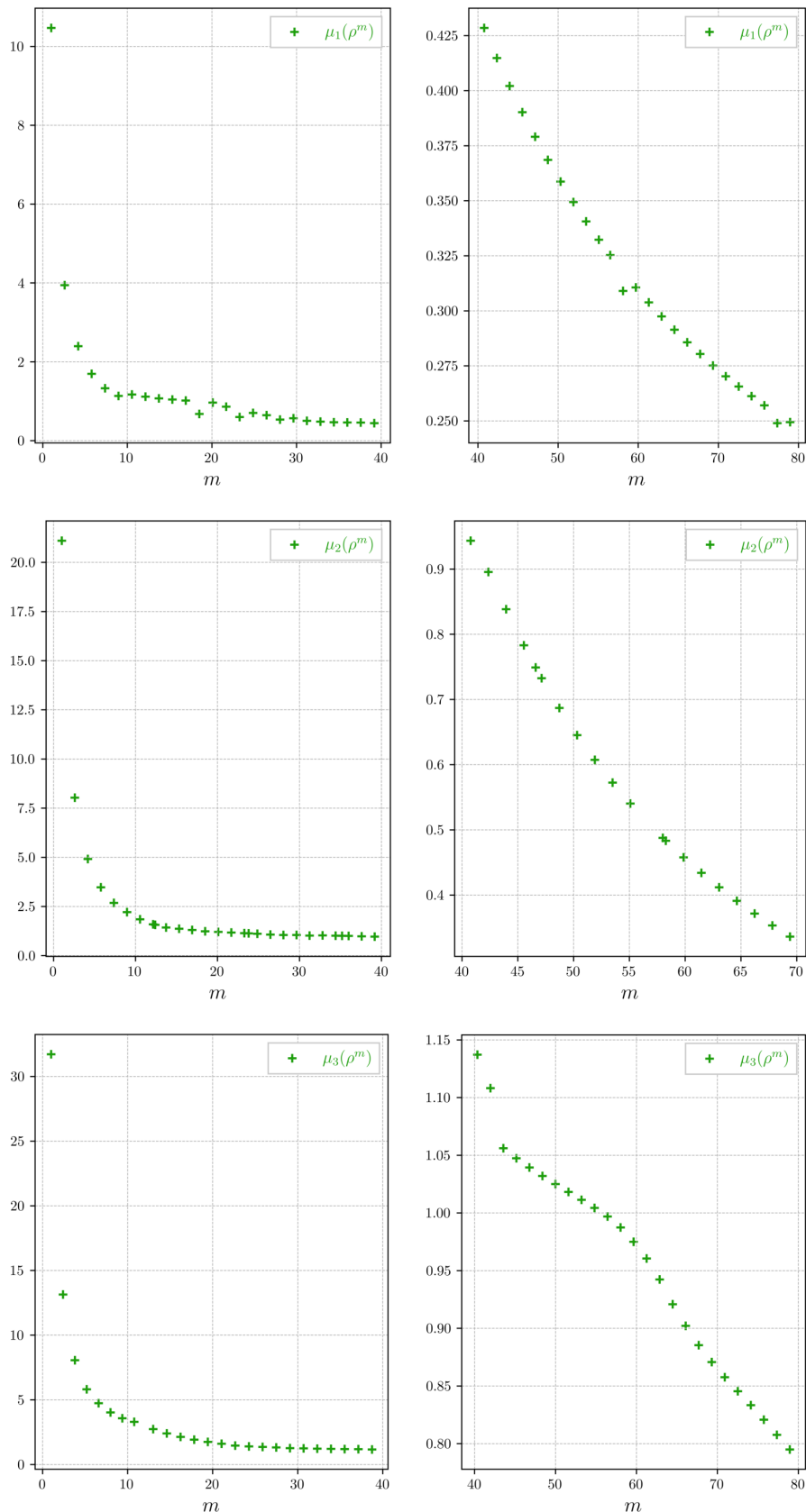


Figure 5.20: Optimal values of μ_1, μ_2 and μ_3 (resp. first, second and third row) obtained by the density method.

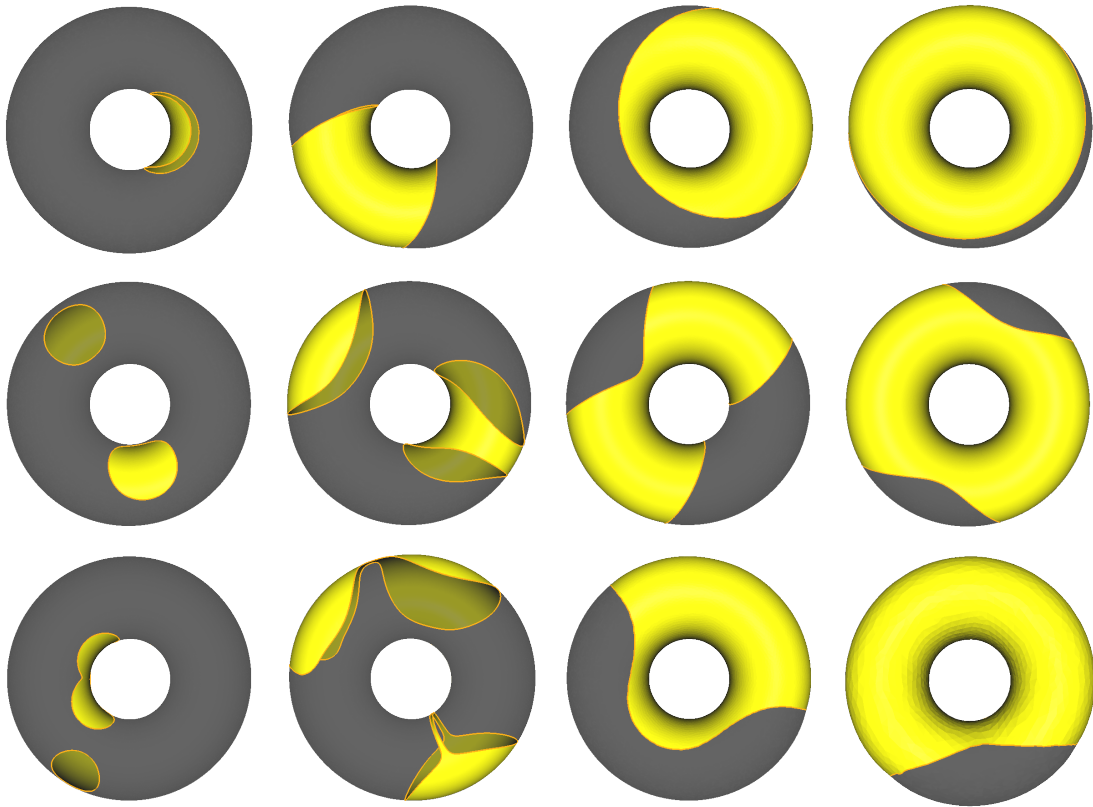


Figure 5.21: Example of optimal domains for μ_1, μ_2 and μ_3 (resp. first, second and third row) for $m \in \{4, 22, 42, 60\}$ approximately.

to the dimensions of the torus, and if it such homogenization happens in flat tori like $(\mathbb{R}^n / \mathbb{Z}^n)$.

In any case, an interesting result would be to get a better grasp on the existence or non-existence of optimal domains on manifold.

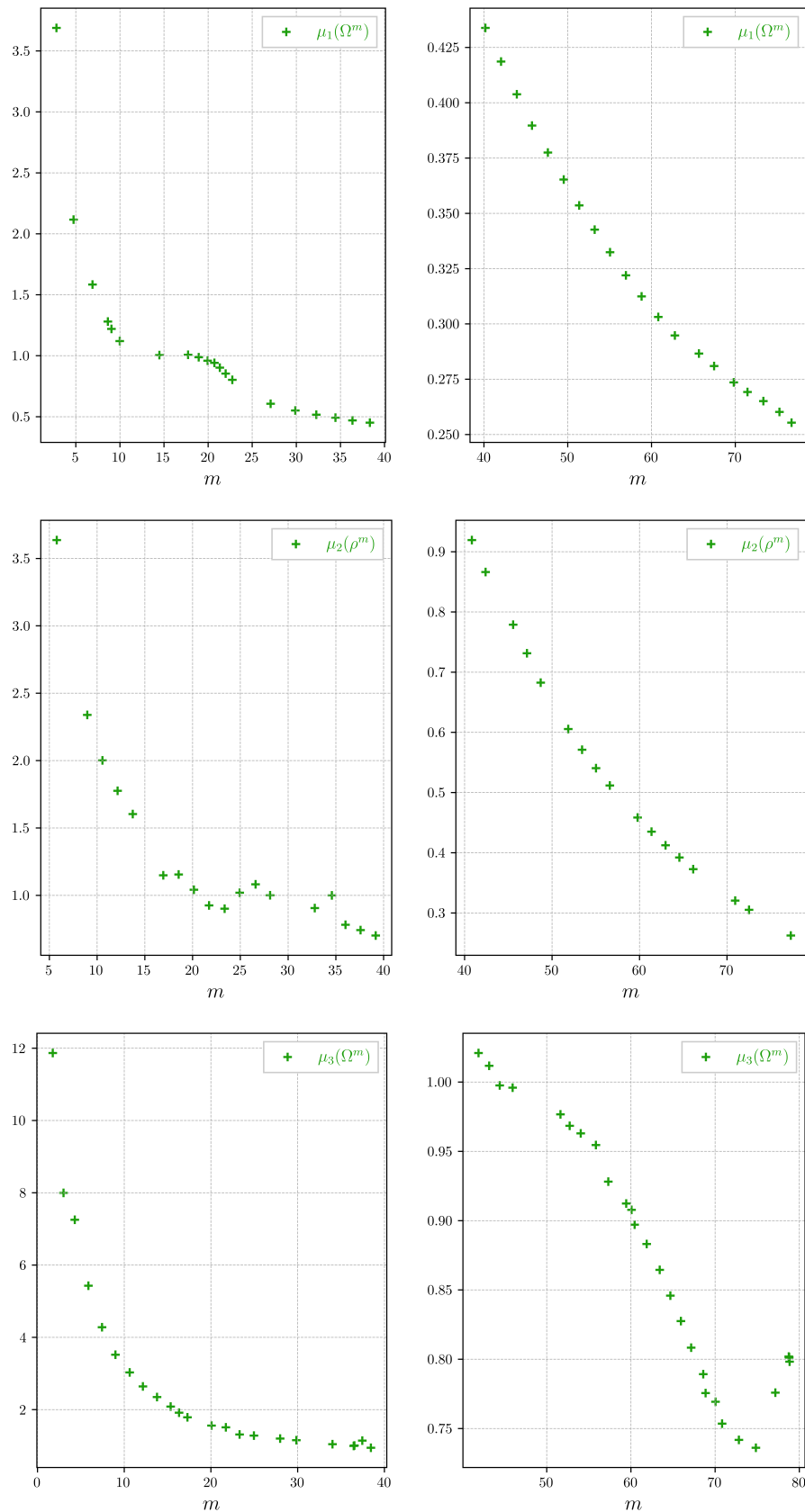


Figure 5.22: Optimal values of μ_1 , μ_2 and μ_3 (resp. first, second and third row) obtained by the level set method.

Bibliography

- [1] G. Allaire, C. Dapogny, and P. Frey. Shape optimization with a level set based mesh evolution method. *Computer Methods in Applied Mechanics and Engineering*, 282:22–53, December 2014.
- [2] Grégoire Allaire. *Analyse numérique et optimisation: une introduction à la modélisation mathématique et à la simulation numérique*. Editions Ecole Polytechnique, 2005.
- [3] Grégoire Allaire, Charles Dapogny, Gabriel Delgado, and Georgios Michailidis. Multi-phase structural optimization via a level set method. *ESAIM: control, optimisation and calculus of variations*, 20(2):576–611, 2014.
- [4] Grégoire Allaire and François Jouve. A level-set method for vibration and multiple loads structural optimization. *Computer Methods in Applied Mechanics and Engineering*, 194(30-33):3269–3290, August 2005.
- [5] Grégoire Allaire. *Shape Optimization by the Homogenization Method*, volume 146 of *Applied Mathematical Sciences*. Springer, New York, NY, 2002.
- [6] Grégoire Allaire, Charles Dapogny, and François Jouve. Chapter 1 - shape and topology optimization. In Andrea Bonito and Ricardo H. Nochetto, editors, *Geometric Partial Differential Equations - Part II*, volume 22 of *Handbook of Numerical Analysis*, pages 1–132. Elsevier, 2021.
- [7] Grégoire Allaire and François Murat. Homogenization of the Neumann problem with nonisolated holes. *Asymptotic Analysis*, 7(2):81–95, January 1993. Publisher: IOS Press.
- [8] P. R. S. Antunes and P. Freitas. Numerical optimization of low eigenvalues of the Dirichlet and Neumann Laplacians. *J. Optim. Theory Appl.*, 154(1):235–257, 2012.
- [9] P. R. S. Antunes and E. Oudet. Numerical results for extremal problem for eigenvalues of the Laplacian. In *Shape optimization and spectral theory*, pages 398–411. De Gruyter Open, Warsaw, 2017.
- [10] P. R. S. Antunes and E. Oudet. Numerical results for extremal problem for eigenvalues of the Laplacian. In *Shape optimization and spectral theory*, pages 398–411. De Gruyter Open, Warsaw, 2017.
- [11] Pedro Antunes and Benjamin Bogosel. Parametric shape optimization using the support function. *Computational Optimization and Applications*, 82, May 2022.
- [12] Pedro R. S. Antunes. Numerical calculation of extremal Steklov eigenvalues in 3D and 4D. *Computers & Mathematics with Applications*, 104:50–58, 2021.
- [13] Pedro R. S. Antunes and Pedro Freitas. Optimisation of Eigenvalues of the Dirichlet Laplacian with a Surface Area Restriction. *Applied Mathematics & Optimization*, 73(2):313–328, April 2016.
- [14] Pedro R. S. Antunes, Pedro Freitas, and James B. Kennedy. Asymptotic behaviour and numerical approximation of optimal eigenvalues of the robin laplacian, 2012.
- [15] Pedro R. S. Antunes and Édouard Oudet. Numerical Minimization of Dirichlet Laplacian Eigenvalues of Four-Dimensional Geometries. *SIAM Journal on Scientific Computing*, 39(3):B508–B521, January 2017.
- [16] Pedro RS Antunes and Pedro Freitas. Numerical optimization of low eigenvalues of the dirichlet and neumann laplacians. *Journal of Optimization Theory and Applications*, 154(1):235–257, 2012.
- [17] Pedro RS Antunes, Pedro Freitas, and David Krejčířík. Bounds and extremal domains for robin eigenvalues with negative boundary parameter. *Advances in Calculus of Variations*, 10(4):357–379, 2017.
- [18] Mark S. Ashbaugh and Rafael D. Benguria. Sharp upper bound to the first nonzero Neumann eigenvalue for bounded domains in spaces of constant curvature. *J. London Math. Soc.* (2), 52(2):402–416, 1995.
- [19] Mark S. Ashbaugh and Rafael D. Benguria. Sharp Upper Bound to the First Nonzero Neumann Eigenvalue for Bounded Domains in Spaces of Constant Curvature. *Journal of the London Mathematical Society*, 52(2):402–416, October 1995.
- [20] Mark S. Ashbaugh and Rafael D. Benguria. A sharp bound for the ratio of the first two Dirichlet eigenvalues of a domain in a hemisphere of S^n . *Trans. Amer. Math. Soc.*, 353(3):1055–1087, 2001.

References

- [21] Catherine Bandle. Isoperimetric Inequality for Some Eigenvalues of an Inhomogeneous, Free Membrane. *SIAM Journal on Applied Mathematics*, 22(2):142–147, March 1972.
- [22] Z. Belhachmi, D. Bucur, G. Buttazzo, and J.-M. Sac-Epée. Shape optimization problems for eigenvalues of elliptic operators. *ZAMM*, 86(3):171–184, March 2006.
- [23] Rafael D. Benguria, Barbara Brandolini, and Francesco Chiacchio. A sharp estimate for Neumann eigenvalues of the Laplace-Beltrami operator for domains in a hemisphere. *Commun. Contemp. Math.*, 22(3):1950018, 9, 2020.
- [24] Pierre Bérard and Bernard Helffer. Sturm’s theorem on zeros of linear combinations of eigenfunctions. *Expo. Math.*, 38(1):27–50, 2020.
- [25] A. Berger. *Optimisation du spectre du Laplacien avec conditions de Dirichlet et Neumann dans \mathbb{R}^2 , \mathbb{R}^3* . Thèse de doctorat en Mathématiques appliquées. Université de Neuchâtel, Université Grenoble Alpes, 2015.
- [26] Daniele Boffi. Finite element approximation of eigenvalue problems. *Acta Numerica*, 19:1–120, May 2010.
- [27] Beniamin Bogosel. The method of fundamental solutions applied to boundary eigenvalue problems. *Journal of Computational and Applied Mathematics*, 306:265–285, 2016.
- [28] Beniamin Bogosel and Pedro R. S. Antunes. Optimization of the Steklov-Lam’s eigenvalues with respect to the domain. May 2022. arXiv:2205.11364 [math].
- [29] Beniamin Bogosel, Doina Bucur, and Alessandro Giacomini. Optimal shapes maximizing the steklov eigenvalues. *SIAM Journal on Mathematical Analysis*, 49(2):1645–1680, 2017.
- [30] Blaise Bourdin, Dorin Bucur, and Édouard Oudet. Optimal Partitions for Eigenvalues. *SIAM Journal on Scientific Computing*, 31(6):4100–4114, January 2010.
- [31] Lorenzo Brasco and Aldo Pratelli. Sharp Stability of Some Spectral Inequalities. *Geometric and Functional Analysis*, 22(1):107–135, February 2012.
- [32] D. Bucur and G. Buttazzo. *Variational methods in shape optimization problems*, volume 65 of *Progress in Nonlinear Differential Equations and their Applications*. Birkhäuser Boston, Inc., Boston, MA, 2005.
- [33] Dorin Bucur and Antoine Henrot. Maximization of the second non-trivial Neumann eigenvalue. *Acta Math.*, 222(2):337–361, 2019.
- [34] Dorin Bucur, Eloi Martinet, and Mickaël Nahon. Sharp inequalities for Neumann eigenvalues on the sphere, August 2022. arXiv:2208.11413.
- [35] Dorin Bucur, Eloi Martinet, and Edouard Oudet. Maximization of Neumann eigenvalues, 2022.
- [36] Dorin Bucur and Nicolas Varchon. Boundary variation for a Neumann problem. *Annali della Scuola Normale Superiore di Pisa - Classe di Scienze*, 29(4):807–821, 2000.
- [37] Giuseppe Buttazzo and Gianni Dal Maso. An existence result for a class of shape optimization problems. *Archive for Rational Mechanics and Analysis*, 122(2):183–195, June 1993.
- [38] Giuseppe Buttazzo and Gianni Dal Maso. An existence result for a class of shape optimization problems. *Arch. Rational Mech. Anal.*, 122(2):183–195, 1993.
- [39] Fabien Caubet, Marc Dambrine, and Rajesh Mahadevan. Shape sensitivity of eigenvalue functionals for scalar problems: computing the semi-derivative of a minimum. page 25.
- [40] Antonin Chambolle and Francesco Doveri. Continuity of neumann linear elliptic problems on varying two-dimensional bounded open sets. *Communications in Partial Differential Equations*, 22(5-6):811–840, January 1997.
- [41] Isaac Chavel. Lowest-eigenvalue inequalities. In *Geometry of the Laplace operator (Proc. Sympos. Pure Math., Univ. Hawaii, Honolulu, Hawaii, 1979)*, Proc. Sympos. Pure Math., XXXVI, pages 79–89. Amer. Math. Soc., Providence, R.I., 1980.
- [42] Denise Chenais. On the existence of a solution in a domain identification problem. *Journal of Mathematical Analysis and Applications*, 52(2):189–219, November 1975.

- [43] Bruno Colbois and Ahmad El Soufi. Spectrum of the Laplacian with weights. *Ann. Global Anal. Geom.*, 55(2):149–180, 2019.
- [44] Bruno Colbois and Ahmad El Soufi. Spectrum of the Laplacian with weights. *Annals of Global Analysis and Geometry*, 55(2):149–180, 2019.
- [45] Bruno Colbois, Ahmad El Soufi, and Alessandro Savo. Eigenvalues of the Laplacian on a compact manifold with density. *Comm. Anal. Geom.*, 23(3):639–670, 2015.
- [46] Luca D’Alessandro, Bichoy Bahr, Luca Daniel, Dana Weinstein, and Raffaele Ardito. Shape optimization of solid-air porous phononic crystal slabs with widest full 3d bandgap for in-plane acoustic waves. *Journal of Computational Physics*, 344:465–484, 2017.
- [47] C. Dapogny, C. Dobrzhynski, and P. Frey. Three-dimensional adaptive domain remeshing, implicit domain meshing, and applications to free and moving boundary problems. *J. Comput. Phys.*, 262:358–378, 2014.
- [48] Charles Dapogny, Cécile Dobrzhynski, and Pascal Frey. Three-dimensional adaptive domain remeshing, implicit domain meshing, and applications to free and moving boundary problems. *Journal of computational physics*, 262:358–378, 2014.
- [49] Charles Dapogny and Pascal Frey. Computation of the signed distance function to a discrete contour on adapted triangulation. *Calcolo*, 49(3):193–219, 2012.
- [50] Frédéric de Gournay. Velocity Extension for the Level-set Method and Multiple Eigenvalues in Shape Optimization. *SIAM Journal on Control and Optimization*, 45(1):343–367, January 2006.
- [51] Michel C. Delfour and J.-P. Zolésio. *Shapes and geometries: metrics, analysis, differential calculus, and optimization*. Number DC22 in Advances in design and control. Society for Industrial and Applied Mathematics, Philadelphia, 2nd ed edition, 2011. OCLC: ocn650821954.
- [52] Lawrence C Evans. *Partial differential equations*, volume 19. American Mathematical Society, 2022.
- [53] Georg Faber. Beweis, dass unter allen homogenen membranen von gleicher fläche und gleicher spannung die kreisförmige den tiefsten grundton gibt. 1923.
- [54] Mouhamed Moustapha Fall and Tobias Weth. Critical domains for the first nonzero Neumann eigenvalue in Riemannian manifolds. *J. Geom. Anal.*, 29(4):3221–3247, 2019.
- [55] Pedro Freitas and Richard Laugesen. From Neumann to Steklov and beyond, via Robin: the Weinberger way, October 2018. arXiv:1810.07461 [math].
- [56] Pedro Freitas and Richard S. Laugesen. Two balls maximize the third neumann eigenvalue in hyperbolic space, 2020.
- [57] Pedro Freitas and Isabel Salavessa. Families of non-tiling domains satisfying pólya’s conjecture, 2022.
- [58] Pedro Freitas and Richard Snyder Laugesen. Two balls maximize the third Neumann eigenvalue in hyperbolic space. *ANNALI SCUOLA NORMALE SUPERIORE - CLASSE DI SCIENZE*, (2021: Forthcoming articles):27, May 2021.
- [59] Harald Garcke, Paul Hüttl, and Patrik Knopf. Shape and topology optimization involving the eigenvalues of an elastic structure: A multi-phase-field approach. *Advances in Nonlinear Analysis*, 11(1):159–197, 2021.
- [60] A. Girouard, N. Nadirashvili, and I. Polterovich. Maximization of the second positive Neumann eigenvalue for planar domains. *J. Differential Geom.*, 83(3):637–661, 2009.
- [61] Alexander Grigor’yan, Yuri Netrusov, and Shing-Tung Yau. Eigenvalues of elliptic operators and geometric applications. In *Surveys in differential geometry. Vol. IX*, Surv. Differ. Geom., IX, pages 147–217. Int. Press, Somerville, MA, 2004.
- [62] Jacques Hadamard. *Mémoire sur le problème d’analyse relatif à l’équilibre des plaques élastiques encastrees*. Mémoires présentés par divers savants à l’Académie des sciences de l’Institut de France, extrait du tome XXXIII. Imprimerie nationale, Paris, 1908.

References

- [63] F. Hecht. New development in freefem++. *J. Numer. Math.*, 20(3-4):251–265, 2012.
- [64] A. Henrot. *Extremum problems for eigenvalues of elliptic operators*. Frontiers in Mathematics. Birkhäuser Verlag, Basel, 2006.
- [65] A. Henrot. *Extremum problems for eigenvalues of elliptic operators*. Frontiers in Mathematics. Birkhäuser Verlag, Basel, 2006.
- [66] Antoine Henrot and Edouard Oudet. Le stade ne minimise pas λ_2 parmi les ouverts convexes du plan. *Comptes Rendus de l'Académie des Sciences - Series I - Mathematics*, 332(5):417–422, March 2001.
- [67] Antoine Henrot and Michel Pierre. *Variation et optimisation de formes: une analyse géométrique*. Number 48 in Mathématiques & applications. Springer, Berlin Heidelberg New York, 2005.
- [68] Antoine Henrot (editor). Shape optimization and spectral theory. Berlin: De Gruyter (ISBN 978-3-11-055085-6/hbk; 978-3-11-055088-7/ebook). x, 464 p., open access (2017)., 2017.
- [69] Jakob S Jensen and Ole Sigmund. Topology optimization of photonic crystal structures: a high-bandwidth low-loss t-junction waveguide. *JOSA B*, 22(6):1191–1198, 2005.
- [70] Tosio Kato. *Perturbation theory for linear operators*, volume 132. Springer Science & Business Media, 2013.
- [71] E. T. Kornhauser and I. Stakgold. A Variational Theorem for $\hat{u}^{\frac{2}{N-2}} u + \|u\| = 0$ and its Application. *Journal of Mathematics and Physics*, 31(1-4):45–54, April 1952.
- [72] Edgar Krahn. Über eine von rayleigh formulierte minimaleigenschaft des kreises. *Mathematische Annalen*, 94(1):97–100, 1925.
- [73] P. Kröger. Upper bounds for the Neumann eigenvalues on a bounded domain in Euclidean space. *J. Funct. Anal.*, 106(2):353–357, 1992.
- [74] Paweł Kröger. On upper bounds for high order Neumann eigenvalues of convex domains in Euclidean space. *Proc. Amer. Math. Soc.*, 127(6):1665–1669, 1999.
- [75] P Kröger. Upper bounds for the Neumann eigenvalues on a bounded domain in euclidean space. *Journal of Functional Analysis*, 106(2):353–357, June 1992.
- [76] Jeffrey J Langford and Richard S Laugesen. Maximizers beyond the hemisphere for the second neumann eigenvalue. *Mathematische Annalen*, pages 1–27, 2022.
- [77] J.J. Langford and R.S. Laugesen. Maximizers beyond the hemisphere for the second neumann eigenvalue. *Math. Ann.*, 2022.
- [78] A. Laptev. Dirichlet and Neumann eigenvalue problems on domains in Euclidean spaces. *J. Funct. Anal.*, 151(2):531–545, 1997.
- [79] Nicolas Lebbe, Charles Dapogny, Edouard Oudet, Karim Hassan, and Alain Gliere. Robust shape and topology optimization of nanophotonic devices using the level set method. *Journal of Computational Physics*, 395:710–746, 2019.
- [80] Adrian S. Lewis and Michael L. Overton. Eigenvalue optimization. In *Acta numerica, 1996*, volume 5 of *Acta Numer.*, pages 149–190. Cambridge Univ. Press, Cambridge, 1996.
- [81] Jiajie Li and Shengfeng Zhu. Shape optimization of the stokes eigenvalue problem. *SIAM Journal on Scientific Computing*, 45(2):A798–A828, 2023.
- [82] P.-L. Lions. The concentration-compactness principle in the calculus of variations. The limit case. I. *Rev. Mat. Iberoamericana*, 1(1):145–201, 1985.
- [83] Yang Liu and Masatoshi Shimoda. Non-parametric shape optimization method for natural vibration design of stiffened shells. *Computers & Structures*, 146:20–31, 2015.
- [84] Z-D Ma, Noboru Kikuchi, and I Hagiwara. Structural topology and shape optimization for a frequency response problem. *Computational mechanics*, 13(3):157–174, 1993.
- [85] Eloi Martinet. Numerical optimization of Neumann eigenvalues of domains in the sphere, March 2023. arXiv:2303.12389 [math].

- [86] Jiří Matoušek. *Using the Borsuk-Ulam theorem*. Universitext. Springer-Verlag, Berlin, 2003. Lectures on topological methods in combinatorics and geometry, Written in cooperation with Anders Björner and Günter M. Ziegler.
- [87] John W. Milnor. *Topology from the differentiable viewpoint*. Princeton Landmarks in Mathematics. Princeton University Press, Princeton, NJ, 1997. Based on notes by David W. Weaver, Revised reprint of the 1965 original.
- [88] Takashi Nakazawa and Hideyuki Azegami. Shape optimization of flow field improving hydrodynamic stability. *Japan Journal of Industrial and Applied Mathematics*, 33:167–181, 2016.
- [89] Édouard Oudet. Numerical minimization of eigenmodes of a membrane with respect to the domain. *ESAIM: Control, Optimisation and Calculus of Variations*, 10(3):315–330, July 2004.
- [90] O. Pironneau. On optimum profiles in stokes flow. *Journal of Fluid Mechanics*, 59(1):117–128, 1973.
- [91] Pierre-Arnaud Raviart, Jean-Marie Thomas, and Jean-Marie Thomas. *Introduction à l’analyse numérique des équations aux dérivées partielles*, volume 6. Elsevier Masson, 1983.
- [92] Yves Renard and Konstantinos Poulios. GetFEM: automated FE modeling of multiphysics problems based on a generic weak form language. *ACM Trans. Math. Software*, 47(1):Art. 4, 31, 2021.
- [93] Jacob T Schwartz. *Nonlinear functional analysis*, volume 4. CRC Press, 1969.
- [94] Alexander Shapiro and Michael K. H. Fan. On eigenvalue optimization. *SIAM J. Optim.*, 5(3):552–569, 1995.
- [95] Anant R. Shastri. *Elements of differential topology*. CRC Press, Boca Raton, FL, 2011. With a foreword by F. Thomas Farrell.
- [96] Robert S. Strichartz. Estimates for Sums of Eigenvalues for Domains in Homogeneous Spaces. *Journal of Functional Analysis*, 137(1):152–190, April 1996.
- [97] C. Sturm. Mémoire sur les équations différentielles linéaires du second ordre. *Journal de mathématiques pures et appliquées 1re série*, 1:106–186, 1836.
- [98] G. Szegö. Inequalities for certain eigenvalues of a membrane of given area. *J. Rational Mech. Anal.*, 3:343–356, 1954.
- [99] B. Andreas Troesch. Elliptical Membranes with Smallest Second Eigenvalue. *Mathematics of Computation*, 27(124):767–772, 1973. Publisher: American Mathematical Society.
- [100] Andreas Wächter and Lorenz T Biegler. On the implementation of an interior-point filter line-search algorithm for large-scale nonlinear programming. *Mathematical programming*, 106(1):25–57, 2006.
- [101] Qiaoling Wang and Changyu Xia. On a conjecture of ashbaugh and benguria about lower eigenvalues of the neumann laplacian, 2018.
- [102] H. F. Weinberger. An isoperimetric inequality for the $\$N\$$ -dimensional free membrane problem. *J. Rational Mech. Anal.*, 5:633–636, 1956.
- [103] H. F. Weinberger. An isoperimetric inequality for the N -dimensional free membrane problem. *J. Rational Mech. Anal.*, 5:633–636, 1956.
- [104] Hermann Weyl. Über die asymptotische verteilung der eigenwerte. *Nachrichten von der Gesellschaft der Wissenschaften zu Göttingen, Mathematisch-Physikalische Klasse*, 1911:110–117, 1911.
- [105] Sven Andreas Wolf and Joseph B. Keller. Range of the first two eigenvalues of the Laplacian. *Proc. Roy. Soc. London Ser. A*, 447(1930):397–412, 1994.
- [106] D.Z. Zanger. Eigenvalue variations for the neumann problem. *Applied Mathematics Letters*, 14(1):39–43, 2001.
- [107] V. Šverák. On optimal shape design. *J. Math Pures Appl.*, 72-6, 1993.

List of Figures

1.1	Représentation de \mathcal{S}_4 (gauche) et \mathcal{S}_{16} (droite)	4
1.2	Ensemble Ω_ε consistant en l'union du carré unité et d'un carré de côté ε relié par un fin rectangle de hauteur ε^2	4
1.3	Exemple de domaine en peigne avec respectivement 20 (gauche) et 60 dents (droite).	5
1.4	Approximation des huit premières densités optimales.	11
1.5	Graphe de ρ^6 comme une fonction de la latitude $\theta \in [0, \pi]$ (gauche) et sa représentation sur la sphère (droite).	12
1.6	Exemples de densités optimales pour μ_1, μ_2, μ_3 (respectivement première, deuxième et troisième ligne) pour différentes valeurs de m	13
1.7	Exemples de domaines optimaux pour μ_1, μ_2, μ_3 (respectivement première, deuxième et troisième ligne) pour différentes valeurs de m	14
1.1	Representation of \mathcal{S}_4 (left) and \mathcal{S}_{16} (right).	19
1.2	Set Ω_ε consisting in the union of the unit square and a square of size ε linked by a thin rectangle of height ε^2	19
1.3	Example of a comb-shaped domain with 20 (left) and 60 teeth (right).	20
1.4	Approximation of the first eight optimal densities.	25
1.5	Graph of ρ^6 as a function of latitude $\theta \in [0, \pi]$ (left) and its representation on the sphere (right).	26
1.6	Examples of optimal densities for μ_1, μ_2, μ_3 (respectively first, second and third row) for different values of m	27
1.7	Examples of optimal domains for μ_1, μ_2, μ_3 (respectively, the first, second, and third row) for different values of m	28
3.1	The function h for $k = 1$ and a function g_P for $k = 2$	53
3.2	One spurious mode	63
3.3	Approximation of the first eight optimal densities	66
5.1	The meshes used for the density method.	88
5.2	Example of optimal densities for μ_1 for $m \in \{2.17, 5.0\}$ when ρ is supported outside of a ball.	89
5.3	Optimal value of μ_1 obtained by the density method, with the constraint that the support of ρ is located outside of a ball.	89
5.4	Optimal value of μ_1 obtained by the density method.	90
5.5	Optimal value of μ_1 near $m \approx 5.0$	90
5.6	Example of optimal densities for μ_1 for $m \in \{2.0, 4.98, 8.05, 11.2\}$ (top) along with their latitudinal profile (bottom).	91
5.7	Mesh-refinement procedure one 1D for different values of m	92
5.8	Optimal value of μ_2 obtained by the density method.	93
5.9	Example of optimal densities for μ_2 for $m \in \{2.31, 5.46, 8.23, 11.01\}$	93
5.10	Optimal value of μ_3 obtained by the density method.	94
5.11	Example of optimal densities for μ_3 for $m \in \{2.0, 5.0, 8.03, 11.0\}$	94
5.12	Optimal value of μ_1 obtained by the level-set method.	99
5.13	Rotational view of the optimal shape obtained by the level-set method for large m	99
5.14	Example of optimal domains for μ_1 for $m \in \{2.03, 5.1, 8.0, 10.85\}$	100
5.15	Optimal value of μ_2 obtained by the level-set method.	100
5.16	Example of optimal domains for μ_2 for $m \in \{2.12, 5.1, 8.13, 11.17\}$	101
5.17	Optimal value of μ_3 obtained by the level-set method.	101
5.18	Example of optimal domains for μ_3 for $m \in \{2.0, 5.22, 8.0, 11.04\}$	101

5.19 Example of optimal densities for μ_1, μ_2 and μ_3 (resp. first, second and third row) for $m \in \{3, 22, 43, 68\}$ approximately	103
5.20 Optimal values of μ_1, μ_2 and μ_3 (resp. first, second and third row) obtained by the density method	104
5.21 Example of optimal domains for μ_1, μ_2 and μ_3 (resp. first, second and third row) for $m \in \{4, 22, 42, 60\}$ approximately	105
5.22 Optimal values of μ_1, μ_2 and μ_3 (resp. first, second and third row) obtained by the level set method	106

List of Tables

3.1	Spurious modes persistence. Eigenvalues computed with the approximation (3.24) containing spurious modes (left) and with the approximation (3.23) (right)	63
3.2	Values comparison	66